Synthetic CRISPR tools for information processing in bacteria

Ava Karanjia

A dissertation
submitted in partial fulfillment of the
requirements for the degree of

Doctor of Philosophy

University of Washington
2025

Reading Committee:
James M. Carothers, *Chair*
Jesse G. Zalatan, *Chair*
Jorge Marchand

Program Authorized to Offer Degree:
Chemical Engineering

University of Washington

Abstract

Synthetic CRISPR tools for information processing in bacteria

Ava Karanjia

Chairs of the Supervisory Committee:

James M. Carothers

Department of Chemical Engineering

Jesse G. Zalatan

Department of Chemistry

CRISPR Cas tools enable programmable control over gene expression and editing in bacteria. However, CRISPR activation in bacteria faces challenges including strict target site requirements, unreliable performance across native genes, and interference from native gene regulation. This work aims to overcome these challenges by creating versatile and robust CRISPR tools in bacteria. We systematically evaluated and developed PAM-flexible dCas9 variants, engineered bacterial activators, and mRNA-responsive molecular switches. First, with PAM-flexible dCas9 variants, we observe activation at previously inaccessible gene targets, and we observe a tradeoff between fold-activation and PAM flexibility. Our work provides a framework to choose the most effective dCas9 variant for a given endogenous gene target. Next, we characterized bacterial activator proteins with a set of engineered synthetic promoters. We found that optimal target sites for different activators could vary upstream of the gene start site and combinations of activators often resulted in antagonistic behavior. Last, we combined CRISPR tools to create mRNA-responsive gene switches for molecular recording and programmable, permanent expression changes. This dual-Cas9 approach uses reprogrammable RNAs to sense mRNA signals and convert them into gene activation, achieving high editing efficiency and high activation of a fluorescent reporter. These advancements enhance CRISPR tools for dynamic, programmable regulation and highlight future strategies for next-generation bacterial gene circuits.

Table of Contents

Reading Guide

Chapter 1 is relevant sections of our review published in Annual Review of Chemical and Biomolecular Engineering, “CRISPR Tools for Engineering Prokaryotic Systems: Recent Advances and New Applications”, which serves as an introduction to CRISPR-Cas systems and their potential applications in gene regulation and gene editing.

Chapter 2 is our manuscript published in ACS Synthetic Biology, “Expanding the Scope of Bacterial CRISPR Activation with PAM-Flexible dCas9 Variants”. In this work, we systematically evaluate a panel of PAM-flexible dCas9 variants for their ability to activate bacterial genes. We provide a framework to choose the most effective dCas9 variant for a given set of gene targets, which will further expand the utility of CRISPRa/i gene regulation in bacterial systems.

Chapter 3 is our manuscript submitted to ACS Synthetic Biology, “Systematic Mapping of Bacterial CRISPRa Design Rules and Implications for Synergistic Gene Activation”. In this work, we identified potential effectors for synergistic activation and systematically characterized these effectors with a set of engineered synthetic promoters. We did not find combinations that produced synergistic activation, and we found that many combinations were antagonistic. This investigation highlights fundamental mechanistic differences between bacterial and eukaryotic transcriptional activation systems.

Chapter 4 presents our manuscript in preparation, “mRNA-responsive Bacterial Genetic Programs through Coupled CRISPR-Cas Tools”. In this work, we engineered a dual CRISPR system that pairs mRNA-responsive tracrRNAs (Rptrs) with CRISPR base editing and CRISPR activation tools to build mRNA-responsive genetic switches. This work lays the foundation for applying mRNA-responsive CRISPR tools to sense endogenous signals and control bacterial gene expression dynamically.

Chapter 1: Introduction to CRISPR Tools for Engineering Prokaryotic Systems

Diego Alba Burbano[+,1,2], Cholpisit Kiattisewee[+,1,2], Ava V. Karanjia[1,2], Ryan A.L. Cardiff[1], Ian D. Faulkner[1,2], Widianti Sugianto[1,2], James M. Carothers*[,1,2]

1: Molecular Engineering & Sciences Institute
and Center for Synthetic Biology
University of Washington
Seattle, WA 98195
United States

2: Department of Chemical Engineering
University of Washington
Seattle, WA 98195
United States

+: These authors contributed equally

*: Corresponding author

jcaroth@uw.edu
206-221-4902

Three key sections from a review article published in *Annual Review in Chemical and Biomolecular Engineering* on July 3, 2024.
DOI: 10.1146/annurev-chembioeng-100522-114706

***Note**: This chapter contains collaborative work. The introduction was drafted by D. A. Burbano and edited by A. V. Karanjia and others. For the main sections presented, A. V. Karanjia drafted initial versions of each section. A. V. Karanjia and D. A. Burbano edited and finalized sections 1.1 and 1.3, while A. V. Karanjia, D. A. Burbano and C. Kiattisewee edited and finalized section 1.2. D. A. Burbano made all figures used in this chapter. The other contributors prepared figures and written text relevant to their contributions. The introduction, tables, and future prospects sections were compiled and written collaboratively.

1.1. Introduction

Synthetic biologists seek to understand and harness biological systems to engineer solutions in a wide variety of fields, ranging from chemical bioproduction to medicine, agriculture, and energy.[1,2] In the past decade, CRISPR-Cas tools have revolutionized biological research by simplifying the design and multiplexing of complex genetic functions. This ability to rapidly modify genetic material is streamlining reverse engineering of genotype-phenotype relationships and genetically encoding new desired functions. To expand beyond these applications, molecular tools that facilitate novel genetic manipulation are in great demand.[3]

Sequence-specific DNA-binding domains combined with different nucleases, transcriptional regulators, and base editors, have been successful in many genetic engineering applications.[4–6] Protein-based tools consisting of DNA-binding domains derived from zinc-finger nucleases (ZFNs) or transcription activator-like effector proteins (TALEs) offer robust and very precise behaviors.[7] However, tuning their effect and designing these proteins to target multiple genes is relatively difficult. In contrast, CRISPR tools facilitate targeting of multiple sites simultaneously since targets are encoded through simple Watson-Crick interactions in short guide RNA (gRNA) sequences. In terms of designability, the discovery of new CRISPR systems, paired with a wide variety of tethered effectors, have greatly expanded the palette of genetic engineering tools.[8–11]

Genetic engineering can be subdivided into 1) gene editing to change the underlying genetic information and 2) gene regulation to change how the information is processed. To date, a wide range CRISPR-Cas techniques have been developed for gene editing, from DNA breaks by Cas nucleases to large DNA integrations via CRISPR-assisted transposases.[12–15] Base editing is another promising gene editing technique that introduces point mutations into DNA or RNA by using nickase or catalytically-dead Cas proteins (nCas or dCas) to localize nucleobase editor enzymes to precise target sites.[16–18] Additionally, many CRISPR-based tools are now available for up- and down-regulation of gene expression by fusing dCas proteins to transcriptional or translational regulators. dCas9 was rapidly repurposed for programmable transcriptional repression, termed CRISPR interference (CRISPRi), by physically blocking the transcription initiation or elongation processes.[13,19] Other dCas proteins have also been implemented in the same fashion, including dCas9s from different species and dCas12.[20–22] The transcriptional activation

counterpart, termed CRISPR activation (CRISPRa), was promptly developed in eukaryotes based on transcription factors widely applicable in any eukaryotic system, e.g. VP64.[23,24] In contrast, prokaryotic CRISPRa lagged behind due to limited universal transcriptional activators and stringent design rules for implementation.[25,26] Nevertheless, these genetic engineering tools are now broadly applied in different bacteria.[27]

The versatility of CRISPR gene regulation and gene editing tools has fueled many applications across diverse bacteria as well as cell-free systems (Figure 1). In bacteria, CRISPR tools are being used for rapid strain engineering in model organisms such as *E. coli*, mainly for bioproduction applications.[28,29] More recently, CRISPR tools have also been implemented in non-model microbes such as *C. necator*, *R. sphaeroides*, and *C. autoethanogenum* due to their unique metabolisms and wide range of substrate utilization, including CO_2.[30–33] Beyond metabolic engineering applications, biotherapeutic bacteria harboring CRISPR tools are now capable of recording changes in their environment and deploying novel antimicrobials.[34–38] In cell-free systems, purified Cas enzymes and gRNAs are widely used as biosensors for *in vitro* diagnostics of nucleic acids, small molecules, proteins, and even bacteria.[39,40] Moreover, cell-free expression systems (CFES) that also contain the molecular machinery required for gene expression, such as PURE or lysate-based TXTL, have accelerated the characterization of new CRISPR systems and the development of CRISPR genetic circuits.[41–47] In turn, these advancements are paving the way for cell-free bioproduction platforms and biosensors that can multiplex input signals and launch appropriate CRISPR programs in response.[42,48–51]

This article reviews CRISPR-based genetic engineering tools developed to date and their cutting-edge applications across diverse bacteria and cell-free systems. For eukaryotic counterparts, several reviews were recently published.[18,52–54] We first showcase the designability and modularity of CRISPR systems by covering the constituent components, namely the different Cas proteins, tethered effectors, and gRNAs, and how they can be designed for specific genetic engineering applications (Figure 1). We then examine how CRISPR-tools can be integrated into genetic circuits, granting a new layer of programmability and a framework for genetic information processing. We describe how these different CRISPR systems are being used for engineering complex biosensing, bioproduction, and biotherapeutics platforms. Lastly, we discuss the current challenges that CRISPR technologies encounter and explore the next-generation of CRISPR applications in prokaryotes.

Figure 1.1. CRISPR Tools for Genetic Engineering Prokaryotic Systems

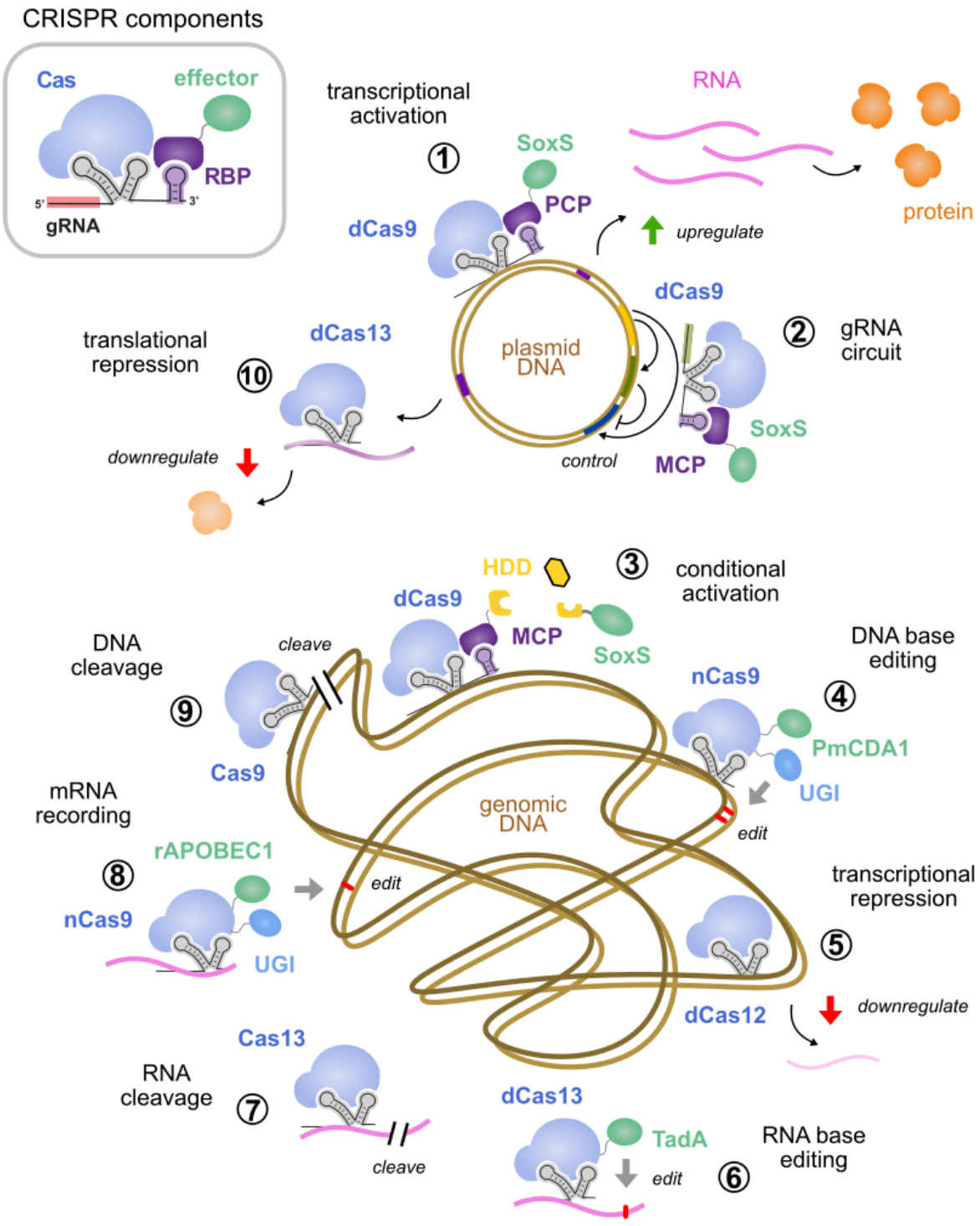

Figure 1: Schematic of different CRISPR tools and their mode of action. The top left panel depicts the main components of a CRISPR tool: Cas protein, guide RNA (gRNA), effector, and RNA binding protein (RBP). For simplicity, different Cas proteins are depicted the same and labeled accordingly. Plasmid and genomic DNA could be used interchangeably. (1) A dCas9-based transcriptional activation tool that recruits the SoxS activator through the RBP PP7 coat protein (PCP) and once localized to a gene of interest and upregulates RNA transcription. (2) A CRISPR circuit operating through the regulated expression of gRNAs that target other gRNAs and controls a gene of interest. In this case, SoxS is recruited through the MS2 coat protein (MCP). (3) A transcriptional activation tool in which recruitment of the effector SoxS is mediated by heterodimerization domains (HDD) responsive to a small-molecule. (4) A nCas9-based tool that uses *Petromyzon marinus* cytidine deaminase 1 (PmCDA1), which catalyzes the irreversible conversion of cytidine to uridine, and uracil DNA glycosylase inhibitor (UGI) for making DNA edits at a location specified by the gRNA. (5) A dCas12-based transcriptional repression tool capable of downregulation transcription of a gene of interest. (6) A dCas13-based tool tether to tRNA adenosine deaminase A (TadA), which catalyzes the irreversible conversion of adenosine to inosine, capable of targeting specific RNAs for base editing. (7) A Cas13-based tool that cleaves target RNA and can trigger collateral cleavage activity of any RNA. (8) A nCas9 tool capable of recording the presence of an mRNA by making DNA edits with the tethered rat apolipoprotein B mRNA editing enzyme catalytic subunit 1 (rAPOBEC1). (9) A Cas9 system capable of making precise DNA double stranded cuts. (10) A dCas13 translational repression system that downregulates protein translation from a specific mRNA.

1.2. Type II: the Cas9 workhorse for DNA targeting

The DNA binding activity of Type II CRISPR systems can easily be controlled by an engineered small guide RNA (gRNA), making them particularly well-suited for DNA manipulation applications. In general, type II systems consist of a Cas9 protein and two RNAs, a trans-activating RNA (tracrRNA) and a CRISPR RNA (crRNA). The tracrRNA serves as the binding scaffold for the Cas9 protein, while the crRNA is the complementary sequence or spacer for the target DNA. In native systems, the tracrRNA and crRNA hybridize; however, many engineered systems fuse the two into a single guide RNA (sgRNA) with similar performance in vitro.[12] Cas9 DNA targeting requires two key features: i) DNA target and gRNA spacer complementarity, and ii) a protospacer adjacent motif (PAM) directly flanking the DNA target, necessary for preventing self-digestion of the gRNA encoding sequence. Mechanistically, Cas9 first scans DNA for potential PAMs and then checks guide-target complementarity. Once guide-target complementarity is validated, the nuclease domains of Cas9 generate double-stranded breaks (DSBs) into the target DNA.[55,56] While mismatched spacer sequences can be tolerated, strict PAM requirements often limit Cas9 targeting.[56,57] For instance, the density of PAM sequences from the most widely used Cas9, SpyCas9 from *Streptococcus pyogenes*, is only ~1 PAM (5'-NGG-3') every 10 bases in the regions upstream of endogenous promoters in the *E. coli* genome (50.5% GC).[25] PAM density for SpyCas9 is potentially higher in organisms whose genome has high GC-content (e.g. *P. putida* 61.5% GC) but will be lower in AT-rich bacterial genome (e.g. *C. autoethanogenum* 31.1% GC). Therefore, engineering non-model organisms with low GC-content could be challenging with SpyCas9 alone.

To increase the range of PAMs and associated loci for targeting, many groups have bioinformatically mined for new orthologs.[58,59] Other type II Cas9s systems were found to have completely different consensus PAMs, a wide range of sizes, and distinct tracrRNAs (Table 1). For example, SmacCas9 from *Streptococcus macacae* has adenine-rich PAM preference (5′-NAAN-3′).[60] Sth1Cas9 and Sth3Cas9 from *Streptococcus thermophilus* have more stringent PAMs, 5′-NNAGAAW-3′ and 5′-NGGNG-3′; however, longer PAMs offer significantly lower off-target effects.[61,62] Computational pipelines to predict functional PAM sequences of uncharacterized CRISPR-Cas systems were also constructed.[63,64] For instance, a type II CRISPR system from *M. heyeri* was found with flexible PAM sequences (5'-GSNN-3'). Additional details on the size and compatibility of PAMs from different Cas9 orthologs beyond the scope of this review can be found in the recent review by Collias & Beisel 2021 et al.[65]

Table 1: Class 2 Cas proteins prevalent in Prokaryotic Applications

Type	Cas protein	Sources	Size (aa)	PAM/PFS	Target substrates	Refs.
Type II	SpyCas9	*Streptococcus pyogenes*	~1400	NGG	dsDNA	[12]
	xCas9-NG	SpyCas9[a]	~1400	NGN	dsDNA	[66,67]
	SpRYCas9	SpyCas9[a]	~1400	NRN > NYN	dsDNA	[68]
	SmacCas9	*Streptococcus macacae*	~1400	NAA	dsDNA	[60]
	Sth1Cas9, Sth3Cas9	*Streptococcus thermophilus*	~1200	NNAGAAW, NGGNG	dsDNA	[61,62]
	ScCas9	*Streptococcus canis*	~1400	NNG	dsDNA	[69]
	Nme1Cas9, Nme2Cas9, Nme3Cas9	*Neisseria meningitidis*	~1000	N4GYTT, N4CC, N4CAAA	dsDNA	[70]
	SauCas9	*Staphylococcus aureus*	~1000	NNGRRT	dsDNA	[71]
	CjCas9	*Campylobacter jejuni*	~1000	N4RYAC	dsDNA	[72]
	SauriCas9	*Staphylococcus auricularis*	~1000	NNGG, NAAN	dsDNA	[73]

Note: [a]These Cas proteins were engineered from widely used Cas proteins.

Protein engineering has also been successfully employed to increase PAM-flexibility (Table 1). These efforts have ranged from chimera construction, random mutagenesis, structure-guided design, and high-throughput PAM determination assays.[66–68,74,75] Hu et al. used phage-assisted continuous evolution of the α-helical recognition domain to evolve expanded PAM SpyCas9 variants capable of targeting 5′-NG-3′ (xCas9-3.7), 5′-GAA-3′, and 5′-GAT-3′.[66] In pursuit of similar goals, Nishimasu et al. screened structure-guided designs to develop another expanded PAM variant, SpCas9-NG, also targeting 5’-NG-3’ PAMs.[67] Comparison of xCas9 and SpCas9-NG demonstrated that SpCas9-NG has superior 5’-NG-3’ PAM recognition.[75,76] Similar engineering efforts were also conducted in other Cas9 variants.[77–79] Overall, near PAM-less Cas9 variants, whose specificity depends

predominantly on target-spacer complementarity, have shown to improve target accessibility and efficacy in both eukaryotic and bacterial systems.[68,75,76,79–81]

However, PAM expansion can lead to extended timescales for target recognition and increased off-target effects.[56,57,82] To address off-target effects, both rational engineering and enzyme selection approaches have been used to develop high-fidelity SpyCas9 variants with reduced off-target activity.[83–88] Introducing mutations that confer high-fidelity traits into a PAM-expanded variant could also mitigate the off-target effect instigated by PAM flexibility.[89] However, most of the high-fidelity variants have yet to be characterized in prokaryotes.

In the case of nuclease-deactivated Cas9 (dCas9), Spy dCas9 has also been shown to bind non-specifically to NGG PAM sites and to off-target genomic loci with up to six mismatched nucleotides that differ from the spacer.[82,90] dCas9 exhibits toxicity rooting from this promiscuous DNA binding effect when expressed at high level in bacteria.[91,92] Although previous works have demonstrated that Cas9 off-target binding directly scales with PAM flexibility, we observed that increased dCas9 PAM-flexibility has no additional growth defect compared to original dCas9, possibly due to reducing CRISPRi-like effect.[67,74,80,89] This finding suggests that adverse effects from Cas engineering might behave differently depending on the biological function of the Cas proteins.

Overall, PAM expansion has increased our targeting ability with Cas9-based genetic tools, but not without functional tradeoffs. For instance, although PAM-flexible dCas9 variants exhibit greater CRISPRa efficiency, CRISPRi gene repression efficiency with the same variants is decreased.[80] Hence, frameworks for choosing the most effective variant for a given set of targets and specific applications are necessary. A database with systematic characterization of Cas9 variants across bacteria will streamline the process of choosing the optimal Cas9 variant for a given set of target genes and specific applications.[93]

1.3. Expanding CRISPR functionality with tethered effectors

Abolishing Cas nuclease activity generates nickase or catalytically-dead Cas proteins (nCas or dCas, respectively), opening a new paradigm of CRISPR tools for sequence-specific nucleic acid modifications and gene expression regulation. Point mutations in one of the Cas nuclease domains generates a ‘nicking’ variant that only cleaves one strand of DNA, while mutations in both domains form a 'catalytically-dead' variant with no cleavage activity. In prokaryotes, dCas9 was rapidly repurposed for programmable transcriptional repression by physically blocking the transcription initiation or elongation processes. Tethering effector domains to the CRISPR complex enabled sequence-specific localization of effectors to a DNA or RNA of interest, for applications such as transcriptional activation and base editing.[6] Effector tethering has been achieved through covalent fusion to the Cas protein, protein-protein interactions (PPI), or recruitment of effectors fused to RNA binding proteins (RBP) that interact non-covalently with modified guide RNAs (scaffold RNA, scRNA). Importantly, orthogonal effector recruitment can be programmed with multiple PPI systems or RBP-RNA hairpin pairs (Figure 2). In contrast to eukaryotes, where CRISPR transcriptional activation (CRISPRa) can readily be achieved with a universal transcriptional activator, CRISPRa across prokaryotes remains challenging due to the distinct transcriptional regulation mechanisms present in different bacteria.[25,26,94,95] Here we focus on the development of transcriptional activators for prokaryotic CRISPRa as well as recent advancements in tethering effectors for CRISPR gene editing.

1.4. Effectors for CRISPR-based gene regulation

Bikard et al. showed that transcriptional activation could be achieved through recruitment of accessory proteins in prokaryotes similarly to previous works in eukaryotes. They developed a CRISPRa system in *E. coli* by fusing a RNA polymerase (RNAP) omega subunit (RpoZ) to dCas9.[96] One limitation of this system was the need to delete the endogenous *rpoZ* gene. Later work from our group found that bacterial CRISPRa could also function through an RBP-based recruitment using a bacterial transcription factor, SoxS, that interacts with the C-terminus of an alpha subunit of RNAP (RpoA).[97] Notably, SoxS-based CRISPRa does not require modification of the genomic background, which streamlines the portability to other bacterial systems. SoxS-RpoA interaction motif is conserved across diverse bacteria and was demonstrated to be functional in *P. putida,* despite the absence of SoxS-homolog.[97,98] Another approach by Liu et al. achieved CRISPRa through the RBP

recruitment of the transcriptional activator PspF.[99] Interestingly, we found that PspF and SoxS could be implemented simultaneously through orthogonal RNA hairpin-RBP pairs —MS2/MCP for SoxS and BoxB/λN22 for PspF— and also work complementary to each other. SoxS can activate a broad range of σ^{70} superfamily promoters but is ineffective toward σ^{54}-family promoters.[25] On the other hand, PspF system works specifically on the σ^{54}-family promoters due to its unique ATP-dependent activation mechanism but cannot activate σ^{70} family promoters.[99] In both cases, strategies to abolish the DNA-binding of transcriptional effectors proved to be crucial since CRISPRa DNA targeting should be governed by dCas9 rather than the transcriptional effectors. In PspF-based CRISPRa, this was achieved by truncating the helix-turn-helix (HTH) DNA-recognition motif of PspF.[99] In SoxS-based CRISPRa, we reduced the DNA-binding capacity of heterologous SoxS through multiple mutations, leading to key improvement in CRISPRa performance.[25]

Through characterization of different CRISPRa elements and target genes, we have found that CRISPRa performance relies on i) composition of the target promoter, and ii) position of target sequence relative to the transcription start site (Figure 2A).[25,48] These design factors remain consistent across multiple transcriptional activation systems.[25,99] For instance, the dynamic range of CRISPR-based gene overexpression is dependent on DNA helical phases (Figure 2B). We also found that these two systems exhibited consistent design rules in both *E. coli* and *P. putida*.[100]

Figure 2: Prokaryotic CRISPRa Sequence and Distance Requirements

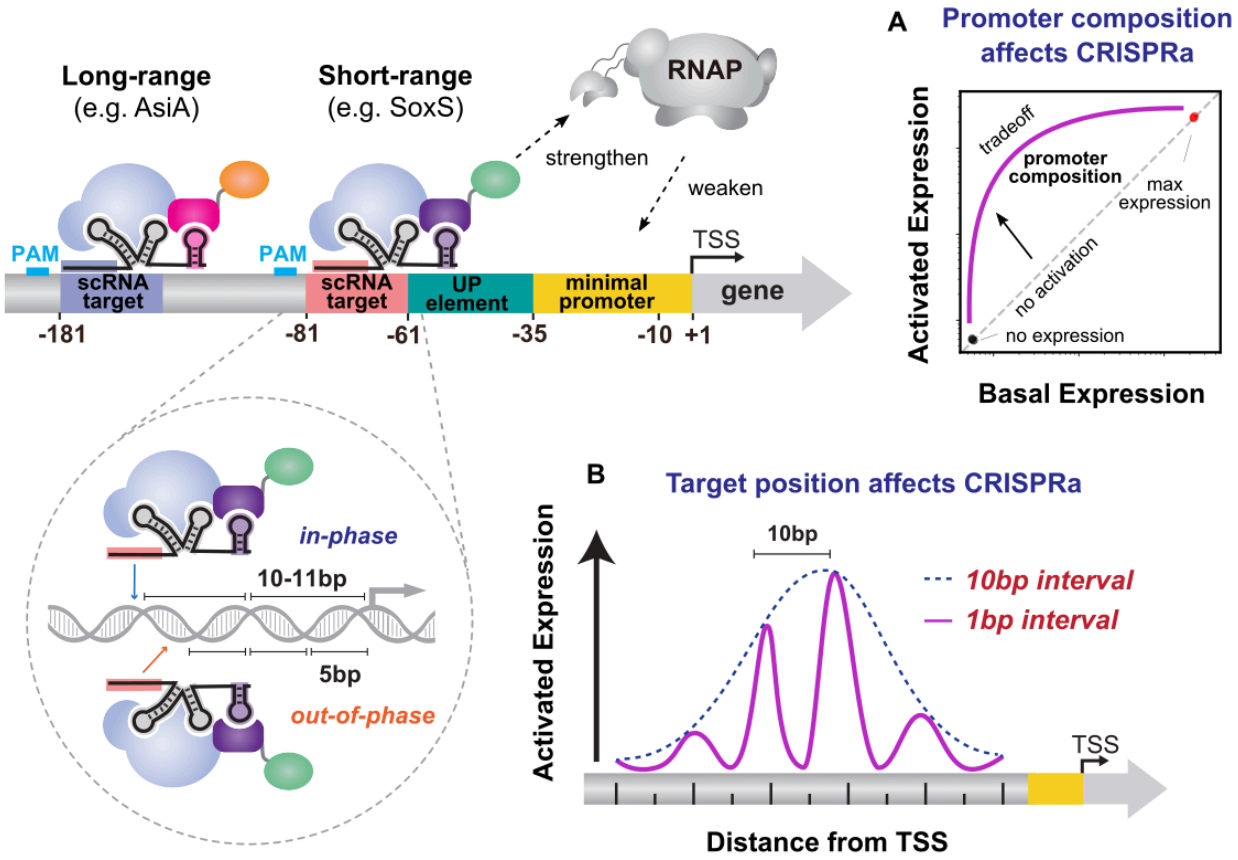

Figure 2: Schematic of a prokaryotic promoter showing stringent requirements for bacterial CRISPRa. RNAP affinity for the minimal promoter and UP-element determines basal expression levels. When CRISPRa is targeted to a promoter with a correct PAM and complementary scRNA target site, RNAP is recruited by the transcriptional activator. A) Promoter composition determines RNAP-promoter and CRISPRa-promoter interactions and hence affects CRISPRa-mediated expression levels. B) CRISPRa-mediated expression is highly dependent on the distance of CRISPRa with respect to the transcription start site (TSS), and exhibits a periodic dependence with peak activities every 10–11 bases, corresponding to a single turn of DNA helix.

Bacterial CRISPRa systems are effective in a narrow range of target positions covering 60 to 100 bp upstream of the TSS (Figure 2 and Table 2A). There have been several attempts to develop CRISPRa systems for targeting alternative positions and promoter contexts. Directed evolution of AsiA, an anti-sigma70 protein from T4 bacteriophage, covalently fused to dCas9 provides long distance CRISPRa beyond previously reported systems.[101] This system was tested in a massively-parallel fashion by replacing a minimal promoter with a library of promoter sequences derived from a metagenomic dataset. Although only 3% (248 out of ~8000) of the promoters could be upregulated, these data do provide a proof-of-concept that targeting regions can be expanded through molecular engineering. Another strategy to overcome the stringent CRIPSRa distance requirements has been to use circular permuted dCas9 (cpdCas9) variants to change the positioning of the tethered effector.[102] They achieved increased targeting flexibility by screening a library of cpdCas9s that recruited the N-terminal domain of RpoA (αNTD) of 8 different bacterial species through heterospecific coiled-coiled peptides (SYNZIPs) recruitment.[102,103] With the advent of new CRISPRa systems, it could be possible to implement multiple CRISPRa systems together simultaneously for more effective activation and more target sites.

Even though most of the CRISPRa systems in bacteria rely on dCas9 to recruit effector proteins, other Cas systems could also be implemented in a similar manner. Direct fusion of RpoZ or SoxS effectors to dCas12a were implemented for CRISPR activation in *P. polymyxa* and *C. glutamicum*, respectively.[104,105] Type I-E Cascade-mediated bacterial CRISPRa is also recently demonstrated in a CRISPR-free *E. coli* using αNTD as an effector (Table 2A).[106] It should be noted that CRISPRa could be improved from engineering efforts on other parts beyond the effector domain and could also be developed in parallel from effector-specific optimization, e.g. dCas9 engineering for PAM-flexibility and reporter engineering to improve dynamic range.[48,80]

Table 2A: Effectors for prokaryotic CRISPRa, their mechanisms, and design rules.

CRISPRa systems	Mechanism	Optimal sites [a]	Strand	Organisms	Refs.
Effectors tethered directly to dCas					
dCas9-RpoZ	RNAP assembly	-60 to -100	NT	*E. coli,* *B. subtilis,* *L. enzymogenes,* *M. xanthus*	96,107–109
dCas9-RpoA	RNAP assembly	-267 to -415	T	*B. subtilis*	96,107–109
dCas9-SYNZIP-αNTD	RNAP assembly	-60 to -100	NT	*E. coli*	102,103
dCas9-RpoD	RNAP assembly	-199 to -216	NT	*S. oneidensis*	110
dCas9-AsiA [b]	RpoD and RpoB binding	-182 to -252	T	*E. coli,* *S. enterica,* *K. oxytoca*	101
Effectors tethered via guide RNA hairpin					
SoxS [b] (MCP or PCP or MCP + SYNZIP)	RpoA and RpoD binding	-60 to -100	NT	*E. coli, P. putida,* Cell-Free System, Hydrogel	25,45,48,97,98,111
TetD (MCP)	RpoA and RpoD binding	-60 to -100	NT	*E. coli*	25,97
RpoZ (MCP)	RNAP assembly	-91	NT	*E. coli*	25,97
αNTD (MCP)	RNAP assembly	-60 to -100	T	*E. coli*	25,97
PspF [b] (λN22 or MCP)	RpoN recruitment [c]	-91 to -131[d]	NT	*E. coli,* *K. oxytoca,* Cell-Free System	99,112

**__Note__: [a]Relative to transcription start site (TSS), [b]Engineered proteins, [c]RpoN promoter is distinct to other bacterial promoters of RpoD-promoter superfamily, [d]DNA looping is present in the promoter*

1.5. Effectors for CRISPR-based gene editing

CRISPR base editors (BEs) with tethered nucleobase editor enzymes, or deaminases, can be used to introduce sequence-specific, single-nucleotide modifications, such as to abolish enzyme activity through precise point mutations or early stop codons (Figure 1).[113] In comparison to traditional CRISPR editing technologies that induce DSB breaks, BEs only nick one strand of DNA. In bacteria, given the species-dependent variations in editing efficiency and the lethality of generating DSB in unintended targets, BE is often favored over traditional editing through native Cas cleavage and DNA repair mechanisms.[8,9,114–116] Current prokaryotic BEs rely on direct tethering of the deaminase to inactivated Cas proteins, such as dCas9, nCas9, and dCas12a (Table 2B). After Cas recruitment to the DNA, the deaminase recognizes and edits the target ssDNA in the R-loop structure formed between the gRNA and the target DNA. Each BE system targets a characteristic proximal stretch of ssDNA, termed editing window, based on the deaminase and tethering approach (Table 2B). Adenosine base editors (ABE) generate A>G through A>I deamination, while cytidine base editors (CBEs) generate C>T substitutions through C>U deamination and subsequent DNA replication (Table 2B). Most CBE systems also tether a uracil glycosylase inhibitor (UGI) to prevent base excision repair and reversal of the point mutation.[117] Notably, CBEs are more widely used, likely due to the higher editing efficiency and high GC content of host genomes.[113] Developing RBP-tethered BEs could allow for simultaneous regulation of multiple genes and even opportunities for multiplexed applications with other effector proteins.[118] The potential for multiplexing BE has been shown in multiple non-model organisms.[11,119–122]

Table 2B: Effectors for CRISPR-based gene editing and their editing window.

Editing system	Effector	Cas protein	Organisms	Editing window	Refs.
CBE	rAPOBEC1	Cas9n	*E. coli*, *B. melitensis*	4 to 8	[123]
		Cas9n	*C. glutamicum*	4 to 7	[120]
		Cas9n	*S. typhimurium*	5 to 10	[35]
		enCas9	*P. putida*	3 to 8	[124]
		dCas9	*B. subtilis*	17 to 20	[121]
	PmCDA1	dCas9	*E. coli*	1 to 5	[119]
		dCas9	*B. subtilis*	1 to 5	[122]
		dCas9	*Streptomyces spp.*	1 to 5	[125]
		dCas9	*P. polymyxa*	17 to 20	[122]
		dCas9	*Agrobacterium spp.*	16 to 20	[126]
ABE	TadA	dCas9/nCas9	*E. coli*	4 to 8	[127]
		Cas9n	*S. aureus*	4 to 8	[128]
		dxCas9/nxCas9	*P. putida*, *Pseudomonas spp.*	4 to 8	[129]

A major bottleneck for base editing is that gRNA spacer design is more challenging than traditional spacer design as it must also factor the constraints imposed by the editing effector.[113] Spacers designed for BE must factor in deaminase type, editing window, target nucleotide position, and desired translation product. Hence, traditional gRNA spacer design tools often cannot be directly translated into designing spacers for base editing. While a few tools exist to support BE-gRNA design in eukaryotes, their development in bacterial systems is fairly limited.[130–133]

Even when gRNAs can be successfully designed, editing applications are still limited by the toxic effects of different combinations of effectors and Cas proteins.[119,134] Hence, most studies require tedious screening combinations of Cas9 variants, deaminases, and expression cassettes to find a balance between efficiency and toxicity.[121,124,135] Moreover, sequencing-based BE efficiency analysis is currently expensive and time-consuming, and *in vivo*, real-time assessment of editing efficiency is only available in mammalian cells.[136,137] Adaptation of these tools for bacterial systems would enable rapid comparison of Cas9 nucleases and deaminases across diverse genetic backgrounds, elucidating the design rules for predictable implementation.

Tethering different effector domains to different Cas proteins has enabled a wide range of functions beyond nucleic acid cleavage. These CRISPR gene regulation and base editing tools have already been implemented individually across different microbes.[27,138–140] Moving forward, simultaneous integration of multiple CRISPR tools in the diverse prokaryotic hosts should be within reach.[141] Discovery and engineering of orthogonal hairpins-RBP pairs will enable the multiplexed recruitment of different effectors to specific sites. Moreover, multi-Cas systems for combined DNA and RNA targeting could be achieved with a better understanding of which Cas variants are better suited for each host as well as expression mechanisms to minimize burden effects.[142,143] Taken together, these advancements will fuel the next generation of prokaryotic CRISPR tools capable of concerted editing and regulation.[144]

1.6. References

(1) Nielsen, J.; Keasling, J. D. Engineering Cellular Metabolism. *Cell* **2016**, *164* (6), 1185–1197. https://doi.org/10.1016/j.cell.2016.02.004.

(2) Voigt, C. A. Synthetic Biology 2020–2030: Six Commercially-Available Products That Are Changing Our World. *Nature Communications* **2020**, *11* (1), 6379. https://doi.org/10.1038/s41467-020-20122-2.

(3) Cameron, D. E.; Bashor, C. J.; Collins, J. J. A Brief History of Synthetic Biology. *Nature Reviews Microbiology* **2014**, *12* (5), 381–390. https://doi.org/10.1038/nrmicro3239.

(4) Flores-Bautista, E.; Hernandez-Guerrero, R.; Huerta-Saquero, A.; Tenorio-Salgado, S.; Rivera-Gomez, N.; Romero, A.; Ibarra, J. A.; Perez-Rueda, E. Deciphering the Functional Diversity of DNA-Binding Transcription Factors in Bacteria and Archaea Organisms. *PLOS ONE* **2020**, *15* (8), e0237135. https://doi.org/10.1371/journal.pone.0237135.

(5) Porto, E. M.; Komor, A. C.; Slaymaker, I. M.; Yeo, G. W. Base Editing: Advances and Therapeutic Opportunities. *Nature Reviews Drug Discovery* **2020**, *19* (12), 839–859. https://doi.org/10.1038/s41573-020-0084-6.

(6) Wang, H.; Russa, M. L.; Qi, L. S. CRISPR/Cas9 in Genome Editing and Beyond. *Annual Review of Biochemistry* **2016**, *85* (1), 227–264. https://doi.org/10.1146/annurev-biochem-060815-014607.

(7) Gaj, T.; Gersbach, C. A.; Barbas, C. F., III. ZFN, TALEN, and CRISPR/Cas-Based Methods for Genome Engineering. *Trends in Biotechnology* **2013**, *31* (7), 397–405. https://doi.org/10.1016/j.tibtech.2013.04.004.

(8) Arroyo-Olarte, R. D.; Bravo Rodríguez, R.; Morales-Ríos, E. Genome Editing in Bacteria: CRISPR-Cas and Beyond. *Microorganisms* **2021**, *9* (4), 844. https://doi.org/10.3390/microorganisms9040844.

(9) Vento, J. M.; Crook, N.; Beisel, C. L. Barriers to Genome Editing with CRISPR in Bacteria. *J Ind Microbiol Biotechnol* **2019**, *46* (9–10), 1327–1341. https://doi.org/10.1007/s10295-019-02195-1.

(10) Vigouroux, A.; Bikard, D. CRISPR Tools To Control Gene Expression in Bacteria. *Microbiology and Molecular Biology Reviews* **2020**, *84* (2), e00077-19. https://doi.org/10.1128/mmbr.00077-19.

(11) Volke, D. C.; Martino, R. A.; Kozaeva, E.; Smania, A. M.; Nikel, P. I. Modular (de)Construction of Complex Bacterial Phenotypes by CRISPR/nCas9-Assisted, Multiplex Cytidine Base-Editing. *Nat Commun* **2022**, *13* (1), 3026. https://doi.org/10.1038/s41467-022-30780-z.

(12) Jinek, M.; Chylinski, K.; Fonfara, I.; Hauer, M.; Doudna, J. A.; Charpentier, E. A Programmable Dual-RNA–Guided DNA Endonuclease in Adaptive Bacterial Immunity. *Science* **2012**, *337* (6096), 816–821. https://doi.org/10.1126/science.1225829.

(13) Qi, L. S.; Larson, M. H.; Gilbert, L. A.; Doudna, J. A.; Weissman, J. S.; Arkin, A. P.; Lim, W. A. Repurposing CRISPR as an RNA-Guided Platform for Sequence-Specific Control of Gene Expression. *Cell* **2013**, *152* (5), 1173–1183. https://doi.org/10.1016/j.cell.2013.02.022.

(14) Tou, C. J.; Orr, B.; Kleinstiver, B. P. Precise Cut-and-Paste DNA Insertion Using Engineered Type V-K CRISPR-Associated Transposases. *Nat. Biotechnol.* **2023**, *41* (7), 968–979. https://doi.org/10.1038/s41587-022-01574-x.

(15) Vo, P. L. H.; Ronda, C.; Klompe, S. E.; Chen, E. E.; Acree, C.; Wang, H. H.; Sternberg, S. H. CRISPR RNA-Guided Integrases for High-Efficiency, Multiplexed

Bacterial Genome Engineering. *Nature Biotechnology* **2021**, *39* (4), 480–489. https://doi.org/10.1038/s41587-020-00745-y.
(16) Komor, A. C.; Kim, Y. B.; Packer, M. S.; Zuris, J. A.; Liu, D. R. Programmable Editing of a Target Base in Genomic DNA without Double-Stranded DNA Cleavage. *Nature* **2016**, *533* (7603), 420–424. https://doi.org/10.1038/nature17946.
(17) Nishida, K.; Arazoe, T.; Yachie, N.; Banno, S.; Kakimoto, M.; Tabata, M.; Mochizuki, M.; Miyabe, A.; Araki, M.; Hara, K. Y.; Shimatani, Z.; Kondo, A. Targeted Nucleotide Editing Using Hybrid Prokaryotic and Vertebrate Adaptive Immune Systems. *Science* **2016**, *353* (6305), aaf8729. https://doi.org/10.1126/science.aaf8729.
(18) Anzalone, A. V.; Koblan, L. W.; Liu, D. R. Genome Editing with CRISPR–Cas Nucleases, Base Editors, Transposases and Prime Editors. *Nature Biotechnology* **2020**, *38* (7), 824–844. https://doi.org/10.1038/s41587-020-0561-9.
(19) Gilbert, L. A.; Horlbeck, M. A.; Adamson, B.; Villalta, J. E.; Chen, Y.; Whitehead, E. H.; Guimaraes, C.; Panning, B.; Ploegh, H. L.; Bassik, M. C.; Qi, L. S.; Kampmann, M.; Weissman, J. S. Genome-Scale CRISPR-Mediated Control of Gene Repression and Activation. *Cell* **2014**, *159* (3), 647–661. https://doi.org/10.1016/j.cell.2014.09.029.
(20) Rock, J. M.; Hopkins, F. F.; Chavez, A.; Diallo, M.; Chase, M. R.; Gerrick, E. R.; Pritchard, J. R.; Church, G. M.; Rubin, E. J.; Sassetti, C. M.; Schnappinger, D.; Fortune, S. M. Programmable Transcriptional Repression in Mycobacteria Using an Orthogonal CRISPR Interference Platform. *Nature Microbiology* **2017**, *2* (4), 16274. https://doi.org/10.1038/nmicrobiol.2016.274.
(21) Fonfara, I.; Richter, H.; Bratovič, M.; Le Rhun, A.; Charpentier, E. The CRISPR-Associated DNA-Cleaving Enzyme Cpf1 Also Processes Precursor CRISPR RNA. *Nature* **2016**, *532* (7600), 517–521. https://doi.org/10.1038/nature17945.
(22) Zetsche, B.; Gootenberg, J. S.; Abudayyeh, O. O.; Slaymaker, I. M.; Makarova, K. S.; Essletzbichler, P.; Volz, S. E.; Joung, J.; van der Oost, J.; Regev, A.; Koonin, E. V.; Zhang, F. Cpf1 Is a Single RNA-Guided Endonuclease of a Class 2 CRISPR-Cas System. *Cell* **2015**, *163* (3), 759–771. https://doi.org/10.1016/j.cell.2015.09.038.
(23) Casas-Mollano, J. A.; Zinselmeier, M. H.; Sychla, A.; Smanski, M. J. Efficient Gene Activation in Plants by the MoonTag Programmable Transcriptional Activator. *Nucleic Acids Research* **2023**, gkad458. https://doi.org/10.1093/nar/gkad458.
(24) Zalatan, J. G.; Lee, M. E.; Almeida, R.; Gilbert, L. A.; Whitehead, E. H.; La Russa, M.; Tsai, J. C.; Weissman, J. S.; Dueber, J. E.; Qi, L. S.; Lim, W. A. Engineering Complex Synthetic Transcriptional Programs with CRISPR RNA Scaffolds. *Cell* **2015**, *160* (1–2), 339–350. https://doi.org/10.1016/j.cell.2014.11.052.
(25) Fontana, J.; Dong, C.; Kiattisewee, C.; Chavali, V. P.; Tickman, B. I.; Carothers, J. M.; Zalatan, J. G. Effective CRISPRa-Mediated Control of Gene Expression in Bacteria Must Overcome Strict Target Site Requirements. *Nature Communications* **2020**, *11* (1), 1618. https://doi.org/10.1038/s41467-020-15454-y.
(26) Fontana, J.; Sparkman-Yager, D.; Zalatan, J. G.; Carothers, J. M. Challenges and Opportunities with CRISPR Activation in Bacteria for Data-Driven Metabolic Engineering. *Current Opinion in Biotechnology* **2020**, *64*, 190–198. https://doi.org/10.1016/j.copbio.2020.04.005.
(27) Call, S. N.; Andrews, L. B. CRISPR-Based Approaches for Gene Regulation in Non-Model Bacteria. *Front. Genome Ed.* **2022**, *4*. https://doi.org/10.3389/fgeed.2022.892304.
(28) Cho, S.; Shin, J.; Cho, B.-K. Applications of CRISPR/Cas System to Bacterial Metabolic Engineering. *International Journal of Molecular Sciences* **2018**, *19* (4). https://doi.org/10.3390/ijms19041089.

(29) Shi, S.; Qi, N.; Nielsen, J. Microbial Production of Chemicals Driven by CRISPR-Cas Systems. *Current Opinion in Biotechnology* **2022**, *73*, 34–42. https://doi.org/10.1016/j.copbio.2021.07.002.
(30) Fackler, N.; Heffernan, J.; Juminaga, A.; Doser, D.; Nagaraju, S.; Gonzalez-Garcia, R. A.; Simpson, S. D.; Marcellin, E.; Köpke, M. Transcriptional Control of Clostridium Autoethanogenum Using CRISPRi. *Synthetic Biology* **2021**, *6* (1), ysab008. https://doi.org/10.1093/synbio/ysab008.
(31) Luo, Y.; Ge, M.; Wang, B.; Sun, C.; Wang, J.; Dong, Y.; Xi, J. J. CRISPR/Cas9-Deaminase Enables Robust Base Editing in Rhodobacter Sphaeroides 2.4.1. *Microbial Cell Factories* **2020**, *19* (1), 93. https://doi.org/10.1186/s12934-020-01345-w.
(32) Mougiakos, I.; Orsi, E.; Ghiffary, M. R.; Post, W.; de Maria, A.; Adiego-Perez, B.; Kengen, S. W. M.; Weusthuis, R. A.; van der Oost, J. Efficient Cas9-Based Genome Editing of Rhodobacter Sphaeroides for Metabolic Engineering. *Microbial Cell Factories* **2019**, *18* (1), 204. https://doi.org/10.1186/s12934-019-1255-1.
(33) Xiong, B.; Li, Z.; Liu, L.; Zhao, D.; Zhang, X.; Bi, C. Genome Editing of Ralstonia Eutropha Using an Electroporation-Based CRISPR-Cas9 Technique. *Biotechnology for Biofuels* **2018**, *11* (1), 172. https://doi.org/10.1186/s13068-018-1170-4.
(34) Bhattarai-Kline, S.; Lear, S. K.; Fishman, C. B.; Lopez, S. C.; Lockshin, E. R.; Schubert, M. G.; Nivala, J.; Church, G. M.; Shipman, S. L. Recording Gene Expression Order in DNA by CRISPR Addition of Retron Barcodes. *Nature* **2022**, *608* (7921), 217–225. https://doi.org/10.1038/s41586-022-04994-6.
(35) Jiao, C.; Reckstadt, C.; König, F.; Homberger, C.; Yu, J.; Vogel, J.; Westermann, A. J.; Sharma, C. M.; Beisel, C. L. RNA Recording in Single Bacterial Cells Using Reprogrammed tracrRNAs. *Nature Biotechnology* **2023**, *41* (8), 1107–1116. https://doi.org/10.1038/s41587-022-01604-8.
(36) Kiga, K.; Tan, X.-E.; Ibarra-Chávez, R.; Watanabe, S.; Aiba, Y.; Sato'o, Y.; Li, F.-Y.; Sasahara, T.; Cui, B.; Kawauchi, M.; Boonsiri, T.; Thitiananpakorn, K.; Taki, Y.; Azam, A. H.; Suzuki, M.; Penadés, J. R.; Cui, L. Development of CRISPR-Cas13a-Based Antimicrobials Capable of Sequence-Specific Killing of Target Bacteria. *Nature Communications* **2020**, *11* (1), 2934. https://doi.org/10.1038/s41467-020-16731-6.
(37) Rodrigues, M.; McBride, S. W.; Hullahalli, K.; Palmer, K. L.; Duerkop, B. A. Conjugative Delivery of CRISPR-Cas9 for the Selective Depletion of Antibiotic-Resistant Enterococci. *Antimicrob. Agents Chemother.* **2019**, *63* (11), 10.1128/aac.01454-19. https://doi.org/10.1128/aac.01454-19.
(38) Schmidt, F.; Zimmermann, J.; Tanna, T.; Farouni, R.; Conway, T.; Macpherson, A. J.; Platt, R. J. Noninvasive Assessment of Gut Function Using Transcriptional Recording Sentinel Cells. *Science* **2022**, *376* (6594), eabm6038. https://doi.org/10.1126/science.abm6038.
(39) Kaminski, M. M.; Abudayyeh, O. O.; Gootenberg, J. S.; Zhang, F.; Collins, J. J. CRISPR-Based Diagnostics. *Nature Biomedical Engineering* **2021**, *5* (7), 643–656. https://doi.org/10.1038/s41551-021-00760-7.
(40) Tian, T.; Zhou, X. CRISPR-Based Biosensing Strategies: Technical Development and Application Prospects. *Annual Rev. Anal. Chem.* **2023**, *16* (1), 311–332. https://doi.org/10.1146/annurev-anchem-090822-014725.
(41) Garamella, J.; Marshall, R.; Rustad, M.; Noireaux, V. The All E. Coli TX-TL Toolbox 2.0: A Platform for Cell-Free Synthetic Biology. *ACS Synth. Biol.* **2016**, *5* (4), 344–355. https://doi.org/10.1021/acssynbio.5b00296.
(42) Garenne, D.; Thompson, S.; Brisson, A.; Khakimzhan, A.; Noireaux, V. The All-E. coliTXTL Toolbox 3.0: New Capabilities of a Cell-Free Synthetic Biology Platform. *Synthetic Biology* **2021**, *6* (1), ysab017. https://doi.org/10.1093/synbio/ysab017.

(43) Lavickova, B.; Maerkl, S. J. A Simple, Robust, and Low-Cost Method To Produce the PURE Cell-Free System. *ACS Synth. Biol.* **2019**, *8* (2), 455–462. https://doi.org/10.1021/acssynbio.8b00427.
(44) Marshall, R.; Maxwell, C. S.; Collins, S. P.; Jacobsen, T.; Luo, M. L.; Begemann, M. B.; Gray, B. N.; January, E.; Singer, A.; He, Y.; Beisel, C. L.; Noireaux, V. Rapid and Scalable Characterization of CRISPR Technologies Using an E. Coli Cell-Free Transcription-Translation System. *Molecular Cell* **2018**, *69* (1), 146-157.e3. https://doi.org/10.1016/j.molcel.2017.12.007.
(45) Tickman, B. I.; Burbano, D. A.; Chavali, V. P.; Kiattisewee, C.; Fontana, J.; Khakimzhan, A.; Noireaux, V.; Zalatan, J. G.; Carothers, J. M. Multi-Layer CRISPRa/i Circuits for Dynamic Genetic Programs in Cell-Free and Bacterial Systems. *Cell Systems* **2021**, S2405471221004191. https://doi.org/10.1016/j.cels.2021.10.008.
(46) Westbrook, A.; Tang, X.; Marshall, R.; Maxwell, C. S.; Chappell, J.; Agrawal, D. K.; Dunlop, M. J.; Noireaux, V.; Beisel, C. L.; Lucks, J.; Franco, E. Distinct Timescales of RNA Regulators Enable the Construction of a Genetic Pulse Generator. *Biotechnology and Bioengineering* **2019**, *116* (5), 1139–1151. https://doi.org/10.1002/bit.26918.
(47) Wimmer, F.; Mougiakos, I.; Englert, F.; Beisel, C. L. Rapid Cell-Free Characterization of Multi-Subunit CRISPR Effectors and Transposons. *Molecular Cell* **2022**, *82* (6), 1210-1224.e6. https://doi.org/10.1016/j.molcel.2022.01.026.
(48) Alba Burbano, D.; Cardiff, R. A. L.; Tickman, B. I.; Kiattisewee, C.; Maranas, C. J.; Zalatan, J. G.; Carothers, J. M. Engineering Activatable Promoters for Scalable and Multi-Input CRISPRa/i Circuits. *Proceedings of the National Academy of Sciences* **2023**, *120* (30), e2220358120. https://doi.org/10.1073/pnas.2220358120.
(49) Cui, Y.; Chen, X.; Wang, Z.; Lu, Y. Cell-Free PURE System: Evolution and Achievements. *BioDesign Research 2022*, 9847014. https://doi.org/10.34133/2022/9847014.
(50) Karim, A. S.; Liew, F. (Eric); Garg, S.; Vögeli, B.; Rasor, B. J.; Gonnot, A.; Pavan, M.; Juminaga, A.; Simpson, S. D.; Köpke, M.; Jewett, M. C. Modular Cell-Free Expression Plasmids to Accelerate Biological Design in Cells. *Synthetic Biology* **2020**, *5* (1), ysaa019. https://doi.org/10.1093/synbio/ysaa019.
(51) Silverman, A. D.; Karim, A. S.; Jewett, M. C. Cell-Free Gene Expression: An Expanded Repertoire of Applications. *Nature Reviews Genetics* **2020**, *21* (3), 151–170. https://doi.org/10.1038/s41576-019-0186-3.
(52) Brandt, K.; Barrangou, R. Applications of CRISPR Technologies Across the Food Supply Chain. *Annu. Rev. Food Sci. Technol.* **2019**, *10* (1), 133–150. https://doi.org/10.1146/annurev-food-032818-121204.
(53) McCarty, N. S.; Graham, A. E.; Studená, L.; Ledesma-Amaro, R. Multiplexed CRISPR Technologies for Gene Editing and Transcriptional Regulation. *Nature Communications* **2020**, *11* (1), 1281. https://doi.org/10.1038/s41467-020-15053-x.
(54) Simeonov, D. R.; Marson, A. CRISPR-Based Tools in Immunity. *Annu. Rev. Immunol.* **2019**, *37* (1), 571–597. https://doi.org/10.1146/annurev-immunol-042718-041522.
(55) Anders, C.; Niewoehner, O.; Duerst, A.; Jinek, M. Structural Basis of PAM-Dependent Target DNA Recognition by the Cas9 Endonuclease. *Nature* **2014**, *513* (7519), 569–573. https://doi.org/10.1038/nature13579.
(56) Sternberg, S. H.; Redding, S.; Jinek, M.; Greene, E. C.; Doudna, J. A. DNA Interrogation by the CRISPR RNA-Guided Endonuclease Cas9. *Nature* **2014**, *507* (7490), 62–67. https://doi.org/10.1038/nature13011.
(57) Anderson, E. M.; Haupt, A.; Schiel, J. A.; Chou, E.; Machado, H. B.; Strezoska, Ž.; Lenger, S.; McClelland, S.; Birmingham, A.; Vermeulen, A.; Smith, A. van B. Systematic Analysis of CRISPR-Cas9 Mismatch Tolerance Reveals Low Levels of

off-Target Activity. *J Biotechnol* **2015**, *211*, 56–65. https://doi.org/10.1016/j.jbiotec.2015.06.427.
(58) Chylinski, K.; Le Rhun, A.; Charpentier, E. The tracrRNA and Cas9 Families of Type II CRISPR-Cas Immunity Systems. *RNA Biology* **2013**, *10* (5), 726–737. https://doi.org/10.4161/rna.24321.
(59) Fonfara, I.; Le Rhun, A.; Chylinski, K.; Makarova, K. S.; Lécrivain, A.-L.; Bzdrenga, J.; Koonin, E. V.; Charpentier, E. Phylogeny of Cas9 Determines Functional Exchangeability of Dual-RNA and Cas9 among Orthologous Type II CRISPR-Cas Systems. *Nucleic Acids Research* **2014**, *42* (4), 2577–2590. https://doi.org/10.1093/nar/gkt1074.
(60) Chatterjee, P.; Lee, J.; Nip, L.; Koseki, S. R. T.; Tysinger, E.; Sontheimer, E. J.; Jacobson, J. M.; Jakimo, N. A Cas9 with PAM Recognition for Adenine Dinucleotides. *Nature Communications* **2020**, *11* (1), 2474. https://doi.org/10.1038/s41467-020-16117-8.
(61) Horvath, P.; Romero, D. A.; Coûté-Monvoisin, A.-C.; Richards, M.; Deveau, H.; Moineau, S.; Boyaval, P.; Fremaux, C.; Barrangou, R. Diversity, Activity, and Evolution of CRISPR Loci in *Streptococcus Thermophilus*. *J. Bacteriol.* **2008**, *190* (4), 1401–1412. https://doi.org/10.1128/jb.01415-07.
(62) Müller, M.; Lee, C. M.; Gasiunas, G.; Davis, T. H.; Cradick, T. J.; Siksnys, V.; Bao, G.; Cathomen, T.; Mussolino, C. Streptococcus Thermophilus CRISPR-Cas9 Systems Enable Specific Editing of the Human Genome. *Molecular Therapy* **2016**, *24* (3), 636–644. https://doi.org/10.1038/mt.2015.218.
(63) Mendoza, B. J.; Trinh, C. T. In Silico Processing of the Complete CRISPR-Cas Spacer Space for Identification of PAM Sequences. *Biotechnology Journal* **2018**, *13* (9), 1700595. https://doi.org/10.1002/biot.201700595.
(64) Rybnicky, G. A.; Fackler, N. A.; Karim, A. S.; Köpke, M.; Jewett, M. C. Spacer2PAM: A Computational Framework to Guide Experimental Determination of Functional CRISPR-Cas System PAM Sequences. *Nucleic Acids Research* **2022**, *50* (6), 3523–3534. https://doi.org/10.1093/nar/gkac142.
(65) Collias, D.; Beisel, C. L. CRISPR Technologies and the Search for the PAM-Free Nuclease. *Nature Communications* **2021**, *12* (1), 555. https://doi.org/10.1038/s41467-020-20633-y.
(66) Hu, J. H.; Miller, S. M.; Geurts, M. H.; Tang, W.; Chen, L.; Sun, N.; Zeina, C. M.; Gao, X.; Rees, H. A.; Lin, Z.; Liu, D. R. Evolved Cas9 Variants with Broad PAM Compatibility and High DNA Specificity. *Nature* **2018**, *556* (7699), 57–63. https://doi.org/10.1038/nature26155.
(67) Nishimasu, H.; Shi, X.; Ishiguro, S.; Gao, L.; Hirano, S.; Okazaki, S.; Noda, T.; Abudayyeh, O. O.; Gootenberg, J. S.; Mori, H.; Oura, S.; Holmes, B.; Tanaka, M.; Seki, M.; Hirano, H.; Aburatani, H.; Ishitani, R.; Ikawa, M.; Yachie, N.; Zhang, F.; Nureki, O. Engineered CRISPR-Cas9 Nuclease with Expanded Targeting Space. *Science* **2018**, *361* (6408), 1259–1262. https://doi.org/10.1126/science.aas9129.
(68) Walton, R. T.; Christie, K. A.; Whittaker, M. N.; Kleinstiver, B. P. Unconstrained Genome Targeting with Near-PAMless Engineered CRISPR-Cas9 Variants. *Science* **2020**, *368* (6488), 290–296. https://doi.org/10.1126/science.aba8853.
(69) Chatterjee, P.; Jakimo, N.; Jacobson, J. M. Minimal PAM Specificity of a Highly Similar SpCas9 Ortholog. *Science Advances* **2018**, *4* (10), eaau0766. https://doi.org/10.1126/sciadv.aau0766.
(70) Edraki, A.; Mir, A.; Ibraheim, R.; Gainetdinov, I.; Yoon, Y.; Song, C.-Q.; Cao, Y.; Gallant, J.; Xue, W.; Rivera-Pérez, J. A.; Sontheimer, E. J. A Compact, High-Accuracy Cas9 with a Dinucleotide PAM for In Vivo Genome Editing. *Molecular Cell* **2019**, *73* (4), 714-726.e4. https://doi.org/10.1016/j.molcel.2018.12.003.

(71) Ran, F. A.; Cong, L.; Yan, W. X.; Scott, D. A.; Gootenberg, J. S.; Kriz, A. J.; Zetsche, B.; Shalem, O.; Wu, X.; Makarova, K. S.; Koonin, E. V.; Sharp, P. A.; Zhang, F. In Vivo Genome Editing Using Staphylococcus Aureus Cas9. *Nature* **2015**, *520* (7546), 186–191. https://doi.org/10.1038/nature14299.
(72) Schmidheini, L.; Mathis, N.; Marquart, K. F.; Rothgangl, T.; Kissling, L.; Böck, D.; Chanez, C.; Wang, J. P.; Jinek, M.; Schwank, G. Continuous Directed Evolution of a Compact CjCas9 Variant with Broad PAM Compatibility. *Nat Chem Biol* **2023**. https://doi.org/10.1038/s41589-023-01427-x.
(73) Hu, Z.; Wang, S.; Zhang, C.; Gao, N.; Li, M.; Wang, D.; Wang, D.; Liu, D.; Liu, H.; Ong, S.-G.; Wang, H.; Wang, Y. A Compact Cas9 Ortholog from Staphylococcus Auricularis (SauriCas9) Expands the DNA Targeting Scope. *PLOS Biology* **2020**, *18* (3), e3000686. https://doi.org/10.1371/journal.pbio.3000686.
(74) Kleinstiver, B. P.; Prew, M. S.; Tsai, S. Q.; Topkar, V. V.; Nguyen, N. T.; Zheng, Z.; Gonzales, A. P. W.; Li, Z.; Peterson, R. T.; Yeh, J.-R. J.; Aryee, M. J.; Joung, J. K. Engineered CRISPR-Cas9 Nucleases with Altered PAM Specificities. *Nature* **2015**, *523* (7561), 481–485. https://doi.org/10.1038/nature14592.
(75) Legut, M.; Daniloski, Z.; Xue, X.; McKenzie, D.; Guo, X.; Wessels, H.-H.; Sanjana, N. E. High-Throughput Screens of PAM-Flexible Cas9 Variants for Gene Knockout and Transcriptional Modulation. *Cell Reports* **2020**, *30* (9), 2859-2868.e5. https://doi.org/10.1016/j.celrep.2020.02.010.
(76) Kim, N.; Kim, H. K.; Lee, S.; Seo, J. H.; Choi, J. W.; Park, J.; Min, S.; Yoon, S.; Cho, S.-R.; Kim, H. H. Prediction of the Sequence-Specific Cleavage Activity of Cas9 Variants. *Nature Biotechnology* **2020**, *38* (11), 1328–1336. https://doi.org/10.1038/s41587-020-0537-9.
(77) Ma, D.; Xu, Z.; Zhang, Z.; Chen, X.; Zeng, X.; Zhang, Y.; Deng, T.; Ren, M.; Sun, Z.; Jiang, R.; Xie, Z. Engineer Chimeric Cas9 to Expand PAM Recognition Based on Evolutionary Information. *Nature Communications* **2019**, *10* (1), 560. https://doi.org/10.1038/s41467-019-08395-8.
(78) Nishimasu, H.; Ran, F. A.; Hsu, P. D.; Konermann, S.; Shehata, S. I.; Dohmae, N.; Ishitani, R.; Zhang, F.; Nureki, O. Crystal Structure of Cas9 in Complex with Guide RNA and Target DNA. *Cell* **2014**, *156* (5), 935–949. https://doi.org/10.1016/j.cell.2014.02.001.
(79) Teng, Y.; Jiang, T.; Yan, Y. The Expanded CRISPR Toolbox for Constructing Microbial Cell Factories. *Trends in Biotechnology* **2023**. https://doi.org/10.1016/j.tibtech.2023.06.012.
(80) Kiattisewee, C.; Karanjia, A. V.; Legut, M.; Daniloski, Z.; Koplik, S. E.; Nelson, J.; Kleinstiver, B. P.; Sanjana, N. E.; Carothers, J. M.; Zalatan, J. G. Expanding the Scope of Bacterial CRISPR Activation with PAM-Flexible dCas9 Variants. *ACS Synth. Biol.* **2022**, *11* (12), 4103–4112. https://doi.org/10.1021/acssynbio.2c00405.
(81) Klanschnig, M.; Cserjan-Puschmann, M.; Striedner, G.; Grabherr, R. CRISPRactivation-SMS, a Message for PAM Sequence Independent Gene up-Regulation in Escherichia Coli. *Nucleic Acids Research* **2022**, gkac804. https://doi.org/10.1093/nar/gkac804.
(82) Jones, D. L.; Leroy, P.; Unoson, C.; Fange, D.; Ćurić, V.; Lawson, M. J.; Elf, J. Kinetics of dCas9 Target Search in Escherichia Coli. *Science* **2017**, *357* (6358), 1420–1424. https://doi.org/10.1126/science.aah7084.
(83) Casini, A.; Olivieri, M.; Petris, G.; Montagna, C.; Reginato, G.; Maule, G.; Lorenzin, F.; Prandi, D.; Romanel, A.; Demichelis, F.; Inga, A.; Cereseto, A. A Highly Specific SpCas9 Variant Is Identified by in Vivo Screening in Yeast. *Nature Biotechnology* **2018**, *36* (3), 265–271. https://doi.org/10.1038/nbt.4066.
(84) Chen, J. S.; Dagdas, Y. S.; Kleinstiver, B. P.; Welch, M. M.; Sousa, A. A.; Harrington,

L. B.; Sternberg, S. H.; Joung, J. K.; Yildiz, A.; Doudna, J. A. Enhanced Proofreading Governs CRISPR–Cas9 Targeting Accuracy. *Nature* **2017**, *550* (7676), 407–410. https://doi.org/10.1038/nature24268.

(85) Kleinstiver, B. P.; Pattanayak, V.; Prew, M. S.; Tsai, S. Q.; Nguyen, N. T.; Zheng, Z.; Joung, J. K. High-Fidelity CRISPR–Cas9 Nucleases with No Detectable Genome-Wide off-Target Effects. *Nature* **2016**, *529* (7587), 490–495. https://doi.org/10.1038/nature16526.

(86) Kulcsár, P. I.; Tálas, A.; Huszár, K.; Ligeti, Z.; Tóth, E.; Weinhardt, N.; Fodor, E.; Welker, E. Crossing Enhanced and High Fidelity SpCas9 Nucleases to Optimize Specificity and Cleavage. *Genome Biology* **2017**, *18* (1), 190. https://doi.org/10.1186/s13059-017-1318-8.

(87) Lee, J. K.; Jeong, E.; Lee, J.; Jung, M.; Shin, E.; Kim, Y.; Lee, K.; Jung, I.; Kim, D.; Kim, S.; Kim, J.-S. Directed Evolution of CRISPR-Cas9 to Increase Its Specificity. *Nature Communications* **2018**, *9* (1), 3048. https://doi.org/10.1038/s41467-018-05477-x.

(88) Slaymaker, I. M.; Gao, L.; Zetsche, B.; Scott, D. A.; Yan, W. X.; Zhang, F. Rationally Engineered Cas9 Nucleases with Improved Specificity. *Science* **2016**, *351* (6268), 84–88. https://doi.org/10.1126/science.aad5227.

(89) Walton, R. T.; Christie, K. A.; Whittaker, M. N.; Kleinstiver, B. P. Unconstrained Genome Targeting with Near-PAMless Engineered CRISPR-Cas9 Variants. *Science* **2020**, *368* (6488), 290–296. https://doi.org/10.1126/science.aba8853.

(90) Kim, D.; Bae, S.; Park, J.; Kim, E.; Kim, S.; Yu, H. R.; Hwang, J.; Kim, J.-I.; Kim, J.-S. Digenome-Seq: Genome-Wide Profiling of CRISPR-Cas9 off-Target Effects in Human Cells. *Nature Methods* **2015**, *12* (3), 237–243. https://doi.org/10.1038/nmeth.3284.

(91) Cho, S.; Choe, D.; Lee, E.; Kim, S. C.; Palsson, B.; Cho, B.-K. High-Level dCas9 Expression Induces Abnormal Cell Morphology in Escherichia Coli. *ACS Synth. Biol.* **2018**, *7* (4), 1085–1094. https://doi.org/10.1021/acssynbio.7b00462.

(92) Zhang, S.; Voigt, C. A. Engineered dCas9 with Reduced Toxicity in Bacteria: Implications for Genetic Circuit Design. *Nucleic Acids Research* **2018**, *46* (20), 11115–11125. https://doi.org/10.1093/nar/gky884.

(93) Adler, B. A.; Trinidad, M. I.; Bellieny-Rabelo, D.; Zhang, E.; Karp, H. M.; Skopintsev, P.; Thornton, B. W.; Weissman, R. F.; Yoon, P. H.; Chen, L.; Hessler, T.; Eggers, A. R.; Colognori, D.; Boger, R.; Doherty, E. E.; Tsuchida, C. A.; Tran, R. V.; Hofman, L.; Shi, H.; Wasko, K. M.; Zhou, Z.; Xia, C.; Al-Shimary, M. J.; Patel, J. R.; Thomas, V. C. J. X.; Pattali, R.; Kan, M. J.; Vardapetyan, A.; Yang, A.; Lahiri, A.; Maxwell, M. F.; Murdock, A. G.; Ramit, G. C.; Henderson, H. R.; Calvert, R. W.; Bamert, R. S.; Knott, G. J.; Lapinaite, A.; Pausch, P.; Cofsky, J. C.; Sontheimer, E. J.; Wiedenheft, B.; Fineran, P. C.; Brouns, S. J. J.; Sashital, D. G.; Thomas, B. C.; Brown, C. T.; Goltsman, D. S. A.; Barrangou, R.; Siksnys, V.; Banfield, J. F.; Savage, D. F.; Doudna, J. A. CasPEDIA Database: A Functional Classification System for Class 2 CRISPR-Cas Enzymes. *Nucleic Acids Research* **2023**, gkad890. https://doi.org/10.1093/nar/gkad890.

(94) Maeder, M. L.; Linder, S. J.; Cascio, V. M.; Fu, Y.; Ho, Q. H.; Joung, J. K. CRISPR RNA–Guided Activation of Endogenous Human Genes. *Nature Methods* **2013**, *10* (10), 977–979. https://doi.org/10.1038/nmeth.2598.

(95) Perez-Pinera, P.; Kocak, D. D.; Vockley, C. M.; Adler, A. F.; Kabadi, A. M.; Polstein, L. R.; Thakore, P. I.; Glass, K. A.; Ousterout, D. G.; Leong, K. W.; Guilak, F.; Crawford, G. E.; Reddy, T. E.; Gersbach, C. A. RNA-Guided Gene Activation by CRISPR-Cas9–Based Transcription Factors. *Nature Methods* **2013**, *10* (10), 973–976. https://doi.org/10.1038/nmeth.2600.

(96) Bikard, D.; Jiang, W.; Samai, P.; Hochschild, A.; Zhang, F.; Marraffini, L. A. Programmable Repression and Activation of Bacterial Gene Expression Using an Engineered CRISPR-Cas System. *Nucleic Acids Res* **2013**, *41* (15), 7429–7437. https://doi.org/10.1093/nar/gkt520.
(97) Dong, C.; Fontana, J.; Patel, A.; Carothers, J. M.; Zalatan, J. G. Synthetic CRISPR-Cas Gene Activators for Transcriptional Reprogramming in Bacteria. *Nat Commun* **2018**, *9* (1), 2489. https://doi.org/10.1038/s41467-018-04901-6.
(98) Kiattisewee, C.; Dong, C.; Fontana, J.; Sugianto, W.; Peralta-Yahya, P.; Carothers, J. M.; Zalatan, J. G. Portable Bacterial CRISPR Transcriptional Activation Enables Metabolic Engineering in Pseudomonas Putida. *Metabolic Engineering* **2021**, *66*, 283–295. https://doi.org/10.1016/j.ymben.2021.04.002.
(99) Liu, Y.; Wan, X.; Wang, B. Engineered CRISPRa Enables Programmable Eukaryote-like Gene Activation in Bacteria. *Nature Communications* **2019**, *10* (1), 3693. https://doi.org/10.1038/s41467-019-11479-0.
(100) Kiattisewee, C.; Dong, C.; Fontana, J.; Sugianto, W.; Peralta-Yahya, P.; Carothers, J. M.; Zalatan, J. G. Portable Bacterial CRISPR Transcriptional Activation Enables Metabolic Engineering in Pseudomonas Putida. *Metabolic Engineering* **2021**, *66*, 283–295. https://doi.org/10.1016/j.ymben.2021.04.002.
(101) Ho, H.-I.; Fang, J. R.; Cheung, J.; Wang, H. H. Programmable CRISPR-Cas Transcriptional Activation in Bacteria. *Molecular Systems Biology* **2020**, *16* (7), e9427. https://doi.org/10.15252/msb.20199427.
(102) Villegas Kcam, M. C.; Tsong, A. J.; Chappell, J. Rational Engineering of a Modular Bacterial CRISPR–Cas Activation Platform with Expanded Target Range. *Nucleic Acids Research* **2021**, *49* (8), 4793–4802. https://doi.org/10.1093/nar/gkab211.
(103) Ameruoso, A.; Villegas Kcam, M. C.; Cohen, K. P.; Chappell, J. Activating Natural Product Synthesis Using CRISPR Interference and Activation Systems in Streptomyces. *Nucleic Acids Research* **2022**, *50* (13), 7751–7760. https://doi.org/10.1093/nar/gkac556.
(104) Liu, W.; Tang, D.; Wang, H.; Lian, J.; Huang, L.; Xu, Z. Combined Genome Editing and Transcriptional Repression for Metabolic Pathway Engineering in Corynebacterium Glutamicum Using a Catalytically Active Cas12a. *Applied Microbiology and Biotechnology* **2019**, *103* (21), 8911–8922. https://doi.org/10.1007/s00253-019-10118-4.
(105) Schilling, C.; Koffas, M. A. G.; Sieber, V.; Schmid, J. Novel Prokaryotic CRISPR-Cas12a-Based Tool for Programmable Transcriptional Activation and Repression. *ACS Synth. Biol.* **2020**, *9* (12), 3353–3363. https://doi.org/10.1021/acssynbio.0c00424.
(106) Villegas Kcam, M. C.; Tsong, A. J.; Chappell, J. Uncovering the Distinct Properties of a Bacterial Type I-E CRISPR Activation System. *ACS Synth. Biol.* **2022**, *11* (2), 1000–1003. https://doi.org/10.1021/acssynbio.1c00496.
(107) Lu, Z.; Yang, S.; Yuan, X.; Shi, Y.; Ouyang, L.; Jiang, S.; Yi, L.; Zhang, G. CRISPR-Assisted Multi-Dimensional Regulation for Fine-Tuning Gene Expression in Bacillus Subtilis. *Nucleic Acids Research* **2019**, *47* (7), e40–e40. https://doi.org/10.1093/nar/gkz072.
(108) Peng, R.; Wang, Y.; Feng, W.; Yue, X.; Chen, J.; Hu, X.; Li, Z.; Sheng, D.; Zhang, Y.; Li, Y. CRISPR/dCas9-Mediated Transcriptional Improvement of the Biosynthetic Gene Cluster for the Epothilone Production in Myxococcus Xanthus. *Microbial Cell Factories* **2018**, *17* (1), 15. https://doi.org/10.1186/s12934-018-0867-1.
(109) Yu, L.; Su, W.; Fey, P. D.; Liu, F.; Du, L. Yield Improvement of the Anti-MRSA Antibiotics WAP-8294A by CRISPR/dCas9 Combined with Refactoring Self-Protection Genes in Lysobacter Enzymogenes OH11. *ACS Synth. Biol.* **2018**, *7*

(1), 258–266. https://doi.org/10.1021/acssynbio.7b00293.
(110) Chen, Y.; Niu, X.; Cheng, M.; Wang, L.; Sun, P.; Song, H.; Cao, Y. CRISPR/dCas9-RpoD-Mediated Simultaneous Transcriptional Activation and Repression in Shewanella Oneidensis MR-1. *ACS Synth. Biol.* **2022**, *11* (6), 2184–2192. https://doi.org/10.1021/acssynbio.2c00149.
(111) Sugianto, W.; Altin-Yavuzarslan, G.; Tickman, B. I.; Kiattisewee, C.; Yuan, S.-F.; Brooks, S. M.; Wong, J.; Alper, H. S.; Nelson, A.; Carothers, J. M. Gene Expression Dynamics in Input-Responsive Engineered Living Materials Programmed for Bioproduction. *Materials Today Bio* **2023**, *20*, 100677. https://doi.org/10.1016/j.mtbio.2023.100677.
(112) Liu, Y.; Pinto, F.; Wan, X.; Yang, Z.; Peng, S.; Li, M.; Cooper, J. M.; Xie, Z.; French, C. E.; Wang, B. Reprogrammed tracrRNAs Enable Repurposing of RNAs as crRNAs and Sequence-Specific RNA Biosensors. *Nature Communications* **2022**, *13* (1), 1937. https://doi.org/10.1038/s41467-022-29604-x.
(113) Wang, Y.; Liu, Y.; Zheng, P.; Sun, J.; Wang, M. Microbial Base Editing: A Powerful Emerging Technology for Microbial Genome Engineering. *Trends in Biotechnology* **2021**, *39* (2), 165–180. https://doi.org/10.1016/j.tibtech.2020.06.010.
(114) Javaid, N.; Choi, S. CRISPR/Cas System and Factors Affecting Its Precision and Efficiency. *Frontiers in Cell and Developmental Biology* **2021**, *9*.
(115) Jiang, W.; Bikard, D.; Cox, D.; Zhang, F.; Marraffini, L. A. CRISPR-Assisted Editing of Bacterial Genomes. *Nat Biotechnol* **2013**, *31* (3), 233–239. https://doi.org/10.1038/nbt.2508.
(116) Vercoe, R. B.; Chang, J. T.; Dy, R. L.; Taylor, C.; Gristwood, T.; Clulow, J. S.; Richter, C.; Przybilski, R.; Pitman, A. R.; Fineran, P. C. Cytotoxic Chromosomal Targeting by CRISPR/Cas Systems Can Reshape Bacterial Genomes and Expel or Remodel Pathogenicity Islands. *PLOS Genetics* **2013**, *9* (4), e1003454. https://doi.org/10.1371/journal.pgen.1003454.
(117) Wang, L.; Xue, W.; Yan, L.; Li, X.; Wei, J.; Chen, M.; Wu, J.; Yang, B.; Yang, L.; Chen, J. Enhanced Base Editing by Co-Expression of Free Uracil DNA Glycosylase Inhibitor. *Cell Research* **2017**, *27* (10), 1289–1292. https://doi.org/10.1038/cr.2017.111.
(118) Zhang, S.; Feng, S.; Jiang, W.; Huang, X.; Chen, J. Construction and Optimization of a Base Editor Based on the MS2 System. *Animal Models and Experimental Medicine* **2019**, *2* (3), 185–190. https://doi.org/10.1002/ame2.12080.
(119) Banno, S.; Nishida, K.; Arazoe, T.; Mitsunobu, H.; Kondo, A. Deaminase-Mediated Multiplex Genome Editing in Escherichia Coli. *Nat Microbiol* **2018**, *3* (4), 423–429. https://doi.org/10.1038/s41564-017-0102-6.
(120) Heo, Y. B.; Hwang, G.-H.; Kang, S. W.; Bae, S.; Woo, H. M. High-Fidelity Cytosine Base Editing in a GC-Rich Corynebacterium Glutamicum with Reduced DNA Off-Target Editing Effects. *Microbiol. Spectr.* **2022**, *10* (6), e03760-22.
(121) Kim, M. S.; Kim, H.-R.; Jeong, D.-E.; Choi, S.-K. Cytosine Base Editor-Mediated Multiplex Genome Editing to Accelerate Discovery of Novel Antibiotics in Bacillus Subtilis and Paenibacillus Polymyxa. *Front Microbiol* **2021**, *12*, 691839. https://doi.org/10.3389/fmicb.2021.691839.
(122) Yu, S.; Price, M. A.; Wang, Y.; Liu, Y.; Guo, Y.; Ni, X.; Rosser, S. J.; Bi, C.; Wang, M. CRISPR-dCas9 Mediated Cytosine Deaminase Base Editing in Bacillus Subtilis. *ACS Synth Biol* **2020**, *9* (7), 1781–1789. https://doi.org/10.1021/acssynbio.0c00151.
(123) Zheng, K.; Wang, Y.; Li, N.; Jiang, F.-F.; Wu, C.-X.; Liu, F.; Chen, H.-C.; Liu, Z.-F. Highly Efficient Base Editing in Bacteria Using a Cas9-Cytidine Deaminase Fusion. *Commun Biol* **2018**, *1*, 32. https://doi.org/10.1038/s42003-018-0035-5.
(124) Sun, J.; Lu, L.-B.; Liang, T.-X.; Yang, L.-R.; Wu, J.-P. CRISPR-Assisted Multiplex

Base Editing System in Pseudomonas Putida KT2440. *Front Bioeng Biotechnol* **2020**, *8*, 905. https://doi.org/10.3389/fbioe.2020.00905.
(125) Zhao, Y.; Tian, J.; Zheng, G.; Chen, J.; Sun, C.; Yang, Z.; Zimin, A. A.; Jiang, W.; Deng, Z.; Wang, Z.; Lu, Y. Multiplex Genome Editing Using a dCas9-Cytidine Deaminase Fusion in Streptomyces. *Sci. China Life Sci.* **2020**, *63* (7), 1053–1062. https://doi.org/10.1007/s11427-019-1559-y.
(126) Rodrigues, S. D.; Karimi, M.; Impens, L.; Van Lerberge, E.; Coussens, G.; Aesaert, S.; Rombaut, D.; Holtappels, D.; Ibrahim, H. M. M.; Van Montagu, M.; Wagemans, J.; Jacobs, T. B.; De Coninck, B.; Pauwels, L. Efficient CRISPR-Mediated Base Editing in Agrobacterium Spp. *Proc Natl Acad Sci U S A* **2021**, *118* (2), e2013338118. https://doi.org/10.1073/pnas.2013338118.
(127) Xin, X.; Li, J.; Zhao, D.; Li, S.; Xie, Q.; Li, Z.; Fan, F.; Bi, C.; Zhang, X. Double-Check Base Editing for Efficient A to G Conversions. *ACS Synth. Biol.* **2019**, *8* (12), 2629–2634. https://doi.org/10.1021/acssynbio.9b00284.
(128) Zhang, Y.; Zhang, H.; Wang, Z.; Wu, Z.; Wang, Y.; Tang, N.; Xu, X.; Zhao, S.; Chen, W.; Ji, Q. Programmable Adenine Deamination in Bacteria Using a Cas9–Adenine-Deaminase Fusion. *Chemical Science* **2020**, *11* (6), 1657–1664. https://doi.org/10.1039/C9SC03784E.
(129) Abdullah; Wang, P.; Han, T.; Liu, W.; Ren, W.; Wu, Y.; Xiao, Y. Adenine Base Editing System for Pseudomonas and Prediction Workflow for Protein Dysfunction via ABE. *ACS Synth. Biol.* **2022**, *11* (4), 1650–1657. https://doi.org/10.1021/acssynbio.2c00066.
(130) Dandage, R.; Després, P. C.; Yachie, N.; Landry, C. R. Beditor: A Computational Workflow for Designing Libraries of Guide RNAs for CRISPR-Mediated Base Editing. *Genetics* **2019**, *212* (2), 377–385. https://doi.org/10.1534/genetics.119.302089.
(131) Hwang, G.-H.; Park, J.; Lim, K.; Kim, S.; Yu, J.; Yu, E.; Kim, S.-T.; Eils, R.; Kim, J.-S.; Bae, S. Web-Based Design and Analysis Tools for CRISPR Base Editing. *BMC Bioinformatics* **2018**, *19* (1), 542. https://doi.org/10.1186/s12859-018-2585-4.
(132) Standage-Beier, K.; Tekel, S. J.; Brafman, D. A.; Wang, X. Prime Editing Guide RNA Design Automation Using PINE-CONE. *ACS Synth. Biol.* **2021**, *10* (2), 422–427. https://doi.org/10.1021/acssynbio.0c00445.
(133) Blin, K.; Shaw, S.; Tong, Y.; Weber, T. Designing sgRNAs for CRISPR-BEST Base Editing Applications with CRISPy-Web 2.0. *Synth Syst Biotechnol* **2020**, *5* (2), 99–102. https://doi.org/10.1016/j.synbio.2020.05.005.
(134) Shelake, R. M.; Pramanik, D.; Kim, J.-Y. In Vivo Rapid Investigation of CRISPR-Based Base Editing Components in Escherichia Coli (IRI-CCE): A Platform for Evaluating Base Editing Tools and Their Components. *Int J Mol Sci* **2022**, *23* (3), 1145. https://doi.org/10.3390/ijms23031145.
(135) Chen, Y.; Hysolli, E.; Chen, A.; Casper, S.; Liu, S.; Yang, K.; Liu, C.; Church, G. Multiplex Base Editing to Convert TAG into TAA Codons in the Human Genome. *Nat Commun* **2022**, *13* (1), 4482. https://doi.org/10.1038/s41467-022-31927-8.
(136) Kluesner, M. G.; Nedveck, D. A.; Lahr, W. S.; Garbe, J. R.; Abrahante, J. E.; Webber, B. R.; Moriarity, B. S. EditR: A Method to Quantify Base Editing from Sanger Sequencing. *CRISPR J* **2018**, *1* (3), 239–250. https://doi.org/10.1089/crispr.2018.0014.
(137) Rieffer, A. E.; Chen, Y.; Salamango, D. J.; Moraes, S. N.; Harris, R. S. APOBEC Reporter Systems for Evaluating diNucleotide Editing Levels. *The CRISPR Journal* **2023**. https://doi.org/10.1089/crispr.2023.0027.
(138) Lu, L.; Shen, X.; Sun, X.; Yan, Y.; Wang, J.; Yuan, Q. CRISPR-Based Metabolic Engineering in Non-Model Microorganisms. *Current Opinion in Biotechnology* **2022**, *75*, 102698. https://doi.org/10.1016/j.copbio.2022.102698.

(139) Naduthodi, M. I. S.; Barbosa, M. J.; van der Oost, J. Progress of CRISPR-Cas Based Genome Editing in Photosynthetic Microbes. *Biotechnology Journal* **2018**, *13* (9), 1700591. https://doi.org/10.1002/biot.201700591.
(140) Volke, D. C.; Orsi, E.; Nikel, P. I. Emergent CRISPR–Cas-Based Technologies for Engineering Non-Model Bacteria. *Current Opinion in Microbiology* **2023**, *75*, 102353. https://doi.org/10.1016/j.mib.2023.102353.
(141) Fontana, J.; Sparkman-Yager, D.; Zalatan, J. G.; Carothers, J. M. Challenges and Opportunities with CRISPR Activation in Bacteria for Data-Driven Metabolic Engineering. *Current Opinion in Biotechnology* **2020**, *64*, 190–198. https://doi.org/10.1016/j.copbio.2020.04.005.
(142) Bellato, M.; Frusteri Chiacchiera, A.; Salibi, E.; Casanova, M.; De Marchi, D.; Castagliuolo, I.; Cusella De Angelis, M. G.; Magni, P.; Pasotti, L. CRISPR Interference Modules as Low-Burden Logic Inverters in Synthetic Circuits. *Frontiers in Bioengineering and Biotechnology* **2022**, *9*.
(143) Ceroni, F.; Boo, A.; Furini, S.; Gorochowski, T. E.; Borkowski, O.; Ladak, Y. N.; Awan, A. R.; Gilbert, C.; Stan, G.-B.; Ellis, T. Burden-Driven Feedback Control of Gene Expression. *Nature Methods* **2018**, *15* (5), 387–393. https://doi.org/10.1038/nmeth.4635.
(144) Lian, J.; HamediRad, M.; Hu, S.; Zhao, H. Combinatorial Metabolic Engineering Using an Orthogonal Tri-Functional CRISPR System. *Nature Communications* **2017**, *8* (1), 1688. https://doi.org/10.1038/s41467-017-01695-x.

Chapter 2: Expanding the Scope of Bacterial CRISPR Activation with PAM-Flexible dCas9 Variants

Cholpisit Kiattisewee[+,1], Ava V. Karanjia[+,1,2], Mateusz Legut[3,4], Zharko Daniloski[#,3,4], Samantha E. Koplik[5], Joely Nelson[1], Benjamin P. Kleinstiver[6,7,8], Neville E. Sanjana[3,4], James M. Carothers[*,1,2,5], Jesse G. Zalatan[*,1,2,9]

1: Molecular Engineering & Sciences Institute and Center for Synthetic Biology
University of Washington
Seattle, WA 98195
United States

2: Department of Chemical Engineering
University of Washington
Seattle, WA 98195
United States

3: New York Genome Center
New York, NY 10013
United States

4: Department of Biology
New York University
New York, NY 10013
United States

5: Department of Bioengineering
University of Washington
Seattle, WA 98195
United States

6: Center for Genomic Medicine
Massachusetts General Hospital
Boston, MA 02114
United States

7: Department of Pathology
Massachusetts General Hospital
Boston, MA 02114
United States

8: Department of Pathology
Harvard Medical School
Boston, MA 02115
United States

9: Department of Chemistry
University of Washington
Seattle, WA 98195
United States

#: current affiliation: Beam Therapeutics,
Cambridge, MA 02142
United States

+: These authors contributed equally
*: Corresponding authors
jcaroth@uw.edu
206-221-4902

zalatan@uw.edu
206-543-1670

Published as a research article in *ACS Synthetic Biology* on November 15, 2022.
DOI: 10.1021/acssynbio.2c00405

Graphical abstract

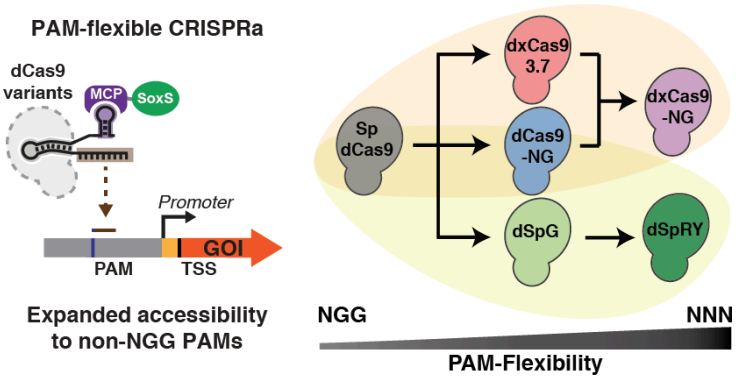

*__Note__: This chapter contains collaborative work. C. Kiattisewee and A. V. Karanjia contributed equally to this work. Both contributed equally to building and testing the CRISPRa PAM reporter libraries. C. Kiattisewee performed the CRISPRi experiments and generated the computational model to evaluate PAMs in endogenous targets. A. V. Karanjia performed CRISPRa at the endogenous promoters. The other contributors prepared figures and written text relevant to their contributions. All sections were written collaboratively with input from J. M. Carothers and J. G. Zalatan.

2.1. Abstract

CRISPR-Cas transcriptional tools have been widely applied for programmable regulation of complex biological networks. In comparison to eukaryotic systems, bacterial CRISPR activation (CRISPRa) has stringent target site requirements for effective gene activation. While genes may not always have an NGG protospacer adjacent motif (PAM) at the appropriate position, PAM-flexible dCas9 variants can expand the range of targetable sites. Here we systematically evaluate a panel of PAM-flexible dCas9 variants for their ability to activate bacterial genes. We observe that dxCas9-NG provides a high dynamic range of gene activation for sites with NGN PAMs while dSpRY permits modest activity across almost any PAM. Similar trends were observed for heterologous and endogenous promoters. For all variants tested, improved PAM-flexibility comes with the tradeoff that CRISPRi-mediated gene repression becomes less effective. Weaker CRISPR interference (CRISPRi) gene repression can be partially rescued by expressing multiple sgRNAs to target many sites in the gene of interest. Our work provides a framework to choose the most effective dCas9 variant for a given set of gene targets, which will further expand the utility of CRISPRa/i gene regulation in bacterial systems.

Keywords: Engineered Cas9, PAM, CRISPRi, CRISPRa

2.2. Introduction

CRISPR-Cas transcriptional regulation enables programmable control over gene activation and repression in bacteria.[1–3] These tools can be used to regulate endogenous gene networks both to probe biological function and to engineer new behaviors. However, effective CRISPR activation (CRISPRa) is limited by complex and stringent target site requirements.[4–7] Previous work has demonstrated a sharply periodic pattern of effective target sites occurring every 10 bp within a 60-100 bp region upstream of the TSS.[2,4,8,9] Targeting these sites with *S. pyogenes* dCas9 requires a compatible protospacer adjacent motif (PAM) at the right position, and endogenous genes that lack an appropriate PAM may be incompatible for activation via Sp-Cas9.

We previously demonstrated that one of the first expanded PAM dCas9 variants, dxCas9(3.7),[10] could activate some genes that lacked an appropriately-positioned NGG PAM.[4] Specifically, dxCas9(3.7) produced at least two-fold increases in gene expression at three out of seven endogenous promoters tested.[4] Although these results were encouraging, all seven of the candidate promoters were predicted to encode PAMs compatible with dxCas9(3.7) and all seven were expected to be activated. Since our initial work with dxCas9(3.7), several new expanded PAM dCas9 variants have been described,[11–13] raising the possibility that improved variants could further expand the number of targetable genes for CRISPRa in bacteria.

In this work, we demonstrate that PAM-flexible dCas9 variants can improve transcriptional activation at endogenous genes compared to both dCas9 and dxCas9(3.7). We observe activation at previously inaccessible gene targets, and we observe a tradeoff between fold-activation and PAM flexibility. We also demonstrate that expanded PAM dCas9 variants are partially impaired for CRISPR interference (CRISPRi) gene repression. This effect can be mitigated by targeting multiple CRISPR complexes to the desired gene. By systematically characterizing the properties of PAM-flexible dCas9 variants in bacterial CRISPRa/i, we provide a framework to choose the most effective variant for a given gene target or set of targets. This toolbox of dCas9 variants will further expand the utility of CRISPRa/i in bacterial systems for a broad range of applications including metabolic engineering and genome-wide functional screens.

2.3. Results

2.3.1. *In-silico* PAM availability analysis to predict effective CRISPRa sites

In bacterial systems, effective CRISPRa requires a target site that is precisely positioned upstream of the gene of interest.[4] Consequently, the ability to activate an arbitrary gene is dependent on an appropriately positioned PAM at the desired target site. The widely-used *S. pyogenes* Cas9 (Sp-Cas9) is generally limited to NGG PAMs, but several engineered Cas9 variants have been developed with more flexibility to accommodate various PAMs. We examined two groups of engineered Cas9 variants (Figure 1A). The first group includes xCas9-NG, a variant that exhibits high nuclease efficiency and CRISPRa/i performance at NGN PAMs in mammalian systems.[10–12] The second group includes SpG and SpRY.[12–16] The SpRY variant was engineered to be near-PAMless with some preference for NRN PAMs.

We previously identified a set of four precisely-positioned sites upstream of the TSS that are the most effective for CRISPRa with the SoxS activator (positions -70 and -80 for the template strand and -81 and -91 for non-template strand) (Figure 1B).[4] We performed an *in-silico* analysis to identify promoters with accessible PAMs at one or more of the optimal upstream positions in *Escherichia coli* and *Pseudomonas putida*. We restricted the search to promoters with high-confidence TSS positions [17] and with sigma factors previously identified to be effective for CRISPRa with the SoxS activator.[4] Together these criteria were met for 1265 out of 4042 promoters in *E. coli*. PAM compatibility for each Cas9 variant was predicted based on the reported nuclease activity with variable PAM targets (See Methods and Supplementary Methods).[11,13,18] We performed the analysis with 4 deactivated Cas9 variants (dCas9, dxCas9(3.7), dCas9-NG, and dSpRY) of different PAM-flexibility (Table S4). We expect the predictions for dCas9-NG to be representative for dxCas9-NG. Consistent with this expectation, we found that xCas9-NG and Cas9-NG exhibit comparable levels of PAM flexibility in mammalian cell assays for nuclease activity and CRISPRa (Figure S2). The number of promoters with at least one PAM at a suitable position was 47% for dCas9, and increased to almost all promoters for the engineered variants (89% and 93% for dCas9-NG and dSpRY, respectively) (Figure 1C). A similar trend was observed in *P. putida* (Figure S3). It is important to note that these predictions are based on nuclease activity in mammalian cells and may not accurately predict bacterial CRISPRa activity, since binding and cleavage determinants may differ.

2.3.2. CRISPRa on non-NGG PAM is improved with engineered dCas9 variants

To test whether PAM-flexible Cas9 variants can increase the number of available CRISPRa target sites, we constructed expression cassettes for the catalytically-inactive versions of each Cas9 variant (dCas9, dxCas9(3.7), dCas9-NG, dxCas9-NG, dSpG, and dSpRY). Our bacterial CRISPRa system uses dCas9 and a modified guide RNA (termed scaffold RNA, scRNA) with an MS2 hairpin to recruit the MCP-SoxS activator (Figure 2A).[2,4] We first determined whether each dCas9 variant was effective for CRISPRa at a canonical AGG PAM target site. We used a previously-described reporter gene (J3-BBa_J23117-mRFP) with an AGG PAM positioned at -81 relative to the TSS (Fontana et al., 2020). All tested dCas9 variants exhibited similar activation (~40-50-fold) with the canonical AGG PAM (Figure 2). We also evaluated the growth burden associated with each dCas9 variant because dCas9 expression can cause growth defects,[19,20] and PAM-flexible variants can potentially bind the genome non-specifically at many more sites than the parent dCas9,[21,22] For each dCas9 variant, we observed similar growth profiles and similar effects on expression capacity (Figure S4), suggesting that PAM flexibility does not produce additional growth burden effects.

To evaluate the effectiveness of each dCas9 variant for recognizing non-canonical PAM sites (non-NGG), we constructed libraries of reporters with varied PAM sequences. The first group of dCas9 variants (dxCas9(3.7), dCas9-NG, and dxCas9-NG) has a preference for NGN PAMs, so we screened three PAM libraries (NGH, NHG, and NHH, where H is not G). This approach follows the strategy previously used to characterize several Cas9 variants in mammalian systems.[11] Taken together, the data indicate that dxCas9-NG provided the highest fold-activation across the largest number of alternative PAM reporters (Figure 2B). dxCas9-NG was effective at all NGH reporters (23 out of 23, or 100% had >10-fold activation) and most NHG reporters (21 out of 24, or 88% had >10-fold activation), but displayed substantially diminished effectiveness at NHH reporters (19 out of 71, or 27% had >10-fold activation). dCas9-NG performed similarly to dxCas9-NG at NGH and NHH PAMs, but notably weaker at NHG PAMs (NGH: 23 out of 23, or 100% had >10-fold activation; NHH: 22 out of 72, or 31% had >10-fold activation; NHG: 13 out of 24, or 54% had >10-fold activation). dCas9 and dxCas9(3.7) led to consistently reduced fold-activation and activated fewer reporters than dxCas9-NG across all three PAM libraries. The broad effectiveness of dxCas9-NG at NGH/NHG PAMs, along with its ability to activate some NHH PAMs, is consistent with prior reports from mammalian systems.[11]

To evaluate the effectiveness of the dSpRY group of dCas9 variants (Figure 1A), we screened NRN and NYN PAM libraries (R = A or G; Y = C or T) following the previously-determined PAM preferences for dSpRY in mammalian cells.[13,16] As expected, we observed the strongest performance across the broadest range of PAM reporters with dSpRY. This variant produced >10-fold CRISPRa at all tested reporters in the NRN library and 29 out of 64 (45%) of the reporters in the NYN library. In both libraries, dSpRY consistently outperformed both dSpG and dCas9 (Figure 2C).

We proceeded to directly compare the CRISPRa efficiency of dxCas9-NG and dSpRY at specific non-NGG PAMs. We tested reporters with NGH (GGA, GGT, GGC), NAN (CAA, CAT, CAC), and NYN (ATA) PAMs (Figure 2D). We found that dxCas9-NG and dSpRY outperformed both dCas9 and dxCas9(3.7) at all of the non-NGG PAMs. dxCas9-NG exhibited the highest activity at NGH (≥40-fold activation) and moderately weaker activity at NAN and NYN (between 10-fold to 20-fold activation). Compared to dxCas9-NG, dSpRY produced similar or stronger activation at NAN and NYN PAMs (>20-fold activation). These data indicate that different PAM-flexible variants have distinct patterns of optimal PAMs. Together with the PAM library screens, these results suggest a framework for choosing an effective dCas9 variant. For a given target gene of interest, PAMs at the appropriate target site positions should be identified (-70 and -80 for the template strand and -81 and -91 for non-template strand upstream of the TSS). dCas9 should be used for NGG, either dCas9-NG, dxCas9-NG or dSpG should be used for NGH, dxCas9-NG should be used for NHG, and dSpRY should be used for NHH PAMs. When the four potential target sites include multiple alternative PAMs, they should be prioritized in the order NGG, NGH or NHG, and NHH. Following these guidelines, for subsequent experiments we prioritized dxCas9-NG for NGH/NHG PAMs and dSpRY for NHH PAMs.

2.3.3. CRISPRi efficiency is impaired with PAM-flexible dCas9 variants

CRISPRi acts by physically blocking transcription, and effective repression in bacteria can generally be obtained by targeting within the promoter or near the beginning of the gene on the non-template strand.[3,23] CRISPRi is not subject to the same stringent target site requirements as CRISPRa, and there are often many canonical NGG PAMs available in the promoter or at the beginning of the gene. However, because we desire to express a single dCas9 protein to simultaneously target multiple genes for CRISPRa or CRISPRi, it is important to evaluate the performance of expanded PAM variants for CRISPRi. Previous

work in bacterial and eukaryotic systems suggests that expanded PAM variants exhibit impaired CRISPRi function.[11,24] We proceeded to evaluate the PAM-flexible variants dxCas9(3.7), dxCas9-NG, and dSpRY for CRISPRi gene repression. We tested multiple distinct sgRNA target sites, with one site in the promoter region and two sites within the ORF, all with NGG PAMs (Figure 3A). At each of these sites, dCas9 produces ~95-fold repression, while the PAM-flexible variants exhibit varying degrees of impaired repression (Figure 3B and Figure S6). For target sites within the ORF, the PAM-flexible dCas9 variants repress gene expression by 5 to 30-fold; these effects are significant but substantially weaker than the ~95-fold repression obtained with dCas9 at these sites. For the target site at the promoter, the dxCas9(3.7) performs similarly to dCas9, while dxCas9-NG and dSpRY produce weaker repression effects (28-fold and 14-fold, respectively).

CRISPRi repression with dCas9 can be improved by targeting multiple sgRNAs to the same gene.[3] We therefore tested whether pairs of sgRNAs could be used to improve CRISPRi repression with PAM-flexible dCas9 variants. In each case, we observed improved repression (Figure 3B and 3C). Most notably, dSpRY repression can be improved from 14-fold to 26-fold. The dSpRY variants has one of the broadest targeting ranges due to its wide tolerance of PAMs for CRISPRa (Figure 2D), and the ability to improve its CRISPRi function via gRNA multiplexing suggests that dSpRY can be used for multi-gene CRISPRa/i programs with a large dynamic range of activation and repression.

2.3.4. PAM-flexible dCas9 variants improve CRISPRa at endogenous promoters

We previously demonstrated that the expanded PAM variant dxCas9(3.7) enables activation of some endogenous genes that are inaccessible to dCas9.[4] To determine if dxCas9-NG and dSpRY further increase the pool of activatable endogenous genes, we examined four endogenous promoters previously tested with dxCas9(3.7): yajGp, uxuRp, araEp, and ppiDp2. For each endogenous promoter, we tested one NGG and one non-NGG PAM at appropriate positions upstream of the TSS at -70 or -80 (template strand) or at -81 or -91 (non-template strand), following the targeting rules defined previously.[4] For two promoters previously activated by dxCas9(3.7), yajGp and uxuRp, dxCas9-NG and dSpRY produced comparable or improved activation compared to dxCas9(3.7) (Figure 4B). We also observed that two promoters that could not be activated by dxCas9(3.7) were slightly activated with dxCas9-NG and dSpRY: araEp was activated by 1.3-fold by dxCas9-NG while ppiDp2 was activated by 3.1-fold by dSpRY (Figure S7C).

We also tested nine new weakly-expressed endogenous promoters chosen from metabolic pathways related to aromatic amino acid biosynthesis (See Supplementary Methods).[25] None of these promoters have NGG PAMs at the ideal distances relative to the TSS for CRISPR activation. For each promoter, we identified two candidate non-NGG targets that we expected to be compatible with dxCas9-NG or dSpRY (see Table S3). These sites were selected with the target site position rules described above.[4] Out of nine new promoters tested, five can be activated by more than 1.5-fold. Activation of aroKp1 by dxCas9-NG and activation of aroLp by dSpRY demonstrated the largest fold-activation values (16-fold and 8-fold, respectively) (Figure 4C). We observed modest, ~2-fold activation for pheLp, secBp, and aroFp, and no activation (<1.5-fold) for aroHp1, aroHp2, talAp, and serCp (Figure S7D). For all promoters that were activated >1.5-fold, we observed distinct behaviors with different PAM-flexible variants. For aroKp1, dxCas9-NG significantly outperforms other variants at the GGT PAM. For aroLp, dSpRY outperforms other variants at the TAG PAM. These behaviors are consistent with our results from the mRFP reporter assay, which suggested the use of dxCas9-NG at NGN PAMs and dSpRY at NHH PAMs (Figure 2D). Taken together, these results suggest that the newer PAM-flexible variants dxCas9-NG and dSpRY can outperform dCas9 and dxCas9(3.7) for bacterial CRISPRa.

Out of the 13 total endogenous promoters tested, we found that five could not be activated above the 1.5-fold threshold (Figure 4B&C, S6C&D). One possible explanation for the failure of some target promoters to activate is that their basal expression levels are too high or too low. We previously observed that bacterial CRISPRa is sensitive to basal promoter strength, with no activation at the weakest promoters, effective activation at moderately weak promoters, and progressively smaller increases in gene expression as basal expression levels increased.[4] Promoters with innately high expression levels may be inaccessible to high activation (>1.5-fold) due to the metabolic burden associated with increasing protein concentration.[26,27] However, none of the five inaccessible promoters have unusually high basal expression levels (Figure 4D). Four of the promoters with <1.5 fold activation (aroHp1, aroHp2, talAp, and serCp) fall in a basal expression range that is higher than aroLp and lower than aroKp1, the two most highly activated promoters. Other factors beyond basal expression levels may be responsible for the failure of these four promoters to activate. The remaining inaccessible promoter, araEp, has the lowest basal expression level of all promoters tested and may be too weak to be activated with our current CRISPRa system.

2.4. Discussion

In this work, we have demonstrated that PAM-flexible dCas9 variants can improve bacterial CRISPRa in both synthetic and endogenous promoter contexts. Target distance from the TSS has been previously shown to be an important factor for effective bacterial CRISPRa.[4–7] PAM-flexible variants expand the scope of accessible PAM sites and therefore enable targeting at precise, optimal positions upstream of the TSS.

Although PAM-flexible dCas9 variants enable CRISPRa at a majority of previously inaccessible gene targets, not all endogenous promoters with target sites at the appropriate position were able to be activated (Figure 4). Additional native regulatory machinery at endogenous gene targets may be responsible for preventing activation in these cases. We have previously shown that transcription factor binding can interfere with bacterial CRISPRa, presumably by physically obstructing binding of the CRISPRa complex or blocking the SoxS effector protein from engaging with RNA polymerase.[4] We hypothesize that cryptic and unannotated transcription factor binding sites could be responsible for preventing activation at the endogenous genes targeted with PAM-flexible dCas9 variants in this work. Alternatively, we note that our guidelines for effective CRISPRa/i are based on experiments with fluorescent reporter genes, and while many endogenous targets appear to behave according to these rules, some gene sequences could have unexpected, context-specific effects on transcription or translation.

Improved bacterial CRISPRa with PAM-flexible variants comes with tradeoffs. We found that PAM-flexible dCas9 variants exhibited weaker CRISPRi-based gene repression compared to dCas9 (Figure 3B). One possible explanation for this behavior follows from the observation that increasing PAM promiscuity reduces affinity towards NGG PAMs.[10–13,28] This reduced PAM-binding affinity could allow RNA polymerase to more readily displace the CRISPRi complex. Alternatively, a near-PAMless dCas9 variant would be expected to interrogate almost every DNA sequence in the bacterial genome[21,22] and increase the time needed to find the correct target site. During every cell division, the CRISPRi complex is displaced from the genome,[3] and increased time will be needed to bind the target site,[29] which could allow for increased leaky expression and consequently weaker CRISPRi compared to the parent dCas9.

To implement complex, programmable genetic regulatory networks, both upregulation and downregulation controls with broad dynamic ranges are desirable.[30–32] Thus, identifying systems that improve CRISPRa while maintaining effective CRISPRi is crucial. Multiplexing the CRISPRi targets with additional sgRNAs led to significantly higher

fold-repression, although still weaker than CRISPRi with the parent dCas9 (FIgure 3C-3D). It remains to be seen whether these improvements are sufficient for genetic circuit applications. If stronger repression is needed, an alternative approach could be to distribute each engineering task to a different subpool of Cas9 proteins.[22] In this application, a PAM-flexible variant could be used for CRISPRa and an orthogonal Cas protein could be used for CRISPRi.

An additional challenge for multi-gene CRISPRa/i regulation is the possibility that a CRISPRa target site ~80-90 bases upstream of a target gene could have undesired CRISPRi effects on the gene immediately upstream. The average intergenic region upstream of an *E. coli* gene is ~140 bases,[33] so CRISPRa target sites could overlap with promoters or the 3' end of an ORF, depending on the orientation of the preceding gene, and either situation could produce CRISPRi repression.[3] The use of the PAM-flexible dCas9 variants described here has no impact on this challenge, and any DNA-targeting transcriptional activation system in bacteria is likely to face the same issue. Alternative gene regulation methods, including mRNA-targeting CRISPR translational activation systems,[34] could be useful in this scenario.

While this manuscript was under revision, another manuscript was published that reported broadly consistent findings with the dSpRY variant.[35] Our work includes additional comparisons with multiple PAM-flexible dCas9 variants and identifies situations where some of these variants (notably dxCas9-NG) are more effective than dSpRY. We also observed tradeoffs with CRISPRi efficiency that have not been previously described. Overall, the independently-obtained results support the broader idea that PAM-flexible Cas9 variants provide an effective means to overcome challenges associated with bacterial CRISPRa/i gene regulation.

These improvements to bacterial CRISPRa bring us closer to the long-standing goal of performing CRISPRa gain-of-function screens for basic discovery and engineering applications. Previously, some successes have been reported for activating natural product biosynthesis pathways [36,37] but the ability to perform genome-wide CRISPRa screens in bacteria lags far behind eukaryotic systems.[38–41] By unlocking these capabilities in bacteria, CRISPRa screens could enable rapid functional annotation of uncharacterized genes. For bioindustrial applications, we envision identifying genes that can overcome bottlenecks in routing metabolic flux or that confer robustness in harsh, non-native growth conditions. In the long term, combined CRISPRi and CRISPRa screens could provide even more information to map biological functions and deconvolute regulatory networks. In mammalian

cells, combining information from single gene CRISPRa/i screens enabled improved chemical genetic profiling to identify drug targets,[42] and dual-gene activation/repression screens have identified genetic interactions and functional relationships between genes.[43,44] Combined CRISPRa/i screens should be possible in bacteria, as CRISPRi loss-of-function screens have been broadly applied,[45] and it is straightforward to target multiple genes with multiple gRNAs for activation and repression.[2,9,46] Some of these goals are plausibly within reach in bacteria using current CRISPRa tools, and further improvements in CRISPRa systems at endogenous gene targets will enable rapid progress in basic research and bioindustrial applications.

2.5. Materials and methods

Bacterial strains and plasmid constructs

E. coli K-12 substrain MG1655 was used for all CRISPRa tests unless specified. CD38 with highly expressed mRFP was used for CRISPRi experiments (**Supplementary Table S1**). Plasmid constructs were cloned using standard molecular biology methods.[4,9] All PCR fragments were amplified with Phusion DNA Polymerase (Thermo-Fisher Scientific) for Infusion Cloning (Takara Bio). Plasmids were transformed into chemically competent NEB Turbo *E. coli* (New England Biolabs) cells, plated on LB-agar, and cultured in LB media supplied with the appropriate antibiotics used in the following concentrations: 100 μg/mL Carbenicillin, 25 μg/mL Chloramphenicol, 30 μg/mL Kanamycin. All plasmid constructs were confirmed by Sanger sequencing (GENEWIZ). Selected plasmids will be available upon request on Addgene (https://www.addgene.org/Jesse_Zalatan/).

PAM-flexible dCas9 variants were cloned from existing dCas9 and dxCas9(3.7) plasmids (pCD442 and pCD564).[4] dxCas9-NG was cloned by replacing the C-terminus of dxCas9(3.7) with dCas9-NG mutations ordered as a gBlock (IDT). dCas9-NG was cloned by fusing the N-terminus of dCas9 and C-terminus of dxCas9-NG together. dSpG and dSpRY sequences were cloned into a bacterial codon optimized vector (Addgene #101199) and then subcloned into the pCD442 vector. Complete sequences are provided in the supplementary information.

Each dCas9 variant (dCas9, dxCas9, dCas9-NG, dxCas9-NG, dSpG, and dSpRY) was expressed from the endogenous Sp.pCas9 promoter in a p15A vector (**Supplementary Table S2**). MCP-SoxS (R93A, S101A) (abbreviated MCP-SoxS) was expressed from the

BBa_J23107 promoter (http://parts.igem.org) in the same plasmid with dCas9. The single guide RNAs (sgRNA) or modified scaffold RNAs b2.1xMS2 (scRNAs) were expressed from the strong BBa_J23119 promoter, either in the same plasmid with the dCas9-carrying plasmid or in a separate ColE1 plasmid.[2,4] All 20 bp scRNA/sgRNA target sequences are provided in **Supplementary Table S3**. The mRFP reporter was expressed from the weak J3-BBa_J23117 promoter on a pSC101** plasmid (**Supplementary Table S2**). For CRISPRi experiments, a construct expressing mRFP from the strong BBa_J23119 promoter (strain CD38, **Supplementary Table S1**) was integrated into the *E. coli* genome using a previously-described lambda red system.[2,47] For endogenous promoter CRISPRa experiments, we used GFPmut2 reporters on pSC101** vectors as described previously.[25] Reporters were purchased from Horizon Discovery or constructed with the same methodology.[25]

Plate reader experiments

Single colonies from LB plates were inoculated in 400 µL of EZ-RDM (Teknova) supplemented with the appropriate antibiotics and grown in 96-deep-well plates at 37 °C with shaking overnight 900 RPM on a Heidolph titramax 1000. 150 µL of the overnight culture were transferred into flat, clear-bottomed black 96-well plates (Corning) and the OD_{600} and fluorescence were measured in a Biotek Synergy HTX plate reader. Data were analyzed using the BioTek Gen5 2.07.17 software. For mRFP1 detection, the excitation wavelength was 540 nm and emission wavelength was 600 nm. For GFPmut2 or sfGFP detections, the excitation wavelength was 485 nm and emission wavelength was 528 nm.

Flow cytometry

Single colonies from LB plates were inoculated in 400 µL EZ-RDM (Teknova) supplemented with appropriate antibiotics and grown in 96-deep-well plates at 37 °C, 900 RPM on a Heidolph titramax 1000. Cultures were grown overnight and then diluted in 1:100 in Dulbecco's phosphate-buffered saline (PBS) and analyzed on a MACSQuant VYB flow cytometer with the MACSQuantify 2.8 software (Miltenyi Biotec). To select single cells, we used a previously-described gating procedure.[2] A side scatter threshold trigger (SSC-H) was applied to select for single cells until 10000 events were collected. FlowJo 10.0.7 software was used to apply a narrow gate along the diagonal line on the SSC-H vs SSC-A plot to exclude the events where multiple cells were grouped together. Within the selected

population, events that appeared on the edges of the FSC-A vs. SSC-A plot and the fluorescence histogram were excluded.

E. coli growth profiles and expression capacity

To evaluate *E. coli* expression capacity, we incorporated an sfGFP capacity monitor expressed from a constitutive, medium-strength promoter (BBa_J23110) into the mRFP CRISPRa reporter plasmid. This method follows previously-described approaches to evaluate expression capacity.[48] For measurement of expression burden, CRISPRa plasmids with different dCas9 variants and an scRNA (J306 for CRISPRa and hAAVS1 for an off-target control) were co-transformed with the reporter plasmids (pJF143.J3 or pCK760). Single colonies were inoculated in 400 µL EZ-RDM with appropriate antibiotics and endpoint fluorescent protein levels were measured after 18 hours with a plate reader as described above.

Growth profile time courses (OD_{600} vs. time) were obtained with strains inoculated from overnight stationary cultures with a 1:100 dilution. Growth profiles were also initiated from exponentially-growing cultures by first subculturing overnight cultures 1:100 into 2 mL EZ-RDM in 14 mL culture tubes for 2 hours, then diluting all cultures back to OD_{600} = 0.1. 200 µL of subcultures were transferred into flat, clear-bottomed black 96-well plates (Corning). OD_{600} values were measured in a plate reader for 16 hours at 37 °C.

Pooled PAM library construction and screening

To generate the pooled reporter library with different PAMs at the target site -81 bp from the TSS, we used pJF143.J3 (Supplementary Table S2) as a PCR template with oCK679_NNN (5'-CTCGTCTCCTCACTTTNNNACGGAGCGTTCTGGACACAACG-3') as a forward primer and oCK680 (5'-AAGTGAGGAGACGAGCGAACGC-3') as a reverse primer. Amplified linear fragments were treated with DpnI to remove the parental vector and circularized with Infusion. oCK679_NNN oligos with NGH, NHG, NHH, NRN, and NYN were used to construct each corresponding PAM library. For each screened variant, the number of colonies picked was 2X the number of sequence variants. For example, we picked 24 colonies for NGH (12 possible sequences) and 64 colonies for NRN (32 possible sequences). Fold activation was calculated relative to a strain with pJF143.J3 and an off-target scRNA.

CRISPRa at endogenous promoters

CRISPRa at endogenous promoters was performed with a three plasmid system — dCas9 plasmid, scRNA plasmid, and reporter plasmid. The reporter plasmids were adapted from the *E. coli* promoter collection (Dharmacon), a commercially available library of promoter-GFPmut2 fusions.[25] We have previously confirmed that CRISPRa effects on these fluorescent protein reporters are also observed by RT-qPCR of the endogenous genomic transcript.[4] Four promoters tested here (yajGp, uxuRp, araEp, and ppiDp2) were evaluated previously with dxCas9(3.7).[4] These promoters were chosen based on the criteria: 1) genes should not be highly expressed, and 2) genes should be regulated by the sigma70 family.[4] A second set of endogenous promoters (aroKp1, aroLp, pheLp, secBp, aroFp, aroHp1, aroHp2, talAp, and serCp) were selected from genes involved in aromatic amino acid biosynthesis pathways that meet the same criteria described above. scRNAs for each promoter were designed to target the optimal positions (-70 and -80 for the template strand and -81 and -91 for non-template strand relative to the TSS). One scRNA from each strand was chosen, based on which PAM was predicted to be accessible to the highest number of dCas9 variants. Accessibility was assessed based on the moderate performance threshold cutoff (see Supplemental Table S4 and Supplementary Methods).

Bioinformatic analysis of targetable genes

Previously reported data for the activity of PAM-flexible dCas9 variants were used to predict the targetable genes for each dCas9 variant. To identify the compatible PAMs for each engineered dCas9 variant, we used data from Cas9 nuclease assays for each variant [11,13,18]. Predicted compatible PAMs for each variant are provided in **Supplementary Table S4** (see Supplementary Methods for further details). We then examined *E. coli* and *P. putida* genome sequences for PAM availability. For *E. coli*, 1265 omoters with strong confidence in TSS were retrieved from RegulonDB.[17] For *P. putida*, 1104 experimentally-confirmed primary transcriptional units were used for the analysis.[49] The PAMs at optimal target site positions were retrieved: -70 and -80 for the template strand and -81 and -91 for non-template strands relative to the TSS. The promoters with at least one compatible PAM out of four target sites were considered targetable. Further information can be found in **Figure S3**.

Data analysis

Flow cytometry analysis was conducted on FlowJo 10.0.7 software or Python FlowCytometryTools on Jupyter Notebooks and then further processed with Microsoft Excel and Graphpad Prism. Data represents the average and standard deviation of at least three

biologically-independent replicates, unless specified. Fold activation and fold repression were calculated by comparing sample fluorescence with a strain expressing off-target scRNA/sgRNA.

Disclosure and competing interests statement

B.P.K. is an inventor on patents and/or patent applications filed by Mass General Brigham that describe genome engineering technologies, including for the development of SpRY. B.P.K. is a consultant for EcoR1 capital and ElevateBio, and is an advisor to Acrigen Biosciences, Life Edit Therapeutics, and Prime Medicine. N.E.S. is an advisor to Vertex and Qiagen. J.M.C. and J.G.Z. are advisors to Wayfinder Biosciences.

Author contributions

C.K., A.V.K., J.M.C., and J.G.Z. developed the initial concept; B.P.K. and N.E.S. provided additional insight to the project; C.K. and J.N. performed bioinformatic analysis; C.K., A.V.K., and S.K. performed experiments in bacteria and analyzed the results; M.L. and Z.D. performed experiments in mammalian cells; C.K. and M.L. analyzed the results from mammalian cells; C.K., A.V.K., J.M.C., and J.G.Z. wrote the manuscript with input from all authors.

Data availability

Screen data generated during this study have been deposited to GEO with an accession number GSE217559. Screen data generated during this study will be deposited to GEO.

Acknowledgements

We thank Benjamin I. Tickman, Ian D. Faulkner, Diego Alba Burbano, Ryan Cardiff, and members of Carothers and Zalatan laboratories for thorough discussion during the experimental planning and data collection/analysis strategy. We also thank Madelynn N. Whittaker for cloning the original bacterial codon optimized dSpG and dSpRY constructs. This work was supported by NSF Award 1817623 (J.M.C, J.G.Z.), DOE Award DE-EE0008927 (J.M.C, J.G.Z.), and NIH/NHGRI DP2HG010099 (N.E.S.). B.P.K. acknowledges funding from an MGH ECOR Howard M. Goodman Award. This material is based upon work supported by the National Science Foundation Graduate Research Fellowship Program under Grant No. DGE-2140004 (A.V.K.). Any opinions, findings, and conclusions or recommendations expressed in this material are those of the author(s) and do not necessarily reflect the views of the National Science Foundation.

2.6. References

(1) Bikard, D.; Jiang, W.; Samai, P.; Hochschild, A.; Zhang, F.; Marraffini, L. A. Programmable Repression and Activation of Bacterial Gene Expression Using an Engineered CRISPR-Cas System. *Nucleic Acids Res* **2013**, *41* (15), 7429–7437. https://doi.org/10.1093/nar/gkt520.

(2) Dong, C.; Fontana, J.; Patel, A.; Carothers, J. M.; Zalatan, J. G. Synthetic CRISPR-Cas Gene Activators for Transcriptional Reprogramming in Bacteria. *Nat Commun* **2018**, *9* (1), 2489. https://doi.org/10.1038/s41467-018-04901-6.

(3) Qi, L. S.; Larson, M. H.; Gilbert, L. A.; Doudna, J. A.; Weissman, J. S.; Arkin, A. P.; Lim, W. A. Repurposing CRISPR as an RNA-Guided Platform for Sequence-Specific Control of Gene Expression. *Cell* **2013**, *152* (5), 1173–1183. https://doi.org/10.1016/j.cell.2013.02.022.

(4) Fontana, J.; Dong, C.; Kiattisewee, C.; Chavali, V. P.; Tickman, B. I.; Carothers, J. M.; Zalatan, J. G. Effective CRISPRa-Mediated Control of Gene Expression in Bacteria Must Overcome Strict Target Site Requirements. *Nat. Commun.* **2020**, *11* (1), 1618. https://doi.org/10.1038/s41467-020-15454-y.

(5) Ho, H.-I.; Fang, J. R.; Cheung, J.; Wang, H. H. Programmable CRISPR-Cas Transcriptional Activation in Bacteria. *Mol. Syst. Biol.* **2020**, *16* (7), e9427. https://doi.org/10.15252/msb.20199427.

(6) Liu, Y.; Wan, X.; Wang, B. Engineered CRISPRa Enables Programmable Eukaryote-like Gene Activation in Bacteria. *Nat. Commun.* **2019**, *10* (1), 3693. https://doi.org/10.1038/s41467-019-11479-0.

(7) Villegas Kcam, M. C.; Tsong, A. J.; Chappell, J. Rational Engineering of a Modular Bacterial CRISPR–Cas Activation Platform with Expanded Target Range. *Nucleic Acids Res.* **2021**, *49* (8), 4793–4802. https://doi.org/10.1093/nar/gkab211.

(8) Fontana, J.; Sparkman-Yager, D.; Zalatan, J. G.; Carothers, J. M. Challenges and Opportunities with CRISPR Activation in Bacteria for Data-Driven Metabolic Engineering. *Curr. Opin. Biotechnol.* **2020**, *64*, 190–198. https://doi.org/10.1016/j.copbio.2020.04.005.

(9) Kiattisewee, C.; Dong, C.; Fontana, J.; Sugianto, W.; Peralta-Yahya, P.; Carothers, J. M.; Zalatan, J. G. Portable Bacterial CRISPR Transcriptional Activation Enables Metabolic Engineering in Pseudomonas Putida. *Metab. Eng.* **2021**, *66*, 283–295. https://doi.org/10.1016/j.ymben.2021.04.002.

(10) Hu, J. H.; Miller, S. M.; Geurts, M. H.; Tang, W.; Chen, L.; Sun, N.; Zeina, C. M.; Gao, X.; Rees, H. A.; Lin, Z.; Liu, D. R. Evolved Cas9 Variants with Broad PAM Compatibility and High DNA Specificity. *Nature* **2018**, *556* (7699), 57–63. https://doi.org/10.1038/nature26155.

(11) Legut, M.; Daniloski, Z.; Xue, X.; McKenzie, D.; Guo, X.; Wessels, H.-H.; Sanjana, N. E. High-Throughput Screens of PAM-Flexible Cas9 Variants for Gene Knockout and Transcriptional Modulation. *Cell Rep.* **2020**, *30* (9), 2859-2868.e5. https://doi.org/10.1016/j.celrep.2020.02.010.

(12) Nishimasu, H.; Shi, X.; Ishiguro, S.; Gao, L.; Hirano, S.; Okazaki, S.; Noda, T.; Abudayyeh, O. O.; Gootenberg, J. S.; Mori, H.; Oura, S.; Holmes, B.; Tanaka, M.; Seki, M.; Hirano, H.; Aburatani, H.; Ishitani, R.; Ikawa, M.; Yachie, N.; Zhang, F.; Nureki, O. Engineered CRISPR-Cas9 Nuclease with Expanded Targeting Space. *Science* **2018**, *361* (6408), 1259–1262. https://doi.org/10.1126/science.aas9129.

(13) Walton, R. T.; Christie, K. A.; Whittaker, M. N.; Kleinstiver, B. P. Unconstrained Genome Targeting with Near-PAMless Engineered CRISPR-Cas9 Variants. *Science* **2020**, eaba8853. https://doi.org/10.1126/science.aba8853.

(14) Kleinstiver, B. P.; Pattanayak, V.; Prew, M. S.; Tsai, S. Q.; Nguyen, N. T.; Zheng, Z.;

Joung, J. K. High-Fidelity CRISPR–Cas9 Nucleases with No Detectable Genome-Wide off-Target Effects. *Nature* **2016**, *529* (7587), 490–495. https://doi.org/10.1038/nature16526.
(15) Kleinstiver, B. P.; Prew, M. S.; Tsai, S. Q.; Topkar, V. V.; Nguyen, N. T.; Zheng, Z.; Gonzales, A. P. W.; Li, Z.; Peterson, R. T.; Yeh, J.-R. J.; Aryee, M. J.; Joung, J. K. Engineered CRISPR-Cas9 Nucleases with Altered PAM Specificities. *Nature* **2015**, *523* (7561), 481–485. https://doi.org/10.1038/nature14592.
(16) Walton, R. T.; Hsu, J. Y.; Joung, J. K.; Kleinstiver, B. P. Scalable Characterization of the PAM Requirements of CRISPR–Cas Enzymes Using HT-PAMDA. *Nat. Protoc.* **2021**, *16* (3), 1511–1547. https://doi.org/10.1038/s41596-020-00465-2.
(17) Santos-Zavaleta, A.; Salgado, H.; Gama-Castro, S.; Sánchez-Pérez, M.; Gómez-Romero, L.; Ledezma-Tejeida, D.; García-Sotelo, J. S.; Alquicira-Hernández, K.; Muñiz-Rascado, L. J.; Peña-Loredo, P.; Ishida-Gutiérrez, C.; Velázquez-Ramírez, D. A.; Del Moral-Chávez, V.; Bonavides-Martínez, C.; Méndez-Cruz, C.-F.; Galagan, J.; Collado-Vides, J. RegulonDB v 10.5: Tackling Challenges to Unify Classic and High Throughput Knowledge of Gene Regulation in E. Coli K-12. *Nucleic Acids Res.* **2019**, *47* (D1), D212–D220. https://doi.org/10.1093/nar/gky1077.
(18) Kim, N.; Kim, H. K.; Lee, S.; Seo, J. H.; Choi, J. W.; Park, J.; Min, S.; Yoon, S.; Cho, S.-R.; Kim, H. H. Prediction of the Sequence-Specific Cleavage Activity of Cas9 Variants. *Nat. Biotechnol.* **2020**. https://doi.org/10.1038/s41587-020-0537-9.
(19) Cho, S.; Choe, D.; Lee, E.; Kim, S. C.; Palsson, B.; Cho, B.-K. High-Level DCas9 Expression Induces Abnormal Cell Morphology in Escherichia Coli. *ACS Synth. Biol.* **2018**, *7* (4), 1085–1094. https://doi.org/10.1021/acssynbio.7b00462.
(20) Zhang, S.; Voigt, C. A. Engineered DCas9 with Reduced Toxicity in Bacteria: Implications for Genetic Circuit Design. *Nucleic Acids Res.* **2018**, *46* (20), 11115–11125. https://doi.org/10.1093/nar/gky884.
(21) Anders, C.; Niewoehner, O.; Duerst, A.; Jinek, M. Structural Basis of PAM-Dependent Target DNA Recognition by the Cas9 Endonuclease. *Nature* **2014**, *513* (7519), 569–573. https://doi.org/10.1038/nature13579.
(22) Collias, D.; Beisel, C. L. CRISPR Technologies and the Search for the PAM-Free Nuclease. *Nat. Commun.* **2021**, *12* (1), 555. https://doi.org/10.1038/s41467-020-20633-y.
(23) Peters, J. M.; Colavin, A.; Shi, H.; Czarny, T. L.; Larson, M. H.; Wong, S.; Hawkins, J. S.; Lu, C. H. S.; Koo, B.-M.; Marta, E.; Shiver, A. L.; Whitehead, E. H.; Weissman, J. S.; Brown, E. D.; Qi, L. S.; Huang, K. C.; Gross, C. A. A Comprehensive, CRISPR-Based Functional Analysis of Essential Genes in Bacteria. *Cell* **2016**, *165* (6), 1493–1506. https://doi.org/10.1016/j.cell.2016.05.003.
(24) Wang, J.; Teng, Y.; Zhang, R.; Wu, Y.; Lou, L.; Zou, Y.; Li, M.; Xie, Z.-R.; Yan, Y. Engineering a PAM-Flexible SpdCas9 Variant as a Universal Gene Repressor. *Nat. Commun.* **2021**, *12* (1), 6916. https://doi.org/10.1038/s41467-021-27290-9.
(25) Zaslaver, A.; Bren, A.; Ronen, M.; Itzkovitz, S.; Kikoin, I.; Shavit, S.; Liebermeister, W.; Surette, M. G.; Alon, U. A Comprehensive Library of Fluorescent Transcriptional Reporters for Escherichia Coli. *Nat. Methods* **2006**, *3* (8), 623–628. https://doi.org/10.1038/nmeth895.
(26) Gyorgy, A.; Jiménez, J. I.; Yazbek, J.; Huang, H.-H.; Chung, H.; Weiss, R.; Del Vecchio, D. Isocost Lines Describe the Cellular Economy of Genetic Circuits. *Biophys. J.* **2015**, *109* (3), 639–646. https://doi.org/10.1016/j.bpj.2015.06.034.
(27) Wu, G.; Yan, Q.; Jones, J. A.; Tang, Y. J.; Fong, S. S.; Koffas, M. A. G. Metabolic Burden: Cornerstones in Synthetic Biology and Metabolic Engineering Applications. *Trends Biotechnol.* **2016**, *34* (8), 652–664. https://doi.org/10.1016/j.tibtech.2016.02.010.

(28) Corsi, G. I.; Qu, K.; Alkan, F.; Pan, X.; Luo, Y.; Gorodkin, J. CRISPR/Cas9 GRNA Activity Depends on Free Energy Changes and on the Target PAM Context. *Nat. Commun.* **2022**, *13* (1), 3006. https://doi.org/10.1038/s41467-022-30515-0.
(29) Jones, D. L.; Leroy, P.; Unoson, C.; Fange, D.; Ćurić, V.; Lawson, M. J.; Elf, J. Kinetics of DCas9 Target Search in *Escherichia Coli*. *Science*, 2017, *357*, 1420–1424.
(30) Alon, U. Network Motifs: Theory and Experimental Approaches. *Nat. Rev. Genet.* **2007**, *8* (6), 450–461. https://doi.org/10.1038/nrg2102.
(31) Brophy, J. A. N.; Voigt, C. A. Principles of Genetic Circuit Design. *Nat. Methods* **2014**, *11* (5), 508–520. https://doi.org/10.1038/nmeth.2926.
(32) Tickman, B. I.; Burbano, D. A.; Chavali, V. P.; Kiattisewee, C.; Fontana, J.; Khakimzhan, A.; Noireaux, V.; Zalatan, J. G.; Carothers, J. M. Multi-Layer CRISPRa/i Circuits for Dynamic Genetic Programs in Cell-Free and Bacterial Systems. *Cell Syst.* **2021**, S2405471221004191. https://doi.org/10.1016/j.cels.2021.10.008.
(33) Fontana, J.; Voje, W. E.; Zalatan, J. G.; Carothers, J. M. Prospects for Engineering Dynamic CRISPR-Cas Transcriptional Circuits to Improve Bioproduction. *J Ind Microbiol Biotechnol* **2018**. https://doi.org/10.1007/s10295-018-2039-z.
(34) Otoupal, P. B.; Cress, B. F.; Doudna, J. A.; Schoeniger, J. S. CRISPR-RNAa: Targeted Activation of Translation Using DCas13 Fusions to Translation Initiation Factors. *Nucleic Acids Res.* **2022**, *50* (15), 8986–8998. https://doi.org/10.1093/nar/gkac680.
(35) Klanschnig, M.; Cserjan-Puschmann, M.; Striedner, G.; Grabherr, R. CRISPRactivation-SMS, a Message for PAM Sequence Independent Gene up-Regulation in Escherichia Coli. *Nucleic Acids Res.* **2022**, gkac804. https://doi.org/10.1093/nar/gkac804.
(36) Ameruoso, A.; Villegas Kcam, M. C.; Cohen, K. P.; Chappell, J. Activating Natural Product Synthesis Using CRISPR Interference and Activation Systems in Streptomyces. *Nucleic Acids Research*, 2022.
(37) Ke, J.; Robinson, D.; Wu, Z.-Y.; Kuftin, A.; Louie, K.; Kosina, S.; Northen, T.; Cheng, J.-F.; Yoshikuni, Y. CRAGE-CRISPR Facilitates Rapid Activation of Secondary Metabolite Biosynthetic Gene Clusters in Bacteria. *Cell Chem. Biol.* **2022**, *29* (4), 696-710.e4. https://doi.org/10.1016/j.chembiol.2021.08.009.
(38) Joung, J.; Engreitz, J. M.; Konermann, S.; Abudayyeh, O. O.; Verdine, V. K.; Aguet, F.; Gootenberg, J. S.; Sanjana, N. E.; Wright, J. B.; Fulco, C. P.; Tseng, Y.-Y.; Yoon, C. H.; Boehm, J. S.; Lander, E. S.; Zhang, F. Genome-Scale Activation Screen Identifies a LncRNA Locus Regulating a Gene Neighbourhood. *Nature* **2017**, *548* (7667), 343–346. https://doi.org/10.1038/nature23451.
(39) Kampmann, M. CRISPRi and CRISPRa Screens in Mammalian Cells for Precision Biology and Medicine. *ACS Chem. Biol.* **2018**, *13* (2), 406–416. https://doi.org/10.1021/acschembio.7b00657.
(40) Sanson, K. R.; Hanna, R. E.; Hegde, M.; Donovan, K. F.; Strand, C.; Sullender, M. E.; Vaimberg, E. W.; Goodale, A.; Root, D. E.; Piccioni, F.; Doench, J. G. Optimized Libraries for CRISPR-Cas9 Genetic Screens with Multiple Modalities. *Nat. Commun.* **2018**, *9* (1), 5416. https://doi.org/10.1038/s41467-018-07901-8.
(41) Schmidt, R.; Steinhart, Z.; Layeghi, M.; Freimer, J. W.; Bueno, R.; Nguyen, V. Q.; Blaeschke, F.; Ye, C. J.; Marson, A. CRISPR Activation and Interference Screens Decode Stimulation Responses in Primary Human T Cells. *Science*, 2022, *375*, eabj4008.
(42) Jost, M.; Chen, Y.; Gilbert, L. A.; Horlbeck, M. A.; Krenning, L.; Menchon, G.; Rai, A.; Cho, M. Y.; Stern, J. J.; Prota, A. E.; Kampmann, M.; Akhmanova, A.; Steinmetz, M. O.; Tanenbaum, M. E.; Weissman, J. S. Combined CRISPRi/a-Based Chemical Genetic Screens Reveal That Rigosertib Is a Microtubule-Destabilizing Agent. *Mol. Cell* **2017**, *68* (1), 210-223.e6. https://doi.org/10.1016/j.molcel.2017.09.012.

(43) Boettcher, M.; Tian, R.; Blau, J. A.; Markegard, E.; Wagner, R. T.; Wu, D.; Mo, X.; Biton, A.; Zaitlen, N.; Fu, H.; McCormick, F.; Kampmann, M.; McManus, M. T. Dual Gene Activation and Knockout Screen Reveals Directional Dependencies in Genetic Networks. *Nat. Biotechnol.* **2018**, *36* (2), 170–178. https://doi.org/10.1038/nbt.4062.
(44) Najm, F. J.; Strand, C.; Donovan, K. F.; Hegde, M.; Sanson, K. R.; Vaimberg, E. W.; Sullender, M. E.; Hartenian, E.; Kalani, Z.; Fusi, N.; Listgarten, J.; Younger, S. T.; Bernstein, B. E.; Root, D. E.; Doench, J. G. Orthologous CRISPR–Cas9 Enzymes for Combinatorial Genetic Screens. *Nat. Biotechnol.* **2018**, *36* (2), 179–189. https://doi.org/10.1038/nbt.4048.
(45) Todor, H.; Silvis, M. R.; Osadnik, H.; Gross, C. A. Bacterial CRISPR Screens for Gene Function. *Host-Microbe Interact. Bact. Viruses* **2021**, *59*, 102–109. https://doi.org/10.1016/j.mib.2020.11.005.
(46) Wu, Y.; Liu, Y.; Lv, X.; Li, J.; Du, G.; Liu, L. CAMERS-B: CRISPR/Cpf1 Assisted Multiple-Genes Editing and Regulation System for Bacillus Subtilis. *Biotechnol Bioeng* **2020**, *117* (6), 1817–1825. https://doi.org/10.1002/bit.27322.
(47) Fontana, J.; Dong, C.; Ham, J. Y.; Zalatan, J. G.; Carothers, J. M. Regulated Expression of SgRNAs Tunes CRISPRi in E. Coli. *Biotechnol J* **2018**, *13* (9), e1800069. https://doi.org/10.1002/biot.201800069.
(48) Ceroni, F.; Algar, R.; Stan, G.-B.; Ellis, T. Quantifying Cellular Capacity Identifies Gene Expression Designs with Reduced Burden. *Nat. Methods* **2015**, *12* (5), 415–418. https://doi.org/10.1038/nmeth.3339.
(49) D'Arrigo, I.; Bojanovič, K.; Yang, X.; Holm Rau, M.; Long, K. S. Genome-Wide Mapping of Transcription Start Sites Yields Novel Insights into the Primary Transcriptome of Pseudomonas Putida. *Environ. Microbiol.* **2016**, *18* (10), 3466–3481. https://doi.org/10.1111/1462-2920.13326.

2.7. Figures

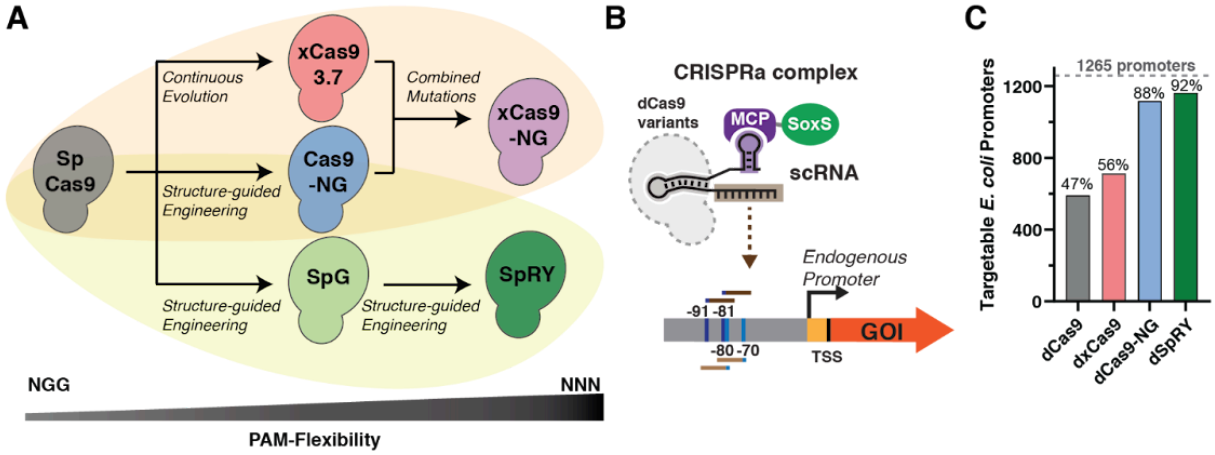

Figure 1. Engineered PAM-flexible Cas9 variants and PAM availability analysis

(A) PAM-flexible S. pyogenes Cas9 (Sp-Cas9) have been engineered using various rational design, screening, and directed evolution methodologies (e.g. phage-assisted continuous evolution (PACE), structure-guided engineering monitored via HT-PAMDA).[10–16] (B) The CRISPRa complex consists of dCas9, an scRNA, and the MCP-SoxS activator.[2] Previous work suggests that four precisely-positioned sites upstream of the TSS are most effective for CRISPRa (-70 and -80 for the template strand and -81 and -91 for non-template strand relative to the TSS).[4] (C) 1265 *E. coli* endogenous promoters were analyzed for target site availability with different PAM-flexible dCas9 variants. Promoters were identified as targetable if they have at least one effective target site with a compatible PAM. For each variant, PAM preferences were obtained from previously-reported nuclease screening experiments (see Methods; PAMs with at least 20% of Sp-Cas9 activity at NGG PAMs were considered compatible).

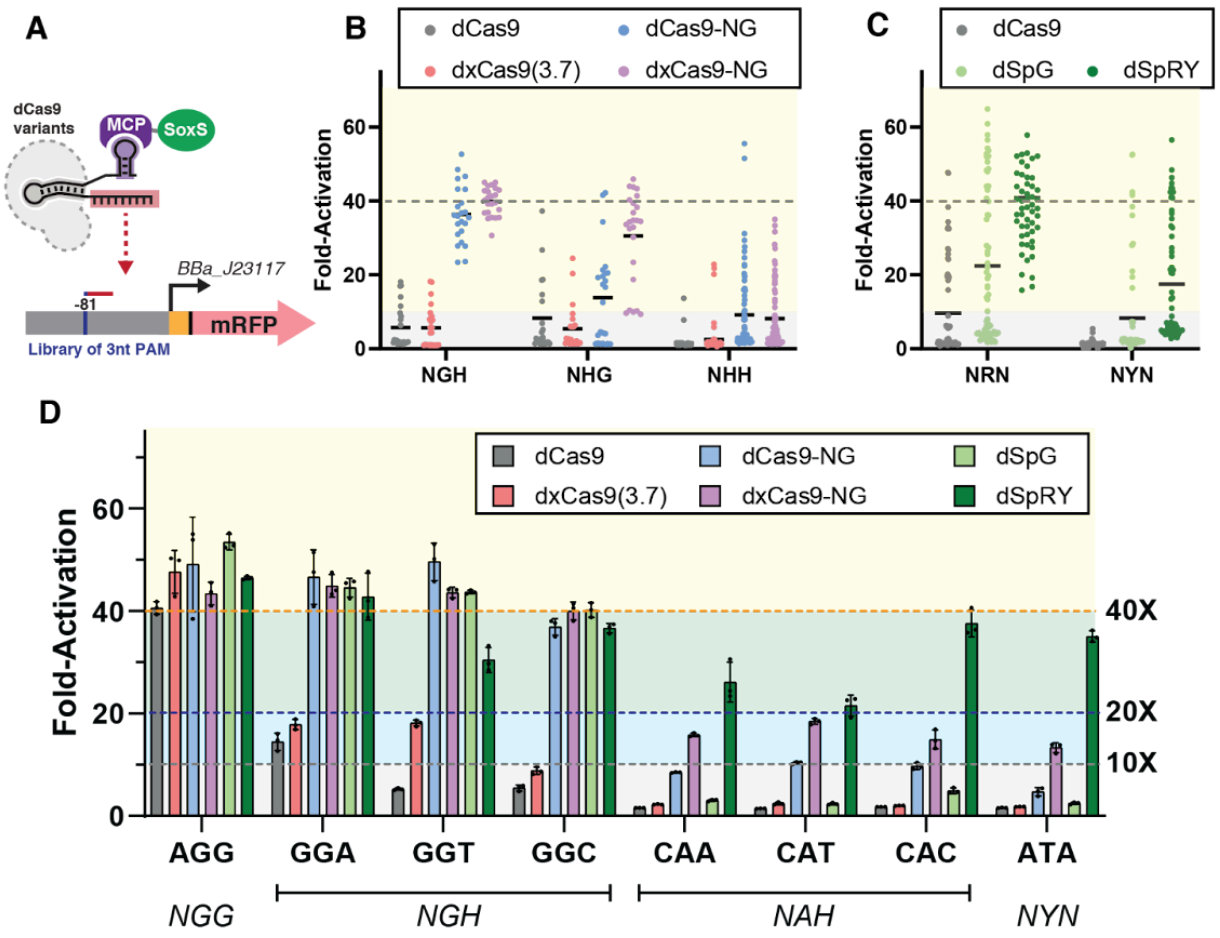

Figure 2. CRISPRa with PAM-flexible dCas9 variants

(A) CRISPRa for PAM-flexible dCas9 variants was tested on an mRFP reporter gene with libraries of alternative 3 nucleotide PAMs at the -81 target site. (B) Reporter gene expression with the dxCas9-NG group (Figure 1A) at NGH, NHG, and NHH PAM libraries. dxCas9-NG outperforms other variants in every PAM library. (C) Reporter gene expression with the dSpRY group (Figure 1A) at NRN and NYN PAM libraries. dSpRY exhibited the highest CRISPRa efficiency. (D) Direct comparisons of reporter gene expression with dCas9, dxCas9(3.7), dCas9-NG, dxCas9-NG, dSpG, and dSpRY at a representative set of PAMs. dCas9-NG, dxCas9-NG, and dSpRY performed best at NGN PAMs while dSpRY outperformed other variants at NAN and NYN PAMs. An scRNA targeting the J306 sequence was used for all library screens and individual PAM assays. To calculate fold-activation, we used an off-target scRNA (hAAVS1) with an AGG PAM reporter to define the basal expression level. Basal reporter expression levels vary <1.5-fold with different dCas9 variants or PAMs (Figure S5). Values in panel D represent the mean ± standard deviation calculated from n = 3.

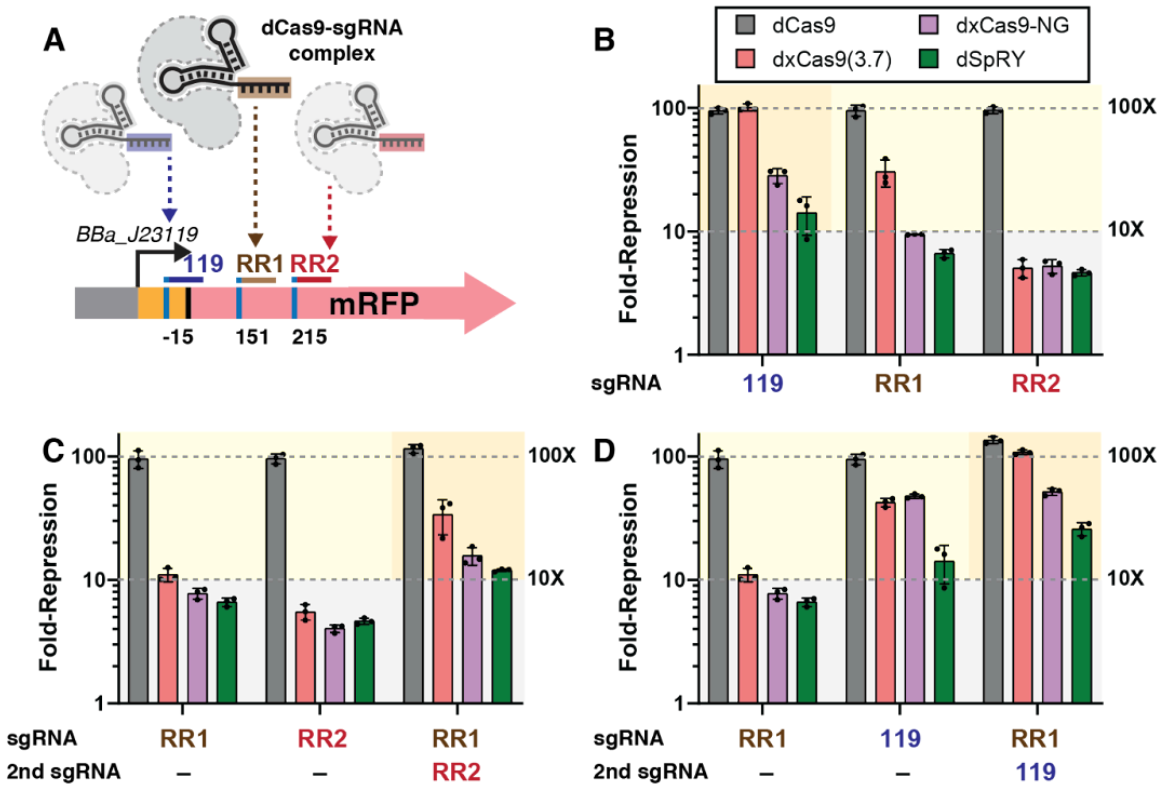

Figure 3. CRISPRi with PAM-flexible dCas9 variants

(A) CRISPRi for PAM-flexible dCas9 variants was tested on an mRFP reporter gene with sgRNAs targeting the promoter (119) or coding sequence (RR1 and RR2), where each target site encodes an NGG PAM. (B) Fold-repression of the mRFP reporter gene with a single expressed sgRNA. (C & D) Comparison of fold-repression with one or two sgRNAs expressed. Fold-repression consistently increases when two sgRNAs are expressed. See Figure S6 for a comparison of all dCas9 variants, including dCas9-NG and dSpG, with single and multiple sgRNAs. Values in panel B, C, and D represent the mean ± standard deviation calculated from n = 3.

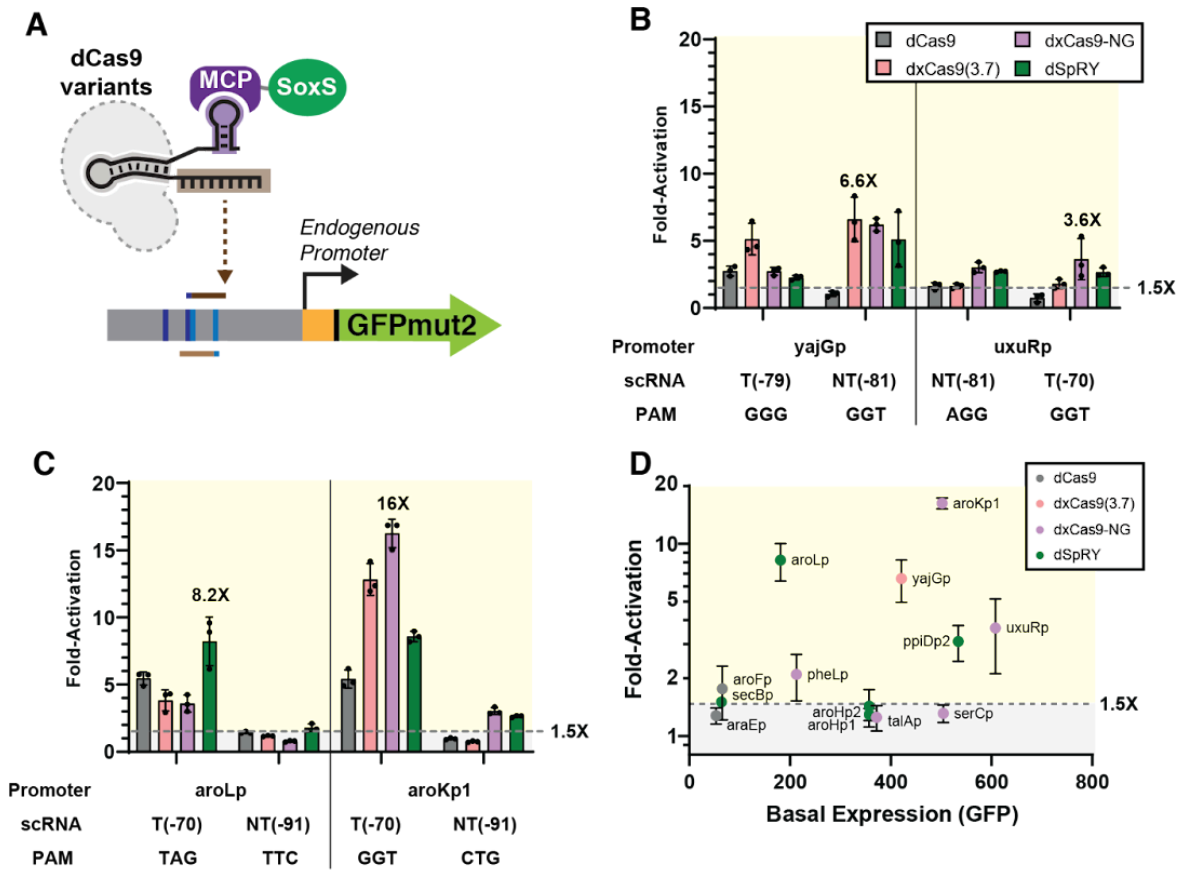

Figure 4. CRISPRa at endogenous promoters is enhanced with PAM-flexible dCas9 variants

(A) CRISPRa at endogenous promoters of *E. coli* was tested using two of the four optimal scRNA positions for each promoter (see Supplemental Methods). (B) CRISPRa at endogenous promoters previously tested with dxCas9(3.7) (yajGp and uxuRp) using NGG or non-NGG PAMs. See Figure S7C for araEp and ppiDp2 promoters. (C) CRISPRa at endogenous promoters involved in aromatic amino acid biosynthesis using non-NGG PAMs. See Figure S7D for additional promoters (D) Plot of fold-activation versus basal expression level for all endogenous promoters tested in (B) & (C). See Table S5 for additional details. Data were collected by flow cytometry and fold-activation was calculated relative to a strain expressing the corresponding dCas9 variant and an off-target hAAVS1 scRNA. Values in panel B, C, and D represent the mean ± standard deviation calculated from n = 3.

2.8. Supplementary Information

Supplementary Figures

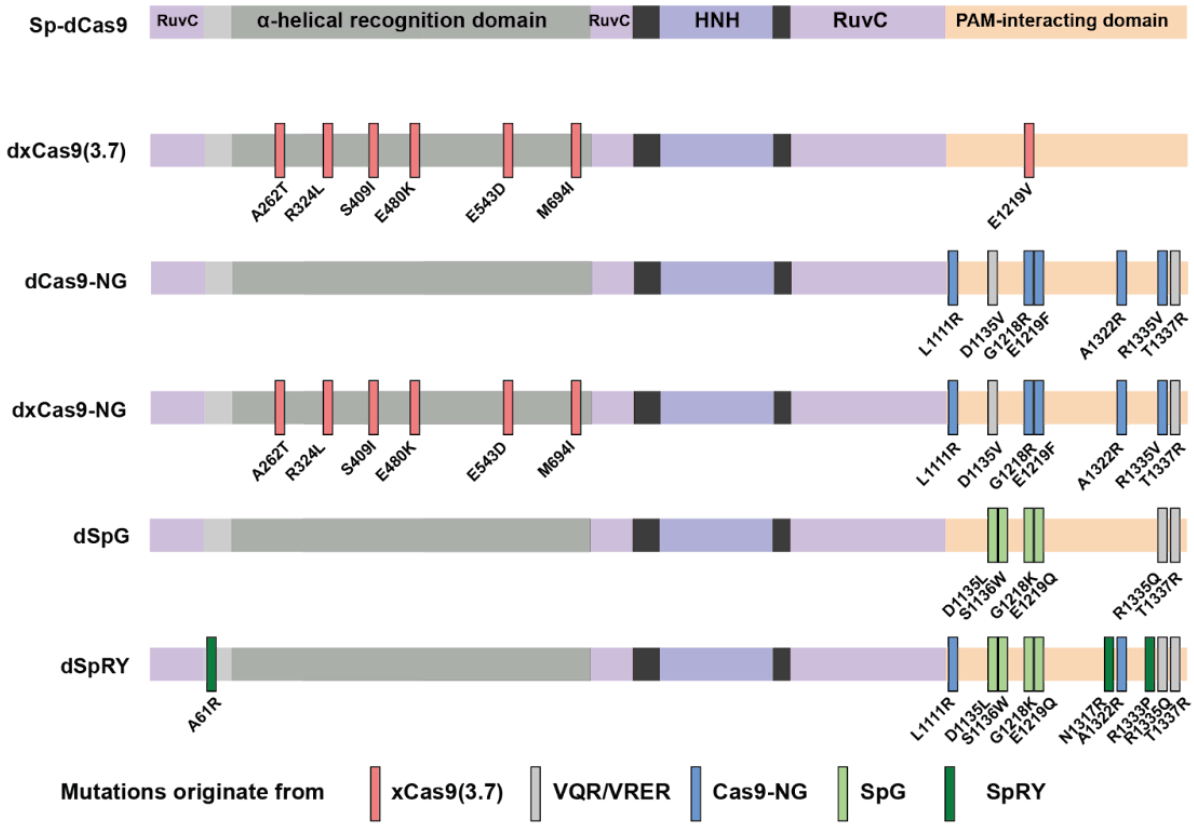

Figure S1. Mutations contributing to PAM-flexibility of engineered dCas9 variants
PAM-flexible dCas9 variants contain differing sets of mutations. All variants share the catalytically-inactivating D10A and H840A mutations of dCas9 (Qi et al., 2013). Mutations of dxCas9(3.7), from phage-assisted continuous evolution (PACE), were mostly at the α-helical recognition domain (Hu et al., 2018). dCas9-NG engineering was guided by the crystal structure with mutations made in the PAM-interacting domain (Nishimasu et al., 2018). dxCas9-NG has combined mutations from dxCas9(3.7) and dCas9-NG (Legut et al., 2020). dSpG and dSpRY were developed through structure-guided engineering with engineering trajectories monitored using a high-throughput PAM determination assay (Walton et al., 2021, 2020). SpG was engineered using mutations from the VRQR variant as a starting point (Kleinstiver et al., 2016, 2015), and SpRY contains mutations from Cas9-NG (Nishimasu et al., 2018). dSpRY is an evolved version of dSpG with a preference for NRN and some NYN PAMs (R is purine nucleotides, Y is pyrimidine nucleotides) (Walton et al., 2020). Mutation colors indicate the origin of each specific mutation. Complete sequences are provided in the DNA sequences section below.

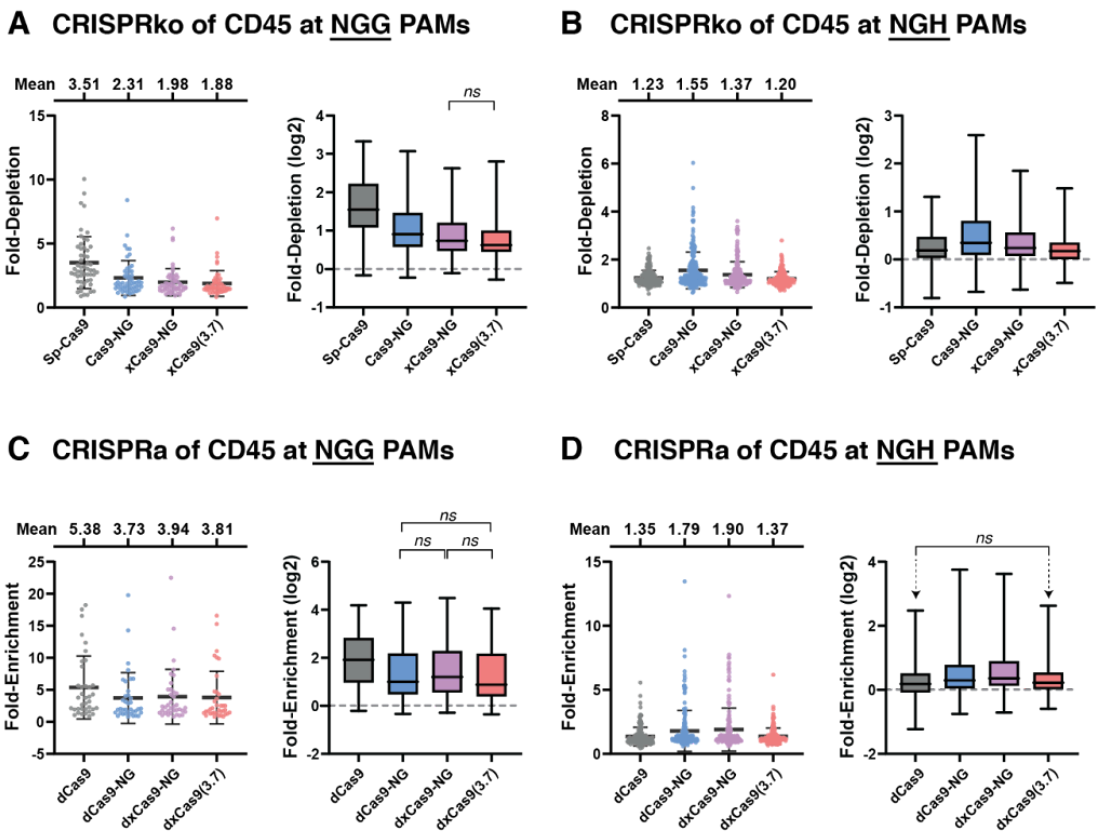

Figure S2: CRISPRko and CRISPRa in mammalian systems with PAM-flexible dCas9 variants

Cas9 variants were evaluated for CRISPRko (knockout) and CRISPRa (activation) at different PAMs. sgRNA-Cas9 effector complexes were targeted to the CD45 gene and changes in expression levels were evaluated by FACS-Seq (see Supplemental Methods). xCas9-NG and Cas9-NG exhibit comparable levels of PAM flexibility and both outperform xCas9(3.7). Data were plotted as fold-change scatter plots (left panel) or log2 fold-change box plots (right panel) for (A) CRISPRko at NGG PAMs, (B) CRISPRko at NGH PAMs, (C) CRISPRa at NGG PAMs, and (D) CRISPRa at NGH PAMs. In the scatter plots, bars and whiskers represent mean and standard deviation, respectively. In the box plots, two-tailed unpaired Welch's *t* test for each dCas9 pair were performed. Only non-significant comparisons (*ns*, $p > 0.05$) are indicated; all other differences (between proteins, within modalities) are significant.

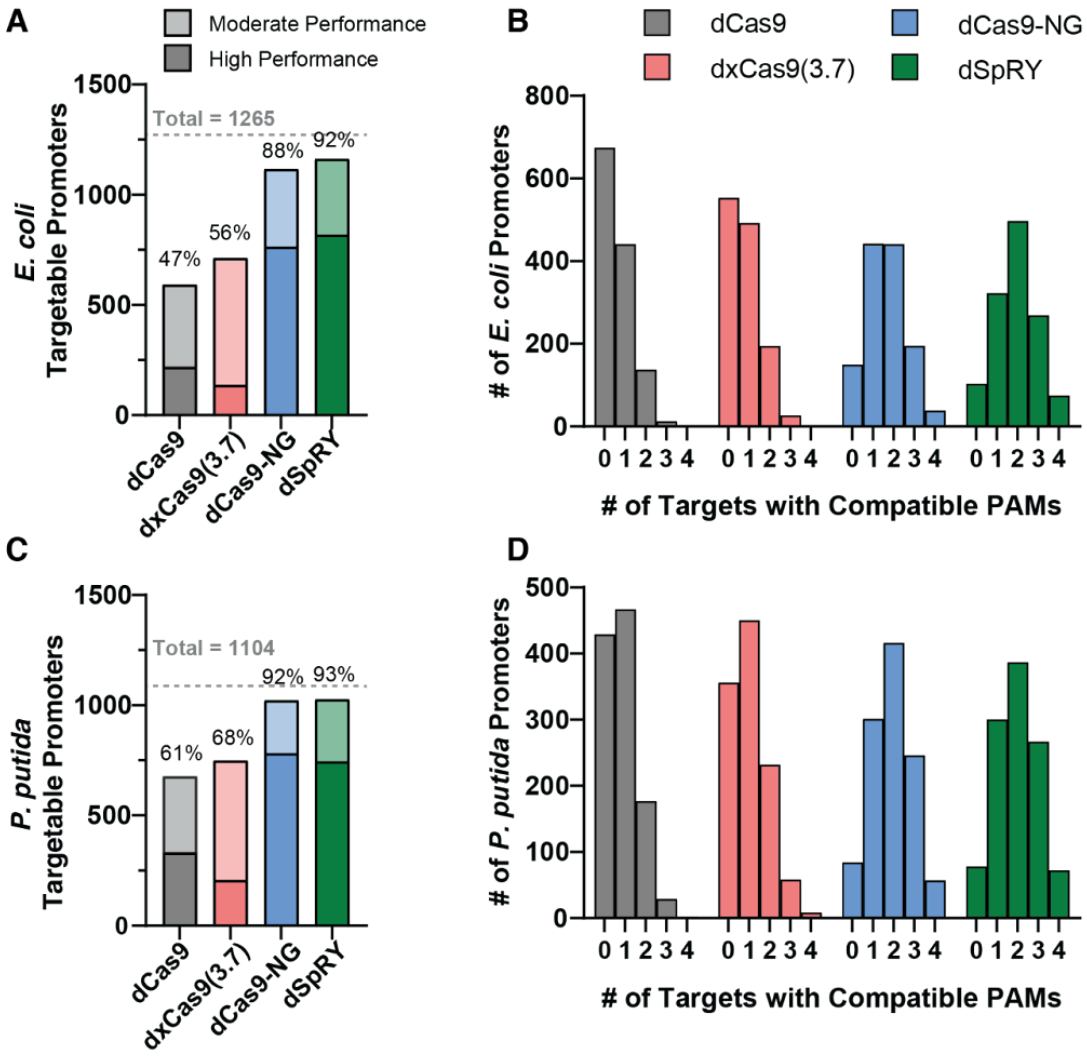

Figure S3: PAM availability and distribution in *E. coli* and *P. putida* promoters

Endogenous *E. coli* and *P. putida* promoters were analyzed for predicted targetable sites with different PAM-flexible dCas9 variants (see Methods section for further details). (A) Number of targetable *E. coli* promoters for different PAM-flexible dCas9 variants. 1265 *E. coli* promoters were analyzed for the presence of a compatible PAM at any of the four effective target site positions upstream of the TSS (see Methods). “High performance” PAMs are classified as PAMs with at least 50% efficiency relative to dCas9 at NGG PAMs. “Moderate performance” PAMs are classified as PAMs with 20-50% efficiency. (B) Distribution of promoters with 0 to 4 compatible PAMs with at least moderate performance in *E. coli*. (C) Number of targetable *P. putida* promoters for different PAM-flexible dCas9 variants. 1104 *P. putida* were analyzed with the same strategy. (D) Distribution of promoters with 0 to 4 compatible PAMs with at least moderate performance in *P. putida*. In both *E. coli* and *P. putida*, dxCas9-NG and dSpRY access more endogenous promoters than dCas9 and dxCas9(3.7). As *P. putida* has a higher GC content than *E. coli* and a correspondingly higher fraction of NGN PAMs, there is an almost identical number of targetable promoters for dCas9-NG and dSpRY.

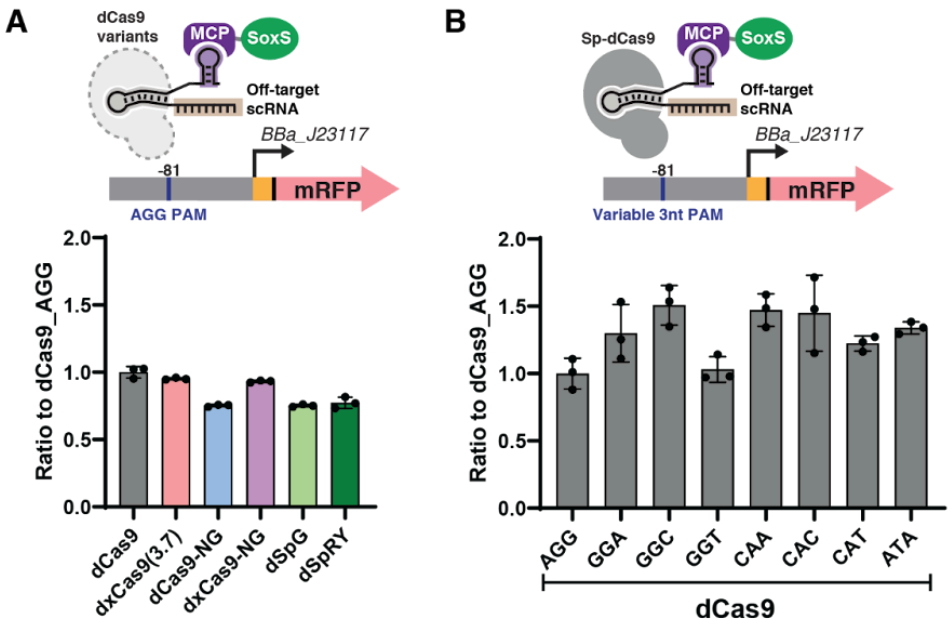

Figure S4: Basal expression of the mRFP reporter gene with different dCas9 variants and PAMs sequences

(A) Expression of different dCas9 variants produces less than 2-fold changes in basal reporter expression level. This experiment was performed with AGG PAM reporter and an off-target scRNA (hAAVS1). These off-target expression levels were used as a basal expression for fold-change calculation with each dCas9 variant in Figure 2. (B) Modified mRFP reporter genes with alternative upstream PAM sites produce less than 2-fold changes in basal reporter expression. This experiment was performed with Sp-dCas9 and an off-target scRNA (hAAVS1). Values in panel A and B represent the mean ± standard deviation calculated from n = 3.

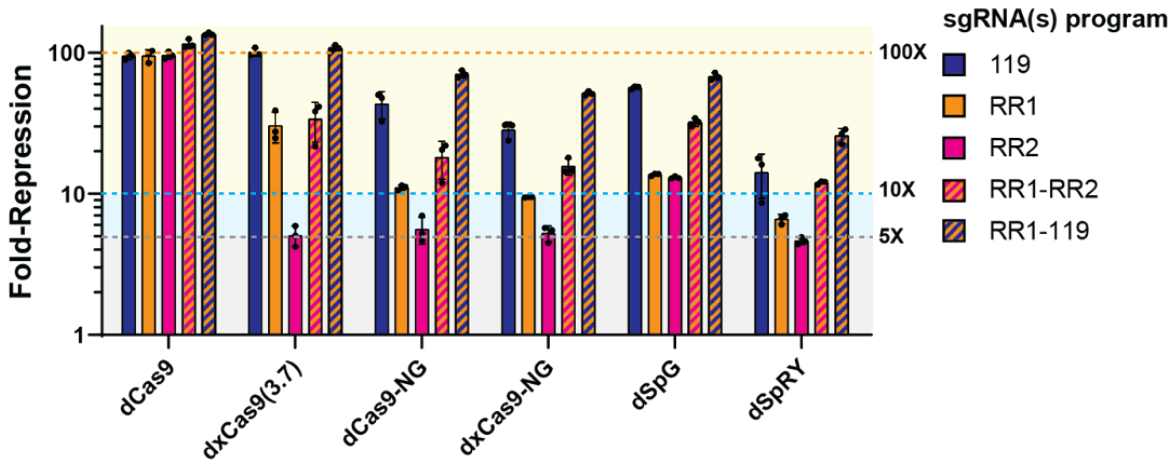

Figure S5: CRISPRi with PAM-flexible dCas9 variants

CRISPRi for PAM-flexible dCas9 variants was tested on an mRFP reporter gene with sgRNAs targeting the promoter (119) or coding sequence (RR1 and RR2) with one or two sgRNAs expressed, each targeting sites harboring NGG PAMs. dCas9 exhibited the highest repression efficiency (>90-fold) among all variants. When only a single sgRNA is expressed, the sgRNA targeting the promoter region (119) produces the largest repression effect with all dCas9 variants. The addition of the second sgRNA (RR1-RR2 or RR1-119) led to significant improvement in repression for all variants. Values represent the mean ± standard deviation calculated from n = 3.

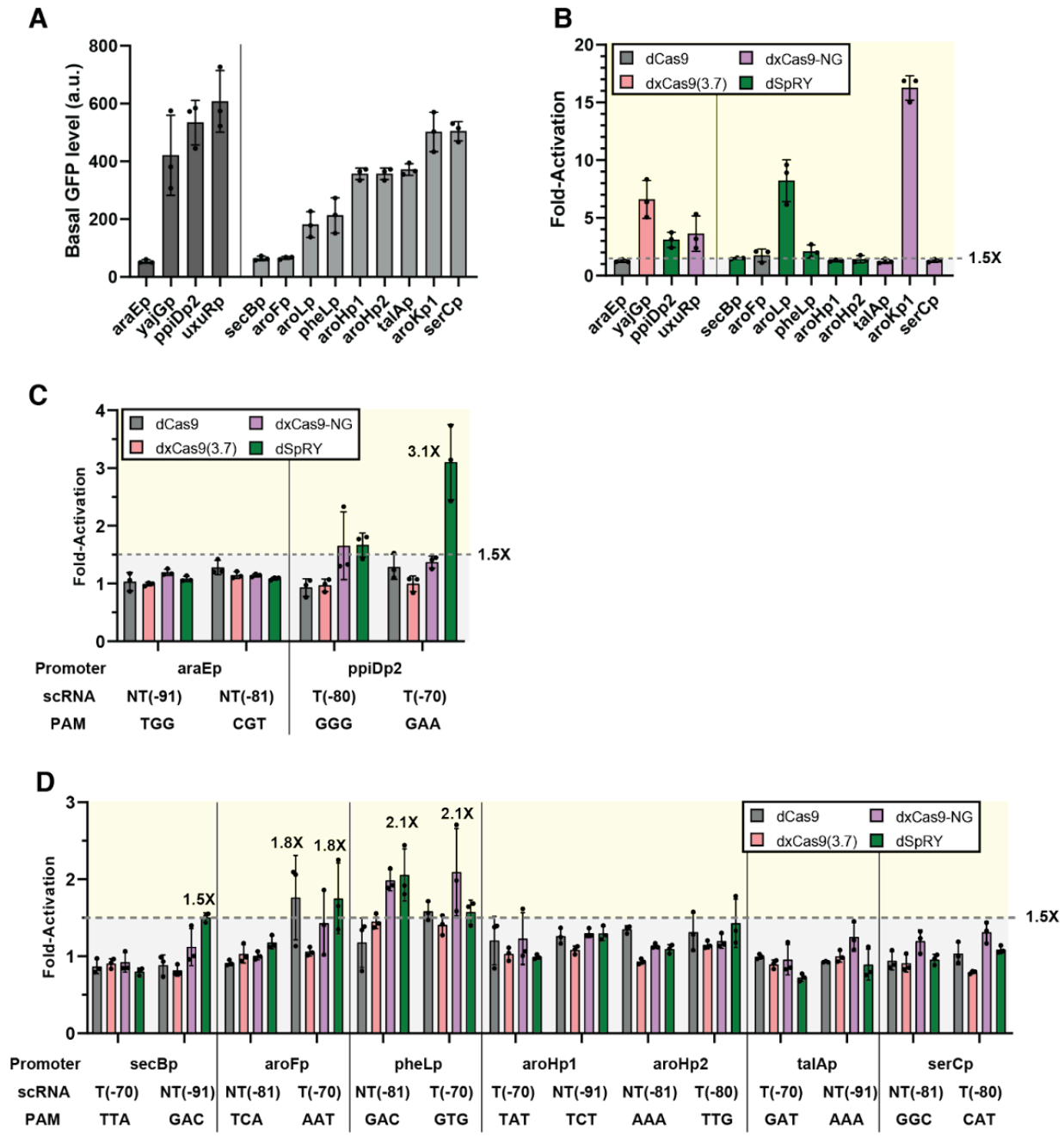

Figure S6: CRISPRa at endogenous promoters with PAM-flexible dCas9 variants
(A) Basal expression levels for endogenous promoters (left: promoters previously tested with dxCas9(3.7) (Fontana et al., 2020); right: new promoters examined in this work). Basal expression levels were measured in a strain expressing the parent dCas9 and an off-target scRNA (hAAVS1). (B) Maximum fold-activation for each endogenous promoter. Bar color indicates the dCas9 variant with the highest fold-activation for the corresponding endogenous promoter. 8 out of 13 endogenous promoters can be activated (>1.5-fold) with PAM-flexible dCas9 variants. (C) CRISPRa at endogenous promoters previously tested with dxCas9(3.7) (araEp and ppiDp2) using NGG or non-NGG PAMs. See main text Figure 4B for the other two promoters from this set (yajGp and uxuRp). (D) CRISPRa at endogenous

promoters involved in aromatic amino acid biosynthesis using non-NGG PAMs (secBp, aroFp, pheLp, aroHp1, aroHp2, talAp, and serCp). See main text Figure 4C for the other two promoters from the aromatic amino acid biosynthesis set (aroLp and aroKp1). Data were collected by flow cytometry and fold-activation was calculated compared to the strain expressing the corresponding dCas9 variant and an off-target hAAVS1 scRNA. Values in panels A-D represent the mean ± standard deviation calculated from n = 3.

Supplementary Tables

Supplementary Table S1: *E. coli* strains.

Strain	Description	Genotype
MG1655	Wildtype *E. coli strain*	F- λ- ilvG- rfb-50 rph-1
CD38	Integrated BBa_J23119-mRFP used for CRISPRi	MG1655 *nsfA*::BBa_J23119-mRFP

Supplementary Table S2: Selected *E. coli* plasmids.

Plasmid	Marker	Origin	Promoter	Gene	Terminator	Reference
pCD442	CmR	p15A	1) Sp.pCas9 2) BBa_J23107	1) dCas9 2) MCP-SoxS	1) BBa_B0015 2) BBa_B1002	(Fontana et al., 2020)
pCD564	CmR	p15A	1) Sp.pCas9 2) BBa_J23107	1) dxCas9(3.7) 2) MCP-SoxS	1) BBa_B0015 2) BBa_B1002	(Fontana et al., 2020)
pCK668	CmR	p15A	1) Sp.pCas9 2) BBa_J23107	1) dCas9-NG 2) MCP-SoxS	1) BBa_B0015 2) BBa_B1002	This work
pCK669	CmR	p15A	1) Sp.pCas9 2) BBa_J23107	1) dxCas9-NG 2) MCP-SoxS	1) BBa_B0015 2) BBa_B1002	This work
pCK340	CmR	p15A	1) Sp.pCas9 2) BBa_J23107	1) dSpG 2) MCP-SoxS	1) BBa_B0015 2) BBa_B1002	This work
pCK341	CmR	p15A	1) Sp.pCas9 2) BBa_J23107	1) dSpRY 2) MCP-SoxS	1) BBa_B0015 2) BBa_B1002	This work
pCK085.scRNA	CmR	p15A	1) Sp.pCas9 2) BBa_J23107 3) BBa_J23119	1) dCas9 2) MCP-SoxS 3) scRNA	1) BBa_B0015 2) BBa_B1002 3) TrrnB	(Tickman et al., 2021)
pCK281.scRNA	CmR	p15A	1) Sp.pCas9 2) BBa_J23107 3) BBa_J23119	1) dxCas9(3.7) 2) MCP-SoxS 3) scRNA	1) BBa_B0015 2) BBa_B1002 3) TrrnB	This work

pCK670.scRNA	CmR	p15A	1) Sp.pCas9 2) BBa_J23107 3) BBa_J23119	1) dCas9-NG 2) MCP-SoxS 3) scRNA	1) BBa_B0015 2) BBa_B1002 3) TrrnB	This work
pCK671.scRNA	CmR	p15A	1) Sp.pCas9 2) BBa_J23107 3) BBa_J23119	1) dxCas9-NG 2) MCP-SoxS 3) scRNA	1) BBa_B0015 2) BBa_B1002 3) TrrnB	This work
pCK363.scRNA	CmR	p15A	1) Sp.pCas9 2) BBa_J23107 3) BBa_J23119	1) dSpG 2) MCP-SoxS 3) scRNA	1) BBa_B0015 2) BBa_B1002 3) TrrnB	This work
pCK364.scRNA	CmR	p15A	1) Sp.pCas9 2) BBa_J23107 3) BBa_J23119	1) dSpRY 2) MCP-SoxS 3) scRNA	1) BBa_B0015 2) BBa_B1002 3) TrrnB	This work
pJF143. J3	AmpR	pSC101**	J3-BBa_J23117	mRFP	BBa_B0015	(Fontana et al., 2020)
pCK284.NNN	AmpR	pSC101**	J3(NNN-PAM)-BBa_J23117	mRFP	BBa_B0015	This work
pCD443.scRNA	AmpR	ColE1	BBa_J23119	scRNA	TrrnB	This work
pCK411.scRNA/sgRNA	AmpR	ColE1	BBa_J23119	scRNA/sgRNA	BBa_K2680405	This work
pCK590.XXX	KmR	pSC101	Endogenous (strand +)	GFPmut2		Same as (Zaslaver et al., 2006)
pCK591.XXX	KmR	pSC101	Endogenous (strand –)	GFPmut2		Same as (Zaslaver et al., 2006)

Supplementary Table S3: scRNA and sgRNA target sites.

sc/sgRNA	DNA sequence	Target strand[a]	Distance to TSS[b]	PAM
J306	TTGTGTCCAGAACGCTCCGT	NT	-81	AGG
hAAVS1	GGGGCCACTAGGGACAGGAT	Off-target	NA	–
RR1	AACTTTCAGTTTAGCGGTCT	NT	151[c]	GGG
RR2	TGGAACCGTACTGGAACTGC	NT	215[c]	GGG
119	AATTCAGATCTATTATACCT	NT	-15	AGG
yajGp_Y1	TTGACGAAATAATCGCCCCT	NT	-81	GGT
yajGp_Y2	CATCAGTGTTTCTTTTACCA	T	-79	GGG
uxuRp_U1	TGATTGACCAGTAAGTCTGT	NT	-81	AGG
uxuRp_U2	GATTACCCTACAGACTTACT	T	-70	GGT
ppiDp2_D1	ACTAAGCGTTGTCCCCAGTG	T	-80	GGG
ppiDp2_D2	GTCCCCAGTGGGGATGTGAC	T	-70	GAA
araEp_E1	TGCGACATGTCGTTATGTGA	NT	-91	TGG
araEp_E2	ATTAAATTGCTGCGACATGT	NT	-81	CGT
pheLp_X06	GCGATACACTCAATATAAAG	NT	-81	GAC
pheLp_X07	AGAGTAGTCCTTTATATTGA	T	-70	GTG
secBp_X07	CACCACGGTTCCCCAGATTT	T	-70	TTA
secBp_X08	AATCTGGGGAACCGTGGTGC	NT	-91	GAC
serCp_X06	ACCGTTGAGGGCAAAAATGT	NT	-81	GGC
serCp_X09	CTTTTGTGTGATGCAAGCCA	T	-80	CAT
talAp_X07	GGTAATAATCCTATAACACT	T	-70	GAT
talAp_X08	GTGTTATAGGATTATTACCA	NT	-91	AAA
aroFp_X06	CAGGCAATTTAGTCGCGCTT	NT	-81	TCA
aroFp_X07	AAGGGTTGAAAGCGCGACTA	T	-70	AAT
aroLp_X07	TGGTGGCTGGAAGTGCAACG	T	-70	TAG
aroLp_X08	GTTGCACTTCCAGCCACCAC	NT	-91	TTC
aroHp1_X07	ATTGCCACCAAGATCCTCGA	T	-70	TAT
aroHp1_X08	CGAGGATCTTGGTGGCAATC	NT	-91	TCT
aroHp2_X06	GTGGTTAGCATGATAACAAA	NT	-81	AAA
aroHp2_X09	TAGTGCATTAGCTTATTTTT	T	-80	TTG
aroKp1_X07	GAGTAAACAGCCGTAAAAGC	T	-70	GGT
aroKp1_X08	CTTTTACGGCTGTTTACTCA	NT	-91	CTG

[a] *Template strand (T) or non-template strand (NT).*

[b] Distance from the 3' end of the guide site (PAM proximal) to the TSS. For synthetic promoters (BBa_J23117 or BBa_J23119, http://parts.igem.org), the TSS is immediately downstream.
[c] For RR1 and RR2 sgRNAs, the positive number refers to the distance downstream of the TSS.

Supplementary Table S4: Predicted compatible PAMs for each dCas9 variants

PAM	Sp-Cas9	xCas9(3.7)	Cas9-NG	SpG	SpRY
AAA	0.18%	2.75%	19.51%	N.A.	27.97%
AAC	0.06%	1.52%	17.62%	N.A.	69.73%
AAG	46.32%	19.04%	43.10%	N.A.	28.35%
AAT	0.25%	3.80%	28.04%	N.A.	6.58%
ACA	0.61%	0.23%	5.03%	N.A.	19.84%
ACC	-0.50%	-0.15%	2.18%	N.A.	N.A.
ACG	17.85%	7.43%	12.10%	N.A.	N.A.
ACT	-0.45%	0.47%	7.07%	N.A.	N.A.
AGA	27.95%	29.33%	60.81%	65.89%	58.50%
AGC	7.82%	16.70%	52.14%	75.97%	56.19%
AGG	99.80%	62.37%	72.89%	38.75%	21.46%
AGT	1.82%	23.39%	68.90%	78.02%	59.55%
ATA	0.78%	0.21%	12.29%	N.A.	43.63%
ATC	-0.56%	-0.34%	5.07%	N.A.	3.20%
ATG	22.04%	5.45%	28.21%	N.A.	N.A.
ATT	-0.13%	0.55%	10.60%	N.A.	N.A.
CAA	-0.01%	6.21%	27.29%	N.A.	53.17%
CAC	-0.53%	2.69%	26.45%	N.A.	19.04%

CAG	44.62%	25.71%	47.15%	N.A.	18.17%
CAT	-0.63%	6.25%	32.92%	N.A.	22.44%
CCA	-0.13%	-0.21%	2.06%	N.A.	N.A.
CCC	-0.65%	-0.31%	0.89%	N.A.	1.01%
CCG	11.47%	3.99%	6.78%	N.A.	9.06%
CCT	-0.22%	-0.37%	3.09%	N.A.	N.A.
CGA	30.35%	36.77%	59.10%	78.85%	N.A.
CGC	10.29%	24.23%	52.31%	70.58%	N.A.
CGG	102.08%	68.15%	72.25%	48.14%	15.80%
CGT	2.47%	32.69%	69.50%	49.23%	23.77%
CTA	-0.23%	0.64%	9.53%	N.A.	20.11%
CTC	-0.52%	0.19%	4.65%	N.A.	25.22%
CTG	17.31%	3.94%	23.82%	N.A.	19.44%
CTT	-0.44%	-0.06%	9.93%	N.A.	2.30%
GAA	1.02%	11.96%	37.31%	N.A.	100.83%
GAC	-0.13%	4.71%	31.57%	N.A.	86.73%
GAG	53.38%	35.04%	57.91%	N.A.	55.14%
GAT	0.05%	10.29%	42.64%	N.A.	35.73%
GCA	-0.05%	0.76%	7.21%	N.A.	55.08%
GCC	-0.26%	0.28%	4.37%	N.A.	21.67%
GCG	13.01%	1.67%	11.22%	N.A.	N.A.
GCT	-0.58%	0.22%	10.36%	N.A.	43.08%
GGA	30.31%	37.93%	60.78%	62.42%	33.41%
GGC	12.24%	22.95%	53.55%	73.33%	41.75%

GGG	101.50%	70.07%	76.36%	67.74%	54.37%
GGT	7.16%	33.76%	69.40%	76.14%	65.25%
GTA	0.05%	1.79%	20.16%	N.A.	37.98%
GTC	-0.34%	0.56%	11.00%	N.A.	N.A.
GTG	23.36%	6.76%	37.60%	N.A.	50.91%
GTT	-0.15%	0.29%	16.20%	N.A.	4.66%
TAA	0.62%	1.36%	16.05%	N.A.	69.86%
TAC	-0.62%	0.15%	11.41%	N.A.	72.28%
TAG	36.56%	11.45%	34.32%	N.A.	30.23%
TAT	-0.22%	1.52%	19.26%	N.A.	44.40%
TCA	-0.36%	0.01%	1.27%	N.A.	N.A.
TCC	-0.81%	-0.28%	0.72%	N.A.	N.A.
TCG	10.87%	3.10%	5.79%	N.A.	N.A.
TCT	-0.15%	-0.37%	2.47%	N.A.	7.00%
TGA	28.62%	29.68%	61.71%	73.33%	45.34%
TGC	7.91%	15.40%	53.76%	88.36%	65.05%
TGG	96.62%	62.22%	72.08%	95.59%	69.12%
TGT	2.32%	24.78%	70.19%	103.69%	N.A.
TTA	0.06%	0.53%	3.71%	N.A.	N.A.
TTC	-1.16%	-0.09%	0.44%	N.A.	N.A.
TTG	9.19%	2.01%	11.05%	N.A.	0.14%
TTT	-0.46%	-0.14%	1.55%	N.A.	11.70%

The predicted PAM compatibility of each PAM-Cas9 pair was reported as indel frequency (in % units) relative to the benchmark efficiency of Sp-Cas9 at NGG PAMs from each

experiment (see Supplementary Methods) (Kim et al., 2020; Walton et al., 2020). Each data point was color-coded based on predicted efficiency: Green (high efficiency, >50% of benchmark), blue (moderate efficiency, 20%–50%), and gray (low efficiency, less than 20%). NGG PAMs are highlighted in yellow. N.A. means data is not available. Some of the reported efficiency values are small negative numbers, likely due to negligible editing frequencies indistinguishable from the background. Comparable data for indel frequencies with xCas9-NG are not available; for this work we assumed Cas9-NG and xCas9-NG were similar based on their comparable performance in nuclease assays (Figure S2).

Supplementary Table S5: CRISPRa on endogenous *E. coli* promoters

Promoter	Max. FA	dCas9 variant	Position	PAM
yajGp	**6.6** 6.2 5.1	**dxCas9(3.7)** dxCas9-NG dSpRY	NT(-81)	GGT
uxuRp	**3.6** 2.6	**dxCas9-NG** dSpRY	T(-70)	GGT
araEp	1.3	dxCas9-NG	NT(-81)	CGT
ppiDp2	**3.1**	**dSpRY**	T(-70)	GAA
aroKp1	**16.3** 12.8	**dxCas9-NG** dxCas9(3.7)	T(-70)	GGT
aroLp	**8.2** 5.5	**dSpRY** dCas9	T(-70)	TAG
aroF	**1.8** **1.8**	**dCas9** **dSpRY**	T(-70)	AAT
aroHp1	1.3	dxCas9-NG	NT(-91)	TCT
aroHp2	1.4	dSpRY	NT(-81)	AAA
pheLp	**2.1** **2.1**	**dxCas9-NG** **dSpRY**	T(-70) NT(-81)	GTG GAC
secBp	**1.5**	**dSpRY**	NT(-91)	GAC
serCp	1.3	dxCas9-NG	T(-80)	CAT
talAp	1.2	dxCas9-NG	NT(-91)	AAA

The top two conditions were shown for each promoter, if >1.5-fold. The best conditions for each promoter is shown in bold. yajGp has three similar activation levels. Promoters with <1.5-fold activation were shaded in gray.

Supplementary Methods

Evaluating PAM accessibility from CRISPR knockout and CRISPR activation screens in mammalian systems

To predict the PAM accessibility for different Cas9 variants, we used data from CRISPR knockout (CRISPRko) and CRISPR activation (CRISPRa) screens in mammalian cells. Previously, screening data has been reported for three Cas9 variants (Sp-Cas9, xCas9(3.7), and Cas9-NG) (Legut et al., 2020). We report here a corresponding screen performed using the same approach with four Cas9 variants: Sp-Cas9, xCas9(3.7), Cas9-NG, and xCas9-NG. Lentiviral sgRNA libraries were constructed to target the CD45 gene, spanning the 3 kb region surrounding the TSS and constitutive CDS exons, using all possible 20-mer sequences upstream of an NG PAM sequence, as described before (Legut et al., 2020). In addition to sgRNAs, each vector also contained a Cas9 variant (nuclease for CRISPRko and catalytically dead Cas9 fusion with VPR transcriptional activators for CRISPRa) and a short barcode downstream of the sgRNA to identify the Cas9 variant in the same Illumina read as the sgRNA. sgRNA library cloning, lentivirus production and cell transduction were done separately for each Cas9 variant. The transduced and selected cells were only pooled together prior to FACS sorting based on the CD45 protein expression. CRISPRko was performed in K562 cells and CRISPRa was performed in A375 cells; both cell lines were obtained from ATCC. The presort samples and 10% top/bottom bins were analyzed by high-throughput Illumina sequencing. To calculate fold-depletion for CRISPRko, the relative frequency (normalized to sequencing depth and median frequency of non-targeting sgRNAs for each Cas9 variant) of each sgRNA from the bottom 10% bin (lowest expression level) was divided by its corresponding frequency in the top 10% bin. To calculate fold-enrichment for CRISPRa, the relative frequency of each sgRNA from the top 10% bin (highest expression) was divided by its corresponding frequency in the bottom 10% bin. For CRISPRko, only sgRNAs targeting within the CDS were included in the analysis; for CRISPRa, only sgRNAs targeting within the core promoter region (as determined previously (Legut et al., 2020), chr1:198638250-198639226) were included. The data were then filtered for designated PAMs (NGG or NGH) to visualize the data as shown in Figure S2.

PAM compatibility analysis

For each dCas9 variant, the ability to target each of the 64 possible 3-nucleotide PAMs was predicted based on previously reported CRISPR nuclease (CRISPRko) data in mammalian systems. (Kim et al., 2020; Walton et al., 2020). Genome editing efficiencies, measured as indel frequencies, have been reported for Sp-Cas9, xCas9(3.7), and Cas9-NG (Kim et al., 2020) and for Sp-Cas9, SpG, and SpRY (Walton et al., 2020). For each Cas9 dataset, sgRNAs with the same 3-nt PAM were grouped together. We then calculated an average indel frequency for all sgRNAs with the same PAM. We assessed PAM compatibility by comparison to the benchmark indel frequency of Sp-Cas9 at NGG PAMs (Table S4). “High performance” PAMs were those with >50% indel frequency relative to the benchmark.

“Moderate performance” PAMs were those with 20-50% efficiency relative to the benchmark. PAMs that were not tested in the previously-reported nuclease assays (Walton et al., 2020) were assumed to be incompatible.

Endogenous promoter and scRNA selection strategy

Gene candidates were selected from metabolic pathways related to aromatic amino acid biosynthesis, including the relevant genes in central metabolic pathways. We selected only promoters that are regulated by sigma70 and are available in the previously characterized *E. coli* endogenous promoter library (obtained from Horizon Discovery) (Zaslaver et al., 2006). To identify potentially activatable promoters with moderately-weak basal expression levels, we compared basal expression to yajGp, which was the strongest endogenous promoter that could be activated in previous work (Fontana et al., 2020). We eliminated any promoters with >10-fold higher expression levels than yajGp, yielding 9 promoters: secBp, aroFp, aroLp, pheLp, aroHp1, aroHp2, talAp, aroKp1, and serCp. Some of these promoters regulate multi-gene operons. Complete sequences of the endogenous promoters used in this study are available in the supplement of our published paper.

Out of selected genes, aroH contains two putative promoters — aroHp1/aroHp2. In Figure S6A, the basal expression levels for aroHp1 and aroHp2 were assumed to be the same value. Expression levels produced by each individual promoter cannot be determined from the fluorescent reporter used in this study because both promoters are upstream of the same fluorescent reporter gene.

In the secBp promoter constructed for the *E. coli* promoter library (Zaslaver et al., 2006), only the sequence to -7 bases from the TSS was included. To include enough sequence for scRNA target sites, we constructed a promoter extending to -137 bases from the TSS.

For each promoter, four scRNAs were identified according to the previously described target site preference. X06 and X08 represent the scRNAs targeting the non-template strand at -81 and -91 positions (Table S3). X07 and X09 represent the scRNAs targeting the template strand at -70 and -80 positions. One target site from the template strand and another from the non-template strand were selected for further analysis based on which PAM was predicted to be accessible to the highest number of dCas9 variants. Accessibility was assessed based on the moderate performance threshold cutoff (Supplemental Table S4).

Chapter 3: Systematic Mapping of Bacterial CRISPRa Design Rules and Implications for Synergistic Gene Activation

Cholpisit Kiattisewee[+,a,b,c,g], Ava V. Karanjia[+,a,b,c], Ryan A. L. Cardiff[+,a,b], Kira E. Olander[a,b], Pansa Leejareon[e,f], Sarah S. Alvi[d], James M. Carothers[*,a,b,c,d], Jesse G. Zalatan[*,a,b,c,e]

a: Molecular Engineering & Sciences Institute
University of Washington
Seattle, WA 98195
United States

b: Center for Synthetic Biology
University of Washington
Seattle, WA 98195
United States

c: Department of Chemical Engineering
University of Washington
Seattle, WA 98195
United States

d: Department of Bioengineering
University of Washington
Seattle, WA 98195
United States

e: Department of Chemistry
University of Washington
Seattle, WA 98195
United States

f: Department of Biochemistry
Mahidol University
Bangkok, 10400
Thailand

g: Current Address:
Institute for Medical Engineering and Science
Massachusetts Institute of Technology
Cambridge, MA, 02139
United States

*: These authors contributed equally
*: Corresponding authors

jcaroth@uw.edu
206-221-4902

zalatan@uw.edu
206-543-1670

Submitted as a research article in *ACS Synthetic Biology* on May 17, 2025.
bioRxiv preprint: https://doi.org/10.1101/2025.05.14.654134

Graphical Abstract

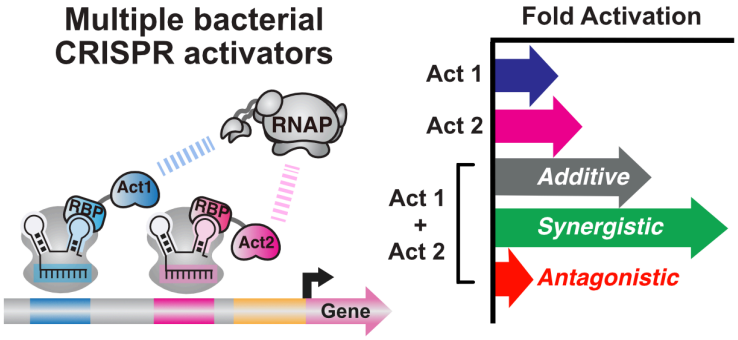

*__Note__: This chapter contains collaborative work. C. Kiattisewee, A. V. Karanjia, and R. A. L. Cardiff contributed equally to this work. C. Kiattisewee screened the design rules for SoxS family activators and combined recruitment of SoxS and PspF. R. A. L. Cardiff screened the design rules for RNAP subunits and assembly mediators. A. V. Karanjia screened the design rules for AsiA and combined recruitment of SoxS and AsiA. All three contributed equally to screening design rules to guide strategies to combine CRISPRa effectors, fusion of tandem effectors, and some experiments on combined recruitment of effectors. The other contributors prepared figures and written text relevant to their contributions. All sections of the paper were written collaboratively with help from J. Zalatan.

3.1. Abstract

CRISPR gene activation (CRISPRa) tools have shown great promise for bacterial strain engineering but often require customization for each intended application. Our goal is to create generalizable CRISPRa tools that can overcome previous limitations of gene activation in bacteria. In eukaryotic cells, multiple activators can be combined for synergistic gene activation. To identify potential effectors for synergistic activation in bacteria, we systematically characterized bacterial activator proteins with a set of engineered synthetic promoters. We found that optimal target sites for different activators could vary by up to 200 bases in the region upstream of the transcription start site (TSS). These optimal target sites qualitatively matched previous reports for each activator, but the precise targeting rules varied between different promoters. By characterizing targeting rules in the same promoter context, we were able to test activator combinations with each effector positioned at its optimal target site. We did not find any activator combinations that produced synergistic activation, and we found that many combinations were antagonistic. This systematic investigation highlights fundamental mechanistic differences between bacterial and eukaryotic transcriptional activation systems, and suggests that alternative strategies will be necessary for strong bacterial gene activation at arbitrary endogenous targets.

Keywords: CRISPR activation, Bacterial CRISPRa, Synergistic activation, transcriptional activators

3.2. Introduction

CRISPR-Cas based transcriptional regulators have become a pivotal tool in genetic programming. CRISPR activation (CRISPRa) and CRISPR interference (CRISPRi) enable massively parallel perturbations at a genome-wide scale.[1–3] In bacterial systems, CRISPRa systems that recruit transcriptional activators to target genes have been used for combinatorial pathway engineering,[4] activating endogenous targets,[5–7] multi-layer dynamic circuits,[8–10] and metabolic engineering in non-model organisms.[11,12] Although past work has estimated that approximately 60% of *E. coli* promoters are targetable with CRISPRa,[7] challenges such as inconsistent activator performance across bacterial promoters, strict design constraints specific to each activator, and interference from native regulatory machinery at endogenous gene targets continue to hinder broader implementation of CRISPRa tools.[6,7,13–15]

To expand our capabilities in bacterial systems, we can look to eukaryotic CRISPRa systems,[16–19] where several groups have demonstrated that delivering multiple effectors can produce potent and synergistic transcriptional activation.[20–22] In both eukaryotic and bacterial systems, synergistic transcriptional effects have been well-established prior to the development of CRISPR technologies.[23–25] Typically, these effects arise from simultaneous recruitment of multiple transcription factors, which can produce expression levels greater than the summed effect of each individual activator. Synergistic CRISPRa in bacteria has yet to be achieved, possibly due to the stringent target site and sequence requirements that govern activation.[6,13–15,26–30] There has been limited progress in engineered bacterial synergistic activators in the ~30 years since the first report of synergistic activation in bacteria, and new approaches are needed to identify bacterial gene activation methods that rival the robust programmability and effectiveness of eukaryotic CRISPRa systems.[31–35]

To determine if improved and potentially synergistic CRISPRa can be achieved, we evaluated gene activation in *E. coli* with combinations of CRISPRa effectors. To identify candidate combinations, we first performed a systematic evaluation of multiple bacterial CRISPRa systems, including several with distinct activation mechanisms.[6,13,14] After identifying optimal target sites for each individual CRISPRa system, we defined strategies to recruit combinations of CRISPRa effectors at their respective optimal target sites. Design rules for these systems have been previously reported,[6,13,14] but we found that it was critical

to characterize candidate systems in the same promoter context because the optimal target sites can vary between different promoters.

Although we identified multiple scenarios where combinations of effectors could be recruited to their respective optimal target sites at a single promoter, we did not observe any significant synergistic CRISPRa effects. Instead, when two effectors were recruited to a single CRISPR-Cas complex, we observed antagonistic effects on activation. When two effectors were recruited to distinct optimal target positions with orthogonal CRISPR-Cas systems, we observed no increase in activation relative to the best single effector. Bacterial effectors typically interact directly with RNA polymerase (RNAP), and our results may indicate that RNAP cannot bind to the minimal promoter and simultaneously interact with two DNA-bound activators, at least for the pairs of effectors tested here. These findings underscore ongoing challenges for synergistic gene activation in bacteria. Although synergistic transcriptional activation has already been achieved in eukaryotes with combinations of CRISPRa effectors,[20–22] our results suggest that alternative strategies may be needed to obtain reliable high-level gene activation at endogenous genes in bacteria.

3.3. Results

Different bacterial CRISPRa strategies have distinct target site preferences depending on their mechanism of interaction with RNAP.[42,43] Here, we focus on four CRISPRa effectors with different RNAP interaction mechanisms: 1) SoxS,[6,27] 2) N-terminal domain of RpoA (αNTD) ,[15,27] 3) AsiA,[13] and 4) PspF (Figure 1).[14] We hypothesized that we could target multiple effectors to the same promoter to increase RNAP recruitment and improve activation. For effectors with the same optimal target sites, we could recruit two effectors to the same CRISPR complex. Alternatively, for effectors with distinct optimal target sites, we could use two orthogonal CRISPR complexes to recruit effectors to their respective sites. However, it is challenging to identify optimal pairs of target sites from the available literature because many CRISPRa systems have been characterized with different model promoters, and the optimal target site position can be sensitive to promoter context.

To facilitate comparisons between CRISPRa systems in a single model promoter, we modified a fluorescent reporter system previously used to characterize SoxS and αNTD.[6,27] The J1 synthetic promoter contains a target site array that includes NGG PAMs oriented every 10 bp upstream from the TSS on both strands, starting from -35 bp from the TSS, and

can be shifted by 1 to 12 base pairs by inserting single base pairs at the 5' end of UP element to characterize target sites preferences at single base resolution. To construct a promoter system for multiple CRISPRa effectors, we modified the J1 promoter to be compatible for testing the design rules of AsiA and PspF activators. For AsiA, we inserted an additional sequence between the J1 target site array and the core promoter, which shifts the target site array further upstream of the TSS previously shown to be optimal for AsiA activation (Figure 2A).[13] For PspF, we changed the core promoter from σ^{70} to σ^{54}, which is required for PspF-mediated activation (Figure 2B). All optimized promoters contain the same J1 target site array, which should enable comparisons between effectors because the promoters have the same target sites and surrounding sequence context. We first validated each CRISPRa system in its original reporter construct and then proceeded to systematically compare these systems using J1 and modified J1 reporters.

3.3.1. Design rules for SoxS family activators

The SoxS transcriptional regulator from *E. coli* is an effective CRISPR activation domain in multiple bacterial species.[12,27,36,44,45] SoxS can be recruited as an MCP-SoxS fusion to an MS2 scaffold RNA (scRNA) and we have previously screened SoxS-mediated CRISPRa at single nucleotide resolution 40-120 bp upstream of the TSS in the J1 synthetic promoter (Figure 2A).[6] SoxS-mediated CRISPRa can activate both the core σ^{70} (RpoD) promoter and other non-housekeeping sigma factor promoters, which includes >95% of *E. coli* promoters.[6] To investigate whether the design rules for SoxS-mediated CRISPRa are generalizable to the other core promoters, we also screened σ^{38} (RpoS), σ^{32} (RpoH), σ^{24} (RpoE), and σ^{54} (RpoN) promoters at 10 bp resolution. We found that CRISPRa at σ^{38}, σ^{32}, and σ^{24} promoters is optimal in the same region as σ^{70} promoters, 60-100 bp upstream of the TSS (Figure S1A). For the σ^{54} promoter, which represents ~3% of *E. coli* promoters, we observed no SoxS-mediated activation at any tested sites. To determine whether the sharp phase dependence observed with σ^{70} promoters was present at other sigma factor promoters, we screened the σ^{38}-dependent sodCp promoter at 1 bp resolution. We found that SoxS-mediated CRISPRa maintains the same optimal target site and sharp phase dependence across σ^{70} and σ^{38} promoters (Figure S1B). These findings suggest that the observed distance preference for SoxS is inherent to the effector itself rather than the minimal sigma factor promoter.

SoxS orthologs are also potentially useful for bacterial CRISPRa. Here we focused on two SoxS orthologs in the AraC/XylS family, MarA and TetD. Previously, we observed modest CRISPRa with TetD and no detectable activation with MarA.[27] We attempted to improve activation by mutating the native DNA binding motifs to prevent the effectors from being sequestered at off-target endogenous sequences. Although this strategy was effective with SoxS,[6,27] the TetD mutants and MarA mutants exhibited no significant increase in CRISPRa (Figure S2). However, TetD remains a candidate for synergistic CRISPRa. Because TetD prefers similar target sites to SoxS,[27] it could potentially be effective when recruited with SoxS to the same target site.

3.3.2. Design rules for RNAP subunits and assembly mediators

RNAP subunits can act as synthetic transcriptional activators in bacteria through subunit-mediated recruitment of the functional RNAP holoenzyme.[46] There are multiple strategies for subunit-mediated recruitment of RNAP to the CRISPR complex, including direct fusion to dCas9[26,30] and noncovalent recruitment via protein-protein or protein-gRNA interactions.[15,27] Several RNAP subunits have been characterized in the J1 reporter context.[6,15,27] In this work, we focus on the N-terminal domain of the alpha subunit (RpoA), termed αNTD, because it has been the most effective and widely used of the RNAP subunits.[5,15,27,30] αNTD is effective when recruited as an αNTD-MCP fusion to an MS2 scRNA, and has similar target site preferences to SoxS (Figure 2A).[6,27]

We first evaluated whether αNTD would be functional when recruited with a different RNA hairpin/RNA-binding protein pair. This approach could be used to independently control different genes, or to recruit multiple effectors to different sites on the same promoter. We tested an αNTD-PCP fusion protein, which can be recruited to a PP7 scRNA. αNTD-PCP exhibited similar target site preferences but lower activity compared to αNTD-MCP (Figure S3). This behavior is analogous to previous results with PCP-SoxS, which has similar target site preferences but modest activity compared to MCP-SoxS.[27] These results provide the design rules necessary to test an orthogonal programming strategy where one CRISPR complex recruits αNTD-PCP and another recruits MCP-SoxS, or vice versa with αNTD-MCP and PCP-SoxS.

In addition to αNTD, RNAP assembly can be facilitated by other RNAP subunits or RNAP assembly factors, with moderate effectiveness in CRISPRa.[11,26,27,47] In this work, we

evaluated an additional candidate effector, the RNAP-σ^{38} assembly factor Crl.[48] We recruited MCP-Crl to a σ^{38}-dependent promoter and observed a small, 1.2-fold increase in gene expression compared to an off-target scRNA (Figure S4). We also found that the presence of MCP-Crl alone, in the absence of any recruitment to the CRISPR complex, increases reporter gene expression by 2.4-fold relative to a strain without MCP-Crl. This effect could arise from nonspecific Crl-mediated activation of σ^{38} promoters. Thus, Crl may not be a useful CRISPRa effector, and αNTD remains the most effective of the RNAP subunits or assembly factors tested for CRISPRa.

3.3.3. Design rules for AsiA

AsiA is an anti-σ^{70} factor that can activate transcription when fused to heterologous DNA binding domains.[27,49,50] An evolved variant AsiA_m2.1 mitigates the toxicity of wild-type AsiA and is effective for CRISPRa as a dCas9 fusion;[13] this variant was used for all AsiA experiments in this work. dCas9-AsiA has been reported to preferentially activate at target sites 90-252 bp from the TSS, further than the 60-100 bp range for SoxS[13]. These findings were reported with a W1 reporter; we confirmed these target site preferences and observed optimal CRISPRa with dCas9-AsiA expressed at basal levels from a pTet promoter in the absence of an inducer (Figure S5).[26] We then tested dCas9-AsiA using the J1 reporter with target sites 40-140 bp from the TSS, but we were unable to detect activation at target sites within this range (Figure 2A). To evaluate target sites further upstream of our original J1 reporter with dCas9-AsiA, we constructed novel synthetic promoters with the J1 array of gRNA target sites placed 100 bp upstream of the J3 promoter. The J3 promoter contains a set of target sites at optimal positions for SoxS-mediated CRISPRa.[6] The new J1-J3(100) hybrid promoter allows us to screen AsiA target sites further than 140 bp at the upstream J1 sites, while maintaining activity with SoxS, αNTD, and TetD at the downstream J3 sites (Figure S6 & S7A). We observed up to 3.2-fold activation at target sites positioned from -160 to -180 bp (Figure S7B), much less than the 21-fold activation observed at similar positions with the W1 reporter (Figure S5C). We also constructed another hybrid promoter J1-J2(100)-J3(100), which shifts the J1 target sites to 240-340 bp, allowing us to test the same distances as previously reported. With the J1-J2(100)-J3(100) promoter, we still observed only 1.9-fold activation at position -250 (Figure S7B). This small effect is consistent with our observations in the W1 reporter of weaker activation at H5 (-252bp) compared to H4 (-182 bp) (Figure S5C).

Because bacterial CRISPRa can be ineffective at target sites shifted by 1 or 2 bases from optimal sites,[6,13] we constructed the J1-J3(122) promoter, which is shifted by 22 bases from J1-J3(100). This shift moves target sites to -182 bp and -252 bp, which correspond precisely to the optimal positions previously reported with the W1 reporter. Using J1-J3(122), we tested target sites from 162-262 bp upstream of the TSS with dCas9-AsiA. We observed strong, ~30-fold gene activation at -192 or -202 bp target sites, (Figure S7C). Surprisingly, we did not detect significant activation from other target sites, including -182 bp which was the most effective site reported previously.[13] We also found that dCas9-AsiA activation was biased toward the template strand, unlike the previously reported results where activation was observed from template and non-template strand targets. Our observations qualitatively agree with previous results for dCas9-AsiA target site preferences,[13] but we find that the precise positions of effective sites can vary between promoters. Characterizing AsiA and SoxS in the same promoter context is thus a critical step towards a potential multi-effector CRISPRa strategy with AsiA and SoxS.

3.3.4. Design rules for PspF

σ^{54} promoters are inaccessible to SoxS, but they can be activated by PspF.[6,14] PspF is an ATP-dependent transcriptional activator that positively regulates *E. coli psp* operon σ^{54} promoters in response to cellular stresses.[51] To benchmark PspF activity, we evaluated PspF-mediated CRISPRa with a previously-characterized CRISPRa-responsive σ^{54} promoter, pspAp-G6.[14] We observed ~16-fold activation from PspF-mediated CRISPRa (Figure S8A). Previous work has reported much larger fold-activation values for PspF-mediated CRISPRa,[14] but these values were obtained using a different baseline subtraction method. When the raw data are directly compared, our results are consistent with the previously reported values (Figure S8A).

To systematically screen PspF target site distance preferences, we constructed a modified σ^{54} promoter with a J1 array of target sites upstream of a minimal σ^{54} minimal promoter (J1-pspAp). At the most effective target site, located at position -61 on the non-template strand, we observed 8-fold activation (Figure 2B). Compared to pspAp-G6, the optimal target site in J1-pspAp is shifted 30 bases closer to the TSS. This shift could be because J1-pspAp lacks the integration host factor (IHF) binding site that forms a loop to bring PspF closer to the minimal promoter.[52]

We proceeded to screen target site preferences in J1-pspAp at single base resolution. We observed a similar periodic effect as observed previously for both PspF and SoxS,[14,28] and we observed a modest increase in activity at position -60 compared to -61 (Figure S8B). We proceeded to use the -60 target site position for subsequent PspF experiments. Because PspF has distinct target site preferences compared to SoxS and other activators, we expect that it may not be useful as a multi-effector fusion protein targeted to a single site. However, PspF might be effective when multiple, orthogonal CRISPR complexes are used to target different activators to their respective preferred target sites.

3.3.5. Design rules guide strategies to combine CRISPRa effectors

We employed three strategies to combine CRISPRa systems: 1) tandem protein fusion of multiple effectors, 2) recruiting two effectors to a single CRISPR complex using a combination of direct dCas9 fusion and gRNA recruitment, and 3) targeting two orthogonal CRISPRa complexes to different preferred target sites. We used the optimal positioning for each CRISPRa activator to guide our choices on which activator combinations to test with each strategy (Table 1 and Table S7).

3.3.6. Fusion of tandem effectors decreases CRISPRa activity

To test tandem effector fusions, we used SoxS with two alternative activators, TetD and αNTD, that have similar target preferences. This strategy is comparable to the eukaryotic dCas9-VPR system, in which three activators are fused to dCas9 in tandem to produce a synergistic CRISPRa effect.[20] For bacterial CRISPRa, we used a single MS2 scRNA to recruit multi-effector MCP fusion proteins. For SoxS and TetD, we constructed a C-terminal fusion MCP-SoxS-TetD because the individual C-terminal fusion MCP-SoxS and MCP-TetD are effective.[27] We found that at their most effective target sites, MCP-SoxS-TetD produced 7-fold gene activation, while the individual MCP-SoxS or MCP-TetD effectors produced 27-fold or 5-fold activation, respectively. Thus, MCP-SoxS-TetD is modestly more effective than MCP-TetD alone, but significantly impaired when compared to MCP-SoxS (Figure S9). In a similar strategy with SoxS and αNTD, we appended SoxS to the previously validated αNTD-MCP to generate αNTD-MCP-SoxS. We found that at their most effective target sites, αNTD-MCP-SoxS produced 1.3-fold gene activation, which was relatively weak

compared to both αNTD-MCP (3.3-fold) and MCP-SoxS (27-fold) (Figure 3A). Our findings are consistent with previous unsuccessful attempts to improve bacterial gene activation using tandem SoxS and αNTD[29] or tandem α and ω subunit effectors.[30]

We tested an alternative system for simultaneous recruitment of αNTD and SoxS using a SYNZIP pair to recruit αNTD to MCP-SoxS. SYNZIP recruitment has previously been effective for bacterial CRISPRa.[8,15] We observed effective CRISPRa with αNTD-SYNZIP5/MCP-SYNZIP6, confirming that SYNZIP recruitment of αNTD can activate gene expression (Figure S10). However, gene activation did not increase with αNTD-SYNZIP5/MCP-SoxS-SYNZIP6 compared to MCP-SoxS or MCP-SoxS-SYNZIP6 (Figure 3B). Taken together, these results suggest that bacterial CRISPRa may be sensitive to the precise orientation or positioning of the activator fusion protein, and we lack sufficient information to design an effective tandem multi-effector fusion.

3.3.7. Combined recruitment of AsiA and SoxS is antagonistic

We proceeded to test whether SoxS and AsiA activators could be effective when recruited to a single CRISPR complex. To recruit both activators, we used a dCas9-AsiA fusion and an MS2 scRNA to recruit MCP-SoxS to the same complex. This approach is analogous to the eukaryotic CRISPRa SAM system.[21] However, AsiA and SoxS have non-overlapping optimal target sites (Figure 2), so we had low confidence that this strategy would improve activation. We targeted dCas9-AsiA/MCP-SoxS to an optimal AsiA site but observed no increase in gene activation compared to dCas9-AsiA alone (Figure 4A & S11). Unexpectedly, when dCas9-AsiA/MCP-SoxS was targeted to an optimal SoxS site, we observed a substantial decrease in gene expression compared to only dCas9/MCP-SoxS system (Figure 4A). We also targeted dCas9-AsiA/MCP-SoxS to both the optimal AsiA and SoxS target sites simultaneously by expressing two scRNAs, but again observed a substantial decrease relative to dCas9/MCP-SoxS (Figure 4A). These observations suggest that if SoxS and AsiA are recruited to the same target site, they may have incompatible interactions with RNAP that prevent optimal gene activation.

As an alternative strategy, we used orthogonal CRISPR complexes to target AsiA and SoxS separately to their respective optimal target sites. The current AsiA and SoxS CRISPRa complexes are not orthogonal, with AsiA recruited as an *S. pyogenes* dCas9 (Spy-dCas9) fusion and SoxS recruited to Spy-dCas9 with a scRNA. Therefore, we needed to develop alternative orthogonal targeting mechanisms. One option could be recruitment of

SoxS and AsiA to different sites with Spy-dCas9 and orthogonal scRNAs, so we tested MS2 scRNA-mediated recruitment of MCP-AsiA. However, we observed only small, <1.5-fold CRISPRa effects (Figure S12). Another option could be fusion of AsiA to an alternative, orthogonal Cas protein. We tested AsiA fusions to alternative dCas9 ortholog Sth1-dCas9 (Figure S13) or to dCas12a (Figure S14). There was no detectable activation with Sth1-dCas9 fusion and small, <2-fold CRISPRa effects with dCas12a fusions. Finally, we used MS2 scRNAs to recruit SoxS to the Sth1-dCas9 ortholog.[38] We tested three engineered MS2 scRNA variants and obtained 8-fold gene activation from the scRNA design analogous to the most effective MS2 scRNA for Spy-dCas9 (Figure S15). Although the 8-fold activation with Sth1-dCas9/MCP-SoxS is smaller than the 20- to 40-fold activation effects observed with Spy-dCas9/MCP-SoxS in the same promoter context (Figure S6A & S9A), the Sth1 system provides sufficient activation to proceed with testing as part of a multi-activator CRISPRa system.

We proceeded to deliver AsiA and SoxS to their respective optimal target sites using orthogonal dCas9 proteins for each effector, Spy-dCas9-AsiA and Sth1-dCas9/MCP-SoxS (Figure 4B). We used the modified J1-J3(122) promoter with an Sth1-dCas9-compatible PAM at the -81 target (J306) and Spy-dCas9-compatible PAM at the -192 target. With orthogonal dCas9s and both AsiA and SoxS, we observed ~12-fold gene activation, which is lower than the activation observed with either AsiA alone (30-fold) or SoxS alone (14-fold). Thus, there is an antagonistic effect between SoxS and AsiA even when they are recruited by orthogonal CRISPRa complexes placed >100 bp away from each other. From these results, we believe that there might be competitive, incompatible interactions with RNAP from SoxS and AsiA together. We also cannot rule out the possibility that AsiA and SoxS directly interact and interfere with each other. Although our design rules suggest plausible synergistic activation with AsiA and SoxS, we are unable to design an effective multi-activator CRISPRa system.

3.3.8. Combined recruitment of SoxS and PspF is ineffective

Finally, we evaluated recruitment of the SoxS and PspF activators, each to their respective optimal target site. Because these established systems are based on orthogonal engineered scRNAs, we can recruit SoxS to one dCas9 complex and PspF to another. However, SoxS and PspF have apparently incompatible promoter requirements. PspF interacts directly with σ^{54} and is effective only at σ^{54}-dependent promoters (Figure 2),[14,59] while SoxS functions at most promoters except σ^{54} (Figure S1A). The ineffectiveness of

SoxS at σ^{54} promoters is unsurprising because σ^{54} RNAP requires ATP-dependent remodeling.[58] However, it might be possible for SoxS to enhance PspF-dependent activation at a σ^{54} promoter, with PspF engaging directly with the sigma factor while SoxS interacts with the RpoA subunit. We therefore tested simultaneous recruitment using J1-pspAp, the modified σ^{54} promoter with an upstream array of J1 gRNA target sites. As SoxS and PspF prefer distinct minimal promoters, simultaneous recruitment in tandem fusion to the same target site was ineffective (Figure S16).

PspF and SoxS have optimal target sites that are relatively close, at -60 and -81 from the TSS, respectively. Because these sites might overlap, we targeted PspF with a boxB scRNA to its optimal site at -60 and targeted SoxS with an MS2 scRNA to -81 or to additional upstream sites (Figure 5A). This strategy was chosen because SoxS retains activity at some sites upstream of its optimal -81 site (Figure 2A). Several SoxS target sites produced improvements relative to PspF alone. The largest effect was with PspF at -60 and SoxS at -100, which activated gene expression 18-fold, a 1.8-fold improvement relative to PspF alone (Figure 5B, 5C, & S16). Notably, SoxS alone produces no detectable activation with this promoter, indicating a potential synergistic 1.8-fold improvement. We observed similar effects when SoxS was replaced with αNTD or TetD (Figure 5D, S17, & S18). To determine if this apparent synergistic effect results from recruitment of both activators, we targeted dCas9 alone to the -100 bp site with an sgRNA or an MS2 scRNA and kept recruiting PspF to the -60 bp site. Without SoxS, we observed 1.2-fold and 1.6-fold increases relative to PspF alone (Figure 5E). With these results in mind, we believe the 1.8-fold synergistic effect arises from a combination of small effects: 1.2-fold from recruiting a second dCas9 complex upstream of PspF, 1.3-fold (1.6/1.2) from the MS2 hairpin, and 1.1-fold (1.8/1.6) from SoxS recruitment together with PspF. Taken together, we observed what appears to be a true synergistic effect for the first time with bacterial CRISPRa, but the total 1.8-fold effect is relatively small and only 1.1-fold of the effect comes from the cooperative action of the PspF and SoxS activators.

3.4. Discussion

To improve gene activation with bacterial CRISPRa, we attempted to recruit multiple effectors to simultaneously engage RNAP and cooperatively activate transcription.[23,24] To implement this strategy, we first needed to know where to recruit each effector in the region upstream of the promoter. Bacterial CRISPRa systems typically have strict requirements for target site positions,[6,13,14] so we first systematically mapped preferred target sites for different

CRISPRa systems (Figure 2 and Table 1). We used a set of promoters compatible with multiple CRISPRa systems, which was critical because the preferred target sites for each CRISPRa system can vary in different promoter contexts. Despite defining optimal target sites, we did not observe any large synergistic effects on gene activation. When we recruited the potent activator SoxS together with other SoxS-family activators or with RNA polymerase subunits at the same target site, we observed either impaired or unchanged activation compared to SoxS alone (Figure 3). We observed similar behavior when recruiting the two potent activators SoxS and AsiA at distinct target sites (Figure 4). These antagonistic effects could arise if the RNAP interactions are incompatible and cannot form simultaneously. Finally, we observed a modest but potentially significant ~2-fold synergistic effect when both SoxS and PspF were recruited together (Figure 5). However, this effect arises largely due to simultaneous binding of two CRISPR-Cas complexes, and only a small fraction of the effect is due to the simultaneous action of both SoxS and PspF. We also expect this effect to have limited practical utility at endogenous bacterial gene targets because it is restricted to σ^{54} promoters, which constitute a small fraction of the bacterial genome. Thus, despite careful analysis to identify effective combinations of effectors for synergistic CRISPRa, we remain largely unable to improve upon the gene activation that can be obtained with individual CRISPRa systems.

Our findings emphasize the challenges of bacterial CRISPRa compared to eukaryotic CRISPRa. Prior to the advent of CRISPR-Cas gene regulation, it was well understood that eukaryotic gene activation could be enhanced by recruiting multiple effectors together.[17,19,60,61] These insights were readily transferred to eukaryotic CRISPRa systems, where recruiting multiple effectors produces enhanced and frequently synergistic activation.[17–21,62,63] Similar effects in bacterial CRISPRa systems have not emerged, possibly due to fundamental differences in the mechanisms of gene activation. In eukaryotes, transcription factors interact with multi-protein complexes of coactivators and chromatin modifiers that in turn recruit RNAP.[64,65] Eukaryotic CRISPRa effectors that interact with these complexes can be effective at a broad range of upstream target sites,[66,67] and it is therefore straightforward to enhance gene activation with multiple CRISPRa effectors. In contrast, bacterial CRISPRa effectors typically directly contact RNAP and are subject to strict positioning requirements for productive gene activation.[6,13,14] These precise positioning requirements have made it difficult to identify compatible positions to recruit multiple bacterial effectors. Although we systematically identified sites that should be compatible, we

were unable to enhance bacterial CRISPRa with multiple effectors, suggesting that other structural constraints or unknown factors remain to be addressed.

In principle, synergistic CRISPRa in bacteria should be possible because native transcriptional activators can produce synergistic effects. The best characterized system is the *E. coli* catabolite activator protein (CAP), also known as the cAMP receptor protein (CRP).[24,31,33,34,68,69] Two appropriately positioned CAP sites can simultaneously contact RNAP to synergistically activate transcription. Based in part on this precedent, we originally screened CAP as a potential CRISPRa effector in *E. coli*, but we did not detect any significant transcriptional activation.[27] Given the efficacy of CAP as a synergistic activator, and the failure of existing CRISPRa effectors to achieve synergistic activation, it may be worth revisiting CAP as a potential CRISPRa effector, either with engineered variants or homologs. More broadly, it could be informative to generate structural models of candidate CRISPRa complexes with RNAP and promoter DNA, although the sizes of such complexes are beyond the limits of the current publicly-available Alphafold3 server.[70] These structural models could help to identify combinations of CRISPRa complexes that could simultaneously and cooperatively engage with RNAP to initiate transcription. Ultimately, we hope these approaches will help us towards the long-term goal to achieve predictable and robust activation of any desired endogenous genes in bacteria.

3.5. Materials and Methods

Bacterial strains and plasmid constructs

The bacterial strains used in this study are listed in Table S1. All PCR fragments were amplified with Phusion DNA Polymerase (Thermo-Fisher Scientific) for Infusion Cloning (Takara Bio). Plasmids were transformed into chemically competent *E. coli* DH10B (Thermo Fisher Scientific) or NEB turbo (New England Biolabs) cells, plated on LB-agar, and cultured in LB media with the appropriate antibiotics used in the following concentrations: 100 μg/mL Carbenicillin, 25 μg/mL Chloramphenicol, 30 μg/mL Kanamycin. Plasmids were constructed following previously described methods.[6,27,36] Detailed descriptions of each plasmid used in this work are provided in Table S2. Different CRISPRa plasmids harboring catalytically-inactive Cas9 (dCas9) were constructed using pCD442 (constitutive expression) or pSLQ1055 (aTc-inducible) as backbones.[6,37] dCas9 and Spy-dCas9 refer to

Streptococcus pyogenes dCas9. Sth1-dCas9 refers to a dCas9 homolog from *Streptococcus thermophilus.*[38] *Lachnospiraceae bacterium* dCas12a (Lb-dCas12a or Lb-dCpf1) was used for all dCas12a experiments.[39,40] The SoxS effector used in this study contains two mutations (R93A/S101A) as previously described.[6] The PspF effector used in this study lacks a DNA binding domain as previously reported.[14] AsiA_m2.1, referred to as AsiA in this study, was designed with the amino acid sequence as reported previously by Ho and coworkers.[13] Modified guide RNA sequences were constructed as described previously.[14,27] Throughout the manuscript, "-" will indicate direct protein fusions and "/" will indicate non-covalent recruitment. For example, dCas9-AsiA represents direct fusion of dCas9 and AsiA while dCas9/MCP-SoxS represents MCP-SoxS recruitment to dCas9 via the interaction of MCP with the MS2 RNA hairpin. All plasmid constructs were confirmed by Sanger sequencing (Genewiz/Azenta Life Sciences) or Nanopore sequencing (Primordium/Plasmidsaurus). All relevant sequences are provided in the Supporting Information DNA sequences section. Plasmid maps are deposited as Supporting Information. Selected plasmids will be available on Addgene.

Reporter design and distance screening

To characterize the target site preferences of each CRISPRa system, promoters were designed with J1 upstream sequences (170 bp) containing NGG PAMs every 10bp on both strands.[27] Because the average intergenic region upstream of *E. coli* genes is ~140 bp, the 170 bp sequence covers most targetable sites of *E. coli* promoters.[41] The previously described J1-BBa_J23117-mRFP reporter was used for the σ^{70}-compatible CRISPRa systems. For AsiA, where the optimal target position is further upstream, the J1 array was moved further upstream by inserting additional sequences (100, 200, or 122 bp) between the J1 array and the BBa_J23117 minimal promoter. J1-J3(100) has 100 bp of J3 inserted between J1 and the minimal promoter. J1-J2(100)-J3(100) has 100 bases of J2 and 100 bases of J3 inserted (200 bases total). J1-J3(122) has 122 bases of J3 inserted. The J2 and J3 sequences were described previously.[6,10] Complete sequences of J1-J3(100), J1-J2(100)-J3(100), and J1-J3(122) are provided in the Supporting Information. These designs mimic the W1 promoter used for AsiA activation.[13,26] The J3 sequence adjacent to the minimal promoter includes a J306 target site positioned to be compatible with SoxS/αNTD/TetD CRISPRa (Figure S6 & S7). For PspF-mediated CRISPRa at σ^{54} promoters, the BBa_J23117 minimal promoter was replaced with 35 bp of the pspAp minimal promoter.[14] gRNA target sites are listed in Table S3. Single nucleotide phase-shift

promoters were designed by addition of N bp (+N) between J1 and the minimal promoter or by deletion of N bp (-N) proximal to the minimal promoter. For alternative dCas proteins with PAM preferences different from the NGG used by Spy-dCas9, new promoter systems were designed by mutating the NGG PAM sequence into a compatible PAM or using a strategy previously used for J1 sequence design by tiling PAMs (see Supporting Methods).[27]

Gene expression measurements via fluorescent reporter

Single colonies of bacteria from LB plates were inoculated in 400 µL of EZ-RDM (Teknova) supplemented with the appropriate antibiotics and grown in 96-deep-well plates at 37 °C with shaking overnight at 900 RPM on a Heidolph titramax 1000 for 18 h. 150 µL of the overnight culture were transferred into flat, clear-bottomed black 96-well plates (Corning) and the OD_{600} and fluorescence were measured in a Biotek Synergy HTX plate reader. Data were analyzed using the BioTek Gen5 2.07.17 software. For mRFP1 detection, the excitation wavelength was 540 nm and emission wavelength was 600 nm. For constructs controlled by an aTc-inducible promoter (pCK320, pCK321, and pAK007), single colonies were first inoculated in the inducer-free EZ-RDM. After overnight incubation, the starter cultures were diluted 100-fold into EZ-RDM containing appropriate antibiotics with or without 200 nM anhydrotetracycline (aTc), unless specified. The cultures were further incubated overnight before fluorescent protein measurement.

Supporting information

The Supporting Information is available free of charge.

Supporting methods, CRISPRa effects with alternative effectors and reporters, bacterial strains, plasmids, guide RNA spacer sequences, and sequences of reporter genes, proteins, and guide RNAs.

Authors Contribution

C.K., A.V.K., R.C., K.O., J.M.C. and J.G.Z. conceptualized the research; C.K., A.V.K., R.C., K.O., P.L. and S.S.A. performed experiments; C.K., A.V.K., R.C. and K.O. analyzed the data. C.K., A.V.K., R.C., J.M.C., and J.G.Z. wrote the manuscript with input from all of the authors.

Conflicts of Interest

J.M.C. and J.G.Z. have financial interests in Wayfinder Biosciences, Inc. The remaining authors declare no competing interests related to this work.

Acknowledgements

We thank members of the Carothers and Zalatan groups for helpful discussion. This work was supported by NSF Award MCB 1817623 (J.G.Z. and J.M.C.), MCB 2032794 (J.M.C. and J.G.Z.), CBET 1844152 (J.M.C.), DOE Awards DE-EE0008927 and DE-SC0023091 (J.M.C, J.G.Z.). This material is based upon work supported by the National Science Foundation Graduate Research Fellowship Program under Grant No. DGE-2140004 (A.V.K.). Any opinions, findings, and conclusions or recommendations expressed in this material are those of the author(s) and do not necessarily reflect the views of the National Science Foundation.

3.6. References

(1) Kampmann, M. CRISPRi and CRISPRa Screens in Mammalian Cells for Precision Biology and Medicine. *ACS Chem. Biol.* **2018**, *13* (2), 406–416. https://doi.org/10.1021/acschembio.7b00657.

(2) Sanson, K. R.; Hanna, R. E.; Hegde, M.; Donovan, K. F.; Strand, C.; Sullender, M. E.; Vaimberg, E. W.; Goodale, A.; Root, D. E.; Piccioni, F.; Doench, J. G. Optimized Libraries for CRISPR-Cas9 Genetic Screens with Multiple Modalities. *Nat. Commun.* **2018**, *9* (1), 5416. https://doi.org/10.1038/s41467-018-07901-8.

(3) Schmidt, R.; Steinhart, Z.; Layeghi, M.; Freimer, J. W.; Bueno, R.; Nguyen, V. Q.; Blaeschke, F.; Ye, C. J.; Marson, A. CRISPR Activation and Interference Screens Decode Stimulation Responses in Primary Human T Cells. *Science* **2022**, *375* (6580), eabj4008. https://doi.org/10.1126/science.abj4008.

(4) Fontana, J.; Sparkman-Yager, D.; Faulkner, I.; Cardiff, R.; Kiattisewee, C.; Walls, A.; Primo, T. G.; Kinnunen, P. C.; Garcia Martin, H.; Zalatan, J. G.; Carothers, J. M. Guide RNA Structure Design Enables Combinatorial CRISPRa Programs for Biosynthetic Profiling. *Nat. Commun.* **2024**, *15* (1), 6341. https://doi.org/10.1038/s41467-024-50528-1.

(5) Ameruoso, A.; Villegas Kcam, M. C.; Cohen, K. P.; Chappell, J. Activating Natural Product Synthesis Using CRISPR Interference and Activation Systems in Streptomyces. *Nucleic Acids Res.* **2022**, *50* (13), 7751–7760. https://doi.org/10.1093/nar/gkac556.

(6) Fontana, J.; Dong, C.; Kiattisewee, C.; Chavali, V. P.; Tickman, B. I.; Carothers, J. M.; Zalatan, J. G. Effective CRISPRa-Mediated Control of Gene Expression in Bacteria Must Overcome Strict Target Site Requirements. *Nat. Commun.* **2020**, *11* (1), 1618. https://doi.org/10.1038/s41467-020-15454-y.

(7) Kiattisewee, C.; Karanjia, A. V.; Legut, M.; Daniloski, Z.; Koplik, S. E.; Nelson, J.; Kleinstiver, B. P.; Sanjana, N. E.; Carothers, J. M.; Zalatan, J. G. Expanding the Scope of Bacterial CRISPR Activation with PAM-Flexible dCas9 Variants. *ACS Synth. Biol.* **2022**, *11* (12), 4103–4112. https://doi.org/10.1021/acssynbio.2c00405.

(8) Alba Burbano, D.; Cardiff, R. A. L.; Tickman, B. I.; Kiattisewee, C.; Maranas, C. J.; Zalatan, J. G.; Carothers, J. M. Engineering Activatable Promoters for Scalable and Multi-Input CRISPRa/i Circuits. *Proc. Natl. Acad. Sci.* **2023**, *120* (30), e2220358120. https://doi.org/10.1073/pnas.2220358120.

(9) Barbier, I.; Kusumawardhani, H.; Chauhan, L.; Harlapur, P. V.; Jolly, M. K.; Schaerli, Y. Synthetic Gene Circuits Combining CRISPR Interference and CRISPR Activation in E. Coli: Importance of Equal Guide RNA Binding Affinities to Avoid Context-Dependent Effects. *ACS Synth. Biol.* **2023**, *12* (10), 3064–3071. https://doi.org/10.1021/acssynbio.3c00375.

(10) Tickman, B. I.; Burbano, D. A.; Chavali, V. P.; Kiattisewee, C.; Fontana, J.; Khakimzhan, A.; Noireaux, V.; Zalatan, J. G.; Carothers, J. M. Multi-Layer CRISPRa/i Circuits for Dynamic Genetic Programs in Cell-Free and Bacterial Systems. *Cell Syst.* **2022**, *13* (3), 215-229.e8. https://doi.org/10.1016/j.cels.2021.10.008.

(11) Peng, R.; Wang, Y.; Feng, W.; Yue, X.; Chen, J.; Hu, X.; Li, Z.; Sheng, D.; Zhang, Y.; Li, Y. CRISPR/dCas9-Mediated Transcriptional Improvement of the Biosynthetic Gene Cluster for the Epothilone Production in Myxococcus Xanthus. *Microb. Cell Factories* **2018**, *17* (1), 15. https://doi.org/10.1186/s12934-018-0867-1.

(12) Yin, L.; Xi, D.; Shen, Y.; Ding, N.; Shao, Q.; Qian, Y.; Fang, Y. Rewiring Metabolic Flux in Corynebacterium Glutamicum Using a CRISPR/dCpf1-Based Bifunctional Regulation System. *J. Agric. Food Chem.* **2024**, *72* (6), 3077–3087.

https://doi.org/10.1021/acs.jafc.3c08529.
(13) Ho, H.-I.; Fang, J. R.; Cheung, J.; Wang, H. H. Programmable CRISPR-Cas Transcriptional Activation in Bacteria. *Mol. Syst. Biol.* **2020**, *16* (7), e9427. https://doi.org/10.15252/msb.20199427.
(14) Liu, Y.; Wan, X.; Wang, B. Engineered CRISPRa Enables Programmable Eukaryote-like Gene Activation in Bacteria. *Nat. Commun.* **2019**, *10* (1), 3693. https://doi.org/10.1038/s41467-019-11479-0.
(15) Villegas Kcam, M. C.; Tsong, A. J.; Chappell, J. Rational Engineering of a Modular Bacterial CRISPR–Cas Activation Platform with Expanded Target Range. *Nucleic Acids Res.* **2021**, *49* (8), 4793–4802. https://doi.org/10.1093/nar/gkab211.
(16) Gilbert, L. A.; Horlbeck, M. A.; Adamson, B.; Villalta, J. E.; Chen, Y.; Whitehead, E. H.; Guimaraes, C.; Panning, B.; Ploegh, H. L.; Bassik, M. C.; Qi, L. S.; Kampmann, M.; Weissman, J. S. Genome-Scale CRISPR-Mediated Control of Gene Repression and Activation. *Cell* **2014**, *159* (3), 647–661. https://doi.org/10.1016/j.cell.2014.09.029.
(17) Maeder, M. L.; Linder, S. J.; Cascio, V. M.; Fu, Y.; Ho, Q. H.; Joung, J. K. CRISPR RNA–Guided Activation of Endogenous Human Genes. *Nat. Methods* **2013**, *10* (10), 977–979. https://doi.org/10.1038/nmeth.2598.
(18) Mali, P.; Yang, L.; Esvelt, K. M.; Aach, J.; Guell, M.; DiCarlo, J. E.; Norville, J. E.; Church, G. M. RNA-Guided Human Genome Engineering via Cas9. *Science* **2013**, *339* (6121), 823–826. https://doi.org/10.1126/science.1232033.
(19) Perez-Pinera, P.; Kocak, D. D.; Vockley, C. M.; Adler, A. F.; Kabadi, A. M.; Polstein, L. R.; Thakore, P. I.; Glass, K. A.; Ousterout, D. G.; Leong, K. W.; Guilak, F.; Crawford, G. E.; Reddy, T. E.; Gersbach, C. A. RNA-Guided Gene Activation by CRISPR-Cas9–Based Transcription Factors. *Nat. Methods* **2013**, *10* (10), 973–976. https://doi.org/10.1038/nmeth.2600.
(20) Chavez, A.; Scheiman, J.; Vora, S.; Pruitt, B. W.; Tuttle, M.; P R Iyer, E.; Lin, S.; Kiani, S.; Guzman, C. D.; Wiegand, D. J.; Ter-Ovanesyan, D.; Braff, J. L.; Davidsohn, N.; Housden, B. E.; Perrimon, N.; Weiss, R.; Aach, J.; Collins, J. J.; Church, G. M. Highly Efficient Cas9-Mediated Transcriptional Programming. *Nat. Methods* **2015**, *12* (4), 326–328. https://doi.org/10.1038/nmeth.3312.
(21) Konermann, S.; Brigham, M. D.; Trevino, A. E.; Joung, J.; Abudayyeh, O. O.; Barcena, C.; Hsu, P. D.; Habib, N.; Gootenberg, J. S.; Nishimasu, H.; Nureki, O.; Zhang, F. Genome-Scale Transcriptional Activation by an Engineered CRISPR-Cas9 Complex. *Nature* **2014**, *517*, 583. https://doi.org/10.1038/nature14136.
(22) Tanenbaum, M. E.; Gilbert, L. A.; Qi, L. S.; Weissman, J. S.; Vale, R. D. A Protein-Tagging System for Signal Amplification in Gene Expression and Fluorescence Imaging. *Cell* **2014**, *159* (3), 635–646. https://doi.org/10.1016/j.cell.2014.09.039.
(23) Hochschild, A.; Joung, J. K. Synergistic Activation of Transcription in E. Coli. In *Mechanisms of Transcription*; Eckstein, F., Lilley, D. M. J., Eds.; Nucleic Acids and Molecular Biology; Springer: Berlin, Heidelberg, 1997; pp 101–114. https://doi.org/10.1007/978-3-642-60691-5_8.
(24) Lee, D. J.; Minchin, S. D.; Busby, S. J. W. Activating Transcription in Bacteria. *Annu. Rev. Microbiol.* **2012**, *66* (1), 125–152. https://doi.org/10.1146/annurev-micro-092611-150012.
(25) Lemon, B.; Tjian, R. Orchestrated Response: A Symphony of Transcription Factors for Gene Control. *Genes Dev.* **2000**, *14* (20), 2551–2569. https://doi.org/10.1101/gad.831000.
(26) Bikard, D.; Jiang, W.; Samai, P.; Hochschild, A.; Zhang, F.; Marraffini, L. A. Programmable Repression and Activation of Bacterial Gene Expression Using an Engineered CRISPR-Cas System. *Nucleic Acids Res* **2013**, *41* (15), 7429–7437. https://doi.org/10.1093/nar/gkt520.

(27) Dong, C.; Fontana, J.; Patel, A.; Carothers, J. M.; Zalatan, J. G. Synthetic CRISPR-Cas Gene Activators for Transcriptional Reprogramming in Bacteria. *Nat. Commun.* **2018**, *9* (1), 2489. https://doi.org/10.1038/s41467-018-04901-6.
(28) Fontana, J.; Sparkman-Yager, D.; Zalatan, J. G.; Carothers, J. M. Challenges and Opportunities with CRISPR Activation in Bacteria for Data-Driven Metabolic Engineering. *Curr. Opin. Biotechnol.* **2020**, *64*, 190–198. https://doi.org/10.1016/j.copbio.2020.04.005.
(29) Klanschnig, M.; Cserjan-Puschmann, M.; Striedner, G.; Grabherr, R. CRISPRactivation-SMS, a Message for PAM Sequence Independent Gene up-Regulation in Escherichia Coli. *Nucleic Acids Res.* **2022**, gkac804. https://doi.org/10.1093/nar/gkac804.
(30) Lu, Z.; Yang, S.; Yuan, X.; Shi, Y.; Ouyang, L.; Jiang, S.; Yi, L.; Zhang, G. CRISPR-Assisted Multi-Dimensional Regulation for Fine-Tuning Gene Expression in Bacillus Subtilis. *Nucleic Acids Res.* **2019**, *47* (7), e40–e40. https://doi.org/10.1093/nar/gkz072.
(31) Busby, S.; West, D.; Lawes, M.; Webster, C.; Ishihama, A.; Kolb, A. Transcription Activation by the Escherichia Coli Cyclic AMP: Receptor Protein Receptor Bound in Tandem at Promoters Can Interact Synergistically. *J. Mol. Biol.* **1994**, *241* (3), 341–352. https://doi.org/10.1006/jmbi.1994.1511.
(32) Hoover, T. R.; Santero, E.; Porter, S.; Kustu, S. The Integration Host Factor Stimulates Interaction of RNA Polymerase with NIFA, the Transcriptional Activator for Nitrogen Fixation Operons. *Cell* **1990**, *63* (1), 11–22. https://doi.org/10.1016/0092-8674(90)90284-L.
(33) Joung, J. K.; Koepp, D. M.; Hochschild, A. Synergistic Activation of Transcription by Bacteriophage λ cI Protein and E. Coli cAMP Receptor Protein. *Science* **1994**, *265* (5180), 1863–1866. https://doi.org/10.1126/science.8091212.
(34) Joung, J. K.; Le, L. U.; Hochschild, A. Synergistic Activation of Transcription by Escherichia Coli cAMP Receptor Protein. *Proc. Natl. Acad. Sci.* **1993**, *90* (7), 3083–3087. https://doi.org/10.1073/pnas.90.7.3083.
(35) Richet, E.; Vidal-Ingigliardi, D.; Raibaud, O. A New Mechanism for Coactivation of Transcription Initiation: Repositioning of an Activator Triggered by the Binding of a Second Activator. *Cell* **1991**, *66* (6), 1185–1195. https://doi.org/10.1016/0092-8674(91)90041-v.
(36) Kiattisewee, C.; Dong, C.; Fontana, J.; Sugianto, W.; Peralta-Yahya, P.; Carothers, J. M.; Zalatan, J. G. Portable Bacterial CRISPR Transcriptional Activation Enables Metabolic Engineering in Pseudomonas Putida. *Metab. Eng.* **2021**, *66*, 283–295. https://doi.org/10.1016/j.ymben.2021.04.002.
(37) Qi, L. S.; Larson, M. H.; Gilbert, L. A.; Doudna, J. A.; Weissman, J. S.; Arkin, A. P.; Lim, W. A. Repurposing CRISPR as an RNA-Guided Platform for Sequence-Specific Control of Gene Expression. *Cell* **2013**, *152* (5), 1173–1183. https://doi.org/10.1016/j.cell.2013.02.022.
(38) Rock, J. M.; Hopkins, F. F.; Chavez, A.; Diallo, M.; Chase, M. R.; Gerrick, E. R.; Pritchard, J. R.; Church, G. M.; Rubin, E. J.; Sassetti, C. M.; Schnappinger, D.; Fortune, S. M. Programmable Transcriptional Repression in Mycobacteria Using an Orthogonal CRISPR Interference Platform. *Nat. Microbiol.* **2017**, *2* (4), 16274. https://doi.org/10.1038/nmicrobiol.2016.274.
(39) Tak, Y. E.; Kleinstiver, B. P.; Nuñez, J. K.; Hsu, J. Y.; Horng, J. E.; Gong, J.; Weissman, J. S.; Joung, J. K. Inducible and Multiplex Gene Regulation Using CRISPR-Cpf1-Based Transcription Factors. *Nat. Methods* **2017**, *14* (12), 1163–1166. https://doi.org/10.1038/nmeth.4483.
(40) Zetsche, B.; Gootenberg, J. S.; Abudayyeh, O. O.; Slaymaker, I. M.; Makarova, K. S.;

Essletzbichler, P.; Volz, S. E.; Joung, J.; van der Oost, J.; Regev, A.; Koonin, E. V.; Zhang, F. Cpf1 Is a Single RNA-Guided Endonuclease of a Class 2 CRISPR-Cas System. *Cell* **2015**, *163* (3), 759–771. https://doi.org/10.1016/j.cell.2015.09.038.
(41) Fontana, J.; Voje, W. E.; Zalatan, J. G.; Carothers, J. M. Prospects for Engineering Dynamic CRISPR–Cas Transcriptional Circuits to Improve Bioproduction. *J. Ind. Microbiol. Biotechnol.* **2018**, *45* (7), 481–490. https://doi.org/10.1007/s10295-018-2039-z.
(42) Burbano, D. A.; Kiattisewee, C.; Karanjia, A. V.; Cardiff, R. A. L.; Faulkner, I. D.; Sugianto, W.; Carothers, J. M. CRISPR Tools for Engineering Prokaryotic Systems: Recent Advances and New Applications. *Annu. Rev. Chem. Biomol. Eng.* **2024**, *15* (Volume 15, 2024), 389–430. https://doi.org/10.1146/annurev-chembioeng-100522-114706.
(43) Call, S. N.; Andrews, L. B. CRISPR-Based Approaches for Gene Regulation in Non-Model Bacteria. *Front. Genome Ed.* **2022**, *4*. https://doi.org/10.3389/fgeed.2022.892304.
(44) Bourgade, B.; Xie, H.; Lindblad, P.; Stensjö, K. Development of a CRISPR Activation System for Targeted Gene Upregulation in Synechocystis Sp. PCC 6803. *bioRxiv* **2024**, 2024.10.31.621247. https://doi.org/10.1101/2024.10.31.621247.
(45) Schilling, C.; Koffas, M. A. G.; Sieber, V.; Schmid, J. Novel Prokaryotic CRISPR-Cas12a-Based Tool for Programmable Transcriptional Activation and Repression. *ACS Synth. Biol.* **2020**, *9* (12), 3353–3363. https://doi.org/10.1021/acssynbio.0c00424.
(46) Mencía, M.; Monsalve, M.; Rojo, F.; Salas, M. Substitution of the C-Terminal Domain of the *Escherichia Coli* RNA Polymerase α Subunit by That from *Bacillus Subtilis* Makes the Enzyme Responsive to a *Bacillus Subtilis* Transcriptional Activator. *J. Mol. Biol.* **1998**, *275* (2), 177–185. https://doi.org/10.1006/jmbi.1997.1463.
(47) Chen, Y.; Niu, X.; Cheng, M.; Wang, L.; Sun, P.; Song, H.; Cao, Y. CRISPR/dCas9-RpoD-Mediated Simultaneous Transcriptional Activation and Repression in Shewanella Oneidensis MR-1. *ACS Synth. Biol.* **2022**, *11* (6), 2184–2192. https://doi.org/10.1021/acssynbio.2c00149.
(48) Banta, A. B.; Chumanov, R. S.; Yuan, A. H.; Lin, H.; Campbell, E. A.; Burgess, R. R.; Gourse, R. L. Key Features of σS Required for Specific Recognition by Crl, a Transcription Factor Promoting Assembly of RNA Polymerase Holoenzyme. *Proc. Natl. Acad. Sci.* **2013**, *110* (40), 15955–15960. https://doi.org/10.1073/pnas.1311642110.
(49) Gregory, B. D.; Deighan, P.; Hochschild, A. An Artificial Activator That Contacts a Normally Occluded Surface of the RNA Polymerase Holoenzyme. *J. Mol. Biol.* **2005**, *353* (3), 497–506. https://doi.org/10.1016/j.jmb.2005.08.047.
(50) Gregory, B. D.; Nickels, B. E.; Garrity, S. J.; Severinova, E.; Minakhin, L.; Bieber Urbauer, R. J.; Urbauer, J. L.; Heyduk, T.; Severinov, K.; Hochschild, A. A Regulator That Inhibits Transcription by Targeting an Intersubunit Interaction of the RNA Polymerase Holoenzyme. *Proc. Natl. Acad. Sci.* **2004**, *101* (13), 4554–4559. https://doi.org/10.1073/pnas.0400923101.
(51) Jovanovic, G.; Weiner, L.; Model, P. Identification, Nucleotide Sequence, and Characterization of PspF, the Transcriptional Activator of the Escherichia Coli Stress-Induced Psp Operon. *J. Bacteriol.* **1996**, *178* (7), 1936–1945. https://doi.org/10.1128/jb.178.7.1936-1945.1996.
(52) Danson, A. E.; Jovanovic, M.; Buck, M.; Zhang, X. Mechanisms of Σ54-Dependent Transcription Initiation and Regulation. *J. Mol. Biol.* **2019**, *431* (20), 3960–3974. https://doi.org/10.1016/j.jmb.2019.04.022.
(53) Griffith, K. L.; Shah, I. M.; Myers, T. E.; O'Neill, M. C.; Wolf, R. E. Evidence for "Pre-Recruitment" as a New Mechanism of Transcription Activation in Escherichia Coli:

The Large Excess of SoxS Binding Sites per Cell Relative to the Number of SoxS Molecules per Cell. *Biochem. Biophys. Res. Commun.* **2002**, *291* (4), 979–986. https://doi.org/10.1006/bbrc.2002.6559.
(54) Griffith, K. L.; Wolf, R. E., Jr. Genetic Evidence for Pre-Recruitment as the Mechanism of Transcription Activation by SoxS of Escherichia Coli: The Dominance of DNA Binding Mutations of SoxS. *J Mol Biol* **2004**, *344* (1), 1–10. https://doi.org/10.1016/j.jmb.2004.09.007.
(55) Griffith, K. L.; Becker, S. M.; E. Wolf Jr, R. Characterization of TetD as a Transcriptional Activator of a Subset of Genes of the Escherichia Coli SoxS/MarA/Rob Regulon. *Mol. Microbiol.* **2005**, *56* (4), 1103–1117. https://doi.org/10.1111/j.1365-2958.2005.04599.x.
(56) Dove, S. L.; Joung, J. K.; Hochschild, A. Activation of Prokaryotic Transcription through Arbitrary Protein–Protein Contacts. *Nature* **1997**, *386* (6625), 627–630. https://doi.org/10.1038/386627a0.
(57) Yuan, A. H.; Nickels, B. E.; Hochschild, A. The Bacteriophage T4 AsiA Protein Contacts the β-Flap Domain of RNA Polymerase. *Proc. Natl. Acad. Sci.* **2009**, *106* (16), 6597–6602. https://doi.org/10.1073/pnas.0812832106.
(58) Schumacher, J.; Zhang, X.; Jones, S.; Bordes, P.; Buck, M. ATP-Dependent Transcriptional Activation by Bacterial PspF AAA+Protein. *J. Mol. Biol.* **2004**, *338* (5), 863–875. https://doi.org/10.1016/j.jmb.2004.02.071.
(59) Zhang, N.; Darbari, V. C.; Glyde, R.; Zhang, X.; Buck, M. The Bacterial Enhancer-Dependent RNA Polymerase. *Biochem. J.* **2016**, *473* (21), 3741. https://doi.org/10.1042/BCJ20160741C.
(60) Beerli, R. R.; Segal, D. J.; Dreier, B.; Barbas, C. F. Toward Controlling Gene Expression at Will: Specific Regulation of the erbB-2/HER-2 Promoter by Using Polydactyl Zinc Finger Proteins Constructed from Modular Building Blocks. *Proc. Natl. Acad. Sci.* **1998**, *95* (25), 14628–14633. https://doi.org/10.1073/pnas.95.25.14628.
(61) Carey, M. The Enhanceosome and Transcriptional Synergy. *Cell* **1998**, *92* (1), 5–8. https://doi.org/10.1016/S0092-8674(00)80893-4.
(62) Cheng, A. W.; Wang, H.; Yang, H.; Shi, L.; Katz, Y.; Theunissen, T. W.; Rangarajan, S.; Shivalila, C. S.; Dadon, D. B.; Jaenisch, R. Multiplexed Activation of Endogenous Genes by CRISPR-on, an RNA-Guided Transcriptional Activator System. *Cell Res.* **2013**, *23* (10), 1163–1171. https://doi.org/10.1038/cr.2013.122.
(63) Farzadfard, F.; Perli, S. D.; Lu, T. K. Tunable and Multifunctional Eukaryotic Transcription Factors Based on CRISPR/Cas. *ACS Synth. Biol.* **2013**, *2* (10), 604–613. https://doi.org/10.1021/sb400081r.
(64) Kornberg, R. D. Mediator and the Mechanism of Transcriptional Activation. *Trends Biochem. Sci.* **2005**, *30* (5), 235–239. https://doi.org/10.1016/j.tibs.2005.03.011.
(65) Panne, D. The Enhanceosome. *Curr. Opin. Struct. Biol.* **2008**, *18* (2), 236–242. https://doi.org/10.1016/j.sbi.2007.12.002.
(66) Roth, G. V.; Gengaro, I. R.; Qi, L. S. Precision Epigenetic Editing: Technological Advances, Enduring Challenges, and Therapeutic Applications. *Cell Chem. Biol.* **2024**, *31* (8), 1422–1446. https://doi.org/10.1016/j.chembiol.2024.07.007.
(67) Wang, H.; Russa, M. L.; Qi, L. S. CRISPR/Cas9 in Genome Editing and Beyond. *Annu. Rev. Biochem.* **2016**, *85* (1), 227–264. https://doi.org/10.1146/annurev-biochem-060815-014607.
(68) Beatty Christine M.; Browning Douglas F.; Busby Stephen J. W.; Wolfe Alan J. Cyclic AMP Receptor Protein-Dependent Activation of the Escherichia Coli acsP2 Promoter by a Synergistic Class III Mechanism. *J. Bacteriol.* **2003**, *185* (17), 5148–5157. https://doi.org/10.1128/jb.185.17.5148-5157.2003.
(69) Scott, S.; Busby, S.; Beacham, I. Transcriptional Co-Activation at the ansB Promoters: Involvement of the Activating Regions of CRP and FNR When Bound in Tandem. *Mol.*

Microbiol. **1995**, *18* (3), 521–531. https://doi.org/10.1111/j.1365-2958.1995.mmi_18030521.x.

(70) Abramson, J.; Adler, J.; Dunger, J.; Evans, R.; Green, T.; Pritzel, A.; Ronneberger, O.; Willmore, L.; Ballard, A. J.; Bambrick, J.; Bodenstein, S. W.; Evans, D. A.; Hung, C.-C.; O'Neill, M.; Reiman, D.; Tunyasuvunakool, K.; Wu, Z.; Žemgulytė, A.; Arvaniti, E.; Beattie, C.; Bertolli, O.; Bridgland, A.; Cherepanov, A.; Congreve, M.; Cowen-Rivers, A. I.; Cowie, A.; Figurnov, M.; Fuchs, F. B.; Gladman, H.; Jain, R.; Khan, Y. A.; Low, C. M. R.; Perlin, K.; Potapenko, A.; Savy, P.; Singh, S.; Stecula, A.; Thillaisundaram, A.; Tong, C.; Yakneen, S.; Zhong, E. D.; Zielinski, M.; Žídek, A.; Bapst, V.; Kohli, P.; Jaderberg, M.; Hassabis, D.; Jumper, J. M. Accurate Structure Prediction of Biomolecular Interactions with AlphaFold 3. *Nature* **2024**, *630* (8016), 493–500. https://doi.org/10.1038/s41586-024-07487-w.

3.7. Figures

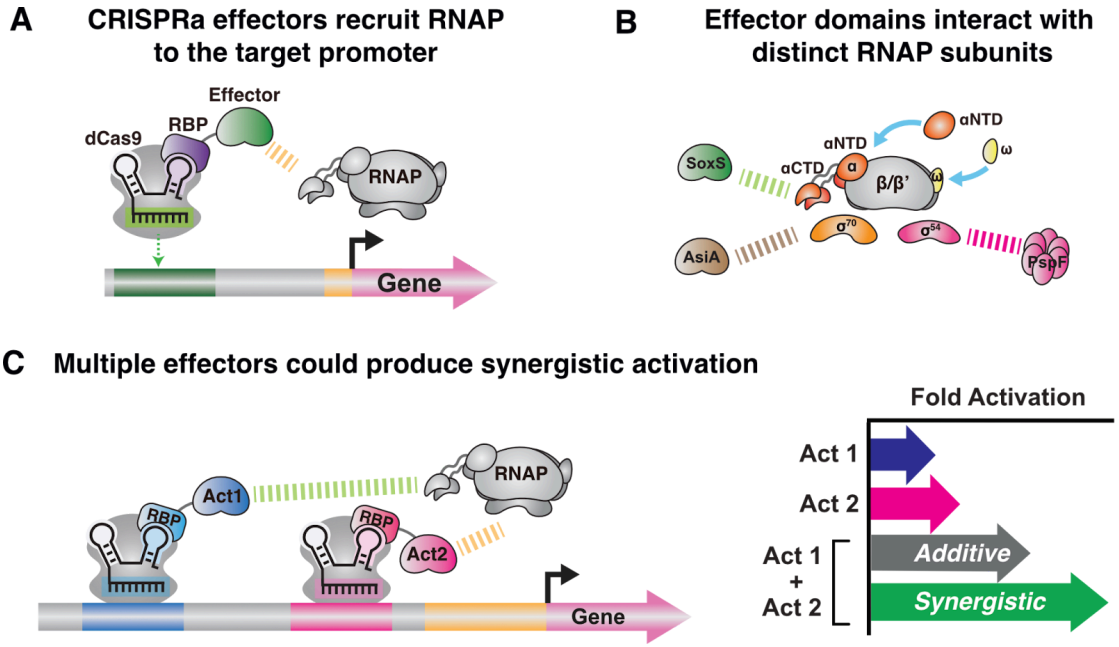

Figure 1. CRISPRa-recruited effector proteins activate gene expression.

A) Bacterial CRISPRa systems recruit transcription factors that interact with RNAP. **B**) Bacterial CRISPRa effectors use various mechanisms to recruit RNAP, including interactions with the α-subunit (RpoA), the σ^{70}-subunit (RpoD), or the σ^{54}-subunit (RpoN). Some strategies use an RNAP subunit itself as the transcriptional effector in the CRISPR-Cas complex. **C**) Proposed model for synergistic activation with multiple CRISPRa complexes providing cooperative interactions with RNAP.

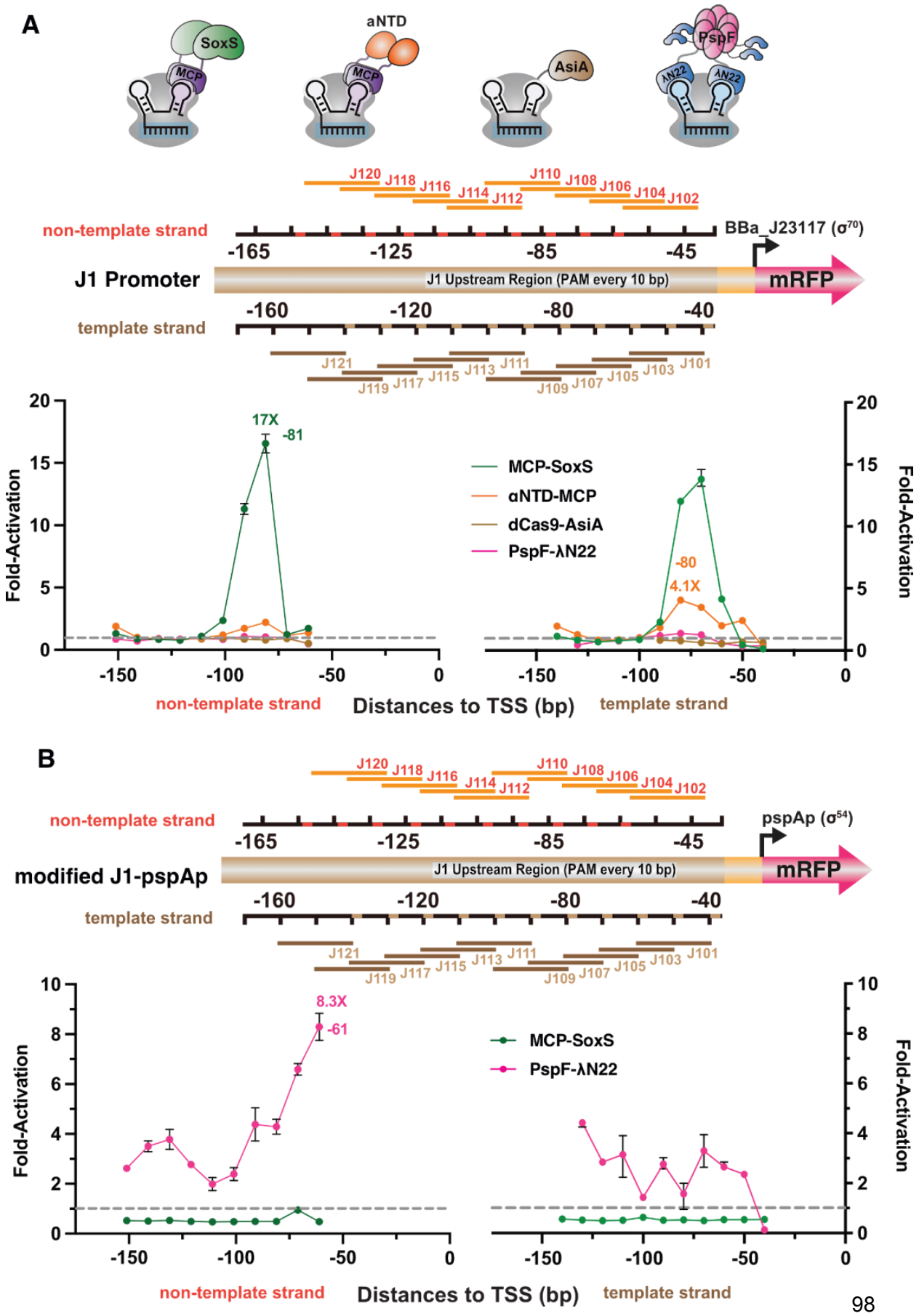
A
SoxS
MCP
aNTD
MCP
AsiA
PspF
λN22
λN22
J120 J118 J116 J114 J112
J110 J108 J106 J104 J102
non-template strand
BBa_J23117 (σ70)
-165 -125 -85 -45
J1 Promoter
J1 Upstream Region (PAM every 10 bp)
mRFP
-160 -120 -80 -40
template strand
J121 J119 J117 J115 J113 J111 J109 J107 J105 J103 J101
17X
-81
-80
4.1X
MCP-SoxS
αNTD-MCP
dCas9-AsiA
PspF-λN22
Fold-Activation
-150 -100 -50 0
non-template strand
Distances to TSS (bp)
template strand
B
modified J1-pspAp
pspAp (σ54)
8.3X
-61
MCP-SoxS
PspF-λN22

Figure 2. CRISPRa is highly sensitive to target site and promoter context.

A) The J1 promoter was used to screen four CRISPRa effectors. J1 contains an array of PAM sequences every 10 bp on both strands upstream of the σ^{70} minimal promoter BBa_J23117 (DNA sequences available in Supporting Information). MCP-SoxS and αNTD-MCP showed optimal fold-activation at -81(NT) and -70(T), respectively. dCas9-AsiA and PspF-λN22 exhibited no activity at any J1 target sites. dCas9-AsiA has activity at target sites further upstream (Figure S7). **B**) Screening for activity with MCP-SoxS and PspF-λN22 using a J1 array upstream of a σ^{54} minimal promoter pspAp. Only PspF showed CRISPRa activity with maximum activity at -61(NT). Values in panel A and B represent the mean ± standard deviation calculated from n = 3.

Table 1. Design rules for different CRISPRa effectors.

Activator	**Mechanism**	**Reported optimal target sites**	**Strand Preference**	**Optimal target sites on J1**
SoxS	RpoA pre-recruitment [53,54]	-60 to -100[27]	Non-template (bottom)	-60 to -100
TetD (SoxS family)	RpoA pre-recruitment[55]	-60 to -100[27]	Non-template (bottom)	-60 to -100
αNTD	RNAP assembly[56]	-60 to -100[27]	Template (top)	-60 to -100
AsiA	RpoD and RpoB binding[49,57]	-182 to -252[13]	Template (top)	-192 to -202
PspF	RpoN recruitment and ATP-dependent activation[51,58]	-91 to -131[14]	Non-template (bottom)	-50 to -80

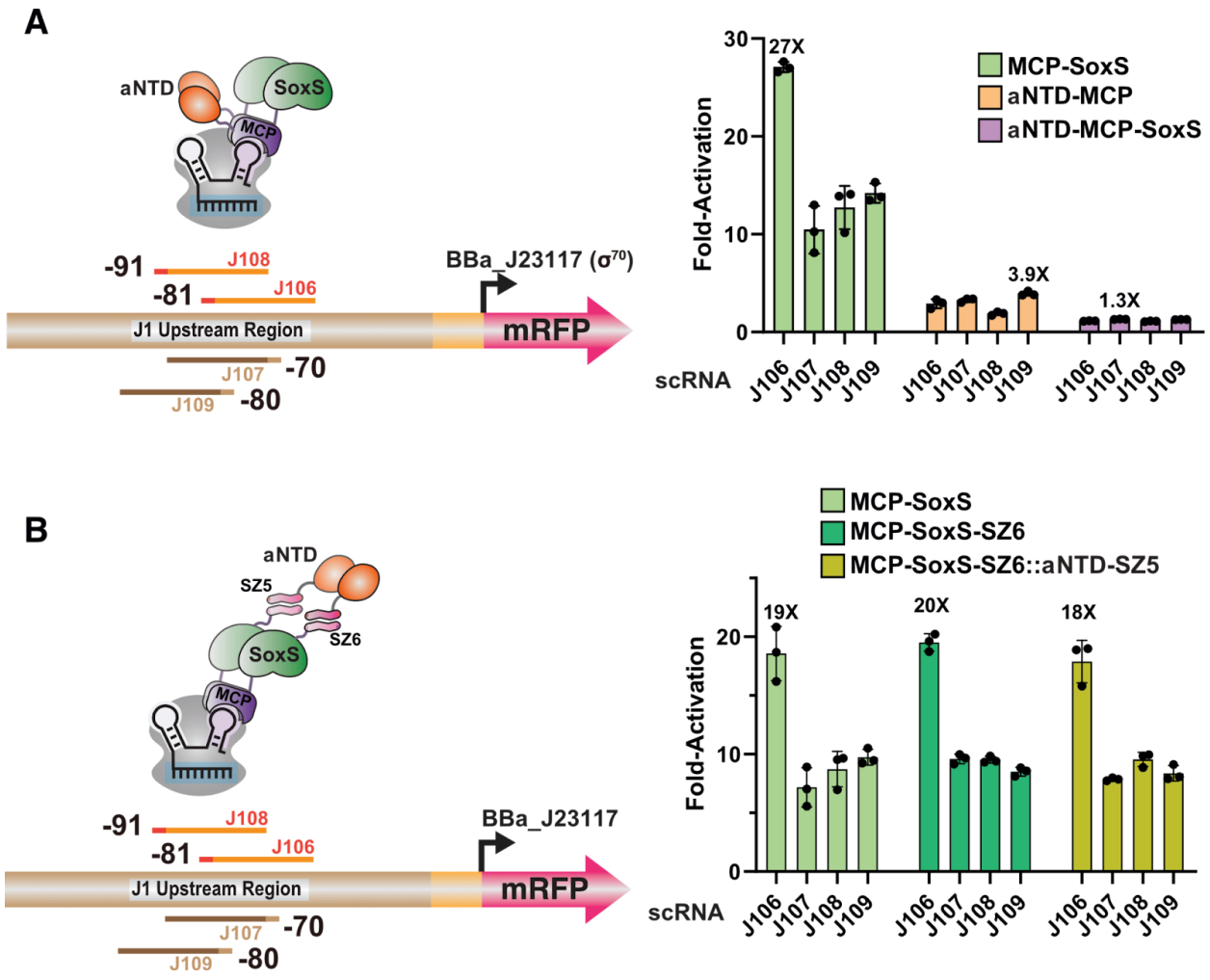

Figure 3. Combined recruitment of SoxS and αNTD is antagonistic or ineffective.

A) Fusion of αNTD-MCP-SoxS (purple) yielded diminished CRISPRa activity compared to αNTD-MCP alone (orange) or MCP-SoxS alone (green) alone. **B)** SYNZIP-mediated recruitment of αNTD to MCP-SoxS does not increase gene expression compared to MCP-SoxS. Values in panel A and B represent the mean ± standard deviation calculated from n = 3.

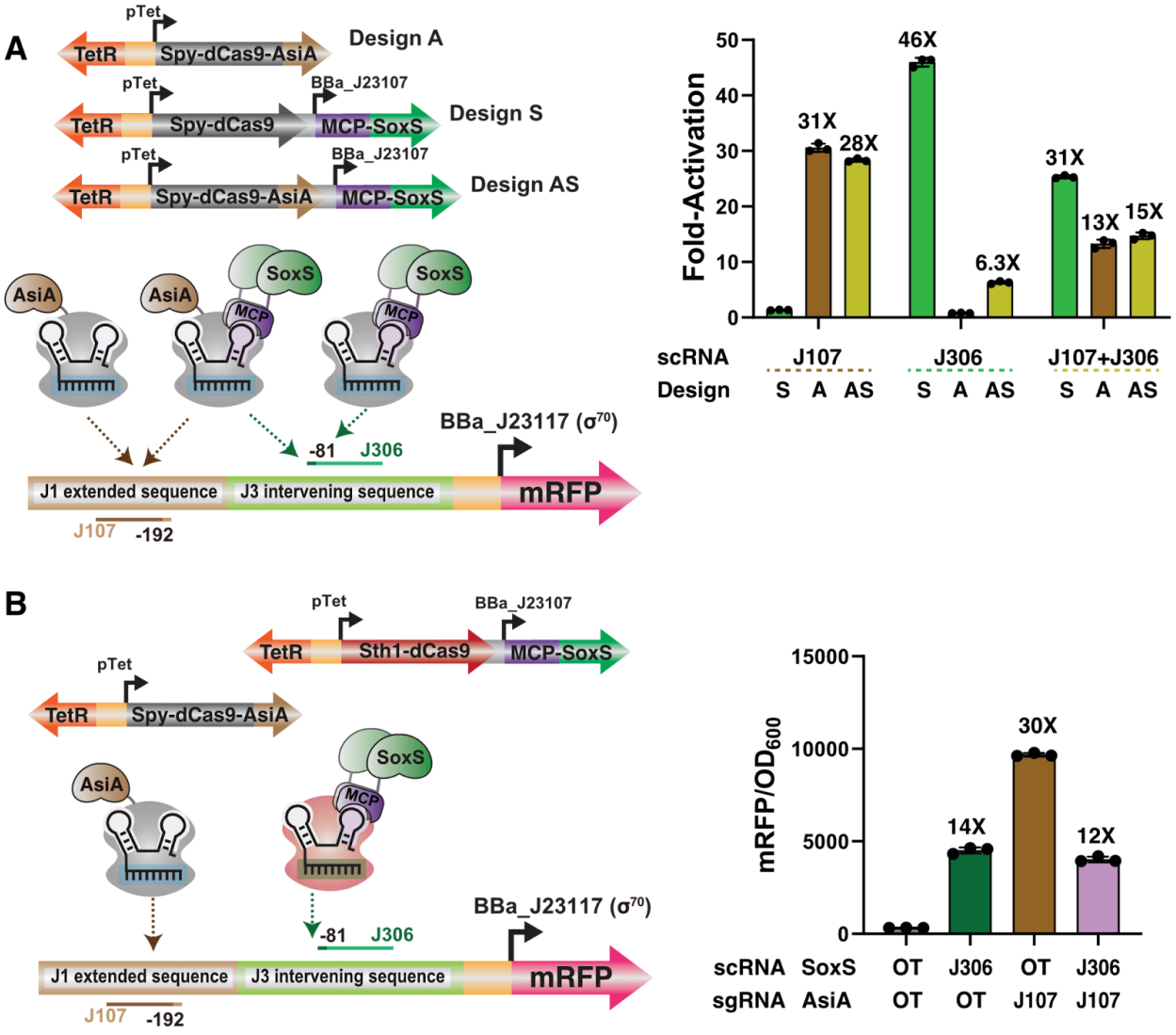

Figure 4. SoxS and AsiA CRISPRa exhibit antagonistic effects.

A) dCas9-AsiA, dCas9/MCP-SoxS, or dCas9-AsiA/MCP-SoxS recruitment to optimal target sites for AsiA (J107, -192) or SoxS (J306, -81). At the optimal AsiA site, dCas9-AsiA/MCP-SoxS does not improve activation relative to dCas9-AsiA. At the optimal SoxS site, dCas9-AsiA/MCP-SoxS is substantially impaired compared to dCas9/MCP-SoxS. With both gRNAs expressed to target the CRISPRa complex to both sites simultaneously, dCas9-AsiA/MCP-SoxS is impaired compared to dCas9/MCP-SoxS and roughly equivalent to dCas9-AsiA. **B)** Targeting AsiA and SoxS to their respective optimal sites with Spy-dCas9-AsiA and Sth1-dCas9/MCP-SoxS. Combined AsiA/SoxS produced lower activation (12-fold) than that observed with either AsiA alone (30-fold) or SoxS alone (14-fold). Values in panel A and B represent the mean ± standard deviation calculated from n = 3.

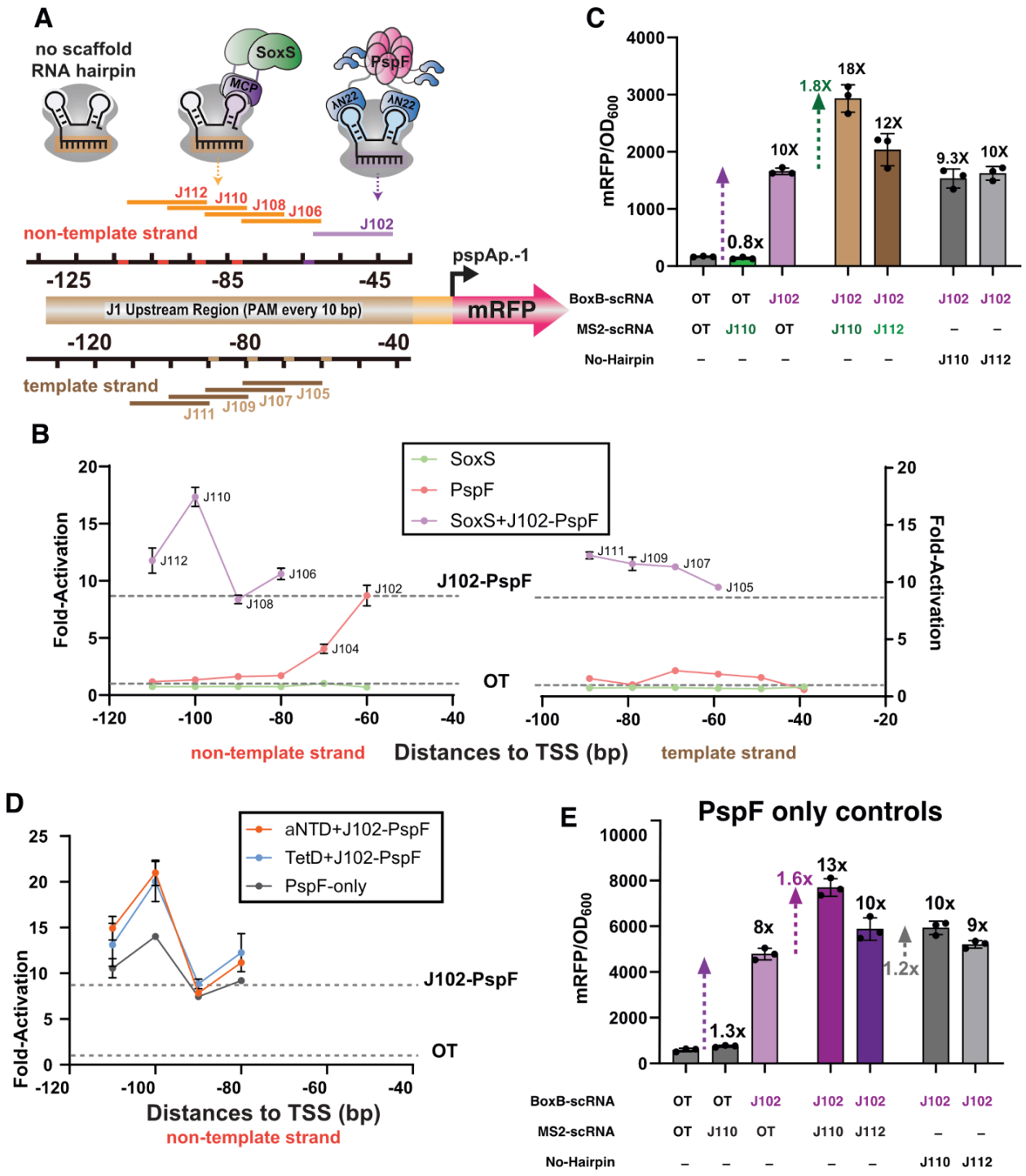

Figure 5. Combined recruitment of PspF and SoxS is ineffective.

A) MCP-SoxS and PspF-λN22 CRISPRa complexes are recruited with orthogonal MS2 and boxB scRNAs, respectively, to the σ^{54} J1-pspAp-1 promoter (Figure S8B). PspF is targeted to its optimal position -60 bp (J102) upstream of TSS and the SoxS-mediated CRISPR complex was screened at target sites from -60 to -110 bp. **B)** CRISPRa with SoxS alone, PspF alone, or SoxS and PspF at a range of sites with the σ^{54} J1-pspAp-1 promoter. For

simultaneous recruitment of PspF and SoxS, PspF is fixed at -60 and the x-axis refers to the target site for SoxS. **C)** Comparison of SoxS alone, PspF alone, or SoxS and PspF with PspF at -60 (J102) and SoxS at -100 (J110) or -110 (J112). With SoxS at -100 and PspF at -60, there is an 18-fold increase in gene expression, above what would be predicted from the combination of SoxS alone (0.8-fold) and PspF alone (10-fold). This increase is dependent on the presence of the MS2 hairpin, which recruits SoxS to the J110 or J112 target sites. **D)** CRISPRa with αNTD+PspF, TetD+PspF, or PspF alone. For simultaneous recruitment of PspF with αNTD or TetD, PspF was fixed at -60 and the x-axis refers to the target site for αNTD or TetD. With αNTD or TetD at -100 and PspF at -60, there is a 20-fold increase in gene expression, similar to the effect observed with SoxS and PspF. **E)** Controls for PspF CRISPRa in the absence of a second activator. With PspF recruited to -60, recruitment of dCas9 to the -100 site with an sgRNA increases gene expression 1.2-fold, and using an MS2 scRNA at -100 increases gene expression 1.6-fold relative to PspF alone. Values in panels B-E represent the mean ± standard deviation calculated from n = 3.

3.8. Supplementary Information

Supporting Methods

Multiple-plasmid systems for CRISPRa screening in *E. coli*

Three plasmids with different replicons and antibiotic markers were used in this study; 1) p15A-CmR, 2) pSC101-AmpR, and 3) ColE1-KmR. For all experiments, dCas9 or dCas9-AsiA were expressed from p15A-CmR. All RBP-activators were expressed on a p15A-CmR plasmid together with dCas9 constructs. Multiple activators were always constructed in a single p15A-CmR plasmid. mRFP reporters with systematically tiled promoters were always on low-copy pSC101-AmpR plasmids. sgRNAs or scRNAs (sgRNAs modified with RNA hairpins) were expressed on ColE1-KmR when delivered as part of a three plasmid system. In some cases, sgRNAs/scRNAs were incorporated into p15A-CmR or pSC101-AmpR for delivery as a two plasmid system. For expression of multiple scRNAs, both gRNA expression cassettes were co-expressed from the same ColE1-KmR plasmid. Details for each plasmid are available in Table S2. Plasmids used for each figure are also listed in Table S5.

AsiA recruitment via engineered gRNA

Following previous work, we used an MS2 scRNA to recruit MCP to the CRISPRa complex.[1,2] In the original report by Dong et al.,[1] expression of wild type AsiA fused with MCP was toxic unless coexpressed with the RpoD F563Y mutant. In the evolved AsiA_m2.1 variant developed by Ho et al.,[2] MCP-AsiA was successfully expressed with an aTc-inducible promoter. When we initially attempted to express MCP-AsiA_m2.1 with a medium constitutive promoter (BBa_J23107), we observed multiple mutations similar to that observed previously when attempting to express wt AsiA.[1] We therefore expressed MCP-AsiA with an aTc-inducible promoter. However, this scRNA-based system showed negligible CRISPRa-mediated gene activation (<1.5-fold) (Figure S12), consistent with previous reports.[2]

Systematically tiled promoters for Sth1-dCas9 and Lb-dCas12a

For CRISPRa with alternative Cas proteins, new promoter systems were designed for systematic characterization using a strategy previously used for J1 sequence design.[1] For *Streptococcus thermophilus* dCas9 fused with AsiA_m2.1, termed Sth1-dCas9-AsiA in this manuscript, we used custom Python scripts to generate 180 nt tiling arrays with NNAGAAW PAM site every 20 nt with 5'-NNAGAAWNNNNNNNNNNNNN-3' as a 20 base spacer sequence for each sgRNA (each 20 base spacer is followed by the NNAGAAW PAM, so the next 20 base spacer begins with NNAGAAW). We randomly generated 100,000 sequences of 180 nt and filtered for endogenous GC content of *E. coli* (50.8%). We discarded any sequences with four consecutive identical nucleotides and sequences containing known *E. coli* transcription factor binding sites.[3] Finally, we omitted sequences that have common restriction enzyme sites and arbitrarily selected one sequence, referred as K1, for further systematic screening with a corresponding set of sgRNAs (K101-K108). We constructed a new promoter (K1T) by modifying the J1-J3(122bp) promoter to replace the upstream J1 array with the K1 array. The K1T promoter has protospacer sequences on the top strand (Figure S13). We constructed a variant promoter K1B with the 180 nt K1 sequence flipped so that the protospacer sequences were on the bottom strand. We also constructed variants of each promoter shifted by 10 nt (K1T+10 and K1B+10). For MCP-SoxS activation with Sth1-dCas9, we constructed a J3-Sth1 promoter by modifying the J3 promoter to replace the *S. py* dCas9 AGG PAM with the Sth1-dCas9 TGAGAAT PAM at the J306 target site 81 nt upstream of the TSS.

For *Lachnospiraceae bacterium* dCas12a fused with AsiA_m2.1, termed dCas12a-AsiA in this work, we generated 170 nt tiling arrays with TTTV PAM sites every 20 nt with 5'-NNNNNNNNNNNNNNNNTTTV-3' as a 20 base spacer sequence for each sgRNA (each 20 base spacer is preceded by the TTTV PAM, so the preceding 20 base spacer ends with TTTV). We randomly generated 100,000 sequences of 170 nt and applied the same selection criteria as described above to generate the I1 sequence and I101-108 crRNAs. I1T and I1B and their +10 nt shifted promoters were constructed in a similar manner as in K1 promoter systems (Figure S14). For the I1T promoter, we also constructed +5 nt to +15 nt variants.

All tested Sth1-dCas9-AsiA and dCas12a-AsiA conditions exhibited no significant change in gene expression. Therefore, MCP-SoxS recruitment by Sth1-dCas9 was prioritized (Figure S15).

Supporting Figures

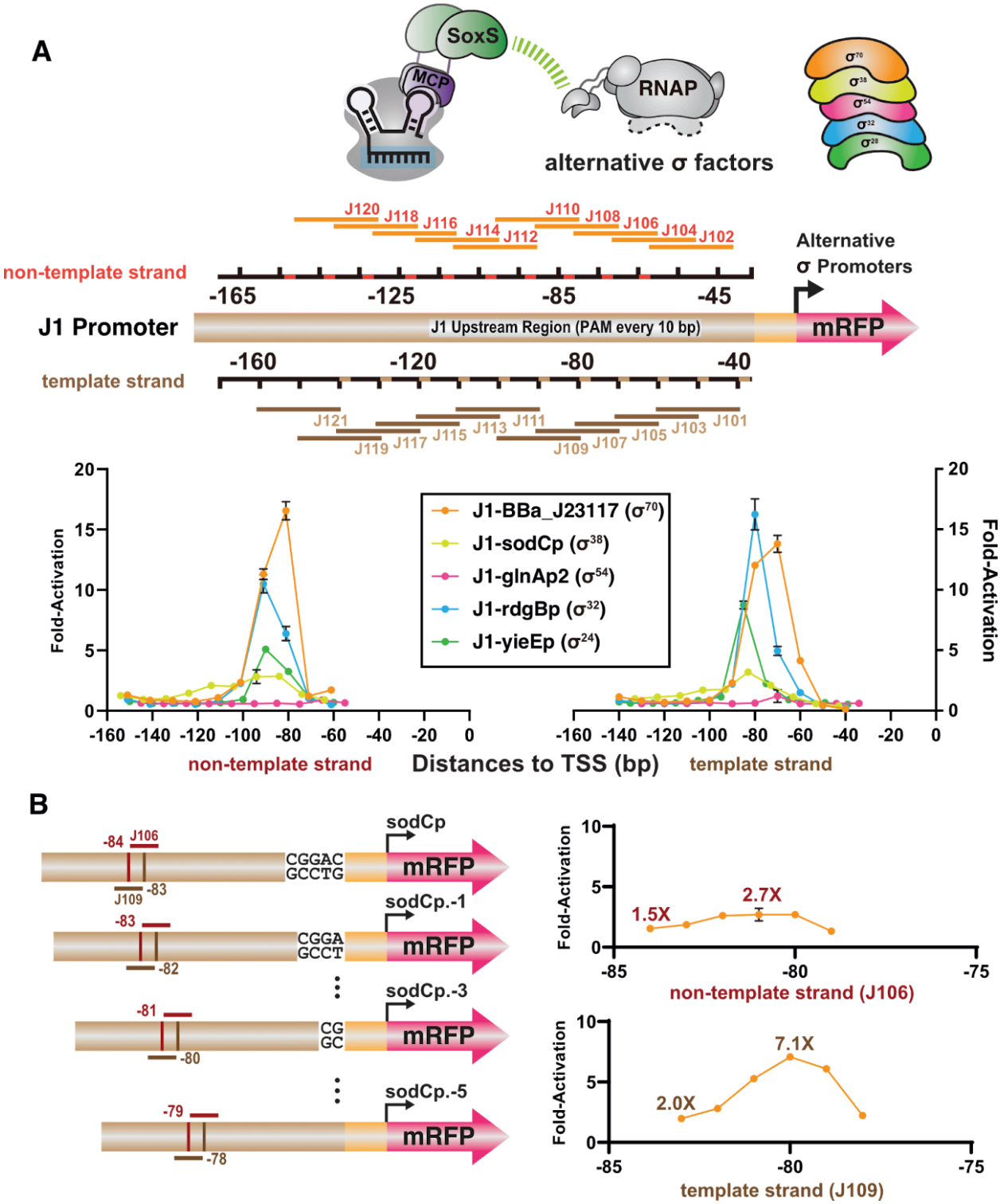

Figure S1. Target site screening for SoxS-mediated CRISPRa at alternative σ-factor promoters.

A) Target site screening from -40 to -170 bp upstream of the TSS in the J1 reporter, following a previously-reported approach.[4] For most of the σ^{70} family promoters, the optimal sites are in a narrow range 60-100 bp upstream of TSS. The σ^{54} promoter, glnAp2, is the exception as it cannot be activated by SoxS. **B)** CRISPRa screening at phase-shifted sodCp (σ^{54}) promoters with 1 bp resolution. Shifting the target sites from -83 bp to -80 bp showed optimal CRISPR activity similar to the optimal phase of σ^{70} promoters. Values in panel A and B represent the mean ± standard deviation calculated from n = 3.

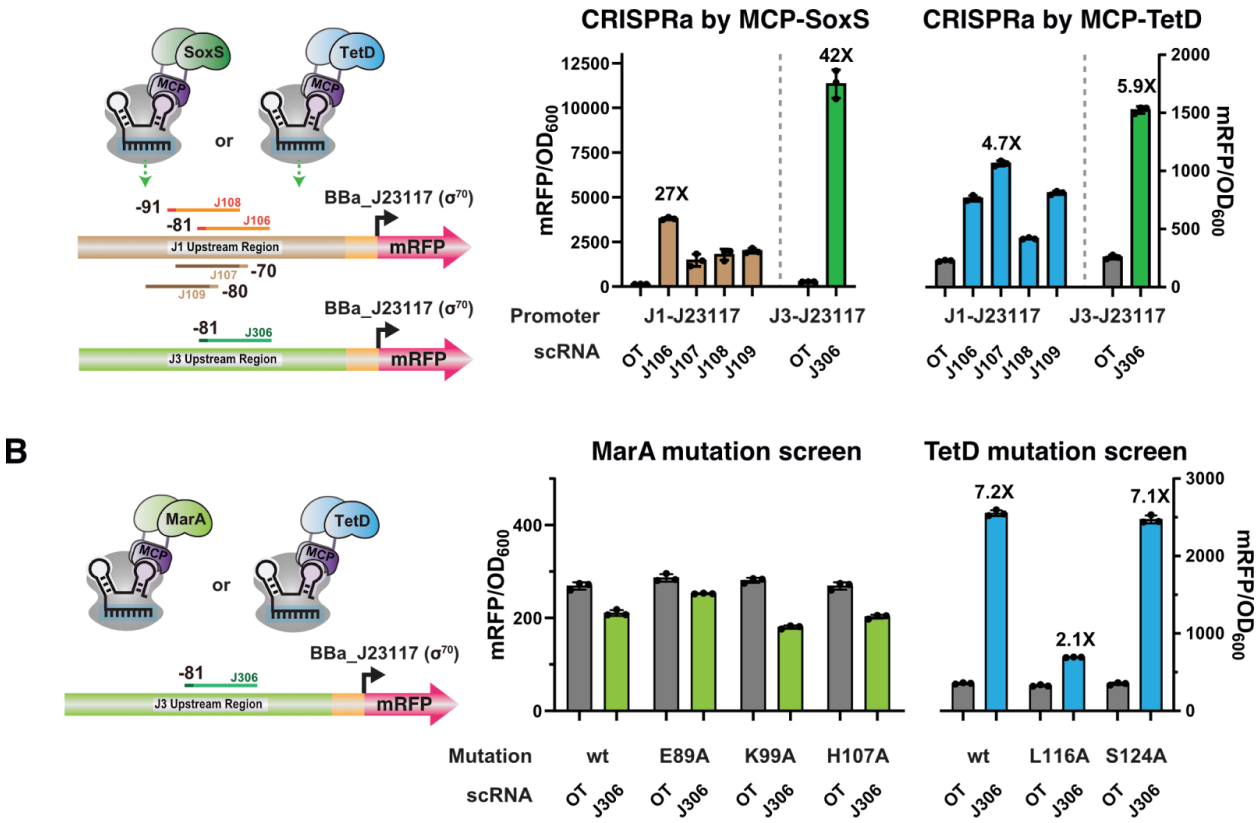

Figure S2. CRISPRa with MarA and TetD mutants.

A) CRISPRa at J1 (J106-J109) and J3 (J306) reporters with MCP-SoxS and MCP-TetD. **B)** CRISPRa with MarA and TetD mutants at a J3 (J306) reporter. MarA mutants showed no improved activation beyond wild-type MarA and TetD mutants showed no improved activation beyond wild-type TetD. hAAVS1 scRNA was used as off-target scRNA in all cases. Values in panel A and B represent the mean ± standard deviation calculated from n = 3.

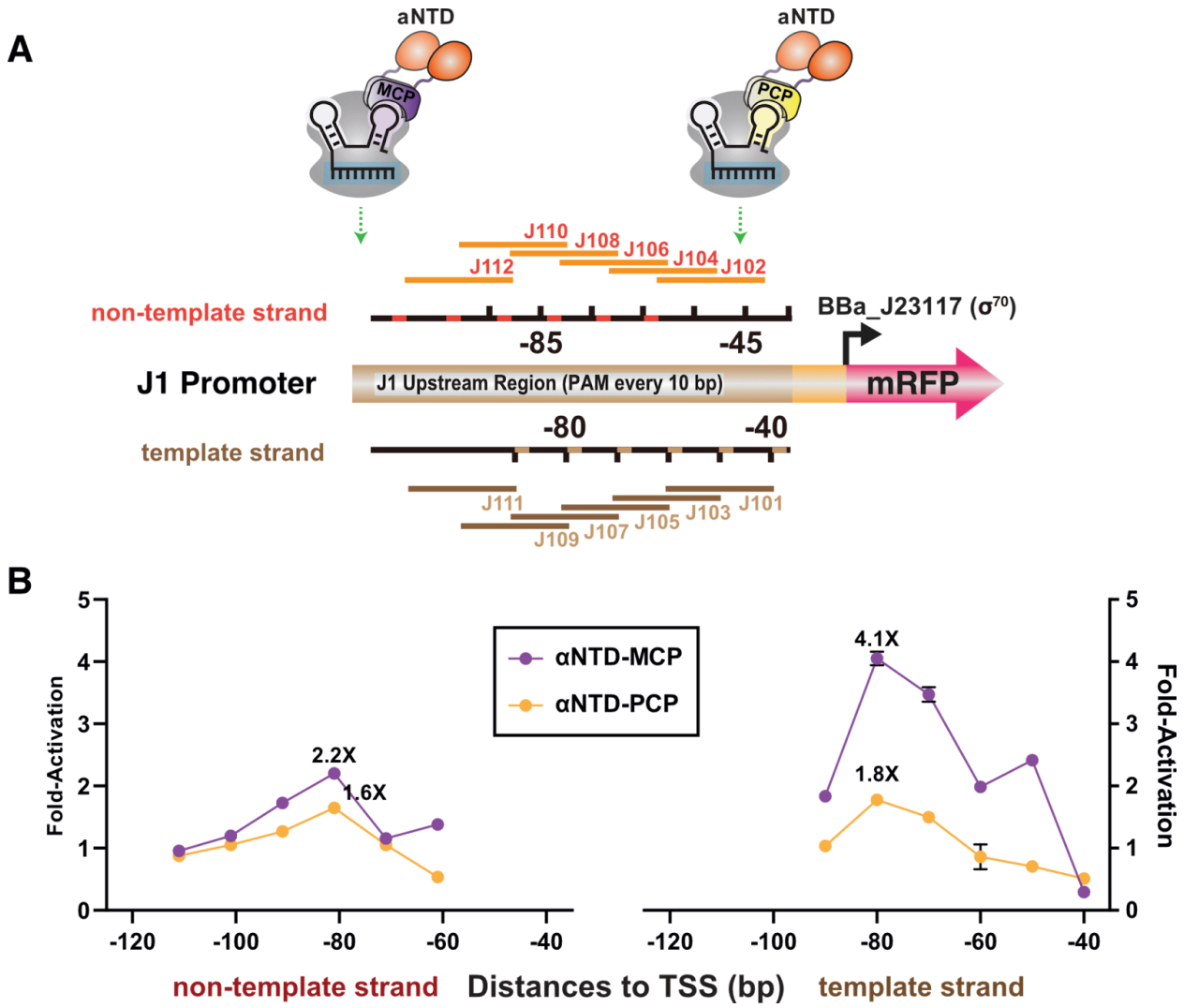

Figure S3. αNTD-mediated CRISPRa with RNA-binding protein recruitment.
A) Conceptual depiction of CRISPRa screening at 40-111 bp (J101-J112) upstream of the TSS by αNTD-MCP and αNTD-PCP. **B)** CRISPRa screening showed that J109 (-80 on the template strand) is the optimal site for αNTD in both MCP- and PCP-based recruitment. Values in panel B represent the mean ± standard deviation calculated from n = 3.

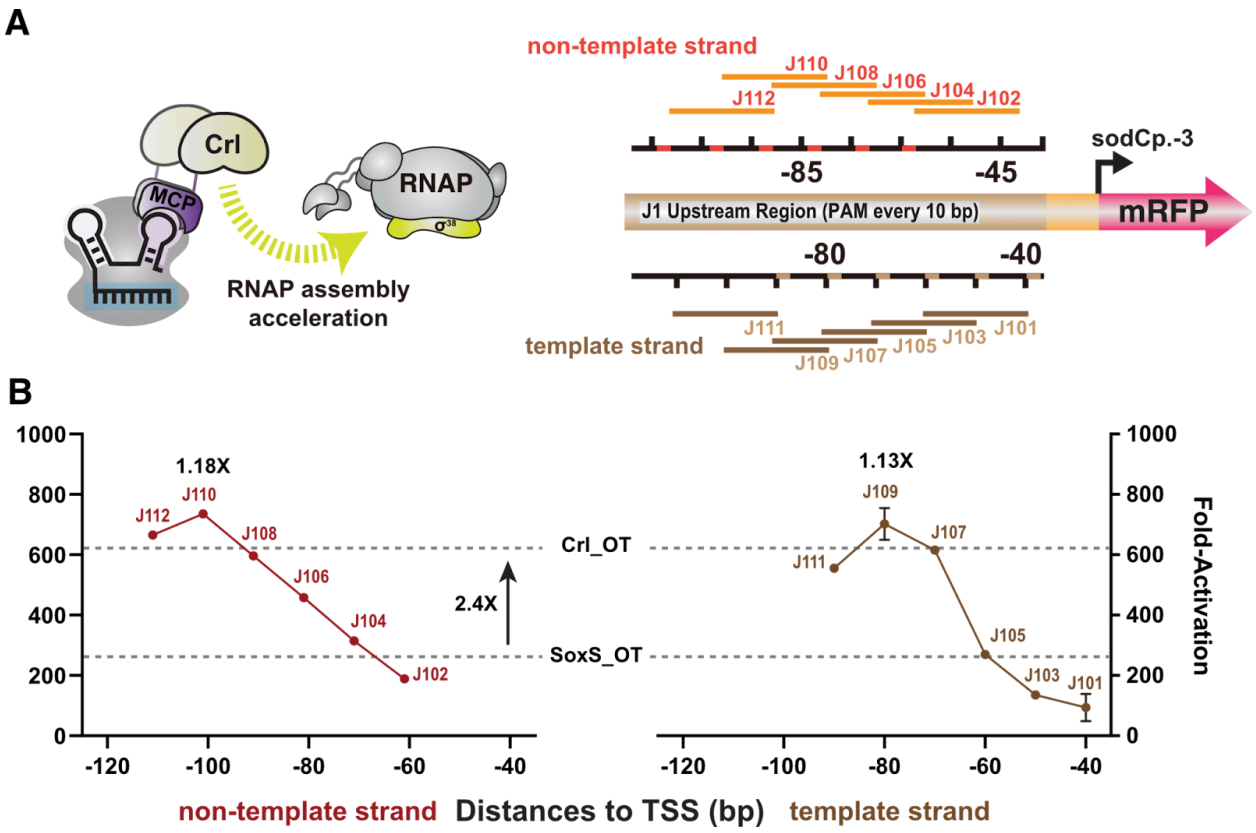

Figure S4. RNAP-σ^{38} assembly using MCP-Crl.

A) Schematic of CRISPRa screening at 40-111 bp (J101-J112) upstream of the TSS at the J1-sodCp.-3 (σ^{38} promoter) by MCP-Crl. **B)** CRISPRa screening showed weak activity at J109 (1.13x) and J110 (1.18x) relative to the Crl off-target control (Crl_OT). The hAAVS1 sequence was used for the off-target scRNA. Significant non-specific gene activation could be observed by expressing MCP-Crl alone (2.4x) compared to MCP-SoxS expression (SoxS_OT). Since the *crl* gene is silent in *E. coli* K-12 MG1655 used in this study,[5] the presence of Crl alone may upregulate RNAP-σ^{38} assembly without localization by CRISPR complex. Values in panel B represent the mean ± standard deviation calculated from n = 3.

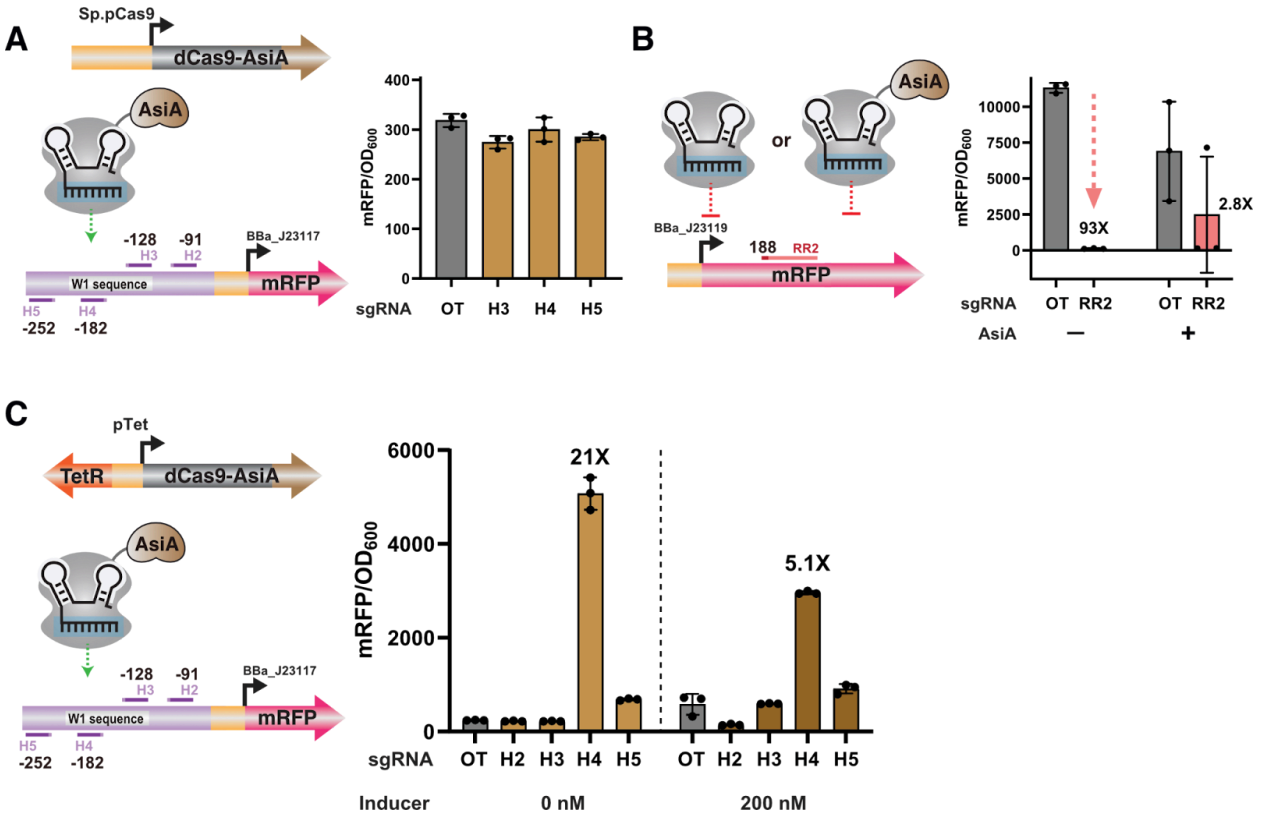

Figure S5. CRISPRa with dCas9-AsiA.

A) CRISPRa screening at the W1 reporter with dCas9-AsiA when expressed under the constitutive Sp.pCas9 promoter showed no significant activation at target sites previously reported to be effective (H4 & H5 at -182 and -252 bp).[2] **B)** CRISPRi using an mRFP-targeting sgRNA (RR2) paired with either dCas9 or dCas9-AsiA showed variable and impaired activity with constitutively-expressed dCas9-AsiA, suggesting unstable expression. **C)** CRISPRa with dCas9-AsiA expressed from an aTc-inducible TetR-Ptet promoter showed 21-fold activation from H4 sgRNA even in an absence of inducer. Induction of dCas9-AsiA led to a 2.4 increase in basal expression (compare OT samples with and without inducer) and a decrease in CRISPRa-mediated expression level. The increase in basal expression may be due to a non-specific effect of dCas9-AsiA.[2] The decrease in CRISPRa-mediated gene expression is unexpected and could be a result of metabolic burden derived from expression of AsiA, as suggested previously.[1] See also Figure S11. Values in panel A, B, and C represent the mean ± standard deviation calculated from n = 3.

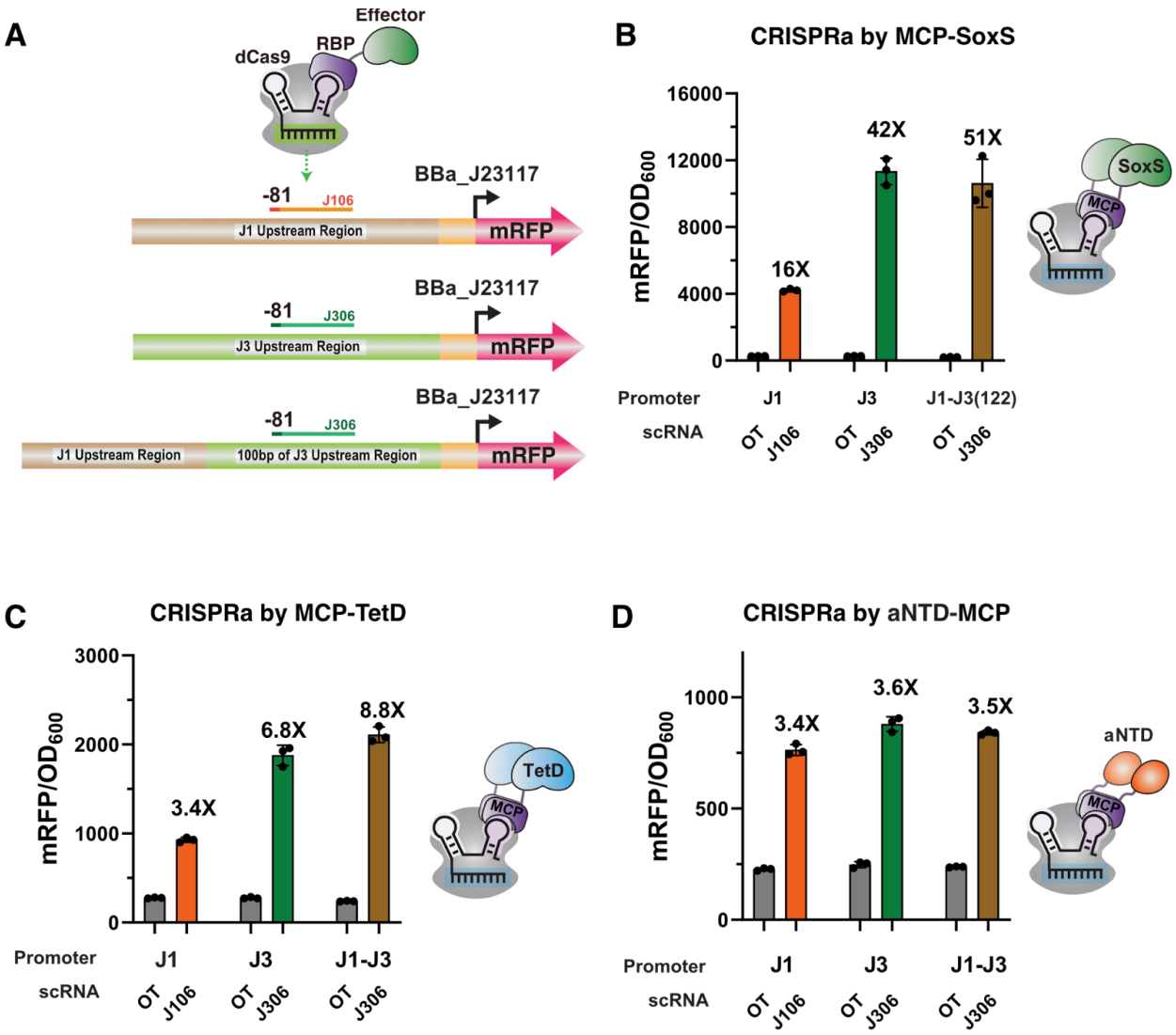

Figure S6. Comparison of different CRISPRa systems at J1, J3, and J1-J3(122) promoters.

A) Schematic of the J1, J3, and J1-J3(122) promoters. **B)** MCP-SoxS activation at J3 showed improved activation with J3 and J1-J3(122) compared to J1. The same experiment was also performed for **C)** MCP-TetD and **D)** αNTD-MCP. MCP-SoxS and MCP-TetD exhibited higher CRISPRa efficiency with the J3 promoter while αNTD-MCP showed similar activity across all three promoters. Values in panel B, C, and D represent the mean ± standard deviation calculated from n = 3.

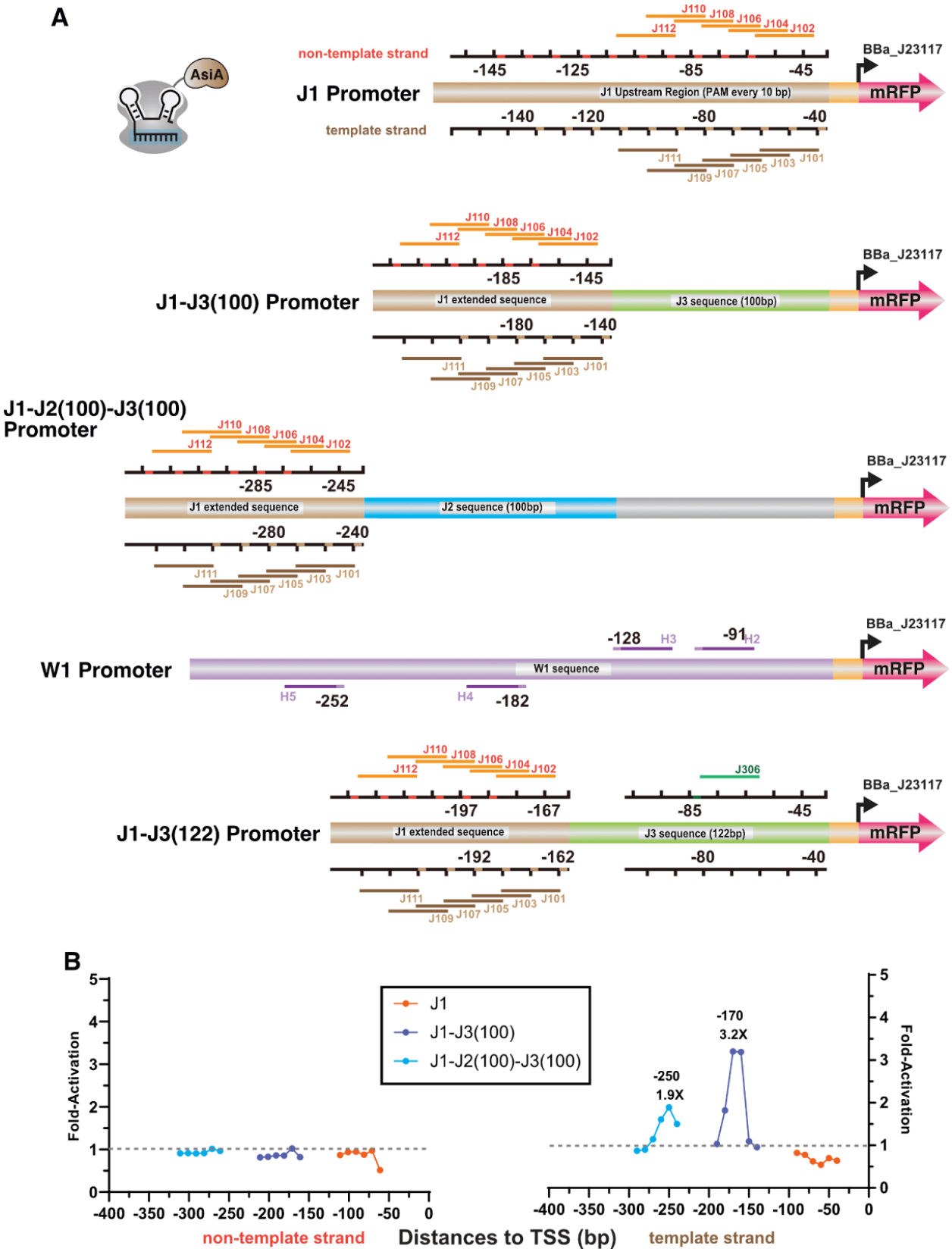
A
AsiA
non-template strand
J1 Promoter
template strand
J110 J108 J106 J104 J102
J112
-145 -125 -85 -45
J1 Upstream Region (PAM every 10 bp)
-140 -120 -80 -40
J111 J109 J107 J105 J103 J101
BBa_J23117
mRFP
J1-J3(100) Promoter
-185 -145
J1 extended sequence
J3 sequence (100bp)
-180 -140
J1-J2(100)-J3(100) Promoter
-285 -245
J2 sequence (100bp)
-280 -240
W1 Promoter
-128 H3
-91 H2
W1 sequence
H5 -252
H4 -182
J306
J1-J3(122) Promoter
-197 -167
-85 -45
J3 sequence (122bp)
-192 -162
-80 -40
B
J1
J1-J3(100)
J1-J2(100)-J3(100)
-250
1.9X
-170
3.2X
Fold-Activation
non-template strand
Distances to TSS (bp)
template strand

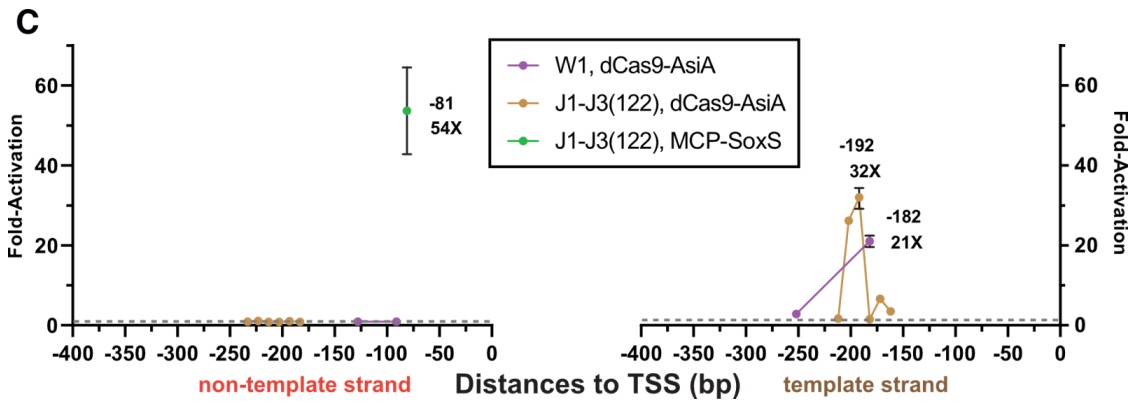

Figure S7. dCas9-AsiA based CRISPRa at target site positions in J1, J3, and J1-J3 promoters.

A) Schematics showing promoters with arrays of sgRNA target sites at different distance ranges upstream of the TSS. The J1-J3(100), J1-J2(100)-J3(100), and J1-J3(122) promoters have 100, 200, and 122 bp added between the J1 array and the minimal promoter, respectively. For promoters with a J3 array, the J306 target site is always maintained at -81 bp for SoxS targeting. Target site positions for each promoter are listed in Table S4. **B)** dCas9-AsiA mediated activation produces relatively small effects at the J1-J3(100) promoter (1.8-fold to 3.2-fold activation between -160 to -180 bp) and the J1-J2(100)-J3(100) promoter (1.5-fold to 1.9-fold activation between -240 to -260 bp). **C)** dCas9-AsiA produces 32-fold activation at -192 bp (J107) in the phase-shifted J1-J3(122) promoter. There is no significant activation at -182 bp (J105) even though 21-fold activation was observed at the same distance with the W1 promoter and the H4 sgRNA (-182 bp). An activation value for dCas9/MCP-SoxS at -81 bp with the J1-J3(122) reporter is included for comparison. Values in panel B and C represent the mean ± standard deviation calculated from n = 3.

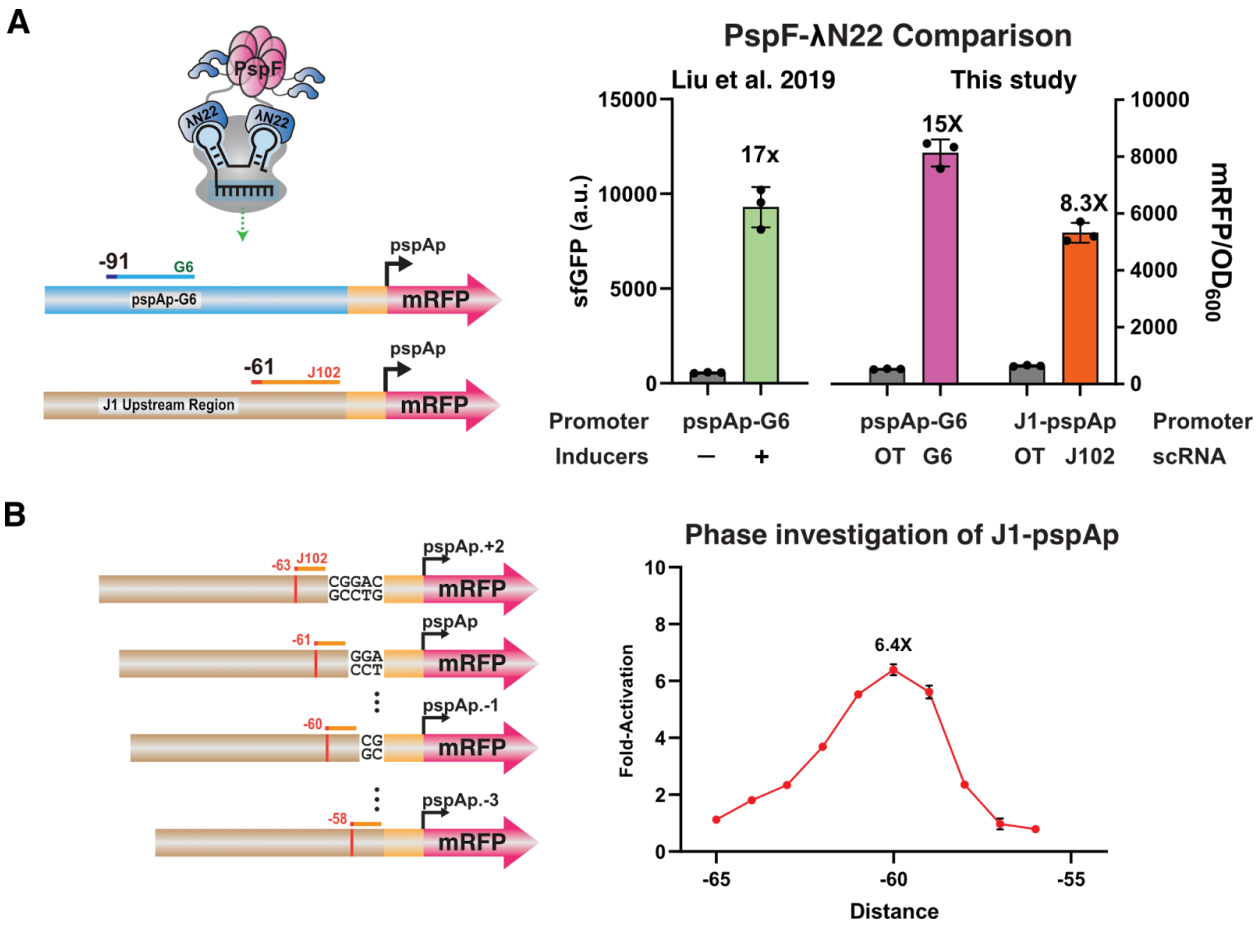

Figure S8. CRISPRa with PspF-λN22 at pspAp-G6 and J1 reporters.
A) CRISPRa by PspF-λN22 at σ^{54} promoters. At the pspAp-G6 promoter, we observe gene activation similar to the raw data reported previously.[6] The most effective activation observed from the J1-pspAp reporter is shown for comparison. See Fig 2 for complete target site characterization at J1. **B)** PspF CRISPRa with J1-pspAp shifted by 1 bp to determine target site preferences at single base resolution. In a side-by-side comparison, position -60 produced a small improvement compared to the original -61 target site in J1-pspAp. Values in panel A and B represent the mean ± standard deviation calculated from n = 3.

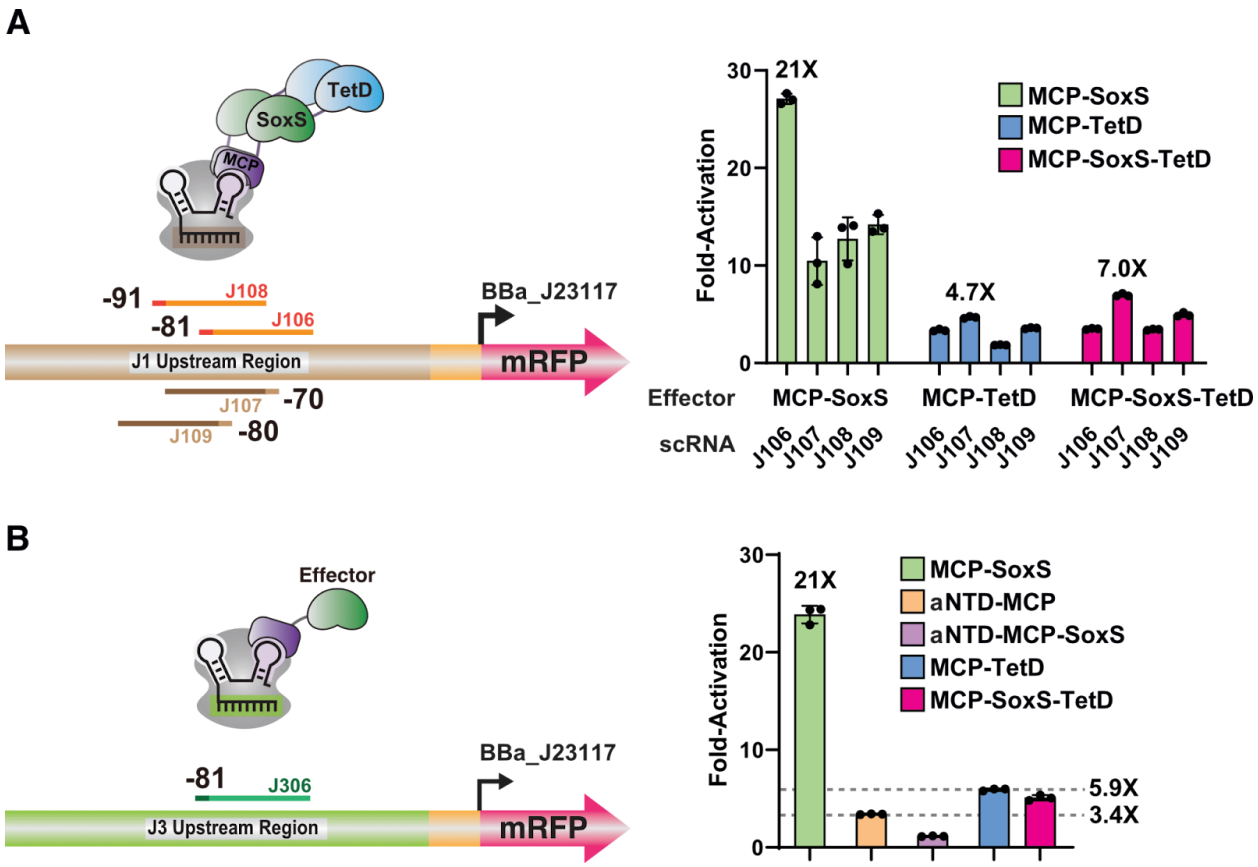

Figure S9. CRISPRa with tandem activator fusions.

A) CRISPRa with MCP-SoxS-TetD compared to MCP-SoxS or MCP-TetD at 60-100 bp (J106-J109) in the J1 reporter. MCP-SoxS-TetD does not improve gene activation relative to MCP-SoxS. **B)** CRISPRa with MCP-SoxS-TetD or αNTD-MCP-SoxS at -81 bp (J306) in the J3 reporter. Neither fusion activator shows improved gene activation relative to MCP-SoxS. Values in panel A and B represent the mean ± standard deviation calculated from n = 3.

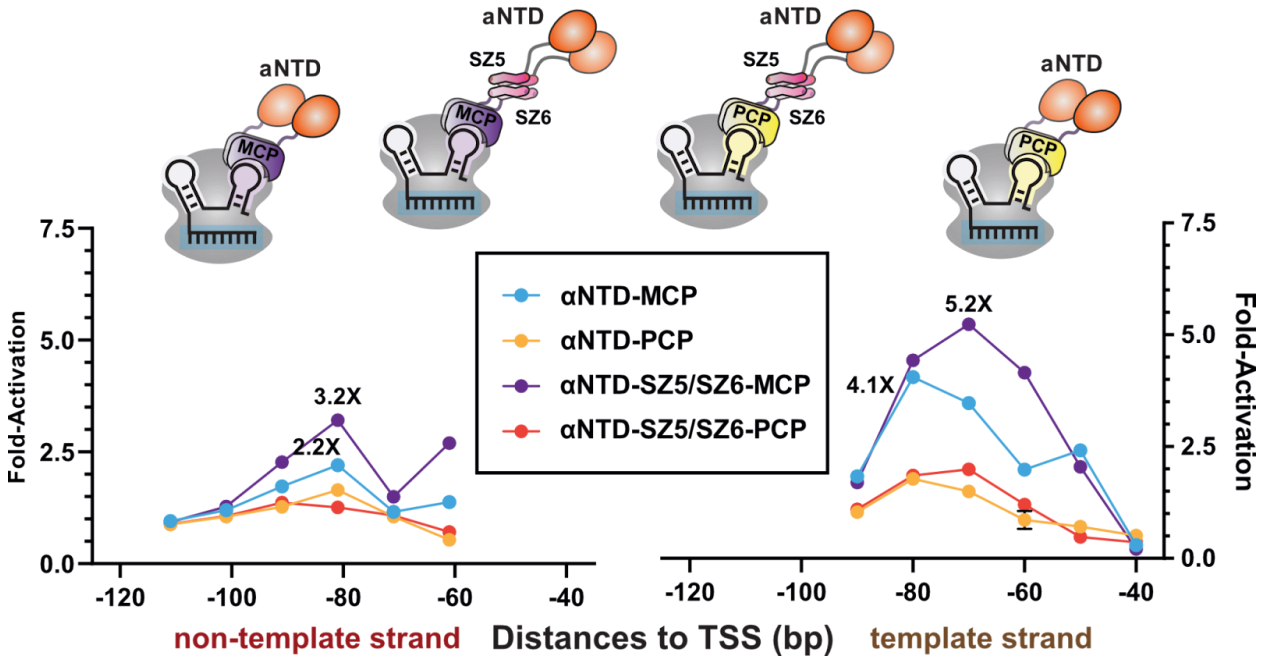

Figure S10. CRISPRa with αNTD using direct fusion or SYNZIP recruitment to RNA binding proteins.

αNTD-mediated CRISPRa with direct fusion or SYNZIP recruitment to RNA binding proteins MCP or PCP. SYNZIP recruitment is performed with αNTD fused to SYNZIP5 (SZ5) and MCP or PCP fused to SYNZIP6 (SZ6). Gene activation was measured at multiple target sites in a J1 reporter with an appropriate scRNA with MS2 to bind MCP or PP7 to bind PCP. Some SYNZIP-mediated complexes show modest improvements compared to the corresponding direct fusion. In general, MCP-mediated recruitment outperforms PCP-mediated recruitment. Values represent the mean ± standard deviation calculated from n = 3.

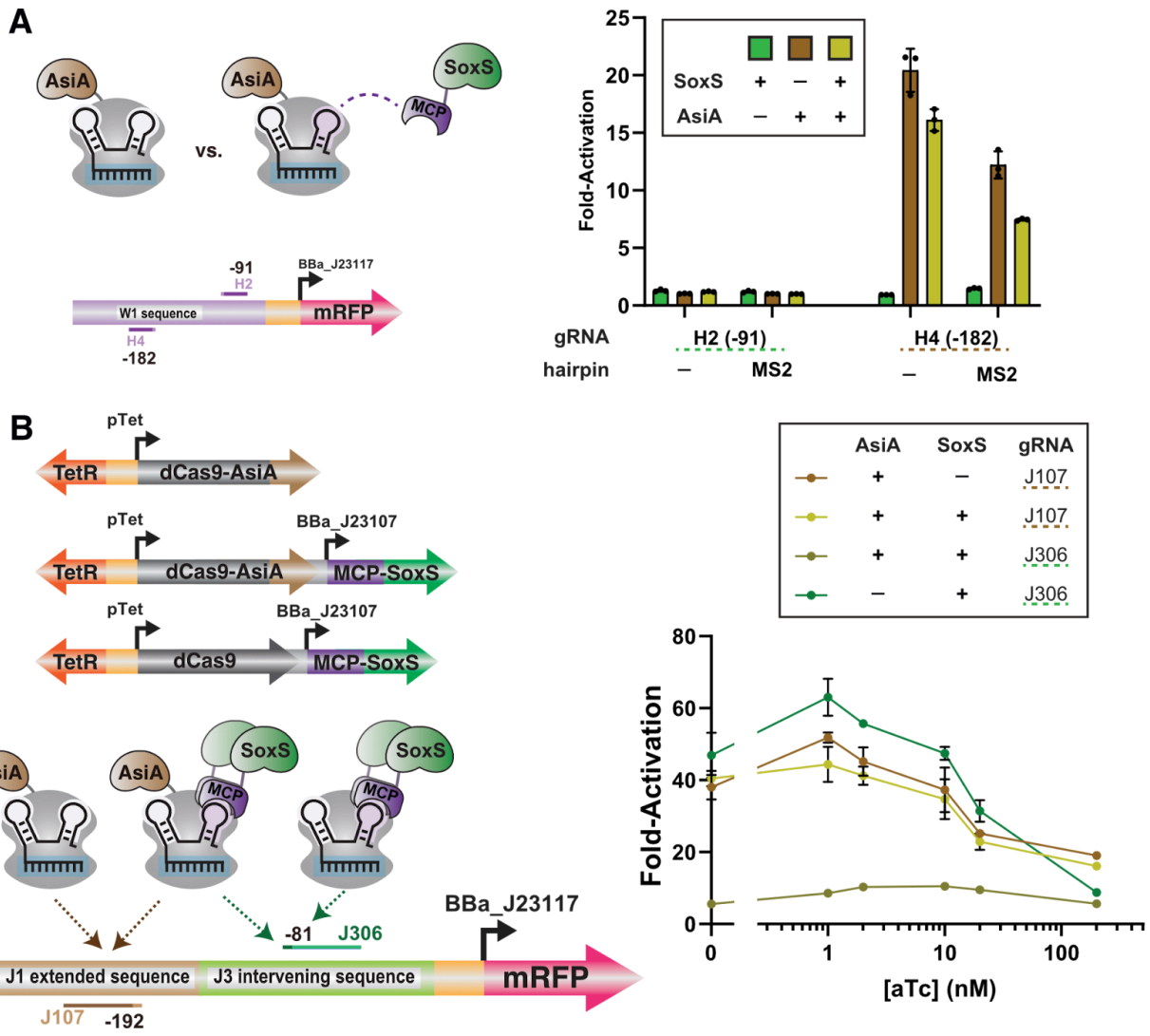

Figure S11. SoxS and AsiA CRISPRa exhibit antagonistic effects.
A) dCas9-AsiA, dCas9/MCP-SoxS, or dCas9-AsiA/MCP-SoxS recruitment to target sites on the W1 promoter, using gRNAs with or without the MS2 hairpin. SoxS recruitment to the CRISPRa complex requires the MS2 hairpin. Only the H4 target site shows significant activation with dCas9-AsiA, and recruitment of SoxS to the dCas9-AsiA complex antagonizes gene activation, similar to effects observed with the J1-J3(122) promoter (Figure 4A). **B)** CRISPRa with dCas9 or dCas9-AsiA expressed from an aTc-inducible TetR-Ptet promoter. Gene activation is optimal at a low induction level with 1 nM aTc, and there is no induction level at which the dCas9-AsiA/MCP-SoxS complex outperforms dCas9-AsiA. Values in panel A and B represent the mean ± standard deviation calculated from n = 3.

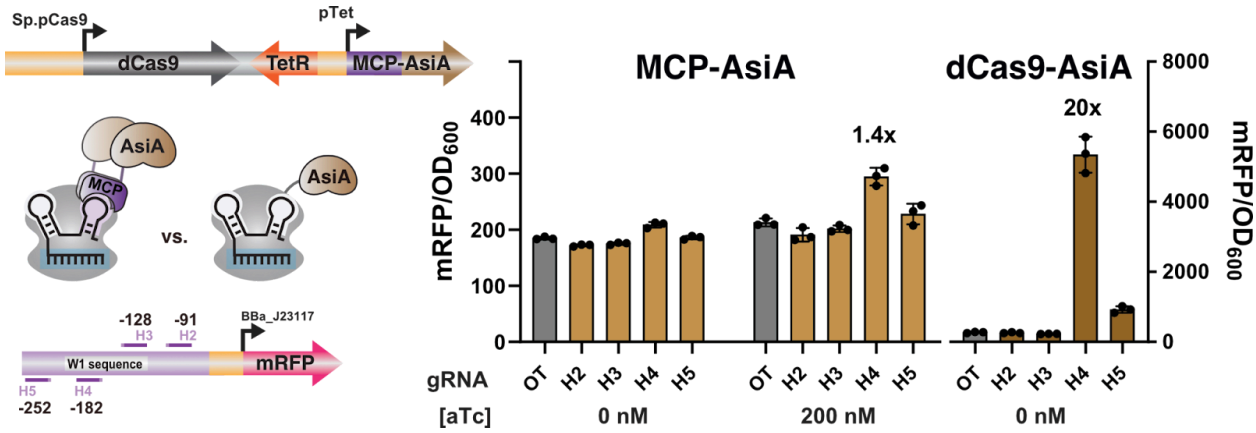

Figure S12. CRISPRa with an MS2 scRNA to recruit MCP-AsiA.
Comparison of CRISPRa with dCas9-AsiA and dCas9/MCP-AsiA, all using the AsiA_m2.1 evolved variant. MCP-AsiA is expressed from an aTc-inducible promoter and tested at either 0 or 200 nM aTc. dCas9-AsiA is effective at 0 nM aTc (Figure S11). CRISPRa was evaluated at four target sites in the W1 promoter and compared to an off-target (OT) negative control. MCP-AsiA produces high basal activation in the OT control, and at most 1.4-fold activation at the H4 target site with 200 nM aTc. This effect is significantly smaller than the ~20-fold activation observed with dCas9-AsiA. Values represent the mean ± standard deviation calculated from n = 3.

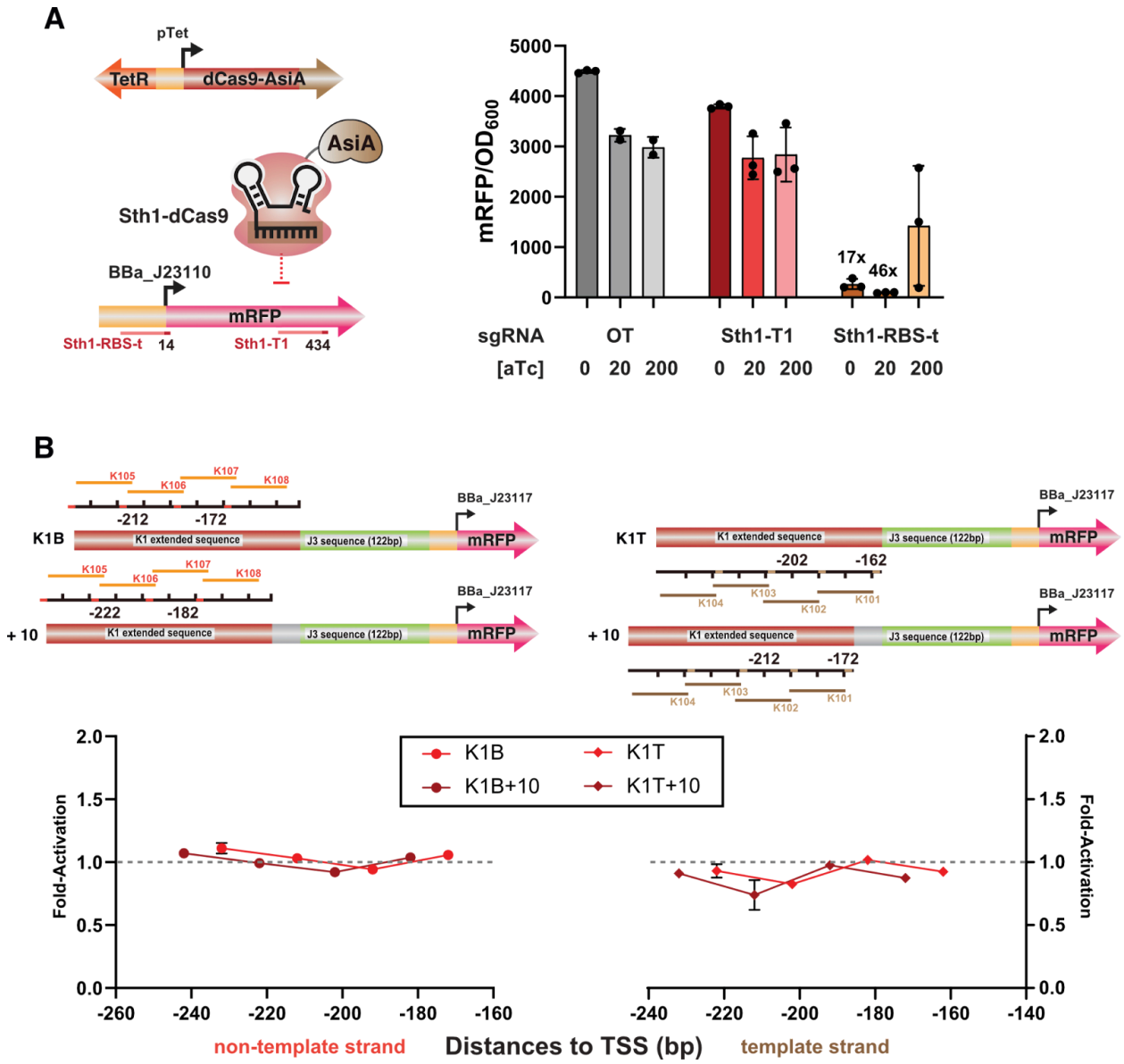

Figure S13. CRISPRa with Sth1-dCas9-AsiA is not effective.
A) CRISPRi gene repression with Sth1-dCas9-AsiA to test expression and DNA-binding function. Sth1-dCas9-AsiA was targeted to target sites in the ribosome binding site (RBS-t) or within the open reading frame (Sth1-T1). Targeting RBS-t produced up to 46-fold repression upon induction with 20 nM aTc. However, 200 nM aTc produced variable CRISPRi effects across the replicates, which could indicate genetic instability. Similar variability in CRISPRi among the individual replicates was observed with Spy-dCas9-AsiA (Figure S5). **B)** CRISPRa with Sth1-dCas9-AsiA on K1 promoters with systematically tiled PAM sites positioned from 162-202 bp from the TSS. There is no significant CRISPRa effect across all tested target sites. Values in panel A and B represent the mean ± standard deviation calculated from n = 3.

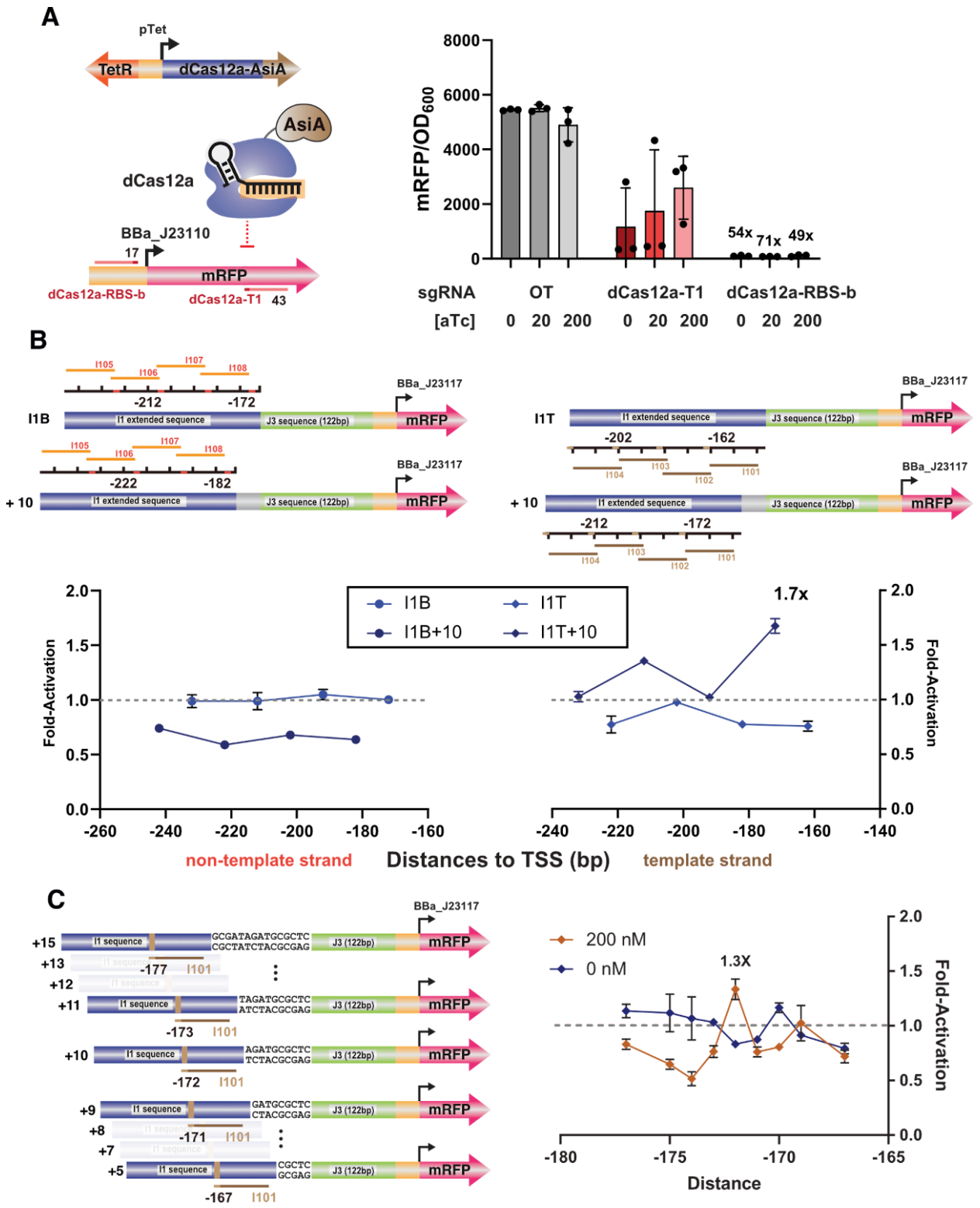

Figure S14. Modest CRISPRa with dCas12a-AsiA.

A) CRISPRi gene repression with Lb-dCas12a-AsiA to test expression and DNA-binding function. Lb-dCas12a-AsiA was targeted to target sites in the ribosome binding site (RBS-b)

or within the open reading frame (dCas12a-T1). Targeting RBS-b produced up to 71-fold repression. Targeting dCas12a-T1 also repressed gene expression to a lesser extent and with substantial variability among replicates (see also Figure S5 & S13). **B)** CRISPRa with Lb-dCas12a-AsiA on I1 promoters with systematically tiled PAM sites positioned from 162-202 bp from the TSS. We observed a small 1.7-fold increase in reporter gene expression at I101 crRNA on the I1T+10 reporter. C) CRISPRa with Lb-dCas12a-AsiA on I1 promoters with target sites shifted by 1-2 nt. In this experiment, 1.3-fold activation was observed. Values in panel A, B, and C represent the mean ± standard deviation calculated from n = 3.

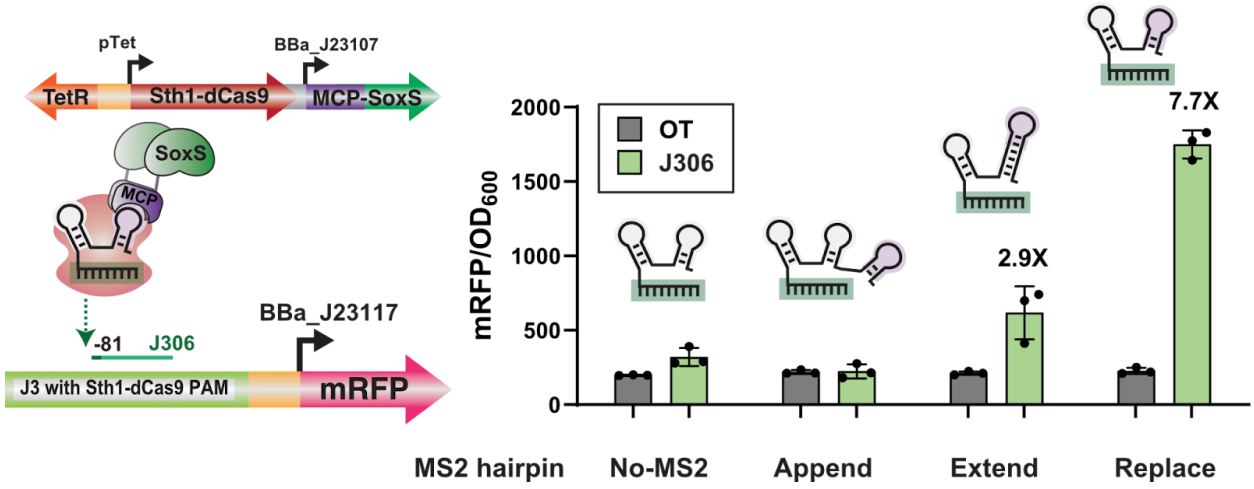

Figure S15. CRISPRa with Sth1-dCas9/MCP-SoxS and MS2 scRNAs.

Three alternative MS2 scRNA designs were screened for CRISPRa function with an mRFP reporter. MS2 was either appended to the 3' end of the Sth1 sgRNA, extended on the TrrnB terminator hairpin, or inserted to replace TrrnB. Complete scRNA sequences are included in the Supporting DNA sequences. Unmodified sgRNA lacking an MS2 hairpin was used as a negative control. The mRFP reporter has a modified J3 sequence with the Spy AGG PAM replaced by the Sth1 TGAGAAT PAM. Both the Extend and Replace scRNA designs produce significant CRISPRa effects, with the highest 7.7-fold effect from the Replace scRNA design. This optimal engineered Sth1 scRNA design is similar to our previously-reported optimal Spy scRNA.b2.[1,4] Values represent the mean ± standard deviation calculated from n = 3.

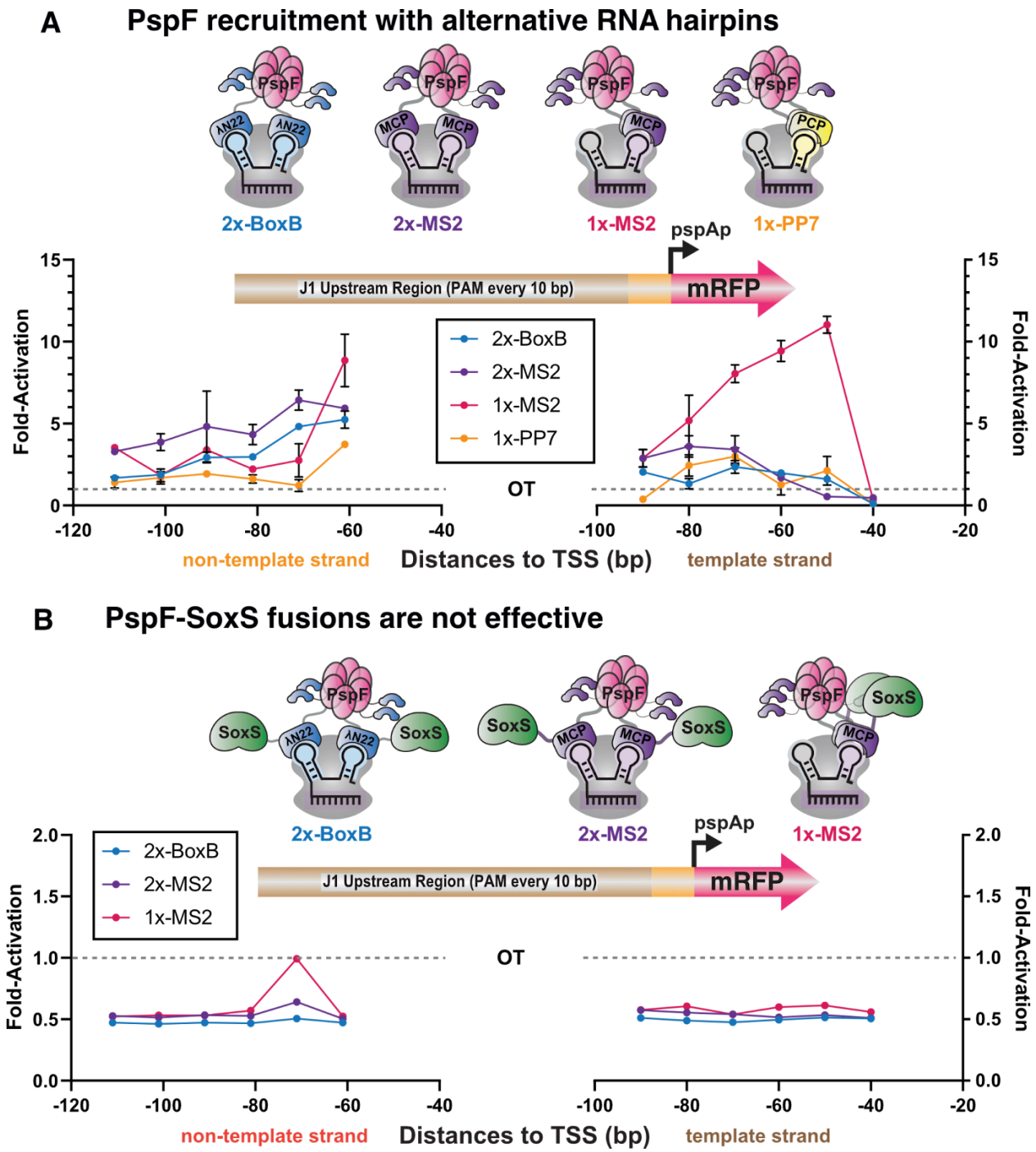

Figure S16. CRISPRa with PspF-SoxS fusions.

A) CRISPRa with PspF recruited via scRNAs with alternative hairpins. 2x-BoxB, 2x-MS2, 1x-MS2, and 1x-PP7 scRNAs recruit PspF-λN22 (BoxB). PspF-MCP (MS2), or PspF-PCP (PP7). 1x-MS2 scRNA yielded the highest performance out of all conditions tested. **B)** CRISPRa with PspF and SoxS recruited together as a PspF-λN22-SoxS or PspF-MCP-SoxS fusion. These constructs were ineffective and exhibited small repression

effects. Values in panel A and B represent the mean ± standard deviation calculated from n = 3.

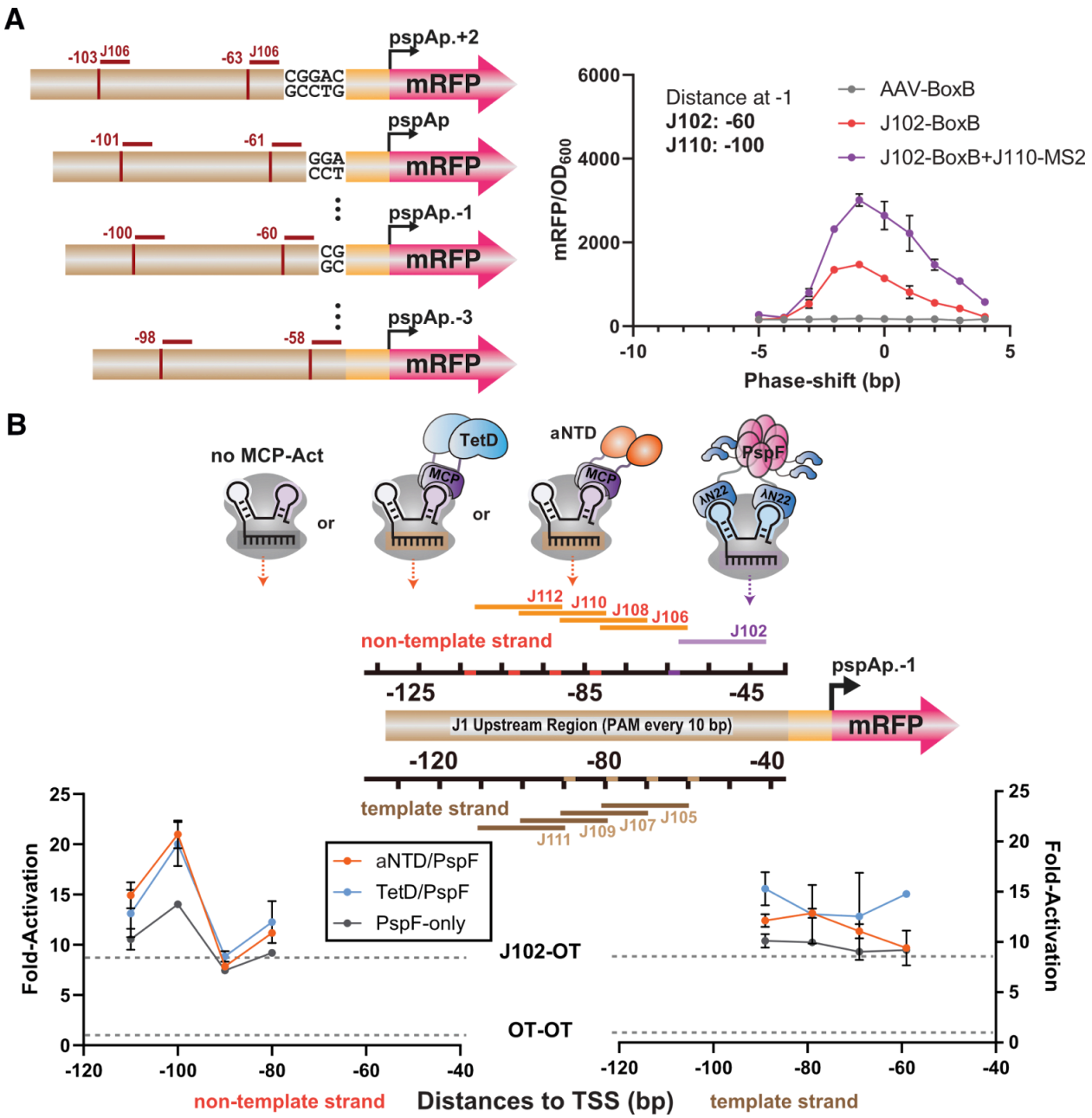

Figure S17. Characterization of PspF CRISPRa with alternative activators.
A) Comparison of PspF-only and combined PspF/SoxS CRISPRa as a function of target site distance at 1 bp resolution, using reporters with DNA insertions to shift target site positions. J102-BoxB scRNA recruits PspF-λN22 and J110-MS2 scRNA recruits MCP-SoxS. The optimal -1 position on the x-axis corresponds to J102-BoxB targeting position -60 and J110-MS2 targeting position -100. **B**) CRISPRa with αNTD+PspF, TetD+PspF, or PspF alone. The non-template data is reproduced from Figure 5D for comparison to the template data shown here. For simultaneous recruitment of PspF with αNTD or TetD, PspF was fixed at -60 on the non-template strand and the x-axis refers to the target site for αNTD or TetD. Values in panel A and B represent the mean ± standard deviation calculated from n = 3.

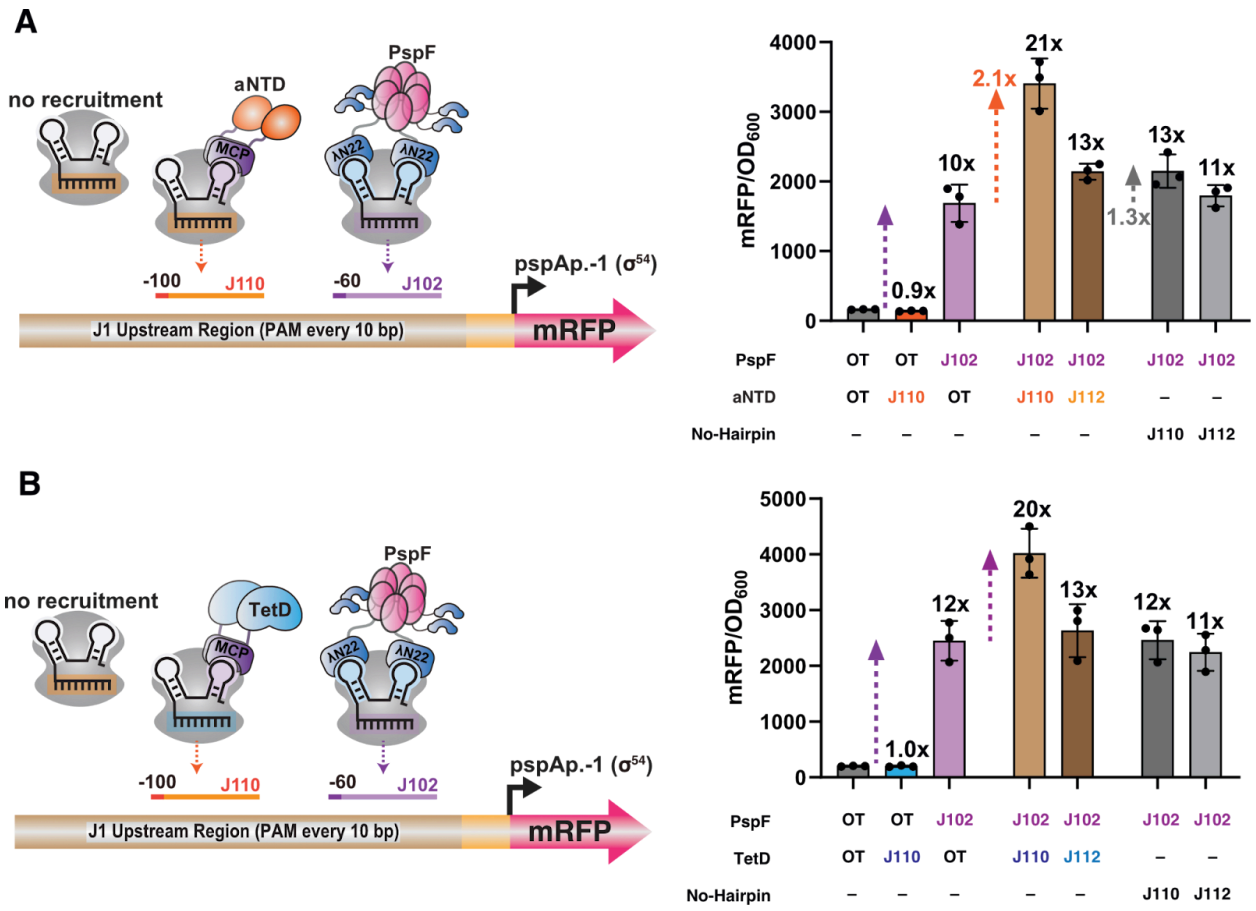

Figure S18. Characterization of CRISPRa with PspF+αNTD and PspF+TetD.

CRISPRa with PspF+αNTD **(A)** or PspF+TetD **(B)**. The observed effects are similar to PspF+SoxS (Figure 5). Values in panel A and B represent the mean ± standard deviation calculated from n = 3.

Supporting Tables

Table S1. Bacterial strains used in this work

Strain	Description	Genotype
MG1655	Wildtype *Escherichia coli strain*	F- λ- ilvG- rfb-50 rph-1
DH10B	Cloning strain	F- mcrA Δ(mrr-hsdRMS-mcrBC) φ80lacZΔM15 ΔlacX74 recA1 endA1 araD139 Δ (ara, leu)7697 galU galK λ- rpsL nupG /pMON14272 / pMON7124
NEB turbo	Cloning strain	F' proA+B+ lacIq ΔlacZM15 / fhuA2 Δ(lac-proAB) glnV galK16 galE15 R(zgb-210::Tn10)TetS endA1 thi-1 Δ(hsdS-mcrB)5
CD38[a]	MG1655 strain with integration of mRFP expressed under a strong constitutive promoter	MG1655_rbsAR::BBa_J23119-mRFP

[a]CD38 was developed previously.[7]

Table S2. List of plasmids used in this work

Plasmid	Marker	Origin	Promoter	Gene	Terminator	Reference
dCas9 + Activator						
pCD442	CmR	p15A	1) Sp.pCas9 2) BBa_J23107	1) dCas9 2) MCP-SoxS[a]	1) BBa_B0015 2) BBa_B1002	Fontana and Dong *et al.* 2020[4]
pCD178	CmR	p15A	1) Sp.pCas9 2) BBa_J23107	1) dCas9 2) MCP-TetD	1) BBa_B0015 2) BBa_B1002	Dong *et al.* 2018[1]
pCD037	CmR	p15A	1) Sp.pCas9 2) BBa_J23107	1) dCas9 2) αNTD-MCP	1) BBa_B0015 2) BBa_B1002	Dong *et al.* 2018[1]
pCD196	CmR	p15A	1) Sp.pCas9 2) BBa_J23107	1) dCas9 2) αNTD-PCP	1) BBa_B0015 2) BBa_B1002	Dong *et al.* 2018[1]
pCK068	CmR	p15A	1) Sp.pCas9 2) BBa_J23107	1) dCas9 2) MCP-CrI	1) BBa_B0015 2) BBa_B1002	This work
pCK226	CmR	p15A	1) Sp.pCas9	1) dCas9-AsiA[b]	1) BBa_B0015	This work
pCK320	CmR	p15A	1) TetR-Ptet	1) dCas9-AsiA[b]	1) BBa_B0015	This work
pAK007	CmR	p15A	1) TetR-Ptet 2) BBa_J23107	1) dCas9 2) MCP-SoxS	1) BBa_B0015 2) BBa_B1002	This work
pCK071	CmR	p15A	1) Sp.pCas9 2) BBa_J23107	1) dCas9 2) PspF-λN22	1) BBa_B0015 2) BBa_B1002	This work
pCK694	CmR	p15A	1) Sp.pCas9 2) BBa_J23107	1) dCas9 2) PspF-MCP	1) BBa_B0015 2) BBa_B1002	This work
pCK934	CmR	p15A	1) Sp.pCas9 2) BBa_J23107	1) dCas9 2) PspF-PCP	1) BBa_B0015 2) BBa_B1002	This work
pCK157	CmR	p15A	1) Sp.pCas9 2) BBa_J23107 3) BBa_J23107	1) dCas9 2) MCP-SYNZIP6 3) αNTD-SYNZIP5	1) BBa_B0015 2) BBa_B1002 3) BBa_B1002	This work
pCK770	CmR	p15A	1) Sp.pCas9 2) BBa_J23107 3) BBa_J23107	1) dCas9 2) PCP-SYNZIP6 3) αNTD-SYNZIP5	1) BBa_B0015 2) BBa_B1002 3) BBa_B1002	This work
pAK010	CmR	p15A	1) Sp.pCas9 2) TetR-Ptet	1) dCas9 2) MCP-AsiA	1) BBa_B0015 2) BBa_B1002	This work
pAK140	CmR	p15A	1) TetR-Ptet 2) BBa_J23107	1) Sth1-dCas9 2) MCP-SoxS	1) BBa_B0015 2) BBa_B1002	This work
pCK1004	CmR	p15A	1) TetR-Ptet	1) Sth1-dCas9-AsiA	1) BBa_B0015	This work
pCK1008	CmR	p15A	1) TetR-Ptet	1) Lb-dCas12a-AsiA	1) BBa_B0015	This work
dCas9 + Activator + gRNA						

Plasmid	Marker	Origin	Promoter	Gene	Terminator	Reference
pCK005.X	CmR	p15A	1) Sp.pCas9 2) BBa_J23107 3) BBa_J23119	1) dCas9 2) MCP-SoxS 3) scRNA	1) BBa_B0015 2) BBa_B1002 3) TrrnB	Fontana and Dong *et al.* 2020[4]
pCD296.X	CmR	p15A	1) Sp.pCas9 2) BBa_J23107 3) BBa_J23119	1) dCas9 2) MCP-TetD 3) scRNA	1) BBa_B0015 2) BBa_B1002 3) TrrnB	Fontana and Dong *et al.* 2020[4]
pCK090.X	CmR	p15A	1) Sp.pCas9 2) BBa_J23107 3) BBa_J23119	1) dCas9 2) MCP-MarA[c] 3) scRNA	1) BBa_B0015 2) BBa_B1002 3) TrrnB	This work
pCK094.X	CmR	p15A	1) Sp.pCas9 2) BBa_J23107 3) BBa_J23119	1) dCas9 2) MCP-TetD[c] 3) scRNA	1) BBa_B0015 2) BBa_B1002 3) TrrnB	This work
pCD297.X	CmR	p15A	1) Sp.pCas9 2) BBa_J23107 3) BBa_J23119	1) dCas9 2) αNTD-MCP 3) scRNA	1) BBa_B0015 2) BBa_B1002 3) TrrnB	Fontana and Dong *et al.* 2020[4]
pRC099.X	CmR	p15A	1) Sp.pCas9 2) BBa_J23107 3) BBa_J23119	1) dCas9 2) αNTD-PCP 3) scRNA	1) BBa_B0015 2) BBa_B1002 3) TrrnB	This work
pCK147.X	CmR	p15A	1) Sp.pCas9 2) BBa_J23107 3) BBa_J23119	1) dCas9 2) PspF-λN22 3) scRNA	1) BBa_B0015 2) BBa_B1002 3) TrrnB	This work
pCK083.X	CmR	p15A	1) Sp.pCas9 2) BBa_J23107 3) BBa_J23119	1) dCas9 2) MCP-CrI 3) scRNA	1) BBa_B0015 2) BBa_B1002 3) TrrnB	This work
pCK309.X	CmR	p15A	1) Sp.pCas9 2) BBa_J23119	1) dCas9-AsiA 2) scRNA	1) BBa_B0015 2) TrrnB	This work
Multiple activators						
pCK692	CmR	p15A	1) Sp.pCas9 2) BBa_J23107	1) dCas9 2) αNTD-MCP-SoxS	1) BBa_B0015 2) BBa_B1002	This work
pCK693	CmR	p15A	1) Sp.pCas9 2) BBa_J23107	1) dCas9 2) MCP-SoxS-TetD	1) BBa_B0015 2) BBa_B1002	This work
pCK321	CmR	p15A	1) TetR-Ptet 2) BBa_J23107	1) dCas9-AsiA[b] 2) MCP-SoxS	1) BBa_B0015 2) BBa_B1002	This work
pKO025	CmR	p15A	1) TetR-Ptet 2) Ptet 3) BBa_J23107	1) dCas9-AsiA 2) Sth1-dCas9 3) MCP-SoxS	1) BBa_B0015 2) BBa_B0015 3) BBa_B1002	This work
pCK660	CmR	p15A	1) Sp.pCas9 2) BBa_J23107 3) BBa_J23107	1) dCas9 2) MCP-SoxS 3) PspF-λN22	1) BBa_B0015 2) BBa_B1002 3) BBa_B1002	This work
pCK761	CmR	p15A	1) Sp.pCas9 2) BBa_J23107	1) dCas9 2) αNTD-MCP	1) BBa_B0015 2) BBa_B1002	This work

Plasmid	Marker	Origin	Promoter	Gene	Terminator	Reference
			3) BBa_J23107	3) PspF-λN22	3) BBa_B1002	
pCK948	CmR	p15A	1) Sp.pCas9 2) BBa_J23107 3) BBa_J23107	1) dCas9 2) MCP-TetD 3) PspF-λN22	1) BBa_B0015 2) BBa_B1002 3) BBa_B1002	This work
pCK882	CmR	p15A	1) Sp.pCas9 2) BBa_J23107	1) dCas9 2) MCP-SoxS-SYNZIP6	1) BBa_B0015 2) BBa_B1002	This work
pCK883	CmR	p15A	1) Sp.pCas9 2) BBa_J23107 3) BBa_J23107	1) dCas9 2) MCP-SoxS-SYNZIP6 3) αNTD-SYNZIP5	1) BBa_B0015 2) BBa_B1002 3) BBa_B1002	This work
pCK695	CmR	p15A	1) Sp.pCas9 2) BBa_J23107	1) dCas9 2) PspF-MCP-SoxS	1) BBa_B0015 2) BBa_B1002	This work
pCK696	CmR	p15A	1) Sp.pCas9 2) BBa_J23107	1) dCas9 2) PspF-λN22-SoxS	1) BBa_B0015 2) BBa_B1002	This work
Reporter						
pJF076	AmpR	pSC101**	J1-BBa_J23117	mRFP	BBa_B0015	Dong *et al.* 2018[1]
pJF143.J3	AmpR	pSC101**	J3-BBa_J23117	mRFP	BBa_B0015	Fontana and Dong *et al.* 2020[4]
pCK001	AmpR	pSC101**	J1-sodCp	mRFP	BBa_B0015	Fontana and Dong *et al.* 2020[4]
pCK002	AmpR	pSC101**	J1-glnAp2	mRFP	BBa_B0015	Fontana and Dong *et al.* 2020[4]
pCK003	AmpR	pSC101**	J1-rdgBp	mRFP	BBa_B0015	Fontana and Dong *et al.* 2020[4]
pCK004	AmpR	pSC101**	J1-yieEp	mRFP	BBa_B0015	Fontana and Dong *et al.* 2020[4]
pCK067.N	AmpR	pSC101**	J1-sodCp_phase-shift	mRFP	BBa_B0015	Fontana and Dong *et al.* 2020[4]
pCD249	AmpR	pSC101**	W1-BBa_J23117	mRFP	BBa_B0015	Dong *et al.* 2018[1]
pCK702	AmpR	pSC101**	J1-J3(100)-BBa_J23117	mRFP	BBa_B0015	This work

Plasmid	Marker	Origin	Promoter	Gene	Terminator	Reference
pCK703	AmpR	pSC101**	J1-J2(100)-J3(100) -BBa_J23117	mRFP	BBa_B0015	This work
pAK011	AmpR	pSC101**	J1-J3(122) -BBa_J23117	mRFP	BBa_B0015	This work
pCK070	AmpR	pSC101**	J1-pspAp	mRFP	BBa_B0015	This work
pCK069	AmpR	pSC101**	pspAp-G6	mRFP	BBa_B0015	This work
pCK662.N	AmpR	pSC101**	J1-pspAp_phase-shift	mRFP	BBa_B0015	This work
pKO021	AmpR	pSC101**	J3-BBa_J23117 with Sth1 PAM	mRFP	BBa_B0015	This work
pCK1006.N	AmpR	pSC101**	K1T-BBa_J23117	mRFP	BBa_B0015	This work
pCK1007.N	AmpR	pSC101**	K1B-BBa_J23117	mRFP	BBa_B0015	This work
pCK1011.N	AmpR	pSC101**	I1T-BBa_J23117	mRFP	BBa_B0015	This work
pCK1012.N	AmpR	pSC101**	I1B-BBa_J23117	mRFP	BBa_B0015	This work
pKO023	AmpR	pSC101**	J1-J3(122)-BBa_J23117 with Sth1 PAM	mRFP	BBa_B0015	This work
Reporter + gRNA						
pCK161.X	AmpR	pSC101**	1) BBa_J23119 2) J1-BBa_J23117	1) scRNA 2) mRFP	1) TrrnB 2) BBa_B0015	This work
pCK101.X	AmpR	pSC101**	1) BBa_J23119 2) J3-BBa_J23117	1) scRNA 2) mRFP	1) TrrnB 2) BBa_B0015	This work
gRNA(s)						
pCK303. scRNA	KmR	ColE1	BBa_J23119	scRNA_b2.MS2	TrrnB	This work
pAK030. sgRNA	KmR	ColE1	BBa_J23119	sgRNA	TrrnB	This work
pCK676. scRNA	KmR	ColE1	BBa_J23119	scRNA_2xBoxB	TrrnB	This work
pCK732. scRNA	KmR	ColE1	BBa_J23119	scRNA_b1.PP7 (1xPP7)	TrrnB	This work

Plasmid	Marker	Origin	Promoter	Gene	Terminator	Reference
pCK697. scRNA	KmR	ColE1	BBa_J23119	scRNA_2xMS2	TrrnB	This work
pKO018. scRNA	KmR	ColE1	BBa_J23119	Sth1-dCas9 scRNA with MS2	TrrnB	This work
pCK1005. sgRNA	KmR	ColE1	BBa_J23119	Sth1-dCas9 sgRNA	TrrnB	This work
pCK1010. crRNA	KmR	ColE1	BBa_J23119	Lb-dCas12a crRNA	TrrnB	This work
pKO024. scRNAs	KmR	ColE1	1) BBa_J23119 2) BBa_J23119	1) Sth1-dCas9 scRNA with MS2.X 2) Spy-dCas9 sgRNA.X	1) TrrnB 2) TrrnB	This work
pCK677. scRNAs	KmR	ColE1	1) BBa_J23119 2) BBa_J23119	1) scRNA_2xBoxB_J102 2) scRNA_b2.MS2.X	1) TrrnB 2) TrrnB	This work
pCK962. gRNAs	KmR	ColE1	1) BBa_J23119 2) BBa_J23119	1) scRNA_2xBoxB_J102 2) sgRNA	1) TrrnB 2) TrrnB	This work

[a]All SoxS genes contain two mutations (R93A and S101A)
[b]All dCas9-AsiA genes in this work are dCas9-AsiA_m2.1 with the same protein sequence as described previously.[2]
[c]MarA and TetD mutants were generated as listed in Figure S2B.

Table S3. sgRNA/scRNA/crRNA spacer sequences

Spacer	DNA sequence	Target strand[a]	Distance to TSS[b]
sgRNA/scRNA for Spy-dCas9			
hAAVS1	GGGGCCACTAGGGACAGGAT	Off-target	NA
J306	TTGTGTCCAGAACGCTCCGT	Non-Template	-81
RR2	TGGAACCGTACTGGAACTGC	Non-Template	188
H2	GAAGATCCGGCCTGCAGCCA	Non-Template	-91
H3	GGCTCGAGTCGACAGTTCAT	Non-Template	-128
H4	CTACGGAACTCTTGTGCGTA	Template	-182
H5	GCAAAAGCTCATTTCTGAAG	Template	-252
G6	AAAGCTGTTGTGGCAAAAAA	Non-Template	-91
J101	TGGGTTCCACCGGATACCTC	Template	-40
J102	AGGTATCCGGTGGAACCCAA	Non-Template	-61
J103	AGGCGTCCTTTGGGTTCCAC	Template	-50
J104	TGGAACCCAAAGGACGCCTT	Non-Template	-71
J105	CGGTTACCAAAGGCGTCCTT	Template	-60
J106	AGGACGCCTTTGGTAACCGC	Non-Template	-81
J107	CGGTGTCCTGCGGTTACCAA	Template	-70
J108	TGGTAACCGCAGGACACCGC	Non-Template	-91
J109	AGGTATCCTGCGGTGTCCTG	Template	-80
J110	AGGACACCGCAGGATACCTG	Non-Template	-101
J111	GGGCGACCTCAGGTATCCTG	Template	-90
J112	AGGATACCTGAGGTCGCCCG	Non-Template	-111
J113	GGGCCACCACGGGCGACCTC	Template	-100
J114	AGGTCGCCCGTGGTGGCCCA	Non-Template	-121
J115	TGGTGACCATGGGCCACCAC	Template	-110
J116	TGGTGGCCCATGGTCACCAT	Non-Template	-131
J117	GGGTGACCTATGGTGACCAT	Template	-120
J118	TGGTCACCATAGGTCACCCT	Non-Template	-141
J119	TGGTTGCCAAGGGTGACCTA	Template	-130
J120	AGGTCACCCTTGGCAACCAA	Non-Template	-151
J121	AGGACACCTTTGGTTGCCAA	Template	-140
sgRNA/scRNA for Sth1-dCas9[a]			

hAAVS1	GGGGCCACTAGGGACAGGAT	Off-target	NA
J306	TTGTGTCCAGAACGCTCCGT	Bottom	-81
Sth1-T1	ccgtccgacggtccggttat	Template	434 from TSS
Sth1-RBS-t	gctagcGAATTCATTAAAGA	RBS	14 from TSS
K101	TGAGAATGGGTTCACAGCGA	Template	-50
K102	CCAGAATAAAGTCTCGCAGA	Template	-70
K103	AGAGAATGCGGACCACTTGA	Template	-90
K104	TGAGAAAGGTGATAGTGCGA	Template	-110
K105	CCAGAAACGACCGGCAGACG	Template	-130
K106	CGAGAATAGACTTCGACTGC	Template	-150
K107	TGAGAATGCCTCCCACCGAG	Template	-170
K108	GGAGAAAGACATCCAAGTCT	Template	-190
crRNA for dCas12a[b]			
hAAVS1	GGGGCCACTAGGGACAGGAT	Off-target	NA
12a-T1	AAAGTTCGTATGGAAGGTTC	Template	42
12a-RBS-b	TCCTCTTTAATGAATTCgct	RBS	17 from TSS
I101	CGTCGAATCATCGGGCTTTC	Template	-40
I102	ATATGGCTCCCGGTCATTTC	Template	-60
I103	GTGGCACAACTATAGGTTTA	Template	-80
I104	TCTGCGGCCAGCACCATTTC	Template	-100
I105	TCGCTATGCGGACGGCTTTA	Template	-120
I106	CTGCCAAGCCTGGGCCTTTA	Template	-140
I107	GCTTTGAAGTCGGTACTTTA	Template	-160
I108	GCTGACACCACAGTCCTTTC	Template	-180

[a]gRNA hairpin of Sth1 dCas9 is distinct from that of Spy-dCas9.
[b]crRNA spacer locates at 3'-end different from that of 5'-end in the Cas9 case. See DNA sequences section for further details.

Table S4. sgRNA target site positions for alternative promoters

Spacer	J1	J1-J3(100)	J1-J2(100)-J3(100)	J1-J3(122)
Non-Template strand[a]				
J101	-40	-140	-240	-162
J103	-50	-150	-250	-172
J105	-60	-160	-260	-182
J107	-70	-170	-270	-192
J109	-80	-180	-280	-202
J111	-90	-190	-290	-212
J113	-100	-200	-300	-222
J115	-110	-210	-310	-232
J117	-120	-220	-320	-242
J119	-130	-230	-330	-252
Template strand[b]				
J102	-61	-161	-261	-183
J104	-71	-171	-271	-193
J106	-81	-181	-281	-203
J108	-91	-191	-291	-213
J110	-101	-201	-301	-223
J112	-111	-211	-311	-233
J114	-121	-221	-321	-243
J116	-131	-231	-331	-253
J118	-141	-241	-341	-263
J120	-151	-251	-351	-273

[a]gRNAs targeting Non-Template strand match the DNA sequence on the Top strand.
[b]gRNAs targeting Template strand match the DNA sequence on the Bottom strand.

Table S5. Plasmids used in each figure

Figures (Activators)	p15A-CmR	pSC101-AmpR	ColE1-KmR
2A (MCP-SoxS)	pCK005.01-21	pJF076 (J1-BBa_J23117)	
2A (αNTD-MCP)	pCD297.01-21	pJF076 (J1-BBa_J23117)	
2A (dCas9-AsiA)	pCK320	pJF076 (J1-BBa_J23117)	pAK030.01-12
2A (PspF-λN22)	pCK147.01-20	pJF076 (J1-BBa_J23117)	
2B (MCP-SoxS)	pCK005.01-21	pAK070 (J1-pspAp)	
2B (PspF-λN22)	pCK147.01-20	pAK070 (J1-pspAp)	
3A (MCP-SoxS)	pCD442	pCK161.06-09 (J1-BBa_J23117)	
3A (αNTD-MCP)	pCD037	pCK161.06-09 (J1-BBa_J23117)	
3A (αNTD-MCP-SoxS)	pCK692	pCK161.06-09 (J1-BBa_J23117)	
3B (MCP-SoxS)	pCD442	pCK161.06-09 (J1-BBa_J23117)	
3B (MCP-SoxS-SYNZIP6)	pCK882	pCK161.06-09 (J1-BBa_J23117)	
3B (MCP-SoxS-SYNZIP6 and αNTD-SYNZIP5)	pCK883	pCK161.06-09 (J1-BBa_J23117)	
4A (MCP-SoxS)	pAK007	pAK011 (J1-J3(122)-BBa_J23117)	pCK303.306 pCK303.107
4A (dCas9-AsiA)	pCK320	pAK011 (J1-J3(122)-BBa_J23117)	pCK303.306 pCK303.107
4A (dCas9-AsiA + MCP-SoxS)	pCK321	pAK011 (J1-J3(122)-BBa_J23117)	pCK303.306 pCK303.107
4B (dCas9-AsiA + Sth1-dCas9 + MCP-SoxS)	pKO025	pKO023 (J1-J3(122)-BBa_J23117 with Sth1 PAM)	pKO024.AAV-AAV pKO024.306-AAV pKO024.AAV-107 pKO024.306-107
5B (MCP-SoxS + PspF-λN22)	pCK660	pCK662.-1 (J1-pspAp.-1)	pCK667.AAV-AAV pCK667.102-AAV pCK667.102-(105-112)
5C (MCP-SoxS + PspF-λN22)	pCK660	pCK662.-1 (J1-pspAp.-1)	pCK667.AAV-AAV pCK667.102-AAV pCK667.AAV-110 pCK667.102-110 pCK667.102-112 pCK962.102-110 pCK962.102-112
5D (αNTD-MCP + PspF-λN22)	pCK761	pCK662.-1 (J1-pspAp.-1)	pCK667.AAV-AAV pCK667.102-AAV pCK667.102-(105-112)
5D (MCP-TetD	pCK761	pCK662.-1 (J1-pspAp.-1)	pCK667.AAV-AAV

Figures (Activators)	p15A-CmR	pSC101-AmpR	ColE1-KmR
+ PspF-λN22)			pCK667.102-AAV pCK667.102-(105-112)
5D (PspF-λN22)	pCK071	pCK662.-1 (J1-pspAp.-1)	pCK667.AAV-AAV pCK667.102-AAV pCK667.102-(105-112)
5E (PspF-λN22)	pCK071	pCK662.-1 (J1-pspAp.-1)	pCK667.AAV-AAV pCK667.102-AAV pCK667.AAV-110 pCK667.102-110 pCK667.102-112 pCK962.102-110 pCK962.102-112
S1A (MCP-SoxS)	pCK005.01-21	pJF076 (J1-BBa_J23117)	
S1A (MCP-SoxS)	pCK005.01-21	pCK001 (J1-sodCp)	
S1A (MCP-SoxS)	pCK005.01-21	pCK002 (J1-glnAp2)	
S1A (MCP-SoxS)	pCK005.01-21	pCK003 (J1-rdgBp)	
S1A (MCP-SoxS)	pCK005.01-21	pCK004 (J1-yieEp)	
S1B (MCP-SoxS)	pCK005.06/09/AAV	pCK001 (J1-sodCp), pCK067.N (J1-sodCp_phase-shift)	
S2A (MCP-SoxS)	pCD442	pCK161.X (J1-BBa_J23117), pCK101.X (J3-BBa_J23117)	
S2A (MCP-TetD)	pCD178	pJF076 (J1-BBa_J23117), pJF143.J3 (J3-BBa_J23117)	
S2B (MCP-MarA-mut)	pCK090.X	pJF143.J3 (J3-BBa_J23117)	
S2B (MCP-TetD-mut)	pCK094.X	pJF143.J3 (J3-BBa_J23117)	
S3B (αNTD-MCP)	pCD297.X	pJF076 (J1-BBa_J23117)	
S3B (αNTD-PCP)	pRC099.X	pJF076 (J1-BBa_J23117)	
S4B (MCP-CrI)	pCK083.X	pCK067.3 (J1-sodCp.-3)	
S5A (dCas9-AsiA)	pCK309.X	pCD249 (W1-BBa_J23117)	
S5B (dCas9-AsiA)	pCD442, pCK226	CD38 (BBa_J23119-mRFP)	pAK030.gAAV pAK030.RR2
S5C (dCas9-AsiA)	pCK320	pCD249 (W1-BBa_J23117)	pAK030.gAAV pAK030.H2-H5
S6B (MCP-SoxS)	pCK005.X	pJF076 (J1-BBa_J23117), pJF143.J3 (J3-BBa_J23117), pAK011 (J1-J3(122)-BBa_J23117)	
S6C (MCP-TetD)	pCD296.X	pJF076 (J1-BBa_J23117),	

Figures (Activators)	p15A-CmR	pSC101-AmpR	ColE1-KmR
		pJF143.J3 (J3-BBa_J23117), pAK011 (J1-J3(122)-BBa_J23117)	
S6D (αNTD-MCP)	pCD297.X	pJF076 (J1-BBa_J23117), pJF143.J3 (J3-BBa_J23117), pAK011 (J1-J3(122)-BBa_J23117)	
S7B (dCas9-AsiA)	pCK320	pJF076 (J1-BBa_J23117), pCK702 (J1-J3(100)-BBa_J23117), pCK703 (J1-J2(100)-J3(100)-BBa_J23117)	pAK030.gAAV pAK030.01-12
S7C (dCas9-AsiA)	pCK320	pCD249 (W1-BBa_J23117), pAK011 (J1-J3(122)-BBa_J23117)	pAK030.gAAV pAK030.01-12 pAK030.H2-H5
S7C (MCP-SoxS)	pCD442	pJF076 (J1-BBa_J23117)	pCK303.AAV pCK303.306
S8A (PspF-λN22)	pCK147.X	pCK069 (pspAp-G6), pCK070 (J1-pspAp)	
S8B (PspF-λN22)	pCK147.X	pCK002 (J1-glnAp2), pCK299 (J1-glnAp2*)	
S8C (PspF-λN22)	pCK147.X	pCK070 (J1-pspAp), pCK662.N (J1-pspAp_phase-shift)	
S9A (MCP-SoxS)	pCD442	pCK161.X (J1-BBa_J23117)	
S9A (MCP-TetD)	pCD178	pCK161.X (J1-BBa_J23117)	
S9A (MCP-SoxS-TetD)	pCK693	pCK161.X (J1-BBa_J23117)	
S9B (MCP-SoxS)	pCD442	pCK101.X (J3-BBa_J23117)	
S9B (αNTD-MCP)	pCD037	pCK101.X (J3-BBa_J23117)	
S9B (αNTD-MCP-SoxS)	pCK692	pCK101.X (J3-BBa_J23117)	
S9B (MCP-TetD)	pCD178	pCK101.X (J3-BBa_J23117)	
S9B (MCP-SoxS-TetD)	pCK693	pCK101.X (J3-BBa_J23117)	
S10 (αNTD-MCP)	pCD297.X	pJF076 (J1-BBa_J23117)	
S10 (αNTD-PCP)	pRC099.X	pJF076 (J1-BBa_J23117)	
S10 (αNTD-SYNZIP5 + MCP-SYNZIP6)	pCK157	pCK161.X (J1-BBa_J23117)	
S10 (αNTD-SYNZIP5 + PCP-SYNZIP6)	pCK770	pJF076 (J1-BBa_J23117)	pCK732.01-12
S11A (MCP-SoxS)	pAK007	pCD249 (W1-BBa_J23117)	pCK303.X pAK030.X

Figures (Activators)	p15A-CmR	pSC101-AmpR	ColE1-KmR
S11A (dCas9-AsiA)	pCK320	pCD249 (W1-BBa_J23117)	pCK303.X pAK030.X
S11A (dCas9-AsiA + MCP-SoxS)	pCK321	pCD249 (W1-BBa_J23117)	pCK303.X pAK030.X
S11B (MCP-SoxS)	pAK007	pAK011 (J1-J3(122)-BBa_J23117)	pCK303.AAV pCK303.306
S11B (dCas9-AsiA)	pCK320	pAK011 (J1-J3(122)-BBa_J23117)	pAK030.gAAV pAK030.107
S11B (dCas9-AsiA + MCP-SoxS)	pCK321	pAK011 (J1-J3(122)-BBa_J23117)	pAK030.gAAV pAK030.107 pCK303.AAV pCK303.306
S12 (MCP-AsiA)	pAK010	pCD249 (W1-BBa_J23117)	pAK030.gAAV pAK030.H2-H5
S12 (dCas9-AsiA)	pCK320	pCD249 (W1-BBa_J23117)	pAK030.gAAV pAK030.H2-H5
S13A (Sth1-dCas9-AsiA)	pCK1004	pJF143.J3.110 (J3-BBa_J23110)	pCK1005.AAV pCK1005.Sth1-T1 pCK1005.RBS-t
S13B (Sth1-dCas9-AsiA)	pCK1004	pCK1006.N (K1T-BBa_J23117), pCK1007.N (K1B-BBa_J23117)	pCK1005.01-08
S14A (Lb-dCas12a-AsiA)	pCK1008	pJF143.J3.110 (J3-BBa_J23110)	pCK1010.AAV pCK1010.12a-T1 pCK1010.RBS-b
S14B (Lb-dCas12a-AsiA)	pCK1008	pCK1010.N (I1T-BBa_J23117), pCK1011.N (I1B-BBa_J23117)	pCK1010.01-08
S14C (Lb-dCas12a-AsiA)	pCK1008	pCK1011.N (I1B-BBa_J23117)	pCK1010.01
S15 (Sth1-dCas9 + MCP-SoxS)	pAK140	pAK021 (J3-BBa_J23117 with Sth1 PAM)	pKO024.X
S16A (PspF-λN22)	pCK071	pCK070 (J1-pspAp)	pCK676.01-12
S16A (PspF-MCP)	pCK694	pCK070 (J1-pspAp)	pCK303.01-12 pCK697.01-12
S16A (PspF-PCP)	pCK934	pCK070 (J1-pspAp)	pCK732.01-12
S16B (PspF-λN22)	pCK696	pCK070 (J1-pspAp)	pCK676.01-12
S16B (PspF-MCP)	pCK695	pCK070 (J1-pspAp)	pCK303.01-12 pCK697.01-12
S17A (MCP-SoxS + PspF-λN22)	pCK660	pCK070 (J1-pspAp), pCK662.N (J1-pspAp.N)	pCK667.AAV-AAV pCK667.102-AAV pCK667.102-110

Figures (Activators)	p15A-CmR	pSC101-AmpR	ColE1-KmR
S17B (αNTD-MCP + PspF-λN22)	pCK761	pCK662.-1 (J1-pspAp.-1)	pCK667.AAV-AAV pCK667.102-AAV pCK667.102-(105-112)
S17B (MCP-TetD + PspF-λN22)	pCK761	pCK662.-1 (J1-pspAp.-1)	pCK667.AAV-AAV pCK667.102-AAV pCK667.102-(105-112)
S17B (PspF-λN22)	pCK071	pCK662.-1 (J1-pspAp.-1)	pCK667.AAV-AAV pCK667.102-AAV pCK667.102-(105-112)
S18A (αNTD-MCP + PspF-λN22)	pCK071	pCK662.-1 (J1-pspAp.-1)	pCK667.AAV-AAV pCK667.102-AAV pCK667.AAV-110 pCK667.102-110 pCK667.102-112 pCK962.102-110 pCK962.102-112
S18B (MCP-TetD + PspF-λN22)	pCK071	pCK662.-1 (J1-pspAp.-1)	pCK667.AAV-AAV pCK667.102-AAV pCK667.AAV-110 pCK667.102-110 pCK667.102-112 pCK962.102-110 pCK962.102-112

Table S6. Design rules of different CRISPRa systems not tested in this work (extended from Table 1)

Activator	**Mechanism group**	**Reported working distance (Strand preference)**[a]	**Organisms**
λcII (Dong et al., 2018)[1]	Interact with RpoA	-71 (T)	*Escherichia coli*
RemA (Wu et al., 2020)[8]	Unknown	-90 (NT)	*Bacillus subtilis*
RpoZ (Bikard et al., 2013; Dong et al., 2018)[1,9]	RNAP assembly	-60 to -100 (NT)	*Escherichia coli, Bacillus subtilis, Lysobacter enzymogenes, Myxococcus xanthus*
RpoA (Lu et al., 2019)[10]	RNAP assembly	-267 to -415 (T)	*Bacillus subtilis*
RpoD (Chen et al., 2022)[11]	RNAP assembly	-199 to -216 (NT)	*Shewanella oneidensis*
RpoN (Peng et al., 2018)[12]	RNAP assembly	-53 to -103 (NT)	*Myxococcus xanthus*
NorR (Liu et al., 2019)[6]	σ^{54} activation	-91 to -131 (NT)	*Escherichia coli*
WtsA (Liu et al., 2019)[6]	σ^{54} activation	-91 to -131 (NT)	*Escherichia coli*

[a]T stands for Template strand and NT stands for Non-Template strand.

Table S7. Potential cooperativity of effectors investigated in this work

Effectors	SoxS-family	RNAP-subunit	AsiA	PspF
SoxS-family	**S**			
RNAP-subunit	**D**	**S**		
AsiA	**O**	**O**	**S**	
PspF	**O**	**O**	**U**	**S**

Representative labels are listed below for each activator pair.

S: Same activator, does not fit different mechanism criteria

U: Unlikely as only one sigma factor will be present

D: Same target site, prefer direct fusion.

O: Distinct target sites, prefer orthogonal recruitment.

Chapter 4: mRNA-responsive Bacterial Genetic Programs through Coupled CRISPR-Cas Tools

Ava V. Karanjia[a,b,c], Chunlei Jiao[d], Kira E. Olander[b,c], Sarah Kono[d], Chase Beisel[d,e], James M. Carothers[a,b,c*], Jesse G. Zalatan[b,c,f*]

a: Department of Chemical Engineering
University of Washington
Seattle, WA 98195
United States

b: Molecular Engineering & Sciences Institute
University of Washington
Seattle, WA 98195
United States

c: Center for Synthetic Biology
University of Washington
Seattle, WA 98195
United States

d: Helmholtz Institute for RNA-based Infection Research
Helmholtz Centre for Infection Research
Würzburg, Germany

e: Medical Faculty
University of Würzburg
Würzburg, Germany

f: Department of Chemistry
University of Washington
Seattle, WA 98195
United States

*: Corresponding authors
jcaroth@uw.edu
206-221-4902

zalatan@uw.edu
206-543-1670

*__Note__: This chapter contains collaborative work. C. J. and S. K. tested the editing window of Sth1-Cas9n-ABE and initial recording experiments. A. V. Karanjia performed the remaining experiments. The other authors provided input on experimental design. All sections were written by A. V. Karanjia with input from J. M. Carothers and J. G. Zalatan.

4.1. Abstract

CRISPR-Cas tools have transformed synthetic biology by providing programmable control over gene expression and gene editing. We have developed a new method to dynamically integrate transient environmental or cellular signals into genetic programs. We combine mRNA-responsive CRISPR based editing with transcriptional activation (CRISPRa) to create permanent gene switches responsive to endogenous mRNAs. Our system employs reprogrammable tracrRNAs (Rptrs) to sense specific mRNAs and convert them into guide RNAs (gRNAs) for CRISPR-Cas effectors. First, an mRNA-responsive Sth1 Cas9 adenine base editor modifies a non-targetable PAM to a targetable PAM at a synthetic reporter. This edit enables a subsequent CRISPRa complex to bind and activate gene expression. We optimized base editing parameters, achieving efficient A-to-G conversions that improve PAM compatibility for Spy CRISPRa. This dual-Cas9 approach uses reprogrammable RNAs to sense mRNA signals and convert them into gene activation, achieving high editing efficiency and high activation of a fluorescent reporter. By integrating RNA sensing with CRISPRa, our system converts transient mRNA signals into stable gene activation, expanding the toolkit for dynamic gene regulation. This approach provides a platform for building mRNA-responsive molecular switches with broad applications in synthetic biology, like phenotype switching and environmental sensing in bacteria.

Keywords: Base editing, CRISPR activation, reprogrammed tracrRNAs, transcriptional switches, multiple dCas9

Highlights

- Developed a dual-Cas9 system that integrates mRNA sensing with CRISPR base editing and CRISPR activation.
- Achieved efficient A-to-G base editing to convert A-rich PAMs to targetable G-rich PAMs that enable Spy CRISPRa.
- Demonstrated a mRNA-responsive switch that activates gene expression with 95% editing efficiency and up to 7.5 fold-activation of a fluorescent reporter.
- Established a platform for creating permanent, cell-state dependent gene switches.

4.2. Introduction

CRISPR-Cas tools have revolutionized biotechnology by simplifying the design and implementation of complex genetic functions. These tools rely on guide RNAs (gRNAs) to direct the CRISPR machinery to specific DNA targets. Many groups have used CRISPR-Cas transcriptional regulation for programmable control over gene activation and repression in bacteria.[1–4] Our group and others have used CRISPR activation (CRISPRa) and CRISPR inhibition (CRISPRi) for combinatorial pathway engineering,[5] activating endogenous targets,[3,6,7] multi-layer dynamic circuits,[8–10] and metabolic engineering in non-model organisms.[11,12] Beyond gene regulation, CRISPR base editors have been used for sequence-specific, single-nucleotide modifications to abolish enzyme activity or record cellular memory.[13,14]

Directly sensing endogenous mRNA signals uniquely enables real-time, sequence-specific incorporation of the current cell state and environment. This allows for an immediate and precise response to intracellular and extracellular changes. To connect CRISPR tools to transient environmental signals, previous groups have developed reprogrammed tracrRNAs (Rptrs) that base pair with a cellular mRNAs and convert the mRNAs to CRISPR gRNAs.[14–16] These Rptrs are designed to base pair with a cellular mRNA, converting the mRNA sequence to the targeting spacer sequence of a CRISPR gRNA. This paired Rptr-mRNA gRNA recruits the CRISPR machinery to a DNA target specified by the mRNA. RNA sensing offers a real-time, sequence-specific approach to directly monitor endogenous gene expression and integrate cell responses into downstream circuits. Rptrs have been used to directly recruit effector proteins including base editors and transcriptional activators.[14–16] Effector recruitment is directly tied to mRNA presence, so when the mRNA disappears, the recruitment stops. A key challenge is maintaining the transcriptional output after the mRNA signal is gone.

By pairing mRNA-responsive CRISPR base editing with CRISPRa (Rptr-CRISPRa), we develop a novel approach to transform transient mRNA signals into permanent genetic switches. Specifically, our system employs the mRNA-guided base editor to introduce sequence-specific genetic edits in a synthetic promoter's protospacer adjacent motif (PAM). This edited PAM functions as the "recording scratchpad" and a permanent switch to turn on downstream expression. Leveraging our and others' research on PAM-flexibility of Spy dCas9, we can identify specific A-to-G base conversions that can generate a PAM compatible with Spy dCas9.[3,7,17] These PAM edits act as a permanent switch for downstream gene activation and ultimately enable other CRISPRa programs. We prototype this tool with a synthetic mRNA and an mRFP fluorescent reporter and show that Rptr-CRISPRa can effectively switch on the expression of a downstream reporter. Then, we use computational tools to design and screen endogenous Rptrs. Our study expands upon current CRISPR capabilities to build mRNA-responsive expression switches.

4.3. Results

Here, we detail the modular design of an mRNA-responsive expression switch that uses base editing to record the mRNA and permanently activate a CRISPRa program. Our groups have previously shown that CRISPR-Cas transcriptional regulation can enable programmable control over gene activation and repression in bacteria. Combined with Rptrs, this design allows for dynamic sensing of endogenous mRNAs and subsequent activation of an arbitrary genetic output. To prototype this system, we modified a fluorescent reporter for recruitment of two CRISPR complexes: 1) a mRNA-responsive CRISPR base editor [Figure 1A] and 2) a CRISPRa complex that recruits the activator MCP-SoxS [Figure 1B].

Once the mRNA is sensed, Rptrs base pair with an RNA of interest and convert the mRNA into a guide RNA (gRNA) for base editing [Figure 1D]. With a fully formed gRNA, the

Sth1 Cas9 with a base editor edits the Spy dCas9 PAM [Figure 1B]. The edit converts the Spy dCas9 PAM from an non-targetable PAM (i.e. NAA) to a targetable PAM (i.e. NGG) [Figure 1C, 1D]. Once the PAM is targetable, Spy dCas9 CRISPRa activates the fluorescent mRFP reporter. The dual Cas9 complexes combine mRNA-guided recording and subsequent activation, achieving a permanent switch to a desired transcriptional program.

4.3.1. Determining appropriate base editor and base editor targets

For the CRISPR base editor, we selected Sth1 Cas9 nickase fused to an adenine base editor, Sth1-Cas9n-ABE, for its precise activity and previous compatibility with reprogrammable tracrRNA (Rptr) designs [Figure 1A]. In addition, Sth1 Cas9 has a strict PAM requirement (5'-NNAGAAW-3') which reduces potential off-target editing. We chose an adenine base editor because our previous PAM screens for Spy dCas9 showed that G-rich PAMs result in higher CRISPR activation, consistent with Spy PAM preference from other studies [Figure 2A].[7,17] For our application, an A-to-G conversion within the Spy dCas9 PAM could trigger Spy dCas9 and downstream activation [Figure 2A]. To determine the best location for an A-to-G conversion, we characterized the optimal editing window of Sth1-Cas9n-ABE. We induced expression of Sth1Cas9-ABE and measured the A-to-G conversion in the recording plasmid, as previously described for other base editors [Figure S1A].[14] We conducted the experiment in biological triplicate and sent purified PCR fragments for Sanger sequencing. We then quantified the relative peak heights of Sanger sequencing chromatograms using EditR.[14,18] We found a peak in activity from A5-A10 and also a context preference, where adjacent cytosine and thymine DNA bases (T ≈ C > G >> A) to the desired edit promoted higher A-to-G conversion [Figure S1B, S1C]. Determining the editing window and context preference will aid in predicting and maximizing the efficiency of A-to-G base editing in future CRISPRa reporter designs.

Next, we measured the recording capability of a synthetic mRNA transcript. As previously reported,[14] we constitutively expressed a synthetic transcript encoded by the CJ8421_04975 gene (CJ mRNA) from *Campylobacter jejuni* CG84-21 in *E. coli* MG1655 along with our designed Rptrs [Figure S2]. Each target in the CJ mRNA had multiple editable adenine bases positioned on the 5' end of the spacer. We saw at least 1 position edit at high efficiency (>80% A-to-G conversion) for all three CJ Rptr DNA targets [Figure S2]. This experiment demonstrated highly efficient recording of a synthetic mRNA using Rptr-guided base editing.

We then identified the most efficient single or double base conversions with CJ Rptrs that would result in an improved PAM for bacterial CRISPRa. Based on our prior work with Spy dCas9 PAMs, edits that convert A-rich PAMs to G-rich PAMs should increase CRISPRa activation with Spy dCas9 MCP-SoxS [Figure 2A]. Through this screening, we identified a single base conversion (A>G) for each Rptr that would result in an improved PAM for bacterial CRISPRa [Figure S2, Figure 2A-B]. For example with Rptr2, a CAA PAM could be converted to CGA, CAG, or CGG PAMs, which would all significantly improve activation of the CRISPRa reporter by Spy-dCas9 MCP-SoxS [Figure 2A].

4.3.2. Testing Rptr-J3 reporters for CRISPR activation

Our goal is to connect the mRNA-responsive base editing system to the Spy dCas9 CRISPRa complex to trigger a permanent change in gene expression after detecting a specific mRNA. To couple these effects, we modified the previously described J3 promoter by overlapping the target sites for both CRISPR effectors [Figure 2B].[3] For each Rptr reporter, we identified an untargetable Spy PAM within the Sth1 target [Figure S2]. This PAM was chosen so that a single A-to-G conversion would lead to the highest predicted increase in CRISPRa [Figure 2A]. We placed the Sth1 target containing the untargetable Spy PAM, directly upstream of the -81 bp site, which is the optimal location for Spy dCas9 CRISPRa.[3]

This precise layering of targets ensures that when Sth1-Cas9n-ABE records an mRNA, it simultaneously edits the Spy dCas9 PAM. This edit acts like a switch, making the Spy PAM targetable and enabling the Spy dCas9 CRISPRa complex to activate the downstream gene [Figure 1D, Figure 2B].

First, we tested Sth1 Cas9n-ABE for its ability to edit each of the Rptr-J3 reporters, where the edit should increase downstream CRISPR activation [Figure 2B]. All three Rptr-J3 reporters yielded measurable editing, with Rptr2 showing almost complete A-to-G at position A8 [Figure 2B]. We observed no editing over baseline with the scrambled tracrRNA (ST) control for each Rptr. To approximate recording at the single-cell level, we plated the culture and performed whole-plasmid sequencing of the DNA target on individual colonies. In each sequenced colony, we observed on-target edits at the A8 position [Figure 2C]. However, one colony had an additional edit within the spacer (A2), while another exhibited an edit beyond the intended target range (A-3). Therefore, multiple differentially edited reporters can be produced within the plasmid population.

Next, we tested Spy dCas9 MCP-SoxS for its ability to activate the Rptr2-J3 reporter [Figure 2C]. We evaluated three differentially edited reporters that each had the desired PAM edit and additional edits observed from Sth1-Cas9n-ABE. We saw 28-fold activation with the PAM-edit only reporter, while no activation was observed with the unedited reporter [Figure 2C]. We also observed that additional edits could significantly impair the resultant CRISPRa efficiency. For example, reporter 2, which has an additional edit directly adjacent to the Spy PAM, exhibited complete loss of CRISPRa activity. This finding is consistent with previously reported mismatch tolerance for Spy Cas9, where the seed region (5-8 bp closest to the PAM) is essential for SpyCas9 target recognition and cleavage efficiency.[19,20] Mismatches in this region can greatly reduce binding stability, which explains why we saw no activation with edit A [Figure 2C]. For future designs, we can remove potential edits (As) at the 5’ end of the spacer. This modification is expected to be tolerated by Sth1, as the

mismatch tolerance is greater at the 5' end of the spacer. These promoter modifications enable us to sequentially recruit each effector complex, bringing us closer to a fully functional mRNA-responsive molecular switch.

4.3.3. Pairing Rptr-base editing with CRISPR activation

We then investigated the dual recruitment of Sth1-Cas9n-ABE and Spy-dCas9 CRISPRa to the Rptr-J3 reporter to enable sequential base editing and CRISPR activation. Initially, both Cas9 complexes were expressed from inducible plasmids previously used in their individual characterizations [Figure 2B, 2C, 3A]. Our initial experiment revealed promising results from an overnight culture, where Sth1-Cas9n-ABE efficiently edited the Spy PAM to approximately ~90% which led to ~6.4x fold activation of an edited mRFP reporter [Figure 3B, 3C].

However, upon extended culturing, specifically after performing two inducer subcultures designed to sequentially activate each CRISPR complex, we observed significant instability across replicates in the dual Cas9 strain [Figure S3A, S3B]. This instability was observed through variable CRISPRa activity in the dual Cas9, dual gRNA (mRNA-Rptr gRNA, CRISPRa scRNA) system. This is likely from burden issues of expressing all components rather than a reversion of the base edit [Figure S4]. Recognizing that the efficiency of the base editor was unaffected, we integrated Spy dCas9 into the MG1655 genome to stabilize the other Cas9 complex. Following this integration, we observed inducer-dependent base editing and CRISPRa with the dual Cas9 system [Figure S3C]. Specifically, we achieved editing efficiencies of approximately 90% and 7.5-fold activation of the mRFP reporter. However, even with the integrated Spy dCas9 CRISPRa system, we still observed instability upon extended culturing [Figure S3C].

Resolving this remaining instability is a critical next step. Our ongoing work will focus on systematically alleviating cellular burden. This includes optimizing the expression levels

of all system components and potentially integrating additional components into the MG1655 genome. Overcoming these burden-related challenges will be essential to building this expression switch that functions reliably over multiple generations.

4.4. Discussion

This study establishes a novel framework for creating mRNA-responsive genetic switches in bacteria by integrating mRNA-responsive base editing with CRISPR activation. This approach enables programmable activation of downstream gene programs, offering a distinct advantage over dynamic control strategies reliant solely on external inducers. By directly incorporating the current cellular state through endogenous mRNA detection, this tool can reprogram native cellular responses to programmable engineered responses.

A core innovation of our system lies in the use of DNA recording to create a permanent “ON” switch for Spy dCas9 CRISPRa. We identified optimal A-to-G conversions of Spy dCas9 PAMs that can turn “ON” Spy dCas9 CRISPRa [Figure 2A]. Our Rptr-guided base editing demonstrated highly efficient recording of a synthetic mRNA, achieving over 80% A-to-G conversion for many different targets with an mRNA. We showed that a single A-to-G edit in a Spy dCas9 PAM can convert a untargetable PAM to a targetable one, and can result in up to 28-fold activation of the downstream mRFP reporter [Figure 2B, 2C]. Although tested separately, these two steps provide the basis for future genetic switches. In addition, our investigation also revealed the critical importance of precise base edit placement for successful CRISPRa. While the desired PAM edit was sufficient for activation, we observed that additional unintended edits could significantly impair CRISPRa efficiency. For instance with reporter 2, with an unintended edit adjacent to the Spy PAM, we observed a complete loss of CRISPRa activity [Figure 2C]. For future designs, we can mitigate off-target effects by removing potential editable adenines at the 5’ end of the spacer.

Initial experiments with dual Cas9 complexes expressed from plasmids demonstrated the feasibility of recruiting both Sth1-Cas9n-ABE and Spy dCas9 CRISPRa to the Rptr-J3 reporter for sequential base editing and CRISPRa. An overnight culture showed promising initial results, with Sth1-Cas9n-ABE efficiently editing the Spy PAM leading to a 6.4-fold activation of the edited mRFP reporter [Figure 3B]. After performing sequential inducer subcultures to induce each CRISPR complex, we observed substantial instability across replicates in the dual Cas9 plasmid-based strain [Figure S3]. These results highlight the importance of component stability when engineering multi-component and multi-Cas9 systems.

This study establishes a foundational framework for creating mRNA-responsive genetic switches in bacteria. Beyond synthetic mRNAs, this system holds significant promise for responding to diverse endogenous cellular signals, enabling advanced applications in dynamic gene regulation. For instance, it could be utilized for metabolic engineering, allowing the permanent activation of a pathway upon detection of a specific metabolic intermediate's mRNA. Similarly in biosensing, it could provide a permanent, detachable readout for the presence of an environmental mRNA. This framework can also be extended to other bacterial species, opening avenues for applications in probiotic therapies, industrial biotechnology, and environmental sensing. Ultimately, our results establish a foundation for leveraging mRNA-responsive CRISPR tools to build dynamic and programmable gene circuits that can respond to cellular states.

4.5. Materials and Methods

Bacterial strains and plasmid constructs

The bacterial strains used in this study are listed in Table S1. All PCR fragments were amplified with Phusion DNA Polymerase (Thermo-Fisher Scientific) for Infusion Cloning (Takara Bio). Plasmids were transformed into chemically competent E. coli DH10B (Thermo Fisher Scientific) or NEB turbo (New England Biolabs) cells, plated on LB-agar, and cultured in LB media with the appropriate antibiotics used in the following concentrations: 100 μg/mL Carbenicillin, 25 μg/mL Chloramphenicol, 30 μg/mL Kanamycin. Plasmids were constructed following previously described methods.[1] Sth1-Cas9n refers to *Streptococcus thermophilus* Cas9 nickase. Spy-dCas9 refers to *Streptococcus pyogenes* deactivated Cas9. Different Sth base editing plasmids were constructed using pCJ787 (IPTG and arabinose inducible) as a backbone. Different Spy CRISPRa plasmids harboring dCas9 were constructed using pSLQ1055 (aTc-inducible) as a backbone. The SoxS effector used in this study contains two mutations (R93A/S101A) as previously described.[1] Throughout the manuscript, "-" will indicate direct protein fusions. All plasmid constructs were confirmed by Sanger sequencing (Genewiz/Azenta Life Sciences) or Nanopore sequencing (Primordium/Plasmidsaurus).

CRISPRa plate reader experiments

Single colonies from LB plates were inoculated in 400 μL of LB supplemented with the appropriate antibiotics and grown in 96-deep-well plates at 37 °C with shaking overnight 900 RPM on a Heidolph titramax 1000. 150 μL of the overnight culture were transferred into flat, clear-bottomed black 96-well plates (Corning) and the OD_{600} and fluorescence were measured in a Biotek Synergy HTX plate reader. Data were analyzed using the BioTek Gen5 2.07.17 software. For mRFP1 detection, the excitation wavelength was 540 nm and emission wavelength was 600 nm. For GFPmut2 or sfGFP detections, the excitation wavelength was 485 nm and emission wavelength was 528 nm.

Sth1-Cas9n-ABE editing window experiment

To identify the editing window of Sth1-Cas9n-ABE, two reporters (W1 and W2) were designed with poly As located in different positions in the guide sequence. Colonies of *E. coli* containing the recording machinery were inoculated in LB + antibiotics medium. Cultures were then grown in 96-deep-well plates at 37 °C with shaking overnight 900 RPM on a Heidolph titramax 1000. The overnight cultures were back diluted 1:20 into 400 uL LB with

antibiotics and inducers and grown for 8h at 37 °C shaking at 900 RPM on a Heidolph titramax 1000. Then 1 uL of induced cultures were used as a template to amplify the edited region with oAK133 and oCK682. The edited region was then purified and extracted with QIAquick or QIAprep 2.0 spin columns (Qiagen) and then sent for Sanger sequencing with primer oCK1005. The web tool, EditR v.1.0.10, was then used to evaluate the editing efficiency.[18]

Non-native transcript recording experiments

Bulk population sequencing of CJ8421_0495, the synthetic mRNA, followed the same procedures outlined in “Sth1-Cas9n-ABE editing window experiment”. To approximate population-level editing, strains were plated for single colonies and then single colonies were sent for whole-plasmid sequencing.

4.6. References

(1) Dong, C.; Fontana, J.; Patel, A.; Carothers, J. M.; Zalatan, J. G. Synthetic CRISPR-Cas Gene Activators for Transcriptional Reprogramming in Bacteria. *Nat. Commun.* **2018**, *9* (1), 2489. https://doi.org/10.1038/s41467-018-04901-6.

(2) Liu, Y.; Wan, X.; Wang, B. Engineered CRISPRa Enables Programmable Eukaryote-like Gene Activation in Bacteria. *Nat. Commun.* **2019**, *10* (1), 3693. https://doi.org/10.1038/s41467-019-11479-0.

(3) Fontana, J.; Dong, C.; Kiattisewee, C.; Chavali, V. P.; Tickman, B. I.; Carothers, J. M.; Zalatan, J. G. Effective CRISPRa-Mediated Control of Gene Expression in Bacteria Must Overcome Strict Target Site Requirements. *Nat. Commun.* **2020**, *11* (1), 1618. https://doi.org/10.1038/s41467-020-15454-y.

(4) Ho, H.; Fang, J. R.; Cheung, J.; Wang, H. H. Programmable CRISPR-Cas Transcriptional Activation in Bacteria. *Mol. Syst. Biol.* **2020**, *16* (7). https://doi.org/10.15252/msb.20199427.

(5) Fontana, J.; Sparkman-Yager, D.; Faulkner, I.; Cardiff, R.; Kiattisewee, C.; Walls, A.; Primo, T. G.; Kinnunen, P. C.; Garcia Martin, H.; Zalatan, J. G.; Carothers, J. M. Guide RNA Structure Design Enables Combinatorial CRISPRa Programs for Biosynthetic Profiling. *Nat. Commun.* **2024**, *15* (1), 6341. https://doi.org/10.1038/s41467-024-50528-1.

(6) Ameruoso, A.; Villegas Kcam, M. C.; Cohen, K. P.; Chappell, J. Activating Natural Product Synthesis Using CRISPR Interference and Activation Systems in Streptomyces. *Nucleic Acids Res.* **2022**, *50* (13), 7751–7760. https://doi.org/10.1093/nar/gkac556.

(7) Kiattisewee, C.; Karanjia, A. V.; Legut, M.; Daniloski, Z.; Koplik, S. E.; Nelson, J.; Kleinstiver, B. P.; Sanjana, N. E.; Carothers, J. M.; Zalatan, J. G. Expanding the Scope of Bacterial CRISPR Activation with PAM-Flexible dCas9 Variants. *ACS Synth. Biol.* **2022**, *11* (12), 4103–4112. https://doi.org/10.1021/acssynbio.2c00405.

(8) Tickman, B. I.; Burbano, D. A.; Chavali, V. P.; Kiattisewee, C.; Fontana, J.; Khakimzhan, A.; Noireaux, V.; Zalatan, J. G.; Carothers, J. M. Multi-Layer CRISPRa/i Circuits for Dynamic Genetic Programs in Cell-Free and Bacterial Systems. *Cell Syst.* **2021**, S2405471221004191. https://doi.org/10.1016/j.cels.2021.10.008.

(9) Alba Burbano, D.; Cardiff, R. A. L.; Tickman, B. I.; Kiattisewee, C.; Maranas, C. J.; Zalatan, J. G.; Carothers, J. M. Engineering Activatable Promoters for Scalable and Multi-Input CRISPRa/i Circuits. *Proc. Natl. Acad. Sci.* **2023**, *120* (30), e2220358120. https://doi.org/10.1073/pnas.2220358120.

(10) Barbier, I.; Kusumawardhani, H.; Chauhan, L.; Harlapur, P. V.; Jolly, M. K.; Schaerli, Y. Synthetic Gene Circuits Combining CRISPR Interference and CRISPR Activation in E. Coli: Importance of Equal Guide RNA Binding Affinities to Avoid Context-Dependent Effects. *ACS Synth. Biol.* **2023**, *12* (10), 3064–3071. https://doi.org/10.1021/acssynbio.3c00375.

(11) Peng, R.; Wang, Y.; Feng, W.; Yue, X.; Chen, J.; Hu, X.; Li, Z.; Sheng, D.; Zhang, Y.; Li, Y. CRISPR/dCas9-Mediated Transcriptional Improvement of the Biosynthetic Gene Cluster for the Epothilone Production in Myxococcus Xanthus. *Microb. Cell Factories* **2018**, *17* (1), 15. https://doi.org/10.1186/s12934-018-0867-1.

(12) Yin, L.; Xi, D.; Shen, Y.; Ding, N.; Shao, Q.; Qian, Y.; Fang, Y. Rewiring Metabolic Flux in Corynebacterium Glutamicum Using a CRISPR/dCpf1-Based Bifunctional Regulation System. *J. Agric. Food Chem.* **2024**, *72* (6), 3077–3087. https://doi.org/10.1021/acs.jafc.3c08529.

(13) Wang, Y.; Liu, Y.; Zheng, P.; Sun, J.; Wang, M. Microbial Base Editing: A Powerful Emerging Technology for Microbial Genome Engineering. *Trends Biotechnol.* **2021**, *39*

(2), 165–180. https://doi.org/10.1016/j.tibtech.2020.06.010.
(14) Jiao, C.; Reckstadt, C.; König, F.; Homberger, C.; Yu, J.; Vogel, J.; Westermann, A. J.; Sharma, C. M.; Beisel, C. L. RNA Recording in Single Bacterial Cells Using Reprogrammed tracrRNAs. *Nat. Biotechnol.* **2023**, *41* (8), 1107–1116. https://doi.org/10.1038/s41587-022-01604-8.
(15) Jiao, C.; Sharma, S.; Dugar, G.; Peeck, N. L.; Bischler, T.; Wimmer, F.; Yu, Y.; Barquist, L.; Schoen, C.; Kurzai, O.; Sharma, C. M.; Beisel, C. L. Noncanonical crRNAs Derived from Host Transcripts Enable Multiplexable RNA Detection by Cas9. *Science* **2021**, *372* (6545), 941–948. https://doi.org/10.1126/science.abe7106.
(16) Liu, Y.; Pinto, F.; Wan, X.; Yang, Z.; Peng, S.; Li, M.; Cooper, J. M.; Xie, Z.; French, C. E.; Wang, B. Reprogrammed tracrRNAs Enable Repurposing of RNAs as crRNAs and Sequence-Specific RNA Biosensors. *Nat. Commun.* **2022**, *13* (1), 1937. https://doi.org/10.1038/s41467-022-29604-x.
(17) Kim, N.; Kim, H. K.; Lee, S.; Seo, J. H.; Choi, J. W.; Park, J.; Min, S.; Yoon, S.; Cho, S.-R.; Kim, H. H. Prediction of the Sequence-Specific Cleavage Activity of Cas9 Variants. *Nat. Biotechnol.* **2020**, *38* (11), 1328–1336. https://doi.org/10.1038/s41587-020-0537-9.
(18) Kluesner, M. G.; Nedveck, D. A.; Lahr, W. S.; Garbe, J. R.; Abrahante, J. E.; Webber, B. R.; Moriarity, B. S. EditR: A Method to Quantify Base Editing from Sanger Sequencing. *CRISPR J.* **2018**, *1* (3), 239–250. https://doi.org/10.1089/crispr.2018.0014.
(19) Jones, D. L.; Leroy, P.; Unoson, C.; Fange, D.; Ćurić, V.; Lawson, M. J.; Elf, J. Kinetics of dCas9 Target Search in Escherichia Coli. *Science* **2017**, *357* (6358), 1420–1424. https://doi.org/10.1126/science.aah7084.
(20) Cho, S.; Choe, D.; Lee, E.; Kim, S. C.; Palsson, B.; Cho, B.-K. High-Level dCas9 Expression Induces Abnormal Cell Morphology in Escherichia Coli. *ACS Synth. Biol.* **2018**, *7* (4), 1085–1094. https://doi.org/10.1021/acssynbio.7b00462.

4.7. Figures

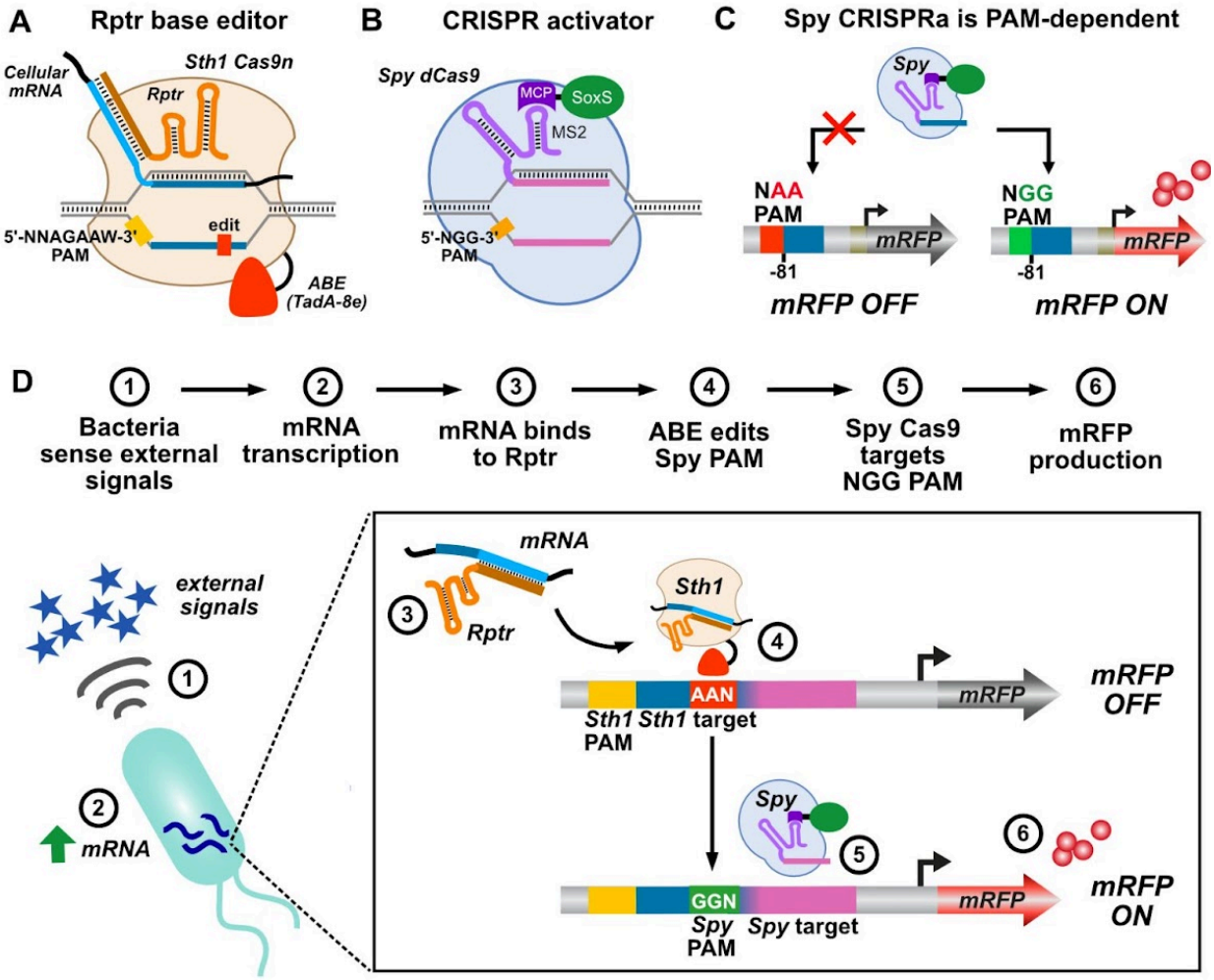

Figure 1. Rptr-CRISPRa can enable mRNA-responsive expression switches.

(A) Sth1-Cas9n-ABE or CRISPR base editor makes base conversions in the DNA target. Sth1-Cas9 has a 5'-NNAGAAW-3' PAM. The deaminase or ABE is TadA-8e. Once the mRNA is sensed, the reprogrammed tracrRNA (Rptr) base pairs with an RNA of interest and converts the mRNA into a guide RNA (gRNA) for base editing. (B) Spy-dCas9 MCP-SoxS or CRISPR activator upregulates genes. Spy-Cas9 has a 5'-NGG-3' PAM. We use a scaffold RNA (scRNA) to recruit a RNA-binding protein (RBP) fused activator, MS2 and MCP-SoxS, respectively. (C) Spy CRISPRa is PAM-dependent, where Spy dCas9 has a PAM preference of G-rich PAMs. (D) Rptr-CRISPR mechanism. The mRNA binds to the Rptr and forms with BE gRNA, which is then used by Sth1-Cas9n-ABE for base editing the Spy PAM. Once edited, the Spy PAM can now be used by Spy-dCas9 for CRISPR activation, which upregulates mRFP production.

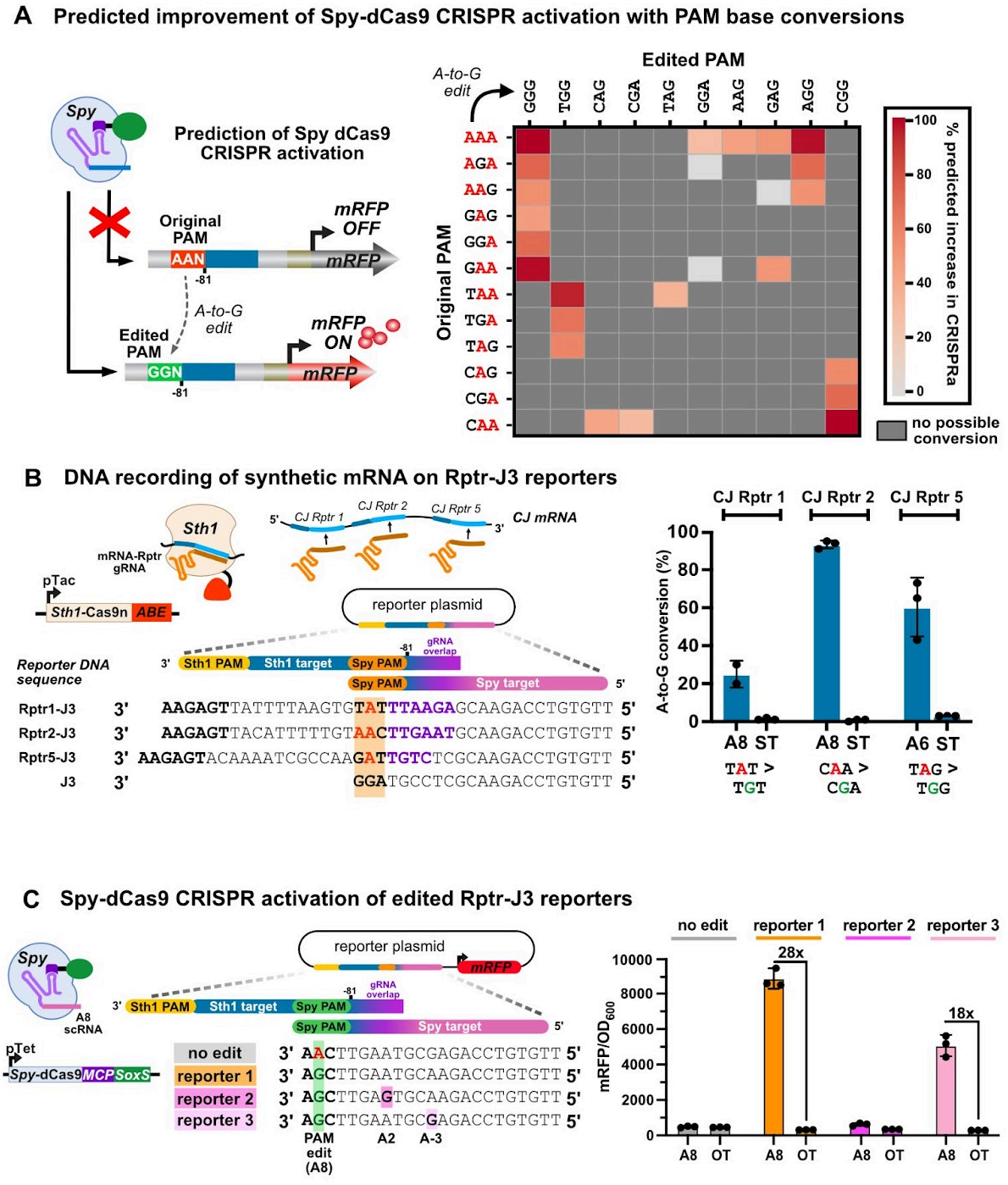

Figure 2. Spy PAM editing can switch on mRFP expression.

(A) Predicted improvement of Spy-dCas9 CRISPR activation with PAM base conversions. Previous work calculated CRISPRa fluorescence from different PAMs for Spy PAM-flexible dCas9 variants (Kiattisewee & Karanjia, et al. 2022). This heatmap calculates the % difference between predicted activation of the original PAM and an edited PAM. (B) Sth1-Cas9n-ABE CRISPR base editing on Rptr-J3 reporters. We found single A-to-G base

conversions that would edit a downstream Spy PAM and tested the editing efficiency. Targets are labeled from the PAM-distal end (i.e. A8 is 8 bp from the 5' end of the spacer). Base editing is relative to a scrambled tracrRNA control (ST). (C) Spy-dCas9 CRISPR activation on edited Rptr-J3 reporters. We observed differential editing across the reporter population and tested CRISPR activation for each of the reporters. Targets are labeled from the PAM-distal end. CRISPRa is relative to an off-target (OT) scRNA.

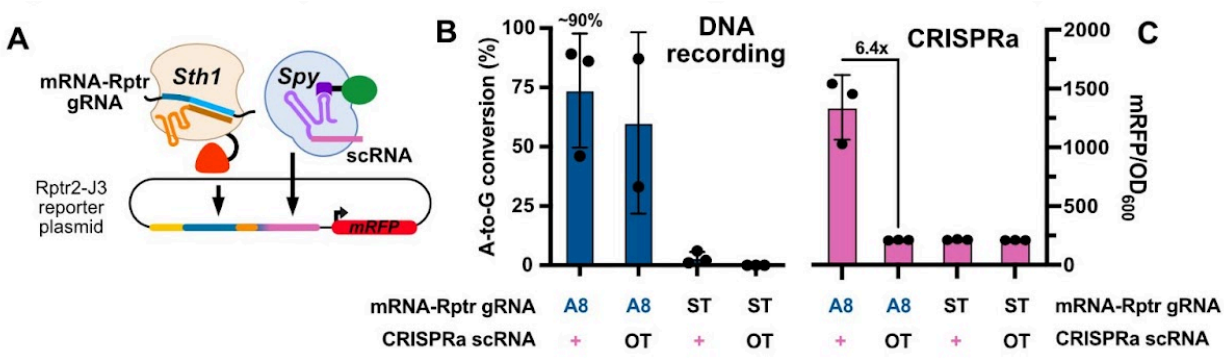

Figure 3. Combined Rptr-CRISPRa can switch on expression of an mRFP reporter.

(A) Dual Cas9 targeting overlapping DNA targets on the reporter plasmid. Sth1-Cas9-ABE performs the base editing first and then Spy-dCas9 MCP-SoxS performs CRISPR activation. (B) Experimental setup for sequential Cas9 recruitment. (C) Multiple methods of Cas9 expression. Base editor gRNAs are either Rptr-mRNA or a scrambled tracrRNA (ST). CRISPRa scRNAs are either on-target guides (+) or off-target guides (OT).

4.8. Supplementary Information

Supporting Figures

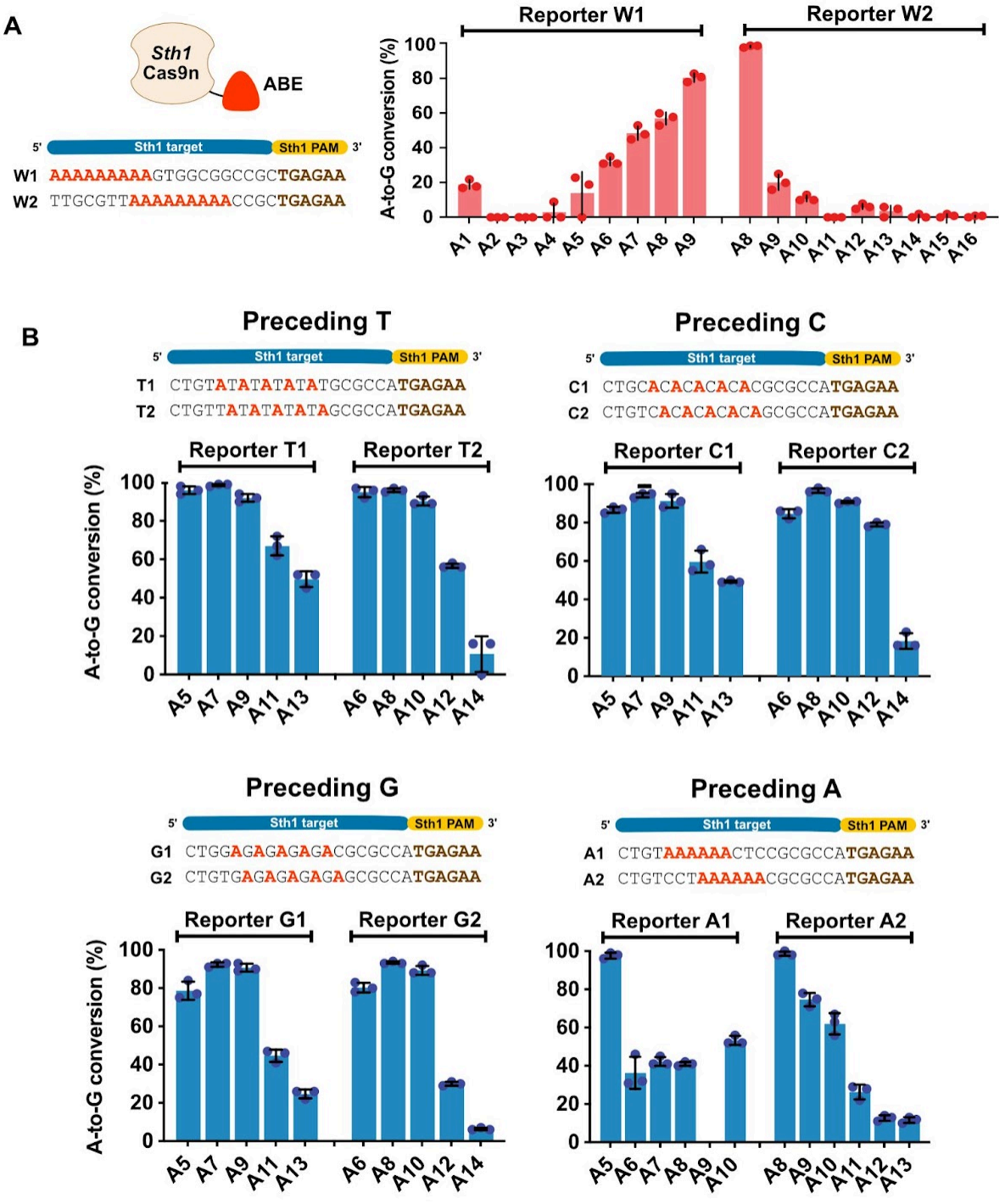

Figure S1. Editing window and context preference of Sth1-Cas9n-ABE
(A) Schematic of Sth1-Cas9n-ABE and a representative target showing the Sth1 target site and Sth1 PAM. Bar graph indicates the A-to-G conversion percentage across various

PAM-distal adenine positions (A1-A16) across two reporter constructs, W1 and W2. (B) Context-dependent editing of PAM-distal adenines. Bar graph again indicates the A-to-G conversion percentage across various PAM-distal adenine positions (A1-A16) across four reporter constructs changing the base pair that precedes the desired edit.

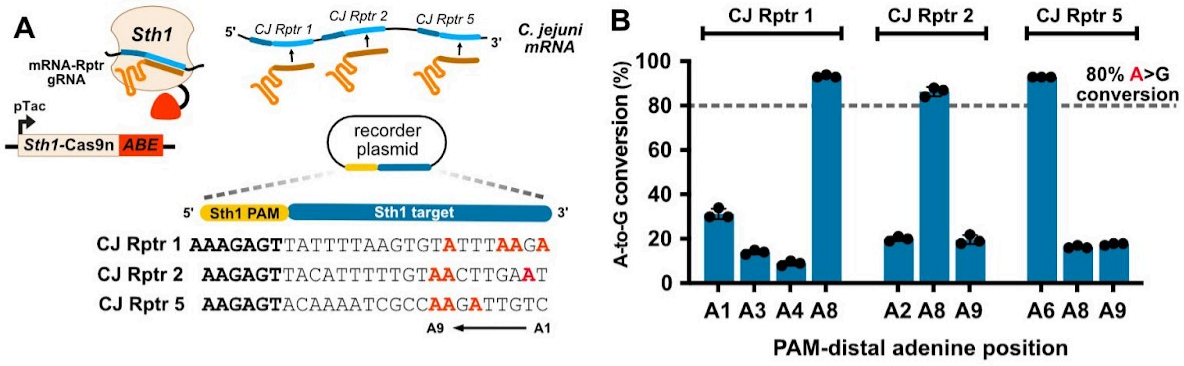

Figure S2. Sth1-Cas9n-ABE can edit synthetic mRNA transcripts.

(A) Schematic of three Rptrs designed for *C. jejuni* mRNA-responsive base editing. Reprogrammed tracrRNAs (Rptrs) bind to mRNA and form a functional gRNA that directs Sth1-Cas9n-ABE to a recorder plasmid that contains the Sth1 PAM and Sth1 target. Sequences for each Rptr are shown, highlighting potential adenine editing positions. (B) Bar graph showing A-to-G conversion percentage at different PAM-distal adenine positions. Efficiencies above 80% are highlighted.

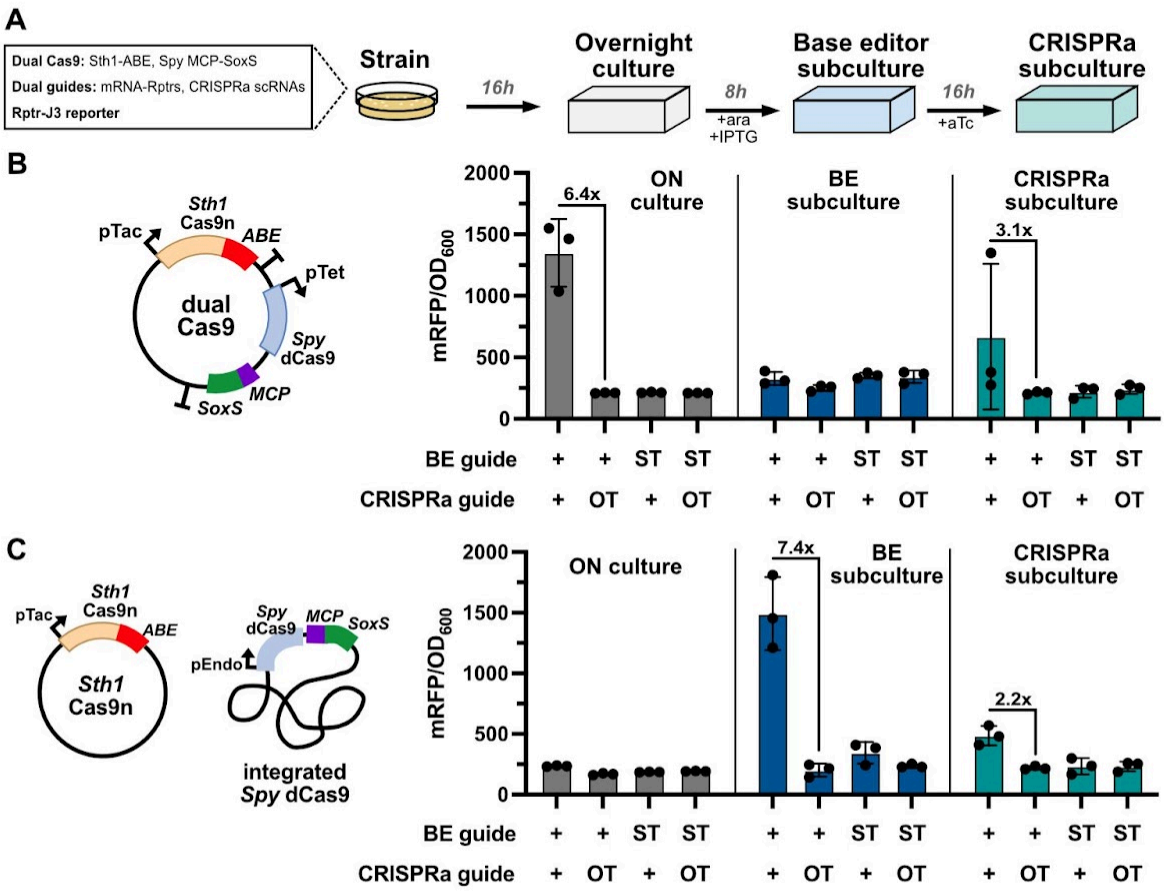

Figure S3. Dual Cas9 system shows variable CRISPRa and potential component instability.

(A) Experiment workflow for testing the dual Cas9 system. The initial strain utilized two separate plasmids encoding Sth1-ABE and Spy dCas9 MCP-SoxS (CRISPRa), along with mRNA-Rptrs and CRISPRa scRNAs. Cultures are subjected to an overnight growth, followed by a base editor subculture with inducers, and a CRISPRa subculture with inducers. (B) mRFP fluorescence measurements indicating CRISPRa activity for the dual Cas9 plasmid. Base editor gRNAs are either Rptr-mRNA or a scrambled tracrRNA (ST). CRISPRa scRNAs are either on-target guides (+) or off-target guides (OT). (C) Schematic illustrating the integrated Spy dCas9 and plasmid-based Sth1-Cas9n-ABE. Same controls and labels as (B).

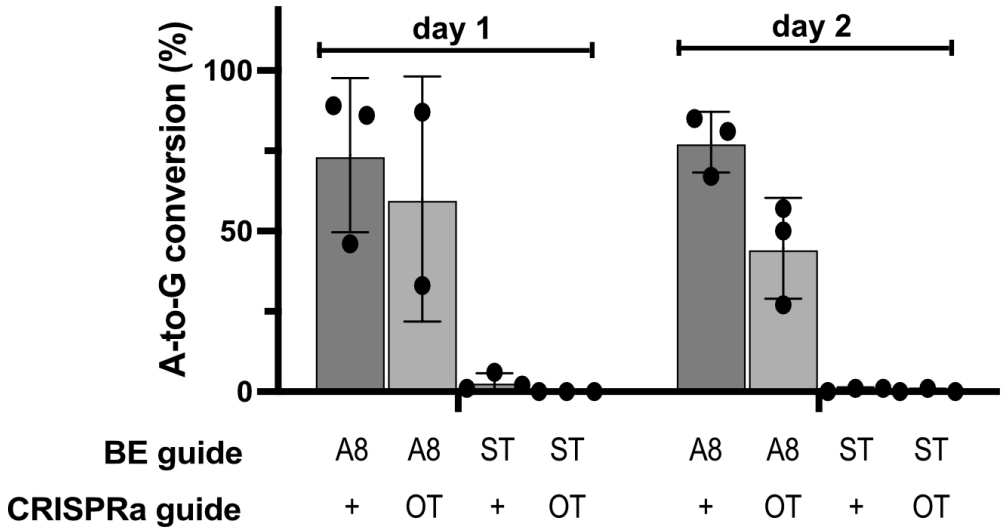

Figure S4. Base editing efficiency is maintained over two days. Base editor gRNAs are either Rptr-mRNA or a scrambled tracrRNA (ST). CRISPRa scRNAs are either on-target guides (+) or off-target guides (OT).

Acknowledgments

Graduate school was quite the journey! It was lots of intense learning, countless ungodly hours in the lab, and plenty of moments filled with imposter syndrome. The actual science wasn't the toughest part of the PhD, it was building up the sheer strength and tenacity to see it through. The work described here and my ability to perform it, would not be possible without the contributions, support, and care from all past, current, and future members of the Carothers and Zalatan labs. I am so honored to have had the opportunity to learn and grow in this environment and have a lot of amazing people to thank!

To my advisors, your combined mentorship has significantly shaped my approach to scientific research. I am really grateful for the immense freedom and opportunity you gave me to explore questions that genuinely excited me – a really unique and invaluable aspect of our research groups.

Jesse, thank you for teaching me the critical importance of asking the right questions and for instilling in me a healthy skepticism. You pushed me to challenge assumptions and look critically beyond what the literature was telling us, which has impacted how I ask research questions.

James, thank you for consistently pushing me to think BIG and frame my research around answering larger, impactful questions. I also appreciate how you've consistently helped me zoom out and see the broader picture and implications of my work.

And to my dissertation committee, Jorge Marchand and Maitreya Dunham, thank you for providing me with suggestions and support that helped me refocus my efforts across all of my different projects.

To my labmates in both Carothers and Zalatan labs, you have been more than just colleagues to me. You have been a fantastic source of collaborations, advice, and community. Thank you for the constant and stimulating discussions, shared laughs, and for making the lab feel like a second home.

To my mentors in both labs, Jason Fontana, Cholpisit Ice Kiattisewee, Joseph Harman, Ian Faulkner, and Emily Cliff: I was completely new to synthetic biology when I joined and you always answered any of my silly questions or helped me fix my mistakes. I have learned a lot from each of you on how to be a good mentor and lead by example.

To my cohort of graduate students in both labs, Diego Alba Burbano, Ryan Cardiff, Widianti Sugianto, Janis Shin, and Noel Jameson: it has been a privilege to learn and grow with you these past 4.5 years. I have so much love for each of you and really cherish the many memories we have built together over the years.

To Kira Olander, Karl Anderson, Nidhi Mehta, Tommy Primo, Yejun Kim, Yujia Huang, and Sam Dyer: it has been so fun to watch each and every one of you grow as scientists and people over the last 2-3 years. I am so honored to have been part of your journey in graduate school and cannot wait to see what you all do next!

Beyond the lab, I have been fortunate to be surrounded by an incredible support system. My graduate school friends have provided me with invaluable commiseration, motivation, and much-needed distraction. Special shout-out to Brendan Butler, Cassandra Maranas, Maria Politi, Evan Komp, Ryan Gharios, Sage Scheiwiller, Chris Yin, and Duncan Reece.

To my friends outside of grad school, thank you for keeping me grounded and reminding me of the world outside of academia. Another special thank you to Akhila Murella, Kayla Tapia, Collin Ganser, Alice Wong, Erin Spielman, Sanchita Galgalikar, and Tomas Bencomo.

I'd also like to thank my broader scientific communities of EBRC and Astrobiology, where their intellectual passion, collaborative spirit, and commitment to learning have been truly inspiring.

To my incredible parents, thank you for your immense sacrifices and unwavering belief in a brighter future for us. Your hard work, dedication, and endless love has been my constant inspiration throughout this journey and I am so grateful to have your never-ending support. And to my sister, thank you for being my built-in best friend! I am so lucky to have you by my side and I am so proud of everything you have accomplished.

Last but not least, I'd like to thank my partner of almost four years (!), Gennaro Olivo. Thank you for being my anchor through the countless late nights, early mornings, and research-filled weekends. You've lovingly taken care of me when I was completely wiped out and you continue to extend your unwavering support to everyone in my life. You have been there from (basically) the very beginning of my graduate school career and I could not have accomplished this without you.